

# University of Southampton Research Repository

Copyright © and Moral Rights for this thesis and, where applicable, any accompanying data are retained by the author and/or other copyright owners. A copy can be downloaded for personal non-commercial research or study, without prior permission or charge. This thesis and the accompanying data cannot be reproduced or quoted extensively from without first obtaining permission in writing from the copyright holder/s. The content of the thesis and accompanying research data (where applicable) must not be changed in any way or sold commercially in any format or medium without the formal permission of the copyright holder/s.

When referring to this thesis and any accompanying data, full bibliographic details must be given, e.g.

Thesis: Author (Year of Submission) "Full thesis title", University of Southampton, name of the University Faculty or School or Department, PhD Thesis, pagination.

Data: Author (Year) Title. URI [dataset]

## **University of Southampton**

Faculty of Medicine

**Clinical Experimental Sciences** 

Interplay between Macrophages and Non-typeable Haemophilus influenzae Biofilms on Respiratory Epithelium

by

Jana Franziska Hueppe

ORCID ID: 0000-0003-1585-7026

Thesis for the degree of Master of Philosophy

March 2025

## **Abstract**

Non-typeable *Haemophilus influenzae* (NTHi) is an opportunistic pathogen that causes respiratory infections in patients with pre-existing conditions, for example, it is the most commonly isolated pathogen from patients with Primary Ciliary Dyskinesia (PCD), an autosomal recessive disorder that is characterised by a reduction or loss of ciliary function. One reason for the persistence of NTHi infection is the formation of biofilms on the airway epithelium. Biofilms are aggregates of bacteria encased in an extracellular matrix that reduces immune clearance and increases antibiotic tolerance. The persistent, yet unresolved nature of the NTHi biofilm leads to the development of chronic inflammation, facilitated in part by tissue resident and recruited macrophages. This project aims to develop an *ex vivo* model of NTHi biofilms on Primary Nasal Epithelial Cells (PNECs) at the air liquid interface (ALI) to investigate the impact of biofilm formation on macrophage mediated clearance. The characterisation of the inflammatory response and the resulting effect on the respiratory epithelium will increase our understanding of the immune response to NTHi biofilms.

The overarching hypothesis of this work is: Monocyte Derived Macrophages (MDMs) are more effective at clearing established Non-typeable *Haemophilus influenzae* (NTHi) biofilms on Primary Nasal Epithelial Cell Air-Liquid Interface (PNEC ALI) culture than established biofilms on an abiotic surface.

In order to address this hypothesis, the aim was to first characterise the biofilm formation of a selection of clinical NTHi isolates, both on an abiotic surface and on PNEC ALI cultures. Subsequently, the impact of primary Monocyte Derived Macrophages (MDMs) on NTHi biofilms was investigated in both of these culture systems.

The planktonic growth characteristics of six clinical isolates of NTHi from PCD patients and a GFP expressing strain were investigated using optical density readings and CFU enumeration. Biofilm formation of all seven NTHi strains was then characterised on an abiotic surface. Crystal violet (CV) staining and colony forming units (CFUs) were used as indicators of biomass and viability respectively. Confocal microscopy was used to visualise and quantify biofilm structure. Antibiotic tolerance of GFP-NTHi and PCD-NTHi 4 biofilms was demonstrated to verify biofilm formation.

Following the characterisation of NTHi biofilms on an abiotic surface, PNECs from healthy volunteers were differentiated to a pseudostratified, ciliated phenotype at ALI for 4 weeks prior to infection with GFP-NTHi and PCD-NTHi 4. A range of multiplicities of infections (MOI) were investigated in order to identify a ratio of bacteria to epithelial cells that allows the model to remain viable over 72

h. Transepithelial electrical resistance (TEER) and CFUs were used as indicators of epithelial viability and biofilm viability respectively. Confocal and scanning electron microscopy were used to visualise the co-cultures.

Primary monocyte derived macrophages (MDMs) were then added to PCD-NTHi 4 biofilms grown on an abiotic surface and on ALI cultures. The impact on biofilm size and viability was measured as before as well as the macrophage response in terms of cytokine and Lactate dehydrogenase (LDH) release.

NTHi biofilm and planktonic growth was found to be highly heterogeneous. Following the characterisation of biofilm formation on plastic, PCD-NTHi 4 was identified as a suitable clinical isolate to take forward to ALI culture alongside GFP-NTHi based on viability, biomass and structural uniformity.

Both PCD-NTHi 4 and GFP-NTHi could be recovered from co-cultures with differentiated PNEC ALI cultures after 72 h. MOI and the length of incubation before removing non-attached bacteria were optimised in order to maximise epithelial cell layer integrity and NTHi recovery. GFP-NTHi was found to be unable to form apical biofilms on ciliated ALI cultures, instead invading the cell layer. The strain was therefore deemed unsuitable for this model.

Primary MDMs could be co-cultured with established PCD-NTHi 4 biofilms on plastic. Though a significant pro-inflammatory response was detected, bacterial viability was not affected by the presence of MDMs. Establishing a triple co-culture of PCD-NTHi 4 and MDMs on PNEC ALI cultures showed that all cell types remained viable within this model.

This work suggests the inability of MDMs to reduce NTHi biofilms, both on plastic and on PNEC ALI cultures despite producing a pro-inflammatory response. Instead, an increased number of NTHi is recovered from triple co-cultures than from NTHi on ALI cultures alone. The model developed to investigate this interaction appeared to remain viable for the 96 h co-culture protocol and serves as a basis for further optimisation and development.

## **Table of Contents**

### Contents

Abst	ract	iii
Tabl	e of Co	ntentsv
Tabl	e of Ta	blesix
Tabl	e of Fig	ruresx
Rese	earch Tl	hesis: Declaration of Authorshipxxii
Ackr	nowled	gements23
Defi	nitions	of Abbreviations24
Chap	oter 1	Introduction28
1.1	Host	t Airway Structure and Immunity28
	1.1.1	Respiratory Epithelium
	1.1.2	Airway Immunity31
1.2	Resp	piratory Pathogen Non-Typeable <i>Haemophilus influenzae</i>
	1.2.1	Persistent Infections and Biofilms39
	1.2.2	Non-typeable Haemophilus influenzae Biofilms41
	1.2.3	Additional Immune Avoidance Mechanisms51
	1.2.4	Non-typeable <i>Haemophilus influenzae</i> in Primary Ciliary Dyskinesia54
1.3	Mod	delling Host-Pathogen Interactions57
	1.3.1	General Methodology57
	1.3.2	Insight into non-typeable <i>Haemophilus influenzae</i> Host-Pathogen Interaction60
1.4	Sum	mary64
1.5		othesis, Aims and Objectives64
	1.5.1	Project context
	1.5.2	Planktonic and Biofilm NTHi characterisation on an Abiotic Surface65
	1.5.3	NTHi-Epithelial Cell Co-culture66
	1.5.4	NTHi-MDM Co-Culture66
	1.5.5	NTHi-MDM-Epithelial cell Triple Co-Culture66

Chapter 2	2 Materials and Methods68
2.1 M	icrobiology Methods68
2.1.	1 Clinical Bacterial Isolates from Study Participants68
2.1.	2 Media and Plate Preparation70
2.1.	3 Planktonic Growth Conditions and Glycerol Stocks of Bacterial Isolates 70
2.1.	4 Planktonic Growth Characterisation71
2.1.	5 Inoculating NTHi Biofilms on Polystyrene72
2.1.	6 Assessing Biomass using Crystal Violet
2.1.	7 Assessing Viability using CFUs72
2.1.	8 Confocal Microscopy73
2.1.	9 Confocal Image analysis73
2.1.	10 Antibiotic Susceptibility74
2.2 Ce	ell Culture Methods75
2.2.	1 Participants75
2.2.	2 Culturing and Biobanking Nasal Brushing Samples75
2.2.	3 Culturing nasal epithelial cells for infection
2.2.	4 Co-culture preparation and Trans-epithelial Electrical Resistance77
2.2.	5 Co-culture with non-typeable <i>Haemophilus influenzae</i> at the Air Liquid Interface78
2.2.	6 Confocal imaging of NTHi-epithelial cell co-cultures79
2.2.	7 Scanning electron microscopy of NTHi-epithelial cell co-cultures80
2.3 M	acrophage Culture Methods80
2.3.	1 Monocyte Derived Macrophage culture80
2.3.	2 Macrophage-NTHi co-culture81
2.4 Su	pernatant Analysis83
2.4.	1 Enzyme-Linked Immunosorbent Assay (ELISA)83
2.4.	2 Lactate Dehydrogenase (LDH) assay86
2.5 St	atistical Analysis86
Chapter 3	3 Characterisation of Planktonic Growth and Biofilm Formation of Non-typeable
	Haemophilus influenzae Strains88

3.1	Intr	oduction	88
3.2	Aim	S	89
	3.2.1	Planktonic characterisation	89
	3.2.2	Biofilm characterisation	89
3.3	Resi	ults	91
	3.3.1	Planktonic Growth	91
	3.3.2	Biofilm Formation	96
	3.3.3	Green Fluorescent Protein Production	98
	3.3.4	Comparing Clinical Isolates	100
	3.3.5	Antibiotic Tolerance	106
3.4	Disc	ussion	111
3.5	Sum	mary and Conclusion	118
Char	oter 4	Non-typeable <i>Haemophilus influenzae</i> on Epithelial Cell Cultu	ıres at the Δir-Liquid
Cital	Jeer 4	Interface	-
4.1	Intr	oduction	
4.2		S	
4.3		ults	
	4.3.1	Co-Culturing GFP-NTHi with Primary Nasal Epithelial Cells  Clinical NTHi isolate Co-Cultured on Primary Epithelial Cells	
	4.3.2	Clinical NTHI Isolate Co-Cultured on Primary Epithelial Cells	125
4.4	Disc	ussion	130
	4.4.1	Strain comparison	130
	4.4.2	Attachment time comparison	132
4.5	Sum	mary and Conclusion	133
Chap	oter 5	Primary Macrophages and Non-typeable Haemophilus influe	enzae Biofilms on an
		Abiotic Surface	135
5.1	Intro	oduction	135
5.2	Aim	S	136

5.3.	.1 Visualising MDM-NTHi co-cultures	137
5.3.	.2 Biofilm Viability	139
5.3.	.3 Macrophage Response	141
5.4 D	Discussion	144
5.5 S	summary and Conclusion	148
Chapter	6 Non-typeable <i>Haemophilus influenzae</i> , Macrophage and Epith	nelial Cell Triple Co
	Culture	149
6.1 Ir	ntroduction	149
6.2 A	Aims	150
6.3 R	Results	150
6.3	.1 Visualising Co-Cultures	150
6.3	.2 ALI culture integrity and viability	153
6.3	.3 Cytokine response	159
6.3.	.4 Biofilm Viability	163
6.4 D	Discussion	164
6.5 S	Summary and Conclusion	169
Chapter	7 Summary and Future Work	170
7.1 S	summary of Results	170
7.2 SI	Shortcomings and Future Work	172
Appendi	ix A Bibliography	175

## **Table of Tables**

Table 1.1: TLRs involved in bacterial pathogen recognition by macrophages35
Table 1.2: Examples of increased antibiotic tolerance by NTHi biofilms compared to planktonic
cultures50
Table 2.1: Diagnostic and clinical details of patients from whom Non-typeable Haemophilus
influenzae isolates were obtained. Pathogenic of likely pathogenic genetic
mutations of PCD genes are bi-allelic unless otherwise stated. NTHi history is
quoted as reported by clinicians. NTHi – Non-Typeable Haemophilus influenzae,
PCD – Primary Ciliary Dyskinesia, TEM – Transmission Electron Microscopy. 69
Table 2.2: Summary of antibodies used for immunofluorescent staining including dilutions 79
Table 2.3 Summary of MBR and corresponding MOIs and actual number of macrophages that wer
added to plastic biofilms82
Table 2.4 Summary of ELISA detection limits, taking into account the dilution of samples86
Table 3.1 MICs of azithromycin and ceftazidime for two strains of planctonic NTHi, GFP-NTHi and
cliical isolate PCD-NTHi 4 in μg/mL (n = 3)106

# **Table of Figures**

Figure 1.1: Cros	ss section of motile cilia. 9 microtubule doublets and 2 microtubule si	nglets. Doublets
	are connected by nexin and lined with dynein motor proteins	30
Figure 1.2: Diag	gram of mucociliary clearance and epithelial defences	31
Figure 1.3 The I	biofilm lifecycle, planktonic cells attach to a surface, produce EPS and	develop into
	mature biofilms. Following dispersal, cells revert to a planktonic ph	enotype.40
Figure 1.4: Bact	terial species reported in 57 PCD studies published 1996 to 2020 sum	marised in
	Gahleitner et al <sup>219</sup> , microbiology review performed by me (JH). The	category
	"other" includes Burkholderia cepacian, Candida albicans, Serratia	mercescens,
	Alcaligenes xylosoxidans, Aspergillus niger, Enterobacter cloacae, E	scherichia coli,
	Proteus spp and Rhodococcus equi	56
Figure 1.5: Prog	gression of co-culture model development. 14. Correspond to the st	udy objectives
	listed in 1.5.1	65
Figure 2.1 Sche	matic of the inoculation protocols investigated	71
Figure 2.2 Over	view of antibiotic tolerance assay	75
Figure 2.3 Sche	matic of Peripheral Blood Mononuclear Cell (PBMC) isolation and diff	erentiation to
	Monocyte Derived Macrophages (MDMs)	80
Figure 2.4 ELISA	A standard curves	85
Figure 3.1: GFP	-NTHi planktonic growth curves comparing inoculation method. Plank	tonic growth
	was measured using optical density (OD600) readings over a 24 h p	eriod. Cultures
	were inoculated either with 200 $\mu L$ of a planktonic pre-culture grow	vn overnight
	(Orange) or a single colony selected from a chocolate agar plate pro	epared the day
	before (Blue). Overnight: n = 2 for 2-12 h, n = 1 for 13 & 24 h. Plate	: n ≥ 2 for 2-12
	h, $n \ge 4$ for 16-18 h, $n \ge 1$ for 14-15 and 20-24 h. Datapoints represe	ent separate
	biological replicates and are shown as means of a minimum of dup	icate cultures,
	lines represent a fitted non-linear model. The difference between t	he inoculation
	methods was not statistically significant (Compare Groups of Grow	th Curves
	permutation test)	92

Figure 3.2 Growth curves of clinical NTHi isolates from PCD patients comparing inoculation method. Planktonic growth was measured using optical density (OD600) readings over a 24-hour period. Two clinical strains were used, PCD-NTHi 1 (Dark Blue & Yellow) and PCD- NTHi 2 (Orange & Teal), for both cultures were inoculated either with 200 µL of a planktonic pre-culture grown overnight (Dark Blue – PCD-NTHi 1, Orange – PCD-NTHi 2) or a single colony selected from a chocolate agar plate prepared the day before (Yellow – PCD-NTHi 1, Teal – PCD-NTHi 2). Overnight: n = 2 for 2-11 h, n = 1 for 12-13 h. Plate n = 2 for 2-11 h, n = 3 for 15-18 h, n = 1 for 12-14 h and 24 h. Datapoints represent separate biological replicates and are shown as means of duplicate cultures. The difference between the inoculation methods was not statistically significant for either strain (Compare Groups of Growth Curves permutation test).

Figure 3.3: Stationary phase regression of GFP-NTHi planktonic cultures grown overnight. Planktonic cultures were inoculated using a colony form a plate and optical density and CFU counts were measured at a range of time points (14-18 h) during incubation. Time points are differentiated by colour, see figure legend for details.  $n \ge 3$  for 16-18 h, n = 1 for 14-15 h. Datapoints represent separate biological replicates and are shown as the means of duplicate cultures. The mean and standard deviation of all time points is represented by the black lines. ................................94

Figure 3.4 Stationary phase planktonic cultures of six clinical NTHi isolates characterised by optical density and CFU counts. Media was inoculated using a colony from an agar plate and incubated for up to 18 h with readings being taken between 14 – 18h. PCD-NTHi strains are shown in different colours, see figure legend for details. n = 12 for PCD-NTHi 1 & 2, n = 5 for PCD-NTHi 3-5, n = 4 for PCD-NTHi 6. Data points represent separate biological replicates and are shown as means of duplicate cultures with the exception of two points for PCD-NTHi 1 & 2 (single cultures). (A) shows the mean OD versus the CFU density for each biological replicate with error bars showing SD. Only PCD-NTHi 2 had a correlation between OD and CFU (Spearman, p < 0.05) (B) shows OD by strain, with solid lines depicting the median for each strain. The dashed line represents the global mean OD (0.611). (B) shows the mean CFU density by strain, solid lines depict the median and the dashed line shows the average across all strains (6.96x108 CFU/mL). The impact of strain on OD

and CFU was analysed using Kruskal-Wallis with Dunn's post hoc test (only	
significant comparisons shown - *p<0.05, **p<0.01)9	95

- Figure 3.8 Characterisation of NTHi biofilms after 72 h of incubation on an abiotic surface. Planktonic overnight cultures of six clinical NTHi isolates from PCD patients were cultured in sBHI. After 72 h, biofilms were washed, and either (A) biomass was quantified using CV staining or (B) bacteria were resuspended and CFUs enumerated. Data points

Figure 3.11: GFP-NTHi biofilm response to antibiotics. Azithromycin and ceftazidime were added to 72 h biofilms at 1, 10 and 100 times the planktonic MIC and incubated for 24 h. No antibiotics were added to the controls. Biofilms were then washed and either scraped and CFUs enumerated or stained with CV to assess biomass. Data points

Figure 4.3 Confocal microscopy images of GFP-NTHi co-cultured for 72 h on healthy volunteer PNECs at ALI. Bacteria were added to the epithelial cell layer at an MOI of 50 and incubated for 72 h before being washed and stained. Cilia were labelled using a RSPH4a antibody with Alexa Fluor 594 as secondary antibody (red), DAPI was used to stain nuclei (blue), while the GFP-strain is green. Examples of GFP-NTHi within the epithelial cell layer are marked by white arrows, examples of cilia by white arrowheads. A) 3D view showing NTHi within the cell layer B) representative max projection of infected non-ciliated area C) representative max projection of a ciliated area without bacteria. Bacteria were observed withing the epithelial layer, not on its surface. Bacteria only appeared in non-ciliated areas (B). Images were taken on a Leica SP8 confocal microscope. One biological repeat was performed as a preliminary investigation. Scale bars represent 20 µm. SEM was used to validate the confocal imaging and provide a better resolution of the epithelial cell surface in order to identify if any bacterial aggregates were present (section 2.2.7). Images showed extensive ciliation of the cell surface (Figure 4.4A). The SEM images confirmed no significant biofilm formation on the epithelial cell surface. Some isolated clusters were observed in the few areas of lower ciliation (Figure 4.4B-C), however it was difficult to determine if these were bacterial clusters or other debris. These data indicate that the GFP strain could not form a biofilm on ALI cultures and therefore the laboratory strain was not taken forwards for this 

Figure 4.4 SEM images of GFP-NTHi/PNEC co-cultures at ALI. Bacteria were added apically to the epithelial cell layer at MOI 50. Co-cultures were incubated for 72 h before being washed, fixed and stained. The majority of the culture was well ciliated (A) with few areas lacking cilia (B). There were no obvious biofilm aggregates identified.

Small aggregates such those shown in (B-C, white arrows) were observed, however they could not be reliably distinguished from debris. Uninfected controls showed the same level of ciliation as infected epithelial cell layers. (A) was taken at 4000x magnification, (B) at 15000x magnification (C) at 20,000x magnification. Respective scale bars shown on images. Images taken with a FEI Quanta 200 SEM ......124

Figure 4.5 SEM image of PCD-NTHi 4 NTHi co-cultured on healthy PNECs at ALI for 72 h. Planktonic bacteria were added to the epithelial cell layer at MOI 50 for 24 h before the

Figure 4.6 Integrity of PNEC layer before and after (yellow and orange respectively) 72 h of coculture with PCD-NTHi 4 at ALI represented by TEER. Ciliated cell cultures were infected with stationary phase planktonic NTHi at a range of MOIs. Bacterial suspensions were removed after (A) 24 h or (B) 1 h. TEER was measured in three positions on each Transwells, averaged per well and corrected for background readings. n > 6 separate biological replicates (each linked by grey dashed lines) except for MOI 100 at 24 h attachment (n = 4). Datapoints show means of a minimum of two duplicate wells except non-infected control treatments which only had single replicates. Solid lines depict medians, the dotted black line marks  $100 \ \Omega.cm^2$ . TEER at 0 h and 72 h was compared for each treatment using multiple Wilcoxon tests (except 24 h MOI 100), no significant difference was observed. 126

Figure 4.7 TEER change within co-cultures before and after 72 h NTHi-PNEC ALI co-culture.

Planktonic PCD-NTHi 4 cell suspension was added for 1 or 24 h before being removed (Attachment time). TEER of PNEC ALI cultures was measured before infection and following 72 h of co-culture. n > 6 separate biological replicates except for MOI 100 at 24 h attachment (n = 4). Datapoints show the calculated difference ( $\Delta\Omega$ .cm²) as a mean of duplicate wells (uninfected controls had single replicate). Solid lines represent the median. Datapoints from the same biological replicates are joined by dashed grey lines. (A) TEER change following an NTHi attachment time of 24 h. (B) TEER change following an NTHi attachment time of 1 h. (C) Shows the comparison of TEER change between the two attachment times. TEER change by MOI for each attachment time (A&B) was analysed using Kruskal-Wallis tests with Dunn's post hoc analysis comparing each MOI to the uninfected control – only significant differences are shown. TEER change by attachment time (C) was compared using multiple Mann-Whitney tests (\*p<0.05, \*\*p<0.01)127

Figure 4.8 Viable PCD-NTHi 4 cells per area recovered after 72 h co-culture on healthy volunteer

PNECs at ALI. Ciliated epithelial cell cultures were infected with a clinical strain of

NTHi at a range of MOIs and co-cultured for 72 h before being scraped, re
suspended and CFU counts performed. Attachment time (before removing the

apical media containing NTHi) was either 24 h or 1 h (A and B respectively). Data

shown as paired averages of duplicate wells, n = 6 separate biological replicates for

24 hr attachment, n = 5 for 1 hr attachment, biological replicates shown as
different shapes joined by dashed grey lines, solid lines depicting the median. Note
that shapes are not equivalent between graph (A) and (B). (C) Comparison of
bacterial attachment periods for each MOI. Data was analysed using Friedman
tests with Dunn's post hoc analysis (A & B) and multiple Mann-Whitney tests,
comparing the difference within each MOI (C) (*p<0.05, **p<0.01)129

- Figure 5.2 SEM images of MDMs on sterile glass coverslips. Macrophages differentiated from monocytes in GM-CSF for 12 days before being dissociated and cultured in low serum antibiotic free medium for 24 h. Macrophage Bacteria Ratio (MBR) refers to the corresponding ratio if the same number of macrophages had been added to an established NTHi biofilm. Intact cells were predominately round with some extending pseudopodia. Light grey bars for scale with representative lengths. (A & B) MBR 0.1 control (300k MDMs) at 500x and 5,000x magnification respectively. (C & D) MBR 0.01 control (30k MDMs) at 500x and 5,000x magnification respectively.
- Figure 5.4 Impact of media change on NTHi biofilms grown on an abiotic surface. PCD-NTHi 4
  biofilms were grown for 72 h in sBHI before the media was either changed to MDM
  media (RPMI), fresh NTHi media (sBHI) or not changed and subsequently incubated
  for a further 24 h. Biofilms were then washed and either resuspended for CFU
  enumeration or stained using CV (A) Biofilm viability as indicated by culturable CFU
  counts. (B) Biomass shown as CV OD readings. CFU: n ≥ 6, Biomass: n ≥ 4 of
  separate biological replicates (linked by dashed grey lines) with data points shown
  as means of technical duplicates where available, otherwise from single wells per

biological replicate. Solid lines indicate the median. Data were analysed using Kruskal-Wallis with Dunn's post hoc analysis test (\*p<0.05, \*\*\*p<0.001). ..140

- Figure 5.7 Supernatant LDH released by MDM-NTHi co-culture. Primary MDMs were co-cultured with established 72 h PCD-NTHi 4 biofilms for 24 h, supernatants were collected and LDH levels quantified. n = 6 separate biological replicates (shapes linked by dashed grey lines), paired datapoints show means of duplicate assay wells from same supernatant sample. Medians depicted by solid lines. Friedman test with Dunn's post-hoc analysis only comparing MDM-NTHi to each control (NTHi only and MDM only cultures), all comparisons shown (\*p<0.05, \*\*p<0.01).......143

- Figure 6.2 SEM images of MDMs and NTHi on ciliated airway epithelial cells. These cultures acted as controls for the triple co-cultures. (A-B) Bacterial aggregates are shown by white arrows (A) in-lay shows zoomed in dashed window. NTHi-ALI cultures were infected with PCD-NTHi 4 and co-cultured for 72 h to allow the formation of biofilms before washing the apical side, replacing the basal media and culturing for a further 24 h. (C-D) MDMs in clusters on ciliated epithelium. MDM-ALI cultures were not infected with NTHi and had MDMs added in antibiotic free media and the co-culture incubated for 24 h. Images are representative of n = 3 biological replicates.151
- Figure 6.4 Epithelial cell layer integrity during triple co-cultures of MDMs on NTHi infected, differentiated PNEC ALI cultures and associated control co-cultures. Ciliated PNEC ALI cultures were infected with PCD-NTHi 4 for 1 h before 72 h co-culture followed by 24 h MDM addition. X axis labelling refers to these time points, A-C will not have NTHi and MDMs added at the corresponding time points (A) Control culture had no bacteria or MDMs added. (B) MDM-ALI was not infected with NTHi but did have MDMs added. (C) NTHi-ALI was infected with NTHi but had no MDMs added. (D) Triple co-culture had both NTHi and MDMs added. TEER was measured in three positions per culture, the mean calculated and corrected for background TEER. n = 6 biological replicates (shapes joined by dashed grey lines), datapoints show the mean of duplicate wells (single technical replicate for Control cultures (A)), solid lines represent the median. Time points were compared using Friedmann Tests with Dunn's post hoc analysis, no significant differences were observed....154
- Figure 6.5 Epithelial cell layer integrity (measured through TEER) of PNEC ALI cultures from different donors during co-culture with PCD-NTHi 4 and MDMs. For Triple co-cultures, ciliated ALI cultures were infected with bacteria for 1 h, co-cultured for 72 h followed by the addition of MDMs for a further 24 h. Control cultures (black) were

- Figure 6.7 LDH released into apical supernatant by PNEC ALI cultures following co-culutres with PCD-NTHi 4, MDMs or both. Ciliated ALI culutres were infected with NTHi for 1 h, co-cultutred for 72 h followed by MDM addition for 24 h. Apical washes were collected and analysed in duplicate and adjusted for media background. n = 6 separate biological replicates (shapes), paired data shows mean OD readings of duplicates. Medians are depicted by solid lines. Data was analysed using Friedmans test with Dunn's post hoc analysis for relevant comparisons, all shown (\*p < 0.05).
- Figure 6.8 Pro-inflammatory cytokines in apical supernatants of PNEC ALI co-cultures. Ciliated PNEC cultures were infected with PCD-NTHi 4 for 1 h, co-cultured for 72 h followed by MDM addition for 24 h. Control co-cultures containing only MDM or NTHi are labelled. Co-cultures were washed apically, and the supernatants assessed for cytokines in duplicate. (A) IL-1 $\beta$  (B) IL-8 (C) IL-6. n = 6 separate biological replicates (shapes), data points are shown as means of technical duplicates, medians are depicted by solid lines. Upper limits of detection are shown by dot/dash lines, lower limits by dotted lines. Data was analysed using Friedman tests with Dunn's post hoc analysis for relevant comparisons, all shown (\*p<0.05, \*\*p<0.01)160
- Figure 6.9 Cytokines with low detection in apical supernatants of PNEC ALI co-cultures. Ciliated PNEC cultures were infected with PCD-NTHi 4 for 1 h, co-cultured for 72 h followed by MDM addition for 24 h. Control co-cultures containing only MDM or NTHi are

labelled. Co-cultures were washed apically, and the supernatants assessed for
cytokines in duplicate. (A) TNF- $\alpha$ (B) IL-10. n = 6 separate biological replicates
(shapes), data points are shown as means of technical duplicates, medians are
depicted by solid lines. Lower limits shown by dotted lines. No statistical difference
was found (Friedman tests with Dunn's post hoc analysis for relevant comparisons
all shown)161

# **Research Thesis: Declaration of Authorship**

Pr	int name:		Jana Franziska Hueppe		
Tit	tle of thesi	is:	Interplay between Macrophages and Non-typeable H Respiratory Epithelium	laemophil	us influenzae Biofilms on
L					
I de	eclare tha	at this	thesis and the work presented in it are my own	and has b	peen generated by me as
the	result of	f my o	own original research.		
l cc	onfirm tha	at:			
1.	This wo	rk wa:	s done wholly or mainly while in candidature for	a researc	h degree at this
	Universi	ity;			
2.	Where a	any pa	art of this thesis has previously been submitted fo	or a degre	ee or any other
	qualifica	ation a	at this University or any other institution, this has	s been cle	early stated;
3.	Where I	l have	consulted the published work of others, this is a	lways cle	arly attributed;
4.	Where I	l have	quoted from the work of others, the source is al	ways give	en. With the exception of
	such qu	otatio	ons, this thesis is entirely my own work;		
5.	I have acknowledged all main sources of help;				
6.	Where t	the th	esis is based on work done by myself jointly with	others, I	have made clear exactly
	what wa	as dor	ne by others and what I have contributed myself;		
7.	Parts of	this v	vork have been published as:		
Fig	ure 1.4 is	syste	ematic review work I (JH) conducted towards:		
Gal	Gahleitner, F. et al. Lower airway clinical outcome measures for use in primary ciliary dyskinesia				
res	research: A scoping review. ERJ Open Res. 7, (2021).				
<u></u>				Data	
SI	gnature:			Date:	

## **Acknowledgements**

I would like to thank my main supervisory team Prof. Dr Jane Lucas, Dr Claire Jackson and Dr Karl Staples. I am so grateful for your guidance, support and patience. Thank you for helping me see this project through to the end.

I'd like to thank my former supervisor Dr Ray Allan, whose lecture on biofilms inspired me to pursue this project and who has supported me throughout my rotation projects and for the first part of this project. I'd also like to thank my former supervisor Dr David Cleary for microbiological guidance.

I'm grateful to the numerous members of the PCD research group and the Pulmonary Immunology group who have helped me with this interdisciplinary project. Thank you for sharing your knowledge, resources and feeding my cells when I could not. Thank you to Janice Coles and Gemma Fryatt for teaching and supporting all my cell culture work, for helping me troubleshoot and for supplying me with all the plastic and cells I could ask for. Many thanks to Dr Jodie Ackland for introducing me to immunology work, taking the time to help me plan and execute techniques new to me and for your general support and chats. I also need to thank Dr Katie Horton for the support both in the lab and in the office, thank you for all your help.

Thank you to everyone at the BIU, especially to Regan Doherty and James Thompson, for helping me with the enchanting work of visualising my experiments. Thank you to the microbiology group at Building 85 for housing me at the start of this project and thank you to the CRF, especially Gavin Babbage, for sharing your space and resources with me.

Naturally, I must extend my deepest gratitude to all the cell donors that made this work possible as well as the AAIR charity and NIHR for generously funding this work.

I would like to extend my deep appreciation to the Student Wellbeing team, my senor tutor, Lucy Dorey, and the NHS for taking care of me when I was struggling with my physical and mental health.

I'd like to thank everyone at Boulder Shack, for welcoming me to the team and being the muchneeded balance to my academic work. To the friends I have made through there who have kept me sane throughout these years, be it climbing, picnics, D&D or Warhammer. You've made this a place worth staying.

And of course, and without a doubt, my deepest gratitude goes to Dr Nic Dinsdale whom I have tested emotionally, musically and financially over this time. Your patience, love and support for my antics and troubles are immeasurable. I promise I'll go find a job now.

## **Definitions of Abbreviations**

Al-2 Autoinducer-2

AMR AntiMicrobial Resistance

BHI Brain Heart Infusion

CBA Chocolate Blood Agar

CD Cluster of Differentiation

CEACAM-1 Carcinoembryonic Antigen-related Cell Adhesion Molecule 1

CF Cystic Fibrosis

CFU Colony Forming Unit

COPD Chronic Obstructive Pulmonary Disease

CV Crystal Violet

DNA Deoxyribonucleic Acid

ECM Extracellular Matrix

eDNA extracellular DNA

EDTA EthyleneDiamineTetraacetic Acid

ELISA Enzyme-Linked ImmunoSorbent Assay

EPS Extracellular Polymeric Substance

GCP-2 Granulocyte Chemotactic Protein 2

GFP Green Fluorescent Protein

GM-CSF Granulocyte-Macrophage Colony-Stimulating Factor

HAP Haemophilus Adhesion Protein

HBSS Hank's Balanced Salt Solution

HIA Haemophilus influenzae adhesion

HiB Haemophilus influenzae type b

HMW Heavy Molecular Weight

HSVM High-Speed Video Microscopy

IL Interleukin

LDH Lactate dehydrogenase

LOS Lipooligosaccharide

LSP Lipopolysaccharide

MDM Monocyte Derived Macrophage

MCP-1 Monocyte Chemotactic Peptide 1

MIC Minimum Inhibitory Concentration

MIP-1β Macrophage Inflammatory Protein 1β

MLST Multilocus Sequence Typing

MOI Multiplicity Of Infection

MRSA Methicillin Resistant Staphylococcus Aureus

MSSA Methicillin Sensitive Staphylococcus Aureus

NAD Nicotinamide Adenine Dinucleotide

NLR NOD-like Receptor

nNO nasal Nitric Oxide

NO Nitric Oxide

NOD Nucleotide binding Oligomerization Domain

NTHi Non-Typeable Haemophilus influenzae

OD Optical Density

ODA Outer Dynein Arms

OMP Outer Membrane Protein

PAF Platelet Activating Factor

PAMP Pathogen-Associated Molecular Pattern

PBMC Peripheral Blood Mononuclear Cell

PBS Phosphate-Buffered Saline

PCD Primary Ciliary Dyskinesia

PCho Phosphorylcholine

PD Protein D

PE Protein E

PF Protein F

PHE Public Health England

PNEC Primary Nasal Epithelial Cell

PRR Pattern Recognition Receptor

ROS Reactive Oxygen Species

RPMI Roswell Park Memorial Institute (media)

sBHI supplemented Brain Heart Infusion

SEM Scanning Electron Microscopy

TAA Trimeric Auto Transporter

TC Tissue Culture

TEER TransEpithelial Electrical Resistance

TEM Transmission Electron Microscopy

Tfp Type IV pili

TLR Toll-Like Receptor

TNF Tumour Necrosis Factor

VBNC Viable But Non-Culturable

## **Chapter 1** Introduction

The aim of this project is to develop a co-culture model to investigate the host-pathogen interaction of airway biofilm infections. This introduction will provide a summary of the airway epithelium and immune response followed by a discussion of the bacterial pathogen *Haemophilus influenzae*. Finally, an overview of models currently used to study the host-pathogen interaction will place this project into context within the work being undertaken in the wider research community. This chapter concludes with a breakdown of hypotheses, aims and objectives for the subsequent chapters.

### 1.1 Host Airway Structure and Immunity

The human airway is part of our respiratory system and can broadly be divided into the lower and the upper airway. The upper airway consists of the nasal cavity, the pharynx and the larynx. The lower airway is made up of the trachea, bronchi, bronchioles and finally alveoli that facilitate the exchange of oxygen and carbon dioxide between the air and our blood stream. This system is exposed to thousands of litres of air every day<sup>1</sup>, and with it a variety of organic and inorganic matter from dust and pollutants to bacterial and viral pathogens. In order to mitigate the harmful impact of these inhaled challenges, the airway is able to utilise a variety of physical and chemical defence mechanisms. Dysregulation of these mechanisms often facilitates chronic infections and the associated inflammatory response. The following section discusses the role that epithelial cells and macrophages play in this host defence mechanism.

#### 1.1.1 Respiratory Epithelium

#### 1.1.1.1 Respiratory Epithelial Cells

The airways are lined with pseudostratified epithelium made up of four cell types: ciliated cells, goblet cells, basal stem cells and club cells. Ciliated cells make up 50-70% of epithelial cells and produce a motile force through ciliary beating that move particles and pathogens trapped in the mucus. Goblet cells make up approximately 25% of the epithelium and are responsible for producing and secreting mucus<sup>2</sup>. Basal stem cells are attached to the basement membrane and regenerate the epithelial cell layer. Club cells secrete anti-inflammatory and immune-modulating proteins into the mucus and increase in number further down the respiratory tract as goblet cells decrease. The

basement membrane is an extracellular matrix made up of collagen that anchors the epithelial layer to the connective tissue underneath and acts as a barrier preventing pathogens and malignant cells from penetrating into the deeper tissue.

The epithelium consists of a single layer of cells; however, the cell nuclei are not found on the same plane, giving the appearance of multiple cell layers, hence the term pseudostratified. The cells are polarised, meaning that there are specific apical and basolateral surfaces, embedded with specific surface protein including receptors and ion channels.

Intercellular junctions maintain the physical integrity and adhesion between adjacent cells. There are three overarching categories of intercellular junctions: anchoring junctions which keep cells attached to the extracellular matrix and each other, communicating junctions which allow diffusion of signals between cells and tight junctions which prohibit the flow of water, molecules, and ions between the apical and basolateral side of the cell layer through the paracellular space. The passage of these substances can therefore be tightly regulated through the epithelial cells themselves, enabling the maintenance of gradients across the cell layer. Tight junctions also prevent surface protein moving between the apical and the basolateral sides and are therefore important for the preservation of cellular polarisation<sup>3</sup>.

The integrity of the epithelial layer can be diminished in disease states such as chronic rhinosinusitis, in which decreased expression of tight junction proteins such as zonula occludens-1 and occludin have been observed<sup>4</sup>. Furthermore, tight junctions prevent pathogens from penetrating the epithelium. In response, many pathogens have evolved strategies of disrupting tight junctions <sup>5</sup> such as bacterial proteases which can cleave tight junction proteins<sup>6</sup>.

Trans-epithelial electrical resistance (TEER) is commonly used as an *in vitro* measurement of tight junction integrity by measuring the ionic permeability of the cell layer<sup>7</sup>. TEER can be affected by pathologies, infections, and exogenous substances. For example, azithromycin exposure has been demonstrated to increase tight junction protein expression and thus TEER<sup>8</sup>. *Haemophilus influenzae* endotoxin has also been shown to increase TEER while increasing inflammatory mediator production<sup>9</sup>.

#### 1.1.1.2 Motile Airway Cilia and Mucociliary Clearance

Motile cilia are hair-like structures that line the apical side of the epithelium in respiratory passages as well as the Eustachian and fallopian tubes. Ciliated cells have approximately 200 cilia each, with

the percentage of ciliated cells decreasing further down the airway. Healthy cilia beat at a frequency of 11 to 20 Hertz (Hz). The co-ordinated beating moves mucus, pathogens and debris out of the airway<sup>10</sup>.

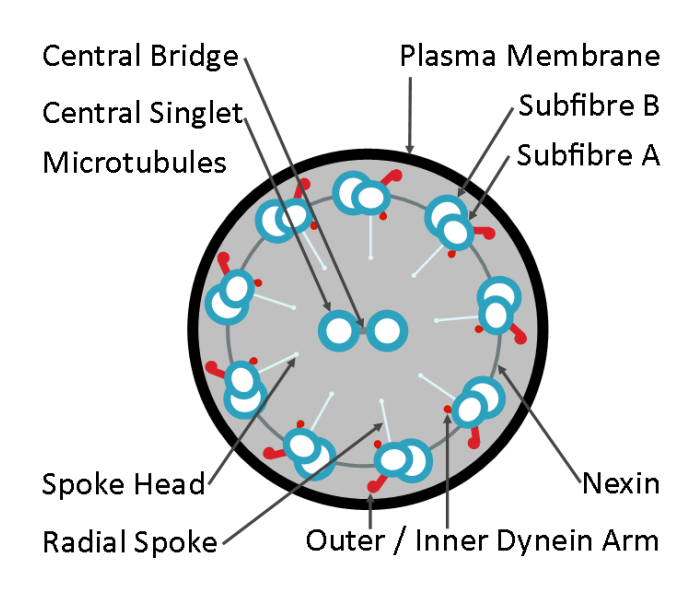


Figure 1.1: Cross section of motile cilia. 9 microtubule doublets and 2 microtubule singlets. Doublets are connected by nexin and lined with dynein motor proteins.

Cilia consist of a cytoskeleton made from microtubules called the axoneme, surrounded by a plasma membrane. The axoneme of motile cilia contains two central microtubule singlets and nine outer doublets (Figure 1.1), hence the term "9 + 2" structure<sup>11</sup>.

At the base of the cilia, basal bodies act as microtubule organising centres by providing an anchoring and nucleation site for the axoneme microtubules. The ciliary stroke is also directed from the basal body<sup>12</sup>.

When functioning normally, cilia beat in a co-ordinated manner. Within each cilium, the motor protein dynein, moves along the adjacent doublet. The nexin joining doublets together forces this movement into an overall bending motion. The resulting motion moves mucus, debris and pathogens up and out of the airway to be removed via coughing or swallowing. This mucociliary clearance is part of the first line of defence against lung infections as it prevents pathogens from settling on the airway epithelium. Coughing and sneezing are reflexes used to clear mucus and the associated pathogens and debris out of the lung and sinonasal cavity repectively<sup>13</sup>.

The airway surface liquid contains two layers: the periciliary fluid surrounding the cilia and the mucus layer sitting on top of the cilia. Mucus contains mainly water and mucins secreted by goblet

cells. Additionally, mucus contains antimicrobial peptides<sup>14</sup>, increasing the defensive function of the mucus layer. The mucus layer acts as a barrier against harmful substances while also maintaining the moisture of the cell surface. The periciliary fluid layer that surrounds the cilia is less viscous than mucus, allowing cilia to beat rapidly. The interciliary space contains macromolecules that prevent mucus from moving down between the cilia, which would obstructing ciliary beating<sup>15</sup>.

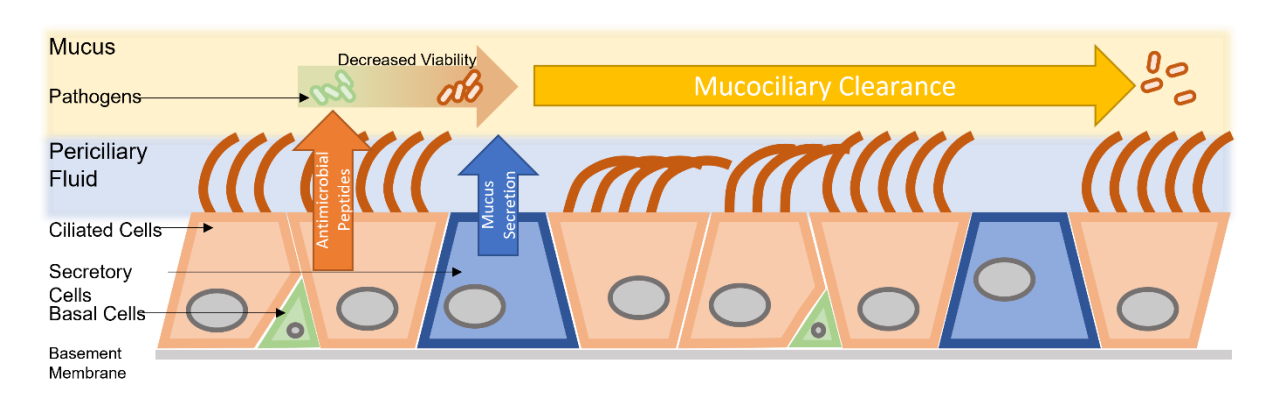


Figure 1.2: Diagram of mucociliary clearance and epithelial defences

#### 1.1.2 Airway Immunity

The air we breathe is filled with potentially dangerous environmental factors including pollutants, pathogens and general debris. The alveoli at the end of our airway are very thin in order to facilitate efficient gas exchange to the blood vessels. They are therefore fragile and need protection from inhaled, potentially harmful factors. Nasal hairs act as a first physical barrier, filtering out larger particles. The mucous membrane lining the airway is the second physical barrier potential pathogens encounter. As discussed above, tight junctions formed by the epithelial cells of the respiratory mucosa prevent pathogens from penetrating deeper into the tissue and mucus traps foreign particles expels them through the mucociliary clearance mechanism. Besides physical protection, the airway also has chemical protection in the form of antimicrobial peptides and microbiological protection in the form of commensal bacteria. These non-pathogenic bacteria help maintain a healthy environment<sup>13</sup>. The loss or dysregulation of the microbiome is often associated with disease states, either as a contributing factor or as an effect of the disease or infection<sup>13</sup>.

An immune response is needed if pathogens are able to persist through these barriers. The immune system is comprised of an innate response and an adaptive response. The innate response is a non-specific response that does not require prior exposure to the pathogen<sup>16</sup>, it is instead aimed at broadly conserved pathogenic patterns. It is initiated first and plays a role in programming the

adaptive response. The adaptive response takes longer to initiate after the initial exposure to a pathogen, but it retains a "memory" that enables a specific response to be mounted faster if the same pathogen is encountered at a later date<sup>17</sup>.

Key components of the innate response in the airway are leukocytes and the epithelial cells that line the airway. The innate response develops in five stages: 1) Recognition of infection or damage, 2) the recruitment of molecules and cells to the site of the infection, 3) elimination of the pathogen, 4) resolution of inflammation, tissue repair and return to homeostasis and 5) induction of the adaptive immune response. These stages may happen concurrently and there are many factors, both from the host and from the microbe that may lead any stage to fail, leading to persistent and chronic infections.

### 1.1.2.1 Epithelial Cell Immune Response

As the airway is lined with epithelial cells, they are usually the first point of contact for pathogens and foreign particles that make it past the nasal filters. Beyond acting as a physical barrier, the epithelium produces a range of antimicrobial compounds to fight off pathogens. The release of cytokines attracts and activates a range of immune cells, effectively "raising the alarm" and coordinating a multi-faceted response. Cytokine responses include the release of IL-1 $\alpha$ , IL-1 $\beta$ , IL-8, TNF- $\alpha$ , IL-6, IL-10, granulocyte-macrophage colony stimulating factor (GM-CSF), granulocyte chemotactic protein 2 (GCP-2) and the chemokines macrophage inflammatory protein 1 $\beta$  (MIP-1 $\beta$ ) and monocyte chemotactic peptide 1 (MCP-1)<sup>18,19</sup>.

Mucus produced by the respiratory epithelium, besides acting as a physical barrier to pathogens, contains several antimicrobial molecules including lysozyme, lactoferrin and peroxide<sup>17</sup>. These factors are produced by a range of airway cells and contribute to an innate defence system. Lysozyme is an enzyme that compromises the bacterial cell wall of gram-positive bacteria leading to cell lysis. Gram negative bacteria have a second membrane preventing lysozyme access to the cell wall. Lactoferrin binds iron, reducing the availability for bacteria. Lactoferrin has also been found to affect the outer membrane of gram negative bacteria, facilitating lysozyme activity against the cell wall<sup>20</sup>. Peroxides released by neutrophils produce radical oxygen species (ROS) whose functions include bacteriostatic and bactericidal properties<sup>21</sup>.

Additional antimicrobial peptides released by the airway epithelium include the cathelicidin LL-37 which is both an antimicrobial and neutralises the bacterial endotoxin lipopolysaccharide (LPS)<sup>22</sup> as

well as acting as a chemokine for immune cells and reducing the permeability and bacterial invasion of the epithelial cell layer<sup>23</sup>.  $\beta$ -defensins are another peptide that displays both antibacterial and immunomodulatory properties<sup>24,25</sup>.

#### 1.1.2.2 Monocytes and Macrophages

Monocytes are a type of leukocyte that act as both regulators and effectors in the innate immune system and as well as influencing the development of adaptive immunity. They develop from hematopoietic stem cells<sup>26</sup> in the bone marrow and make up 10% of circulating leukocytes in peripheral blood. Monocytes that become resident in tissues differentiate into macrophages. It was previously believed that tissue macrophages were derived from the reservoir of circulating blood monocytes, until it was found that the populations of resident tissue macrophages, for example alveolar macrophages, were predominantly maintained by local differentiation in the absence of infection or inflammation<sup>27</sup>. Resident macrophages are embryonically derived and originate in the yolk sac during foetal development<sup>28</sup>. Circulating monocytes can then be rapidly recruited to sites of inflammation to supplement local populations, providing an easily mobilised reservoir whose versatility comes from the ease at which it can reach sites of damage or infection through the circulatory system<sup>29</sup>. Migration occurs along a gradient of signalling proteins released by cells called chemotactic cytokines, or chemokines. The secretion of chemokines by resident cells at the site of infection recruits phagocytes in order to mount a defence against the pathogen. These, in turn, release further chemokines, leading to a positive feedback loop of immune cell recruitment.

Monocytes form a heterogeneous cell population<sup>29</sup>. Based on the identification of differential expression of antigenic markers CD14 and CD16, monocytes were categorised into two major subsets<sup>30</sup>: the "classical" CD14++CD16-, making up 90% of blood monocytes, and the "non-classical" CD14+CD16++. An additional "intermediate" CD14++CD16+ subset was found to make up a small sub-population in humans. Non-classical monocytes are generally considered to have a protective, anti-inflammatory role<sup>31</sup>. Changes in relative subset populations have been associated with the progression of inflammatory diseases<sup>32</sup>.

In the past, the activation of macrophages has been categorised into two groups: M1 or "classically activated" and M2 or "alternatively activated". The understanding was that M1 macrophages performed pro-inflammatory functions such as secreting pro-inflammatory cytokines, phagocytosis of pathogens as well as producing reactive oxygen species and nitrogen radicals in order to kill pathogens. M1 activation is stimulated by IFN-γ and toll-like receptor agonists such as LPS<sup>33</sup>. M2

activation is triggered by signals like IL-4 and IL-13 and leads to macrophages supressing inflammatory signals<sup>34,35</sup> and releasing anti-inflammatory signals like IL-10<sup>36</sup>. M2 macrophages are involved in the resolution of inflammation and the repair of damaged tissue. The discovery of several M2 sub-types complicated the clear categorisation due to overlapping triggers and functions. Our understanding has advanced to show that macrophage phenotype is found on a spectrum between M1 and M2 and that activation depends intricately on the environment of the macrophage<sup>33,37,38</sup>.

The 3 major functions of monocytes are: (1) the presentation of antigens to adaptive immune cells such as T and B cells, (2) immunomodulation through the release of cytokines and (3) phagocytosis<sup>39</sup>. This third function includes the phagocytosis of waste and debris, a part of both healthy tissue renewal and the response to tissue injury and damage, and the phagocytosis of invading pathogens in response to infection.

Both monocytes and macrophages express a wide range of surface proteins which are important for phagocytic activity and innate immune recognition. The recognition of pathogen-associated molecular patterns (PAMPs) by pattern recognition receptors (PRRs) enables a rapid response to bacterial pathogens, leading to immune cell activation and downstream responses. Bacterial PAMP structures are highly conserved and vital to cellular function and therefore cannot be "evolved away" in order to avoid immune detection. PRR classes include Toll-like receptors (TLRs), Nucleotide-binding oligomerisation domain (NOD)-like receptors (NLRs), Retinoic acid-inducible gene (RIG)-I-like receptors (RLRs), AIM2-like receptors (ALRs) and C-type lectin receptors (CLRs)<sup>40</sup>.

The best characterised class of receptors for innate pathogen recognition are TLRs<sup>41</sup> which recognise a wide range of pathogens and their products (Table 1.1). TLR4, for example, recognises LPS from bacterial outer membranes when it forms a complex with CD14 and MD2. The formation of this complex acts as an additional step beyond LPS binding to TLR4 to avoid erroneous activation of the macrophage. TLR signalling converges on NF-κB, leading to the production of pro-inflammatory cytokines<sup>42</sup>.

Table 1.1: TLRs involved in bacterial pathogen recognition by macrophages.

Toll-like receptor (TLR) type	Recognition target	Receptor location
TLR1/TLR2 heterodimer	Bacterial lipoprotein <sup>43</sup>	Cell surface
TLR2/TLR6 heterodimer	<ul> <li>Bacterial peptidoglycans</li> <li>Bacterial lipoprotein<sup>43</sup></li> <li>Lipoteichoic acid <sup>44</sup>(Gram +ve bacterial cell well component)</li> </ul>	Cell surface
TLR4/TLR4 homodimer	<ul> <li>Lipopolysaccharide (Gram -ve bacterial outer membrane component)</li> <li>heat shock protein and fibrinogen from host<sup>40</sup></li> </ul>	Cell surface
TLR5	Bacterial flagellin <sup>40</sup>	Cell surface
TLR9	Bacterial DNA <sup>45</sup>	Cell compartment

Macrophages secrete pro-inflammatory cytokines including IL-1 $\beta$ , CXCL8, TNF $\alpha$ , IL-6 and IL-12. These cytokines activate and recruit other immune cells as well as increasing vascular permeability and adhesin expression on the blood vessel endothelium to allow cells like monocytes to enter the tissue from the blood stream.

Chemokines involved in the recruitment and activation of macrophages include CXCL8, N-formylmethionine-leucyl-phenylalanine (fMLP), leukotriene B4 (LTB4) and complement component 5a (C5a). Macrophages can also activate nitric oxide synthase, enabling cytostatic and cytotoxic activity against pathogens<sup>46</sup>. Additionally, macrophages secrete lysozyme, an antimicrobial protein able to hydrolyse bacterial cell wall components<sup>47</sup>.

Beyond the inflammatory response, macrophages also play a role in the resolution of inflammation and the return to homeostasis. When expressing an anti-inflammatory phenotype, macrophages release IL-10 and IL-1R antagonists<sup>48</sup>. Phagocytosis of apoptotic cells (efferocytosis) and clearance of cellular debris also aids the restoration of damaged tissue.

#### 1.1.2.3 Interaction between Epithelial Cells and Macrophages

The foundation of an effective immune response is the interaction between cell types in response to a pathogen. Macrophages are often removed from their context when being studied, either through blood samples or BAL samples. Cell to cell contact between macrophages and an epithelial monolayer has been shown to affect the phenotype of the macrophages<sup>49</sup>, demonstrating the need for more complex experimental models. For example, when co-cultured, epithelial cell derived signals shifted macrophages to a less phagocytic, more cytotoxic immunophenotype in response to ozone, a pollutant that exacerbates pre-existing airway diseases. CD14 expression was increased in co-culture<sup>50</sup>. Atmospheric particles also elicited a significantly higher pro-inflammatory cytokine response by macrophages in co-culture compared to mono-culture.<sup>51</sup> The expression of mRNA for GM-CSF, a macrophage stimulating cytokine, was more rapidly induced in co-culture exposed to air pollution<sup>52</sup>. This suggests that the contact between the cell types enables a quicker amplifying response to infection through the recruitment and activation of circulating monocytes *in vivo*.

The interaction between epithelial cells and macrophages also plays a role in the resolution and recovery from inflammation as non-inflammatory macrophages promote the proliferation of airway epithelial cells, contributing to the recovery of tissue injury<sup>53</sup>.

The communication between epithelial cells and macrophages includes a range of methods. One is the cytokine signals used by all immune cells. TNF- $\alpha$  is released by macrophages, the corresponding receptor, TNFR1 is constitutively expressed on the alveolar epithelium<sup>54</sup>. Alveolar macrophages release microparticles, cell membrane vesicles containing cytoplasmic molecules, that are taken up by epithelial cells. For example, alveolar inflammation may be inhibited by the uptake of anti-inflammatory proteins SOCS1 and 3 by the epithelial cells<sup>55</sup>. Microparticles are shed by eukaryotic cells and are also involved in pro-inflammatory signals between epithelial cells and macrophages<sup>56</sup>.

Signals may also be passed between cells through direct contact. Pathogen-induced Ca<sup>2+</sup> may travel between epithelial cells and macrophages through gap junction channels (GJCs), allowing messages to be passed between cells<sup>57</sup>. For example, TLR2 on the airway epithelium may be activated by opportunistic pathogens leading to a Ca2+ influx that is the passed along to non-stimulated cells in order to increase the pro-inflammatory response<sup>58</sup>. This includes CXCL8 production and the upregulation of proteases that break down intracellular junction protein, thereby allowing an influx of immune cells through the epithelial layer<sup>59</sup>. Increases in cytosolic Ca<sup>2+</sup> also leads to increased TNF-

 $\alpha$  and ROS production by mitochondria. However,  $Ca^{2+}$  communication has also been shown to have an anti-inflammatory effect in alveolar macrophages<sup>60</sup>.

The complexity of the interactions between macrophages and epithelial cells, both during homeostasis and during infection, underpins the need for multi-cell models. Cells studied in isolation may fail to accurately represent the *in vivo* situation.

# 1.2 Respiratory Pathogen Non-Typeable Haemophilus influenzae

In 1892, a gram-negative coccobacillus was incorrectly identified as the causative agent of influenza by Pfeiffer<sup>61</sup>. Despite the later discovery of viral causation<sup>62</sup>, the bacterium was named *Haemophilus influenzae* in 1920<sup>63</sup>. Since its discovery, *H. influenzae* has been found to exist as both capsulated and non-capsulated strains. The strains expressing the polysaccharide capsules are subdivided into type a to f based on the capsule composition. Non-capsulated strains are considered non-typeable *H. influenzae* (NTHi). These can be classified through biotyping, antigenicity of surface structures, enzyme electrophoretic typing, restriction fragment length polymorphism and random amplification of chromosomal DNA by PCR<sup>64</sup> as well as Multilocus Sequence Typing (MLST).

Encapsulated *H. influenzae* strains are relatively homologous across types, while NTHi strains are genetically and phenotypically diverse<sup>65</sup>. However, there is a genetic pattern associated with serum killing resistance and epithelial cell adhesion that is largely preserved across strains<sup>66</sup>.

NTHi can grow both aerobically and as a facultative anaerobe, the requirement for hemin (factor X) nicotinamide adenine di-nucleotide (NAD, factor V), differentiating it from other *Haemophilus* species. It is a human-restricted opportunistic pathogen that asymptomatically colonises the upper respiratory tract as a harmless commensal. As such, it grows optimally between 34 and 37°C. Generally, standard laboratory strains have a doubling time of approximately 30 min, reaching up to  $10^{10}$  cell/mL in planktonic culture using nutrient rich media. Cells will start dying continuously once maximum capacity is reached. Viable cells can be found within colonies for approximately a week on solid agar when stored at room temperature or at 4 °C<sup>67</sup>.

NTHi can become pathogenic if it reaches privileged anatomical sites due to predisposing conditions such as age, viral infections<sup>68</sup>, reduced immune function or reduced mucociliary clearance. This can lead to otitis media, sinusitis, bronchitis, pneumonia, conjunctivitis and, less commonly, septicaemia and meningitis<sup>69,70</sup>.

About 20% of children are colonised by commensal NTHi strains within a year of birth, over 50% after 5 years<sup>71</sup>, rising to at least 75% amongst healthy adults. Colonising strains vary over time, with new strain acquisition being linked to exacerbations in airway diseases such as COPD<sup>72</sup>. Concurrent colonisation by multiple strains has also been observed<sup>73,74</sup>.

The introduction of a vaccine in 1992<sup>75</sup> against *H. influenzae* type b (Hib), a cause of meningitis and responsible for 90% of *Haemophilus* invasive disease worldwide at the time, has led to an increase in invasive *Haemophilus* disease caused by NTHi, filling the niche left by HiB. NTHi is, however, considered to be primarily a mucosal pathogen, infecting the respiratory tract<sup>76</sup>. It is spread through airborne droplets. The lack of capsule prevents the HiB vaccine from being effective against NTHi, furthermore, the heterogeneity of NTHi makes the development of a new vaccines challenging.

Virulence factors are mechanisms through which bacteria are able to act in a pathogen. These include molecular structures, signalling systems or secreted molecules that aid pathogenic activities such as colonisation, immune evasion, cellular invasion and nutrients acquisition. Virulence factors may cause damage to the host directly, e.g. toxins, or indirectly, e.g. adhesins that enable attachment to the host cells. An individual strain is unlikely to possess the whole array of virulence factors, instead only expressing a subset of them. It has been proposed that the virulence factors available to the NTHi strain affect the niche it is best suited for, thus influencing where a strain might become pathogenic<sup>77</sup>.

The distributed genome hypothesis states that populations of pathogenic bacteria have access to a "supragenome", which is much larger than the genome of any single bacterial cell. All strains within a polyclonal infection possess a core genome, in addition to which, each strain contains a unique distribution of non-core genes<sup>78</sup>. Death of bacterial cells releases genetic material back into the supragenome, making it available to be picked up by new strains. This mechanism relies on the autocompetence and autotransformation abilities of the pathogen. NTHi is naturally competent, meaning they can take up extra chromosomal DNA or plasmids from the environment. The resulting genetic diversity enables populations to rapidly adapt to environmental challenges experienced in the host, supporting persistence. The heterogeneity of NTHi populations means that if one epitope is successfully targeted by the immune system or a vaccine, strain replacement may lead to an alternative strain, without said epitope, filling the niche.

#### 1.2.1 Persistent Infections and Biofilms

The host-pathogen interaction can be considered an arms race between pathogens and both the host defence systems, and the medical interventions developed to combat infections. While acute infections can often be treated in this day and age, persistent infections are now a major battleground in this fight.

Estimated to play a role in approximately 80% of bacterial pathogenesis<sup>79</sup>, biofilms are aggregates of bacteria forming an organised, three-dimensional structure within an extracellular matrix. This matrix is produced by the bacteria and consists of extracellular polymeric substances (EPS), including polysaccharides, lipids, proteins and DNA. Host components can also be incorporated into the matrix. The complex architecture is highly heterogeneous and has been observed to form water channels throughout the biofilm which allow transport of nutrients and oxygen to the cells within <sup>80</sup>. It is possible for multiple species of bacteria to co-exist within a biofilm, both competitively and co-operatively.

The EPS layer shields bacteria from harmful factors, including the host immune response and antibiotics, allowing the bacteria to persist on the host surface. The close contact between bacterial cells also allows for the sharing of nutrients and exchange of DNA, including antibiotic resistance genes, via horizontal gene transfer. This gene transfer gives bacteria an advantage if they do disperse from the biofilm and is a major contributor to the development of antimicrobial resistance (AMR)<sup>81</sup>.

When part of a biofilm, bacterial cells have been demonstrated to form physiologically distinct sub-populations. Cells within biofilms generally have reduced metabolic activity and grow slower than their planktonic counterparts<sup>80</sup>. This further reduces the effectiveness of antimicrobials targeting translation, transcription, and cell wall synthesis associated with cellular replication.

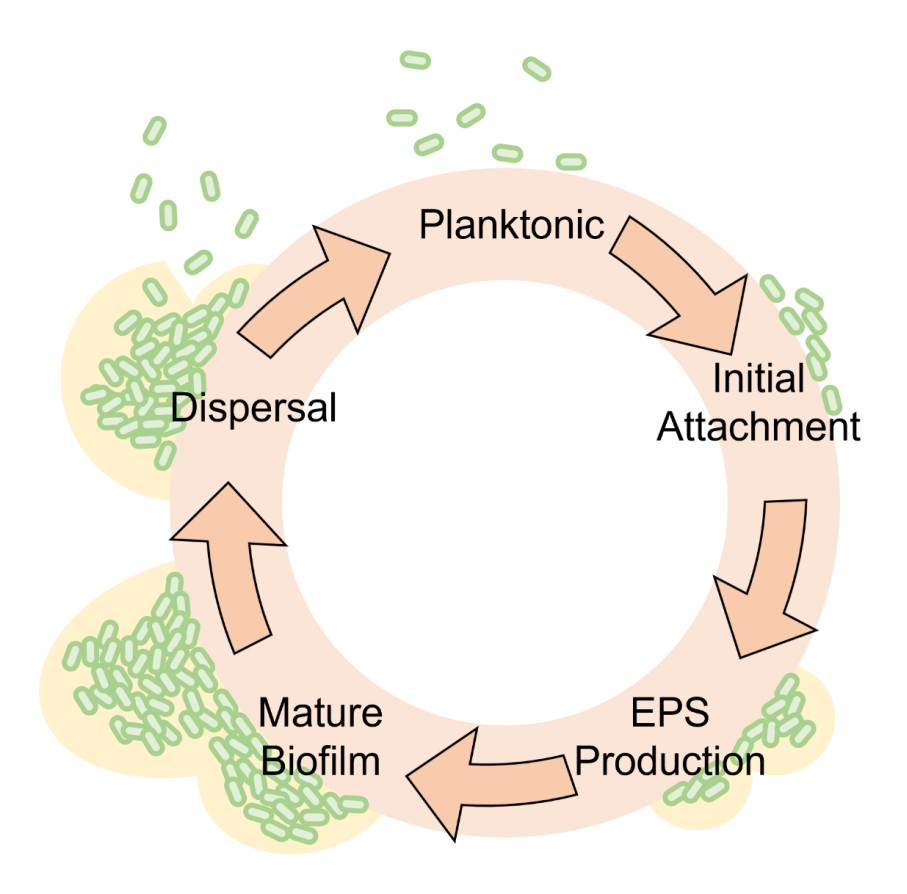


Figure 1.3 The biofilm lifecycle, planktonic cells attach to a surface, produce EPS and develop into mature biofilms. Following dispersal, cells revert to a planktonic phenotype.

The biofilm lifecycle consists of 5 stages: reversible attachment, irreversible attachment, initial growth, maturation, and dispersal.

Within the context of airway infections, biofilm formation requires the attachment of planktonic cells to the host mucosa. The first interactions are through transient van der Waals forces, followed by an irreversible attachment through cell adhesion structures such as pili or fimbria<sup>80</sup>. Non-functional or damaged cilial make this easier for the bacteria as a lack of mucociliary clearance allows bacteria access to the epithelial cell surface.

Once attached, the bacteria begin to divide and produce EPS to generate the biofilm matrix. As the biofilm matures and the EPS matrix grows, both physical and chemical microenvironments develop leading to sub-population formation within the 3D structures of the biofilm. Jurcisek & Bakaletz have considered a biofilm immature after 4-5 days of growth, with a mature biofilm being reached after 21 days<sup>82</sup> in the context of their work. Biofilms grown on abiotic surfaces have been observed to initially form "towers" with water channels after approximately 12 h, these structures became less pronounced by 24 h as the biofilm grew thicker<sup>83</sup>.

Biofilms can disperse by producing enzymes that degrade the EPS in response to environmental stimuli, for example nitric oxide (NO)<sup>84</sup>. As cells revert back to a planktonic lifestyle, the removal of a biofilm can lead to a flood of pathogenic bacteria being released into the surrounding area<sup>80</sup>. Targeting dispersal mechanisms as a treatment strategy can therefore capitalise on the increased antibiotic sensitivity of planktonic cells by combining the induction of biofilm dispersal with adjuvant antibiotic treatment.

# 1.2.2 Non-typeable Haemophilus influenzae Biofilms

One of the earliest evidence of NTHi biofilms was presented by Murphy and Kirkham which immediately established the heterogeneity of biofilm formation between clinically isolated strains of NTHi, even within the infection of origin (OM and COPD)<sup>85</sup>. NTHi biofilms contain aggregates of live and dead bacteria as well as host cell components on the mucosal surface. Furthermore, biofilms can be either associated or dissociated from the host cells<sup>86</sup>. Mokrzan et al proposed that NTHi biofilm formation is a response to the challenges of nasopharyngeal niche such as mechanical stress from breathing and moving surface liquid, ciliary beating, nutrient scarcity and changes in the composition of the surrounding substances<sup>83</sup>.

#### 1.2.2.1 Adhesins

Adhesion is one of the vital first steps of colonisation. NTHi has a variety of adhesins, including trimeric auto transporters (TAAs) and outer membrane proteins (OMPs). Adhesins interact with host cells, mucus and the extracellular matrix, which is especially exposed following damage to the epithelial cell layer lining the airway through infections or inflammation. Not all adhesins are expressed ubiquitously throughout NTHi strains, meaning there is no one size fits all immune or potential vaccine response that would be universally effective.

Trimeric autotransporters (TAAs) are translocated through the inner bacterial membrane to the periplasm where the c-terminal domain forms a pore in the outer membrane through which the adhesion domain reaches the cell surface, remaining anchored to the c-terminal<sup>87</sup>. NTHi can produce several adhesins with a TAA structure: heavy molecular weight proteins 1 and 2 (HMW1/HMW2), *H. influenzae* adhesion (HIA) and Haemophilus adhesion protein (HAP). TAA expression is heterogenous among NTHi strains: 45%-80% express HMW while 8.3%-33% express HIA. 3.1%-8.3% have been found to express both, while a small number containing neither have been found<sup>88</sup>. Generally,

strains expressing one will not express the other and up to 95% of NTHi strains express one of the two adhesin types<sup>88–90</sup>. HAP is found in all NTHi strains<sup>91</sup>

HMW proteins bind host glycans<sup>92</sup> and play a role in the interaction of NTHi with macrophages<sup>93</sup> and epithelial cells<sup>94</sup>. NTHi strains lacking HWM1 and/or HWM2 have been found to show a decreased adherence capacity<sup>94,95</sup>.

HAP is a serine protease which binds to epithelial cells<sup>96</sup> and components of the extracellular matrix such as collagen IV, fibronectin and laminin<sup>97,98</sup>. It is able to undergo autoproteolysis to be released into the extracellular environment<sup>99</sup> where it may disrupt the epithelial cell layer and enable bacterial penetration into the tissue through degradation of host protein. Secreted HAP may also aid immune evasion by interacting with mucosal IgA, reducing the number of antibodies free to interact with surface bound HAP and opsonise NTHi cells. The protease activity of HAP may also directly degrade immune components such as complement and immunoglobulins<sup>99</sup>. HAP plays a role in bacterial aggregation through HAP-HAP interactions<sup>100</sup>, though does not appear to be vital<sup>101</sup>. Autoproteolysis of HAP from the bacterial cell is inhibited by the hosts secretory leucocyte protease inhibitor (SLPI), which is found in the upper respiratory tract<sup>102</sup>. In a strange turn of events this means the host is facilitating the continued adhesion of NTHi cells to the epithelium, the ECM and one another<sup>99</sup>. If NTHi cells and therefore HAP reaches a critical point to outweigh the inhibitive action of SLPI, bacterial cells are dispersed as the adhesin is cleaved<sup>89,99</sup>.

HIA is a lectin that binds to sialylated glycans on host cell surfaces, preferentially Neu5AC, the only sialic acid form expressed by humans<sup>103</sup>. The binding affinity appears to mirror that of HWM1 and 2 combined<sup>103</sup>, meaning that host targets are available to NTHi strains regardless of which adhesin is expressed. HIA appears to remain uncleaved and thus attached to the bacterial cell surface<sup>104</sup>. High levels of HIA expression have been linked to nasopharygeal colonisation<sup>105</sup>.

The roles of HMW and HAP protein in biofilm formation remain relatively unexplored. The expression of both within biofilms has been confirmed, both in the ECM and on the bacterial surface<sup>106</sup>. In one investigation, Hia expressing NTHi strains produced more biofilm than HMW expressing strains<sup>107</sup>.

Non-TAA bacterial surface protein expressed by NTHi include Outer Membrane Proteins (OMPs) 1, 2,4, 5 and 6 as well as Protein D (PD), Protein E (PE) and Protein F (PF). OMP 1, 2, 5 and 6 have been found in biofilms, however presence does not guarantee requirement.

OMP P1 binds to carcinoembryonic antigen-related cell adhesion molecule 1 (CEACAM-1) on the epithelium, facilitating host cell invasion<sup>108</sup>. This interaction is human specific and not observed for homologs in other mammals<sup>108</sup>.

OMP P5 is expressed by all NTHi strains. It appears to bind and upregulate Intercellular Adhesin Molecule 1 (ICAM-1) expressed by leukocytes, endothelial and respiratory epithelial cells<sup>101,109,110</sup>. There have, however, been contrary findings suggesting that while NTHi does interact with N-glycosylated molecules such as ICAM-1, this interaction may not be mediated through OMP P5<sup>101</sup>. Neutrophil recruitment is facilitated by ICAM-1, so an increased expression may lead to an increased presence of immune cells at an infection site. The binding of NTHi to ICAM-1 may help obscure these receptors, decreasing their leukocyte recruiting capacity. OMP P5 appears not to be required for biofilm growth under *in vitro* flow conditions, but does seem to play a major role in the host-pathogen interaction with respiratory epithelial cells and macrophages as well as persistence *in vivo*<sup>101</sup>. Anti-P5 antibodies have been found to reduce, but not eliminate biofilm formation *in vitro*<sup>83</sup>

OMP P2 is a pore forming protein, or porin, that enables passive diffusion of hydrophilic molecules through the bacterial membrane<sup>111</sup>. Playing a role in nutrients uptake, the pores cover approximately half the cell membrane and can vary in diameter through sequence variation, affecting the susceptibility of the bacterial strain to broad spectrum antibiotics<sup>112</sup>. Single base changes have been found to lead to antigenic drift, possibly providing a method of immune evasion as selective pressure is put on strains by OMP P2 recognition by the host immune response<sup>113</sup>. OMP P2 in NTHi has been found to vary to a much higher degree than OMP P2 in Hib<sup>114</sup>. OMPs P2 and P5 bind nasopharyngeal mucins<sup>115</sup>, reducing mucin mediated clearance.

OMP P4, ubiquitous within NTHi strains<sup>89</sup>, binds to ECM components fibronectin, laminin and vitronectin<sup>116</sup>. The OMP P4/vitronectin interaction provides serum resistance<sup>116</sup>. The adhesion to pharyngeal, alveolar and bronchial epithelial cells through P4 appears to be mainly through fibronectin interaction<sup>116</sup>.

OMP P6 has been found to predominantly protrude from the outer membrane into the periplasmic space rather than be orientated outwards toward the extracellular space<sup>117</sup>. Within the periplasm, P6 plays a role in cellular integrity by anchoring the outer membrane to the cell wall<sup>118</sup>. OMP P6 is responsible for triggering a pro-inflammatory cytokine response from host macrophages<sup>119</sup>. P6 has been found in all NTHi strains to date, although there is variation between strains<sup>120</sup>. Through binding to its own gene, P6 appears to self-regulate expression, reducing excess production when

high levels of P6 are present in the cytoplasm<sup>121</sup>. OMP P6 is often used as a marker for NTHi abundance<sup>86</sup> or as a validation tool<sup>122</sup>, speaking for its reliable abundance across all NTHi strains.

Outer membrane proteins 1,2 and 5 have been identified specifically in the extracellular matrix of NTHi biofilms and not the corresponding planktonic culture, both after 24 and 96 hours of biofilm growth <sup>123</sup>. OMP P2, P5 and P6 has been found to be expressed by NTHi colonies growing on agar plates<sup>85</sup>. OMP P6 has been found on the membrane of viable bacteria within biofilms<sup>106</sup>. The secretion of P2 and P5 by NTHi biofilms may make them useful biomarkers for diagnostic detection<sup>124</sup>.

Protein E is involved with adhesion to epithelial cells and, like OMP P5, upregulates ICAM-1 expression<sup>110,125</sup>. It also interacts with ECM component vitronectin and the inactive precursor to plasmin, plasminogen. Plasminogen converts to plasmin while bound to PE, where its action as a serine protease degrades the ECM, enabling invasion<sup>126</sup>. Protein E has been found in over 96% of NTHi strains<sup>89</sup>.

Protein F, like Protein E, also binds vitronectin which in turn binds and inactivates components of the complement system in the vicinity of the bacterial cells, thereby contributing to complement evasion by NTHi<sup>127</sup>. Protein E appears to have a higher affinity to vitronectin than Protein F and double knockout mutant experiments suggest a shared binding site<sup>127</sup>. There is therefore a certain redundancy between Protein E and F.

Protein F has been found to be ubiquitous across NTHi strains<sup>128</sup>. Like many adhesins, Protein F facilitates binding to a range of targets, including epithelial cells, the surrounding extracellular matrix, and the basement membrane. The latter two occur via the binding of laminin<sup>128</sup>, a major protein component of the extracellular matrix and a target with high levels of redundancy across NTHi adhesins. The work of Su et al presents a detailed examination of the "laminin interactome", identifying several novel binding protein and comparing them to previously discussed adhesins<sup>129</sup>. The plethora of laminin binding proteins suggests it to be a vital step for bacterial colonisation.

A further laminin binding lipoprotein adhesin is Protein D<sup>129</sup> which has been found to facilitate adherence to and entry into monocytes<sup>130</sup> as well as impair ciliary function within 12 hours of co-culturing NTHi with ciliated epithelial cells, reducing beat frequency faster and to a greater extent than protein D deficient strains<sup>131</sup>. Infection with protein D expressing strains lead to a greater loss of cilia compared with protein D deficient strains, although Janson et al hypothesise that the observed effect is due to a chain of events involving host inflammatory mediators rather than the

direct interaction of protein D with host cilia<sup>131</sup>. Protein D expression does not appear to be vital for NTHi survival within the host, instead acting predominantly as a virulence factor. Outer membrane protein D (PD) is highly conserved across NTHi strains and is therefore a potential vaccine target <sup>132</sup>.

Type IV pili (Tfp) are involved in twitching motility, adhesion and biofilm formation <sup>82,85,133</sup>. They mediate adhesion to epithelial cells through ICAM-1 interaction <sup>134</sup>. The major component of the pilus is encoded by *pilA* <sup>135,136</sup>. PilA expression remains relatively low during the initial planktonic growth phase, increasing once the stationary growth phase is reached <sup>137</sup>. The increased expression of Tfp, and the associated increase in adhesion and twitching motility, is likely to provide commensal NTHi more versatility when responding to the changing environment, enabling long term colonisation <sup>83</sup>.

PilA expression has been found to be increased within biofilms growing in a nasopharyngeal microenvironment compared to biofilms growing in a middle ear environment as determined by epithelial cell type and temperature, 34°C and 37°C respectively<sup>83</sup>. In the former, pilA expression was observed to be distributed throughout the biofilm rather than concentrated near the substratum as observed in the latter<sup>83</sup>. PilA expression appears to play a role in the development of tower structures<sup>83</sup> within biofilms by enabling twitching motility<sup>135</sup>.

Co-culture with epithelial cells led to increased pilA expression compared with abiotic surfaces, likely influenced by soluble factors released by the epithelial cells<sup>137</sup>. A PilA mutant has been observed to form worse biofilms on epithelial cell layers than the wild type<sup>138</sup>. Pili are able to bind to respiratory mucins<sup>139</sup> along with *H. influenzae* fimbriae (HIF), another NTHi surface protrusion. Fimbriated (*hif* positive) strains are more commonly isolated from asymptomatic carriers than from pathogenic states such as otitis media suggesting a role in reduced pathogenesis/commensal behaviour<sup>89</sup>. Non-fimbriated strains have shown impaired colonisation ability in a knockout study<sup>140</sup>, however, the redundancy amongst adhesins means that it is difficult to draw conclusions when looking at a single factor<sup>131</sup>.

# 1.2.2.2 Lipooligosaccharide

NTHi produces lipooligosaccharide (LOS), a form of lipopolysaccharide (LPS) lacking the terminal variable sugar (O antigen). LOS, like LPS, contains core polysaccharides and lipid A. Lipid A anchors the LOS to the bacterial membrane, where it plays a critical role in membrane integrity. LOS acts as an endotoxin, which means that it is a component of the bacterial cell wall which only acts as a toxin

when it is released through cell lysis, as opposed to being actively secreted by viable bacterial cells. Endotoxins trigger a range of host immune responses, causing inflammation and subsequently damaging the host tissue. Secondary modifications of LOS results in significant heterogeneity between strains<sup>141</sup>.

LOS has been found associated with the EPS of NTHi biofilms, possibly providing stability<sup>106</sup>. NTHi can incorporate host sialic (N-acetyl-neuraminic) acid into its LOS, masking it from host complement recognition<sup>142</sup>. The importance of LOS containing sialic acid for biofilm formation was first demonstrated by Sword et al in 2004 under *in vitro* static and flow conditions as well as a gerbil *in vivo* model<sup>143</sup>. LOS sialyation was subsequently found to promote biofilm formation<sup>144</sup> as well as being essential for biofilm formation in chinchilla ears<sup>145</sup>. Even sialylated non-biofilm forming mutants have been observed to have an increased *in vivo* survival compared to those that contain no sialic acid at all<sup>145</sup>. Sialylation can be reduced through reduced transport (transporter mutants)<sup>146</sup> or reduced incorporation (sialyltransferase mutants).

Phosphorylcholine (PCho or ChoP across the literature) is a well-studied component of LOS that interacts with platelet-activating factor (PAF) receptor, leading to adhesion and cell invasion<sup>147</sup>. Expression of the PAF receptor is increased during chronic airway inflammation, likely leading to a feedback loop of colonisation and inflammation. The role of PCho in NTHi biofilms was first reported in 2006 by West-Barnette et al, noting that the incorporation of PCho into LOS was increased in biofilms compared to planktonic cultures<sup>148</sup>. NTHi relies on phosphatidylcholine (PC) from the host as the source of choline in PCho. One potential mechanism of PCho incorporation is a multi-functional outer membrane lipoprotein: Protein D/glycerophosphodiester phosphodiesterase (PD/GlpQ)<sup>149</sup>.

PCho incorporation by NTHi triggers a weaker immune response from macrophages as measured by TNF- $\alpha$ , IL- $\beta$  and nitric oxide<sup>148</sup>. Mutants unable to incorporate PCho have shown increased initial inflammation within chinchilla middle ear models, as well as a slower increase in bacterial growth<sup>150</sup> and increased clearance<sup>151</sup>. PCho expression correlates with thicker, denser biofilms, both *in vivo*<sup>150</sup> and in under flow conditions<sup>152</sup>. However, clinical isolates under *in vitro* static growth conditions appear not to show this relationship. The viability of established biofilms appears not be affected whether in wild type, PCho knock out mutants or constitutively expressing PCho<sup>152</sup>.

Co-infection of PCho mutants and wild type NTHi lead to both strains being recoverable at ratios similar to the innoculum<sup>150</sup>, suggesting that the immune dampening effect of a subpopulation of NTHi is able to aid the survival of all strains present.

Wild type clinical NTHi isolates are found to have a higher PCho content following *in vivo* biofilm infection compared to planktonic cultures<sup>150,151</sup>. Additionally, a higher PCho content appears to be detrimental for planktonic persitence<sup>152</sup>.

Sialyation and PCho incorporation of NTHi LOS varies spatially and temporally throughout the biofilm life cycle. Sialic acid containing LOS are more prevalent during early infection, decreasing as the infection progresses<sup>153</sup>. PCho appears to be associated with biofilm maturation<sup>152</sup>. Sialylated NTHi is found relatively equally distributed throughout the biofilm while PCho expressing cells appear to cluster within the biofilm<sup>148</sup>.

#### 1.2.2.3 Quorum sensing:

Quorum sensing allows bacteria to co-ordinate behaviour based on the number of bacterial cells present. The autoinducer 2 (AI-2) quorum signal pathway appears to modulate biofilm forming ability of NTHi. The AI-2 component LuxS appears to have an impact on lipooligosaccharide (LOS) composition, with mutants being found to be more virulent<sup>154</sup> and less able to form biofilms<sup>155</sup>. Similar observations were made for RbsB mutants, a protein involved in the uptake of quorum sensing signals<sup>156</sup>. LuxS expression peaks as the biofilm matures, and decreases prior to biofilm dispersal<sup>157</sup>. Expression of LuxS also increases when NTHi invades epithelial cells, however, the invasive capability of LuxS mutants has been found to vary between strains and epithelial cell type<sup>154</sup>. The two-component signalling system QseB/C has been found to play a role in biofilm formation<sup>158</sup>, possibly acting as a receptor for AI-2. The AI-2 signal is derived from a bacterial metabolic by-product, dihydroxypentanedione (DPD), which is conserved across many bacterial species, enabling inter-species communication<sup>159</sup>. The role of quorum sensing in NTHi has only been investigated in a small number of strains, so there may be variation between strains, as with many other aspects of NTHi pathology.

# 1.2.2.4 Extracellular Polymeric Matrix and Biofilm Dispersal

One defining feature of bacterial growth in biofilms compared to planktonic cells is the production of an extracellular polymeric substances (EPS) within which the cells are embedded. The EPS can comprise up to 90% of a biofilms dry mass. The EPS acts as a barrier, keeping nutrients and enzymes within the biofilms and preventing access of harmful substances such as immune cells and antibiotics<sup>160</sup> to the bacteria. EPS include proteins, polysaccharides and extracellular DNA (eDNA)<sup>160</sup>.

Extracellular DNA (eDNA) released by bacteria provides some structure and adds to the overall thickness of biofilms<sup>161</sup>. Both eDNA and the DNA-binding protein are actively released by bacteria through the same machinery associated with the type IV pilus<sup>162</sup>. Additionally, eDNA from both host and bacterial cells can be released through lysis and autolysis<sup>163</sup>.

A family of DNA binding protein, DNABII, stabilise the extracellular matrix by inter-connecting extracellular DNA strands, providing stability to the biofilm structure<sup>163</sup>. Integration host factor (IHF) and the histone like protein HU are DNABII protein found to be critical to biofilm structure<sup>164</sup>. Anti-IHF antibodies cause "catastrophic structural collapse" of NTHi biofilm<sup>165</sup>. To date, DNABII protein are ubiquitous across pathogenic bacterial species<sup>166</sup>, and therefore present a species-independent target for anti-biofilm strategies. A synergistic effect was seen between anti-IHF-antibodies and antibiotics when it came to reducing biofilm biomass, when antibiotics alone caused an increase<sup>167</sup>. This effect may be due to antibiotics gaining access to planktonic cells that are released as the extracellular matrix brakes down<sup>168</sup>, increasing the efficacy and reducing the overall number of viable cells available.

Dispersal triggered by anti-PilA antibodies appears to be linked to LuxS expression, a component of the AI-2 quorum sensing system. The transition of biofilm cells back to planktonic cells appears to take place in a more "gradual top-down" manner when triggered by anti-PilA than that caused by anti-IHF<sup>169</sup>.

#### 1.2.2.5 Antibiotic Resistance

The development of antibiotic tolerance and resistance by bacteria has led to an arms race between nature and medicine. Antibiotics can be grouped based on their mechanism of action: inhibition of cell wall, protein or nucleic acid synthesis, as well as cell membrane depolarisation and metabolic inhibition<sup>170</sup>. Bacterial susceptibility to a given antibiotic is measured as the minimum inhibitory concentration (MIC), i.e. the lowest concentration that prevents bacterial growth.

Resistance genes can be intrinsic, induced or acquired. Intrinsic genes are inherently expressed by a whole species while induced genes may only be expressed following antibiotic exposure. Both intrinsic and induced genes are naturally present in bacteria<sup>170</sup>. Acquired resistance genes are not naturally present in a given bacterial species. Random mutations in bacterial sub-populations may confer an advantage in surviving antibiotic exposure, meaning that this sub-population remains viable and able to reproduce into the space left behind by sub-populations not able to resist the

antibiotic effect. This leads to the overall population shifting towards being more tolerant to the drug in question. Resistant strains may spread from host to host but may also pass on advantageous genes through horizontal gene transfer, increasing resistance in pre-existing populations.

Antibiotic tolerance refers to a decreased response by bacteria following repeated exposure to an antibiotic while resistance refers to the ability to resist the effect completely. Furthermore, persistent bacteria that are not susceptible to antibiotics due to their current, metabolically dormant state, but carry no resistance genes, may become susceptible through changes in metabolic state<sup>170</sup>.

Antibiotic tolerance and resistance functions by: limiting drug uptake, modifying the site targeted by the drug, inactivating the drug and the active removal of a drug from the targeted organism (efflux)<sup>170</sup>.

Biofilms are often observed to have a much higher antibiotic tolerance than planktonic cells of the same species (Table 1.2). The EPS formed by biofilms blocks access to bacterial cells, meaning bacteria are exposed to lower, sub-inhibitory, concentrations of antibiotics. Higher concentrations are therefore needed to achieve the same exposure once the antibiotics have penetrated the biofilm. Bacterial cells in biofilms are also more likely to be sessile, meaning a slower rate of division and metabolism. This removes a common target for antibiotics. The close proximity of bacteria within biofilms also promotes horizontal gene transfer of resistance genes.

Beta-lactamases are enzymes that break open the ring structure characteristic to beta-lactams, a widely used class of antibiotics, thereby inactivating them. There's beta-lactamase-negative ampicillin susceptible and ampicillin resistant (BLNAS and BLNAR) NTHi strains, as determined by a mutation in Pencilin Binding Protein 3 (PBP3). The response to antibiotics varies between biofilms formed by these two groups<sup>171</sup>. NTHi biofilms grown in flow chambers have been observed to vary in antibiotic susceptibility compared to biofilms grown in microtiter assays<sup>171</sup>. Low level exposure to some antibiotics appears to cause an increase in biomass<sup>171</sup>. Fluoroquinolones have been shown to penetrate the exopolysaccharides of the biofilm matrix<sup>171</sup>

The thickness and biomass of *in vitro* biofilms formed over 24 h by strains isolated from otitis media patients does not appear to affect antibiotic susceptibility<sup>172</sup>. These biofilms tolerated over 1000x the concentration of amoxicillin while remaining viable. The failure to eradicate biofilms by clinically relevant antibiotic doses is a critical factor in the persistence of bacterial infection and the spread of antibiotic tolerance.

Table 1.2: Examples of increased antibiotic tolerance by NTHi biofilms compared to planktonic cultures.

Antibiotic (type)	Minimum inhibitory concentration (planktonic growth) (μg/mL)	Minimum biofilm eradication concentration (μg/mL)		
Amoxicillin (Beta-lactam / penicillin)	0.5 - 2 <sup>172</sup>	>1000¹72		
Ceftriaxone (Beta-lactam / cephalosporin)	0.004 - 0.032 <sup>172</sup>	>500 <sup>172</sup>		
Clarithromycin (macrolide)	2 <sup>172</sup> - 8 <sup>171</sup>	64 - >256 <sup>172</sup>		
Azithromycin (macrolide)	0.25 - 2 <sup>172</sup>	4 - >256 <sup>172</sup> 0.6 <sup>171</sup>		
Gatifloxacin (fluoroquinolone)	<0.06 <sup>171</sup>			

In a clinical context, mucosal infections can be treated with oral antibiotics. Otitis media, one of the main diseases caused by NTHi, is treated in the first instance with amoxicillin. Additionally, in cases of beta-lactamase positive NTHi, which account for approximately 25-50% of strains<sup>173,174</sup>, beta-lactamase inhibitors such as clavulanate are used in conjunction. Other antibiotics against beta-lactamase producing bacteria include trimethoprim-sulfamethoxazole, cefuroxime axetil, cefixime, clarithromycin, azithromycin, and fluoroquinolones. Erythromycin, sulfisoxazole or cefaclor may be used in cases of penicillin-allergic patients.

#### 1.2.3 Additional Immune Avoidance Mechanisms

#### 1.2.3.1 Intracellular invasion & survival

Besides biofilms, NTHi is able to avoid detection and immune responses by the host in several ways. Intracellular invasion and persistence of NTHi have been observed since the 1990s<sup>175–177</sup>. The reoccurrence of NTHi infections despite antibiotic therapy, antibodies targeting NTHi and periods of clinically negative culture results, suggested that bacterial cells can remain undetected within host epithelial cells<sup>178</sup>. While inside epithelial cells, NTHi is protected from antibiotic exposure and host antibodies<sup>177</sup>, while being able to re-emerge onto the mucosal surface<sup>176</sup>.

NTHi have been found to survive within airway epithelial cells inside acidic vacuoles. Here the bacteria were observed to be metabolically active but non-proliferative<sup>68</sup>. The ability of internalised NTHi to avoid lysosomal degradation appears to be linked to whether nutrient deprivation acted as a trigger for intracellular invasion through macropinocytosis<sup>179</sup>. Differential gene expression suggests a phenotypic adaptation following intracellularisation<sup>180</sup>. NTHi is also able to invade and survive within macrophages, with the level of invasion and survival varying between strains<sup>130,180–183</sup>. Non-virulent strains, however, did not display the same ability to survive intracellularly<sup>181</sup>.

Invasion involves cytoskeletal rearrangement by the host cell, for example, non-opsonised NTHi can enter monocytes and epithelial cells via receptor mediated endocytosis using the  $\beta$ -glucan receptor. The extent of this varies between NTHi strains, but is generally more able to do so than Hib<sup>184</sup>. NTHi invade type 2 alveolar cells. The increase in intracellular cells early in an infection appears to be mainly due to invasion rather than intracellular replication. NTHi mainly resides in acidic, endocytic vacuoles. As infection progresses, NTHi escapes into cytosol leading to apoptosis of the alveolar cell<sup>185</sup>.

Although a range of adhesins has been found to play a role in cellular invasion (eg: Hap, PCho, Protein E and Protein D), no specific "invasins", dedicated purely to invasion, have been identified 178.

PCho incorporated on LOS can interact with platelet activated factor receptor (PAFR), mediating cellular invasion via PAFR-linked pinocytotic vacuole formation PAFR expression is elevated in chronically inflamed airways 147, potentially providing NTHi with increased opportunity for intracellular persistence. The  $\beta$ -glucan receptor on host cells also appears to mediate non-opsonic receptor dependent endocytosis, both in monocytes and epithelial cells 184.

NTHi has been observed between and underneath respiratory cells both *in vitro* and *in vivo*<sup>178</sup>. There is evidence of paracytosis, passing between cell with intact intercellular integrity<sup>186</sup>. Transcytosis, passing through cells, has also been shown to provide a mechanisms through which NTHi reaches the submucosal layer<sup>187</sup>.

# 1.2.3.2 Antigenic variation

Phase variation is a reversible process that allows bacteria to generate phenotypic diversity. For example, insertions and deletions in "hypermutable" areas of DNA lead to frameshifts. These frameshifts can lead to truncation of the protein, effectively "turning off" the expression. If the opposite mutation occurs at a later point, the gene is frameshifted back into a functional sequence, reverting the gene to the "ON" state. Phase variation allows expression to be turned on and off in a stochastic manner, enabling rapid adaptation to the surrounding environment<sup>188</sup>.

The level of expression of the adhesins HMW and HIA can be altered through phase variation<sup>105,189,190</sup>. This may provide an advantage during long term colonisation as bacterial populations are established, but antibodies are raised against the exposed adhesins<sup>191</sup>.

LOS structure depends on a range of genes that are controlled by phase variation. A screen of almost 7000 transposon mutants by Nakamura et~al. revealed the importance of LOS in avoiding complement mediated killing<sup>192</sup>. PCho incorporation depends on the expression of PCho kinase encoded by the *licA* gene which is controlled through phase variation, meaning PCho incorporation can be turned on and off<sup>193</sup>. PCho plays a role in the interaction of NTHi with the host immune response: on the one hand, PCho appears to decrease the effectiveness of antimicrobial peptide LL- $37^{194}$ . On the other hand, PCho acts as a target for C-reactive protein (CRP) which mediates complement killing via classical pathway activation<sup>195</sup>. NTHi strains isolated from the oropharynx have been found to incorporate PCho more often than strains isolated from blood<sup>196</sup>. Exposure to complement is likely to limit survival of PCho positive strains in the blood, however PCho reduces the release of the pro-inflammatory cytokine IL- $1\beta$  by epithelial cells, aiding colonisation by supressing inflammation<sup>197</sup>. The viability of PCho incorporation is therefore highly niche dependent and rapid adaptation to new environments aids NTHi survival. PCho also reduces LOS endotoxin potency<sup>148</sup>.

The incorporation of a further LOS component, sialic acid, is also under phase variable control. NTHi is not able to synthesise sialic acid and therefore acquires it from the surroundings through a

tripartite ATP-independent periplasmic (TRAP) transporter<sup>142,146</sup>. Incorporation into LOS is mediated by sialyltransferases Lic3A, Lic3B, SiaA or LsgB<sup>198</sup>. Di-sialylation appears to have a stronger protective effect from human serum than non or mono-sialylation<sup>199</sup>.

# 1.2.3.3 Epigenetic regulation

Epigenetic regulation of gene expression involves inheritable yet reversible modifications to DNA without changing the genetic sequence itself. It is a relatively new area of interest within NTHi. The DNA methyltransferase *modA* has been found to be under the control of phase variation<sup>200</sup>. Distinct *modA* alleles (*modA1 – modA22*) have been identified based on the variable DNA recognition domain that determines the DNA sequences to be methylated. NTHi isolates from paediatric otitis media patients and isolates from COPD patients showed distinct differences in *modA* allele profile, suggesting a role in environmental adaptation<sup>200,201</sup>. *ModA2* has been found to affect biofilm formation, otitis media severity and resistance to oxidative stress. NTHi strains with *modA2* in the ON status are less resistant to oxidative stress and neutrophil mediated killing<sup>202</sup> and form thicker but less structured biofilms under alkali conditions which mimic the otitis media environment<sup>203</sup>. Furthermore, *modA2* ON causes more severe otitis media in chinchillas, specifically if the strain was able to shift from OFF to ON<sup>204</sup>. Increased adherence and invasion of airway cells was observed in *modA10* knockout strains, but lower levels of bacteraemia were observed by the knockout strain than by the wild-type *modA10* strain in a rat model<sup>187</sup>.

#### 1.2.3.4 Antibody protease

NTHi encodes IgA1 proteases which cleave and therefore inactivate host IgA antibodies. IgA1 is a human antibody, so the activity of IgA1 proteases and their impact on infection is difficult to investigate in animal models. Human lactoferrin, found in saliva and mucus amongst other fluids, is able to cleave IgA1 proteases as well as the homologous adhesin HAP, suggesting a reduced impact in healthy individuals<sup>205</sup>. Nearly all NTHi strains have the *iga* gene, encoding type I IgA1 protease, though this does not guarantee expression. A subset of NTHi has been found to contain an alternative IgA1 protease gene, *igaB*, coding for a type II IgA1 protease. Strains with *igaB* were more commonly isolated from infections than from commensal carriage<sup>206</sup>. Type II IgA1 protease does not appear to be required for adhesion or cellular invasion but does allow better intracellular persistence. IgA plays a role in complement activation, so bacterial proteases are also likely to reduce complement killing<sup>207</sup>.

#### 1.2.3.5 Outer Membrane Vesicles

Outer membrane vesicles (OMVs) are small lipid vesicles that have diverse functions including transfer of DNA between cells, release of virulence factors and stress response mediation. OMVs are found to be produced by all gram-negative bacteria to date and can bind to human respiratory epithelial cells, leading to internalisation and subsequent immune modulation<sup>208</sup>. OMVs are enriched with outer membrane components including LOS and adhesins and have been investigated as an immunisation strategy<sup>209</sup>.

#### 1.2.4 Non-typeable *Haemophilus influenzae* in Primary Ciliary Dyskinesia

# 1.2.4.1 Impaired Respiratory Epithelial Function in Primary Ciliary Dyskinesia

Primary ciliary dyskinesia (PCD) is an autosomal, recessive genetic disorder. Variations in genes lead to impaired ciliary structure and function. The loss of co-ordinated ciliary beating reduces the natural mucociliary clearance in the airways. This leads to a chronic wet cough, rhinosinusitis and otitis media in the patients<sup>210</sup>. Furthermore, it facilitates persistent and recurring infections<sup>211</sup> and thus chronic inflammation. The continuous inflammatory response damages the airways and leads to bronchiectasis, an abnormal widening of the airways, leading to more infections and exacerbating the problem.

PCD is a rare disease with an estimated incidence between 1 in  $2,000^{212}$  and 1 in  $40,000^{213}$ . This variation in incidence is influenced by variation across demographics, however, Behan *et al* have also suggested that it "reflects differences in access to diagnostic facilities"<sup>213</sup>. The average incidence in Europe is around 1 in  $10,000^{214}$ .

Both the genotype and the phenotype of PCD are highly heterogeneous. To date, over 50 genes have been identified to play a role in PCD<sup>215,216</sup>. About 70% of PCD cases possess mutations in the identified genes<sup>216</sup>. The complex structure of motile cilia, consisting of more than 250 protein<sup>217</sup>, is linked to the genetic heterogeneity. The majority of genes associated with PCD are linked to the dynein component of the ciliary ultrasturcture<sup>216</sup>, though cytoplasmic proteins involved in ciliary assembly have also been linked to ciliopathy<sup>218</sup>.

# 1.2.4.2 Bacterial infections in Primary Ciliary Dyskinesia

In PCD, the reduced mucociliary clearance leads to increased infections as well as more persistent infections. Microbiology is often reported alongside demographic information and diagnostic characteristics. Infection status is not always linked to the study findings or its impact on the stated outcomes.

As part of a scoping review on PCD clinical outcome measures Gahleitner et al analysed 102 studies, 57 of which reported microbiological findings<sup>219</sup>. A summary of the bacterial species reported are shown in Figure 1.4.

There is no uniform panel of bacterial species that is reported across studies. Most commonly, *Haemophilus influenzae* and *Pseudomonas aeruginosa* infection status is reported, followed by *Staphylococcus aureus*. In some studies, a distinction is made between mucoid and non-mucoid strains of *P. aeruginosa*. However, when "mucoid *P. aeruginosa*" is mentioned alongside simply "P. aeruginosa" it is unclear if the latter includes the former. In some studies, *S. aureus* is reported as methicillin sensitive and resistant (MSSA and MRSA respectively). In one case, the stated category of "others" included both *S. aureus* and *Streptococcus pneumoniae*, the 3rd and 4th most commonly isolated pathogens<sup>220</sup>.

A distinction between age groups was not made consistently in studies looking at both paediatric and adult patients. Since the prevalence of bacterial species has been shown to change with age<sup>221</sup>, it would be relevant to report a breakdown of pathogens by age group.

Noone et al highlights under-sampling of sputum in PCD patients compared to CF patients. They recommend sputum sample monitoring 3 to 4 times a year<sup>222</sup>. In many studies, the prevalence stated relies on one positive sample, often taken from patient records. It is often not noted if the samples were taken during exacerbations or clinically stable periods.

One hallmark of PCD is chronic respiratory infections. There is no unified definition of "chronic" across the studies examined. Some studies mention both chronic and non-chronic infection statuses and some only chronic infections. In some cases, total percentage of positive cultures are reported (including the same patient several times). Other times, if a patient has cultured a pathogen once during the study period they are reported as infected.

The prevalence of multiple bacterial species within PCD patients makes cross-species interaction very likely. This should be considered before drawing conclusions based on models using only one species.

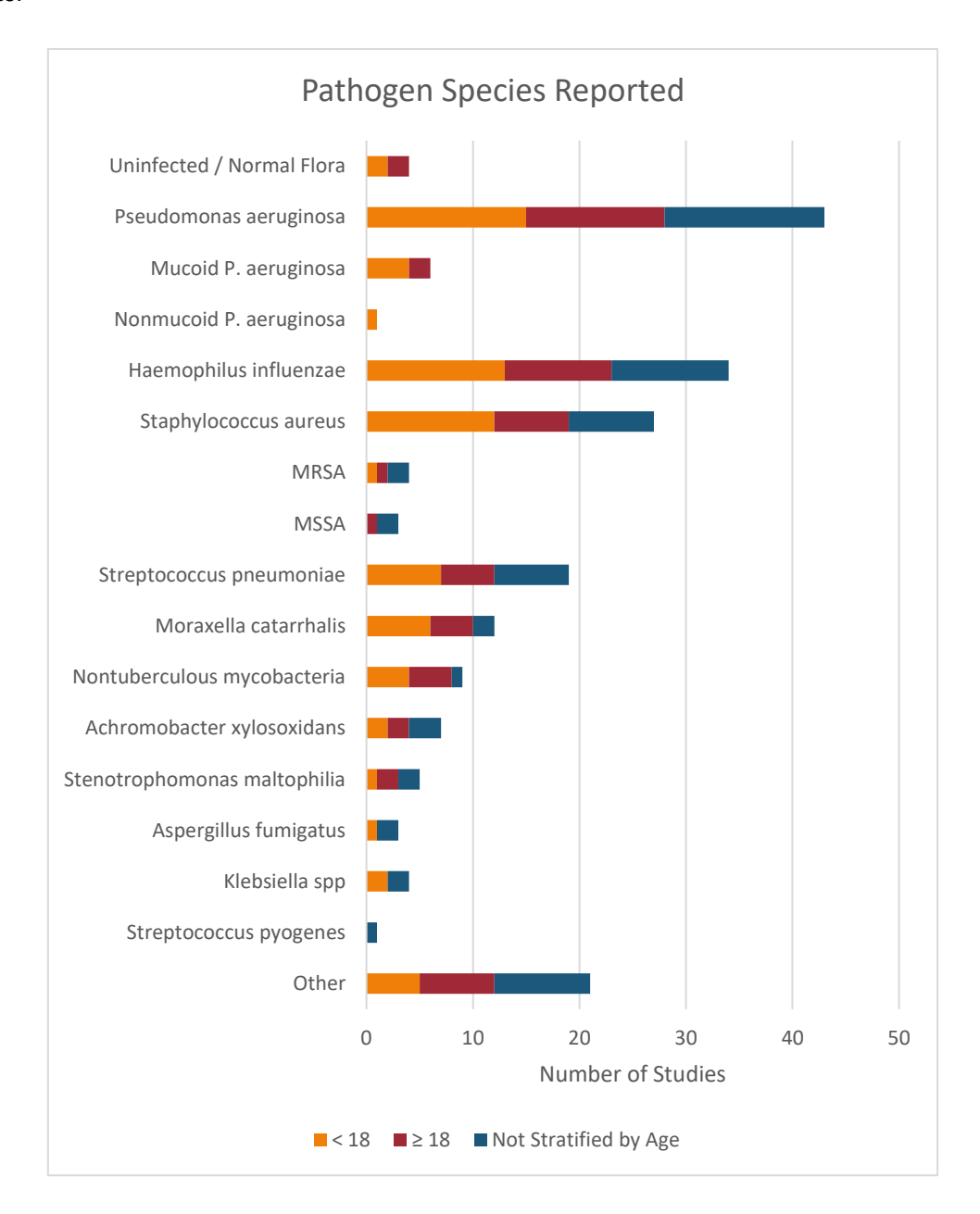


Figure 1.4: Bacterial species reported in 57 PCD studies published 1996 to 2020 summarised in Gahleitner et al<sup>219</sup>, microbiology review performed by me (JH). The category "other" includes *Burkholderia cepacian*, *Candida albicans*, *Serratia mercescens*, *Alcaligenes* 

xylosoxidans, Aspergillus niger, Enterobacter cloacae, Escherichia coli, Proteus spp and Rhodococcus equi.

#### 1.2.4.3 Non-typeable Haemophilus influenzae in Primary Ciliary Dyskinesia

NTHi is the most commonly isolated bacterial pathogen in both paediatric<sup>223</sup> and adolescent/early adult<sup>211</sup> PCD patients. Prevalence has been found to be as high as 80% in children under 18 and 22% in adults<sup>222</sup>. Further studies have found the prevalence to be 32–65% and 21–27% in children and adults respectively<sup>211</sup>, however, there is a general decline in prevalence with age<sup>221</sup>. Alanin *et al.* found 8–31% of patients to be chronically infected, as defined by more than 50% of cultures being positive for a pathogen over a 12-month period<sup>221</sup>.

An increase in NTHi biofilm formation was observed on PCD epithelial cells compared to those of healthy volunteers<sup>224</sup>. The cytokine release by the epithelial cells was found to be similar<sup>224</sup>, suggesting a link between the reduced ciliary function and the increased biofilm.

# 1.3 Modelling Host-Pathogen Interactions

#### 1.3.1 General Methodology

By definition, a model used to study an interaction must have the two components between which the interaction is to be studied. Examples of this include the interaction between immune cells and pathogens, or the interaction between bacteria and epithelial cells. Models using two cell types can help compartmentalise and investigate molecular mechanisms, forming a fundamental component of our current understanding. The relative ease of use, alongside the reduced logistical and economic impact of these techniques make monocultures an important starting point for investigating host-pathogen interactions before moving on to co-cultures involving two or more cell types.

As with all biological systems, interactions are complex and very rarely occur only between two components. This poses the challenge of developing an accurate representation of a given biological situation, including all key components, while maintaining the practicality of the model. Increased complexity leads to greater difficulties setting up a model as well as an increased difficulty obtaining data from it, for example a biofilm in a polystyrene well can easily be quantified with crystal violet dye while a biofilm on an epithelial cell layer cannot.

Introducing more components into a model will also increase the level of stochasticity in the system, meaning that the accuracy of measurements will be impacted by the variability of each component. This makes it difficult to control for experimental variables in the same way that simpler models allow.

The interaction of multiple cell types is often required to produce an effective immune response to pathogenic challenge. The results of investigating the response of single cell types to infection can therefore rarely be extrapolated to *in vivo* systems.

One issue with animal models is that pathogens often have a strict specificity for their hosts<sup>225</sup>, so human pathogens can only be accurately modelled in animals to a limited degree. NTHi is one such human specific pathogen.

#### 1.3.1.1 Cell culture and immortalised cell lines

Cell cultures allow biological systems to be studied in a simplified environment, granting tighter control over the experimental environment and removing possible confounding factors<sup>226</sup>. *In vitro* cell cultures must be continually supplied with nutrients and growth factors that would otherwise be provided by the organism. They also lack the active immune response that would keep them free from contamination *in vivo*, so protection must be provided in the form of antibiotics and fungicides alongside stringent aseptic working technique. In order to grow, cells usually require a substrate to adhere to, so tissue culture plates are coated in collagen to mimic the extracellular matrix <sup>226</sup>.

Immortalised, or continuous, cell lines are able to proliferate almost indefinitely either by originating from tumorous cells, or through artificial manipulation. They can therefore be cultured continuously over several generations<sup>226</sup>. The cells will continue to divide, filling the surface available, so require regular splitting, or "passaging", to avoid inhibiting the growth of neighbouring cells and using up nutrients too rapidly<sup>226</sup>. Immortalised cells lines have the advantage of being comparatively cheap and well characterised as they are used across multiple laboratories, making results more comparable across the research community. However, immortalised cell lines often no longer resemble cells found *in vivo*, displaying dysregulated signalling and gene expression<sup>226,227</sup>. Immortalised cell lines can form monolayers but often do not form a stratified structure of differentiated cells<sup>2</sup> such as those observed *in vivo*.

# 1.3.1.2 Primary cell cultures

Primary cells are obtained directly from patients, volunteers or animals. These cultures are used as an *in vitro* model to study function and mechanisms. Using primary cells can reduce the need for animal models<sup>2</sup>. The limitations of primary cell cultures include price, availability, rate of expansion and the number of times cells can divide (and subsequently number of passages possible)<sup>2</sup>. Methods that increase the number of passages possible enable increased research to be done in situations where primary cells are limited, such as in neonates or diseased patients where collecting samples is associated with discomfort or logistical challenges<sup>2</sup>.

#### 1.3.1.3 ALI Cultures

The respiratory epithelium can be modelled *in vitro* by culturing cells at the air liquid interface (ALI) as opposed to liquid covered culture (LCC). First described as a "biphasic chamber system" in 1988<sup>228</sup>, cells are grown with their basal surfaces on a permeable membrane and exposed to the air on the apical side. Media is added underneath the membrane and regularly exchanged for fresh media, providing the cells with a constant source of nutrients thereby simulating the blood supply and the concentration gradients that cells would be exposed to *in vivo*.

ALI cultures have been shown to develop a pseudostratified structure that more accurately represents the *in vivo* airway than LCCs. Besides the increase in cell layers, the cultures have been shown to ciliate as well as forming microvilli. Although the Calu-3 cell line develops a more similar morphology at ALI than LCC, it does not ciliate in either culturing methodology<sup>229</sup>.

A comparison of human bronchial epithelial cell culturing methods showed that it was possible to get a stratified, differentiated epithelial layer from up to 6 passages using PneumaCult-Ex media<sup>2</sup>. This media also yielded the fastest growth, producing a fully differentiated, 4-6 layered epithelium after 4 weeks of culturing at ALI<sup>2</sup>. The drop off in quality post passage 6 was not uniform across donors, highlighting a variation in differentiation capabilities. Successful expansion and differentiation of human primary nasal epithelial cells (PNECs) following cryostorage<sup>230</sup> has increased the yield of cells from individual samples, greatly expanding the scientific output from each sample.

# 1.3.2 Insight into non-typeable Haemophilus influenzae Host-Pathogen Interaction

#### 1.3.2.1 NTHi Co-cultures

NTHi has been co-cultured in a range of systems with focus on different diseases and mechanisms. Work has mainly been done on epithelial cells, both primary cells<sup>137,224,225,231,232</sup> and cell lines<sup>233–235</sup>, with models at ALI<sup>224,225,232,233</sup> and at LCC<sup>137,231,234,235</sup>. NTHi biofilm grown on an epithelial cell surface, relying on host cells alone for nutrients, show less growth compared to biofilms on abiotic surfaces in rich medium<sup>83</sup>.

Previous work by our group<sup>224</sup> has produced a co-culture system using primary respiratory epithelial cells obtained from PCD patients by nasal brushings. The cells are cultured on membrane in a transwell system that allows basal feeding while maintaining the apical side of the cell layer at ALI. This model produces a differentiated pseudostratified cell layer including ciliation and mucus producing cells. Co-culture with NTHi and biofilm formation has been demonstrated for 72 h. Cytokine release can be measured by sampling the basolateral media or performing apical washes, cell layer integrity can be measured using TEER and bacterial cell counts by CFU enumeration. Additionally, the model can be imaged using confocal and electron microscopy as well as high-speed video light microscopy for live imaging of ciliary behaviour.

A similar model is used by Ren et al to co-culture NTHi from OM patients with normal human bronchial epithelial (NHBE) cells<sup>232</sup>. The epithelial cells are not from a specific disease. Similar to the model developed by Walker et al<sup>224</sup>, TEER and cytokine release is measured along with SEM and TEM. Intracellularisation of bacteria was measured using gentamicin to kill extracellular bacteria, followed by lysis of the epithelial cells and CFU enumeration, similar methodology can be used on macrophages<sup>236</sup>. Ren et al also describe the use the commercially available EpiAirway system (MatTek, Ashland, MA, USA)<sup>232</sup> consisting of human derived tracheal/bronchial epithelial cells cultured at ALI, differentiated to a pseudostratified mucociliary morphology including basal cells, mucus producing goblet cells, tight junctions and beating cilia. A model including normal human fibroblasts is also commercially available (EpiAirwayFT, MatTek, Ashland, MA, USA), modelling the stromal space below the epithelium<sup>237</sup>. A similar model was developed by Marrazzo et al where fibroblasts and the addition of collagen generate a simulated ECM on which primary human tracheabronchial cells were cultured at ALI until fully differentiated to form a columnar epithelial layer<sup>225</sup>. Ciliation and mucus production as well as basement membrane and tight junction formation was confirmed through immunostaining and electron microscopy. Markers for tissue regeneration and

repair were also detected. A clinical NTHi isolate from an OM patient was used to validate the model through the demonstration of an expected invasive phenotype<sup>225</sup>. Bacteria were found in the mucus layer, the epithelial sheet and as aggregates within the stromal layer<sup>225</sup>.

Primary cells have been co-cultured with NTHi in LCCs to investigate PilA expression. The recognition that the contact with epithelial cells stimulates the expression of the type IV pilus<sup>137</sup> underlines the importance of studying pathogenicity in the context of co-cultures.

Using immortalised cell lines allows for faster access to larger volumes of cells, an important factor for RNA extraction protocols. As such it is an attractive alternative for co-cultures involving viral infection<sup>234</sup>. Cell lines have also been used in co-cultures with NTHi to investigate the host pathogen interaction in CF<sup>233</sup> and the antibiotic susceptibility of NTHi isolated from OM patients<sup>238</sup>.

The *in vivo* microbiome is not a monoculture of NTHi alone. NTHi has been co-cultured with other bacterial species to investigate the interactions within a multi-species biofilm. The focus has been on *streptococcus pneumoniae* as the two species are found together as commensals in healthy individuals but play a major pathogenic role in upper airway infections<sup>239,240</sup>.

#### 1.3.2.2 Epithelial cells and NTHi

Epithelial cells play an important role in the recognition of pathogenic NTHi and the subsequent immune response. NTHi interacts with epithelial cell surface receptors such as gangliosides<sup>241</sup> and ICAM-1, upregulating the latter to increase adhesion<sup>242</sup>. NTHi, specifically lipoprotein P6, is recognised by TLR2 on the epithelial cells, leading to an inflammatory response<sup>243</sup>.

Whole NTHi cells have been found to elicit a greater maximum IL-8 and IL-6 response than purified LOS, supporting the idea that the epithelium reacts to more than just LOS when responding to NTHi infection<sup>244</sup>.

# 1.3.2.3 Macrophages and NTHi

The macrophage response to NTHi infection varies with bacterial strain, with expression of RIG-I, CXCL10 and NF-kB as well as cytokine release found to be strain dependent<sup>245</sup>. This means that most findings reliant on a single strain would benefit from being confirmed in a range of strains, preferably clinical isolates.

Additional macrophage receptors involved in the interaction with NTHi include gangliosides, plasma membrane components which are expressed on the surface of most host cells<sup>241,246</sup>. The glycoprotein ICAM-1 plays a role in NTHi adhesion and uptake into macrophages<sup>247</sup>. NTHi can also enter monocytes via receptor mediated endocytosis in a strain dependent manner<sup>184</sup>.

Cytokine release by macrophages in response to NTHi stimulates the anti-bacterial response of immune cells. LPS released by NTHi acts on TLR4 and triggers the release of cytokines including TNF- $\alpha$ , IL-1 $\beta$  and IL-6 from macrophages<sup>248,249</sup>. LPS must be bound to LPS binding protein (LBP) in order for NTHi to elicit a TLR4 response from alveolar macrophages<sup>250</sup>. The response to NTHi appears to be mediated predominantly through TLR4 and MyD88 rather than TLR2 and TRIF<sup>251</sup>, with TLR9 not being significantly involved<sup>252</sup>. A synergistic effect between IFN- $\beta$  and lipoprotein (a TLR2 ligand) has been observed for IL-6 release, but not TNF- $\alpha$ <sup>253</sup>.

IL-8 and macrophage inflammatory protein  $1\alpha$  and  $1\beta$  (MIP- $1\alpha/\beta$ ) are also released in response to NTHi co-incubation<sup>254</sup>. TNF- $\alpha$  knockouts show defects in the recruitment and function of macrophages at the site of infection<sup>255</sup>.

IL-1 $\beta$  is processed into its activated from by the inflammasome. Both NLRP1<sup>256</sup> and NLRP3<sup>257</sup> inflammasomes have been found to be upregulated in macrophages in response to NTHi infection. Impaired inflammasome function leads to significantly reduced IL-1 $\beta$  maturation and subsequent reduction in macrophage recruitment and phagocytic ability<sup>258</sup>.

Macrophages are able to produce the antimicrobial enzyme lysozyme which can aggregate NTHi cells<sup>259</sup>. Alveolar macrophages also produce reactive oxygen species (ROS) in response to NTHi, both in healthy individuals and in COPD patients<sup>260</sup>. The sustained release of ROS is associated with the formation of extracellular trap-like structures involving metalloproteinase-12<sup>261</sup>.

Macrophages are found to preferentially phagocytose NTHi when present compared to apoptotic cells (efferocytosis) $^{262}$ , leading to a reduction in clearance of cellular debris, likely stimulating further inflammation. DNA from internalised NTHi cells stimulates IFN- $\beta$  and CXCL10 expression in both epithelial cells and macrophages $^{263}$ 

Phagocytosis and cytokine release appear calcium mediated, with extracellular calcium leading to improved phagocytosis and cytokine secretion as well as increased expression of receptors involved in bacterial recognition, CD16 and MARCO<sup>254</sup>

Chronic conditions can impact macrophage function. Alveolar macrophages from COPD patients produce less pro-inflammatory cytokines than non -COPD. However this is only observed in alveolar macrophages, not peripheral blood macrophages<sup>264</sup>. Similarly, alveolar COPD macrophages show impaired phagocytosis compared to non-COPD<sup>265</sup>, this is not seen in blood macrophages<sup>264</sup>.

The expression of bacterial recognition receptors decreases in COPD and smokers following NTHi exposure. TLR 4 also decreases in healthy non-smokers when exposed to NTHi<sup>266</sup>. The impaired innate immune response in COPD alveolar macrophages, caused by impaired TLR signalling, is likely to contribute to unresolved infections and disease exacerbations<sup>267</sup>

Impaired phagocytosis of NTHi by macrophages is observed in association with smoke exposure (regular cigarettes, e-cigarrettes<sup>268</sup>, second hand smoke<sup>269</sup> and bushfires<sup>270</sup>), COPD, asthma and bronchiectasis<sup>271</sup>.

The antibiotic azithromycin is antibacterial and anti-inflammatory. It can act on intracellular NTHi in epithelial and macrophages, if the strain is susceptible<sup>272</sup>. Phagocytosis is also improved by azithromycin, even at low doses. This may, however, lead to the development of antibiotic resistance. Novel macrolides with reduced antimicrobial ability have been found to maintain the positive effect of phagocytosis but may exert less selective pressure to develop resistance<sup>271</sup>, instead encouraging NTHi clearance through restored macrophage function.

On the NTHi side, protein D is expressed on the surface of all NTHi strains and promotes adherence and internalisation into monocytes<sup>130</sup>. OMP P5 also plays a role in macrophage recognition and phagocytosis. Hap was not found to be crucial despite being involved in adhesion, possibly indicating a redundancy among adhesion molecules and that hap deficiencies can be compensated for by other NTHi surface molecules<sup>101</sup>.

Besides inducing a substantial increase in TNF- $\alpha$  and IL-8 secretion by macrophages, NTHi membrane protein OMP P6 induces a small amount of IL- $10^{119}$ . Furthermore, NTHi has been observed to shift macrophage polarisation to a more anti-inflammatory phenotype over time by stimulating IL- $10^{119}$ . This decreases the pro-inflammatory response to TLR mediated bacterial recognition, allowing bacteria to persist more readily in the presence of immune cells.

# 1.4 Summary

The host immune response is a complex system of interacting components. Studying these interactions *in vitro* often requires the use of a significantly simplified models, often including only one cell type such as epithelial cells or macrophages. These models are vital for building a basis of understanding the host-pathogen interaction, however, as our comprehension grows, more complex models are needed to allow the interplay of host components to be understood further.

Previous work within our research groups has focused on NTHi infections of both epithelial cells and macrophages within a range of contexts including PCD<sup>224,274,275</sup>, asthma<sup>236</sup> and healthy indeviduals<sup>276</sup>. Building on the methodology established in that body of work, this project sought to combine these two cell types, previously used separately, into one model that allowed the macrophage response to NTHi biofilms to be investigated on an epithelial cell layer model.

# 1.5 Hypothesis, Aims and Objectives

Overall study hypothesis: Monocyte Derived Macrophages (MDMs) are more effective at clearing established Non-typeable *Haemophilus influenzae* (NTHi) biofilms on Primary Nasal Epithelial Cell Air-Liquid Interface (PNEC ALI) culture than established biofilms on an abiotic surface.

# 1.5.1 Project context

The roadmap of the whole project is as follows (illustrated in Figure 1.5):

- 1. Characterise biofilm formation of clinical isolates on an abiotic surface (Chapter 3).
- 2. Establish a bacterial/epithelial cell co-culture (Chapter 4).
- 3. Determine bacteria macrophage interaction (Chapter 5).
- 4. Establish a macrophage/bacteria/epithelial cell triple co-culture (Chapter 6).

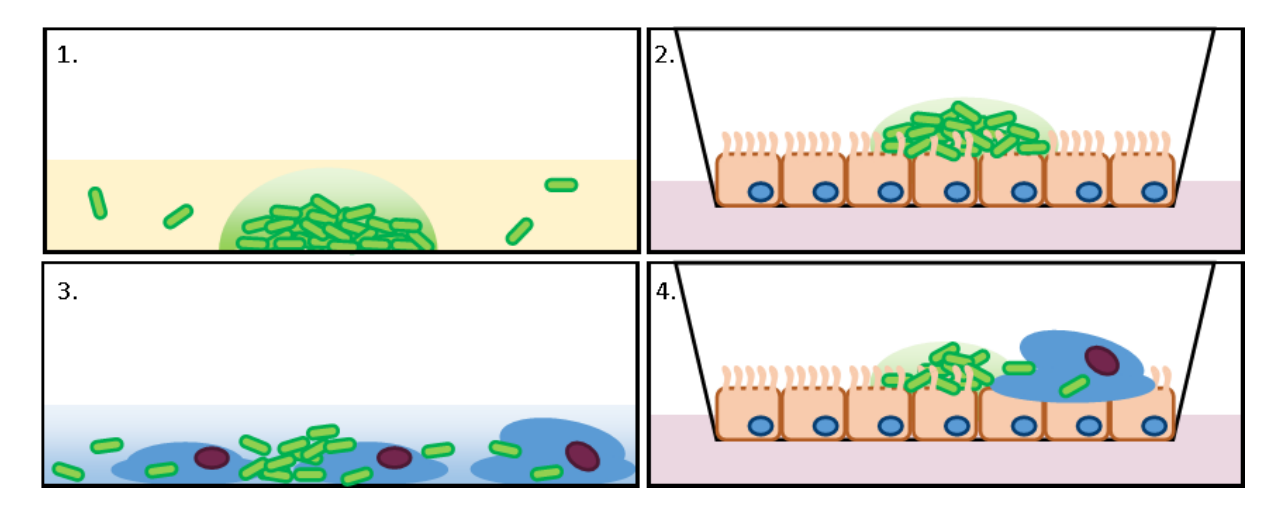


Figure 1.5: Progression of co-culture model development. 1.-4. Correspond to the study objectives listed in 1.5.1

#### 1.5.2 Planktonic and Biofilm NTHi characterisation on an Abiotic Surface

The planktonic and biofilm growth behaviour of NTHi isolates from PCD patients and a GFP producing strain needed to be characterised first. Planktonic growth determined protocol design while biofilm growth was considered in order to select a suitable strain for subsequent work.

The hypothesis, aims and objectives were as follows:

NTHi forms biofilms on abiotic surfaces in a strain dependent manner

- Characterise the planktonic growth of 6 clinical NTHi strains from PCD patients and a GFP strain in order to optimise the inoculation protocol for biofilms
  - a. CFU count and Optical density (OD) growth curves
  - b. Correlate OD and CFU counts during the stationary growth curve
- 2. Confirm and characterise the biofilm formation of NTHi strains on an abiotic surface in order to select a suitable strain for further work
  - a. Quantify biofilm growth over 72 h using CFU counts, CV staining for three NTHi strains
  - b. Comparison of 72 h biofilm endpoint for four further NTHi strains using CFUs, CV and confocal microscopy with live/dead (Syto9/PI) staining
  - c. Demonstrate antibiotic recalcitrance of selected NTHi strains for azithromycin and ceftazidime

#### 1.5.3 NTHi-Epithelial Cell Co-culture

Following the identification of a suitable NTHi isolate and infection protocol, the next step was the optimisation of an NTHi-epithelial cell co-culture. For this, PNECs were differentiated to a ciliated pseudostratified epithelial layer at ALI before being infected with planktonic NTHi and then co-cultured for 72 h.

The hypothesis, aims and objectives were as follows:

GFP- NTHi and a selected clinical strain of NTHi form biofilms on the apical surface of PNEC ALI cultures

- 1. Optimise MOI (1-100) and attachment period (1 h and 24 h) for NTHi/ALI co-cultures to maximise epithelial layer integrity and biofilm formation
  - a. Measure bacterial recovery after 72 h through CFU count
  - b. Validate epithelial cell layer integrity through TEER
  - c. Elucidate biofilm location through SEM and immunofluorescent confocal microscopy

# 1.5.4 NTHi-MDM Co-Culture

In order to compare the impact of MDMs on NTHi biofilms on abiotic and epithelial cells, a NTHi biofilm-MDM model had to be established on plastic first.

The hypothesis, aims and objectives were as follows:

MDMs reduce established NTHi biofilm viability on an abiotic surface

- 1. Assess the ability of MDMs to reduce established NTHi biofilms on plastic controlling for the impact of MDM media
  - a. Visualise the MDM-biofilm interaction through SEM
  - b. Measure changes in biofilm viability through CFU counts and in biomass through CV staining
  - c. Characterise MDM cytokine response through ELISA
  - d. Confirm MDM viability through LDH assay

# 1.5.5 NTHi-MDM-Epithelial cell Triple Co-Culture

Finally, the established NTHi-epithelial cell co-culture was expanded using the addition of MDMs and the results compared to the NTHi-MDM co-cultures on an abiotic surface.

The hypothesis, aims and objectives were as follows:

- 1. Characterise the impact of MDM addition to established NTHi biofilms on ALI cultures, including controls for ALI, ALI-MDM and ALI-NTHi in each experiment.
  - a. Visualise MDM impact, localisation and cell viability through SEM
  - b. Confirm epithelial cell integrity through TEER
  - c. Measure co-culture viability through LDH
  - d. Characterise MDM cytokine response through ELISA
  - e. Measure changes in biofilm viability through CFU counts

# **Chapter 2** Materials and Methods

# 2.1 Microbiology Methods

# 2.1.1 Clinical Bacterial Isolates from Study Participants

Patients were recruited from the National PCD centre at the University Hospital Southampton, UK. They were diagnosed as having PCD in accordance with European evidence-based guidelines<sup>277</sup> and the study was approved by Southampton and South West Hampshire Research Ethics Committee (A) (REC numbers: 06/Q1702/109 and 08/H0502/126, UOS ERGO II 53155). All patients gave written informed consent.

Clinical isolates of NTHi were obtained through Public Health England (PHE), who were notified and asked to provide a sample of the isolated strain when PCD patients were identified to be carrying NTHi on their 3 monthly sputum sample. Bacterial strains were named in order of acquisition, i.e. PCD-NTHi 1, PCD-NTHi 2 etc.

Six isolates were collected from either paediatric or adult patients (Table 2.1). The PCD diagnosis had been reached through nasal nitric oxide (nNO), transmission electron microscopy (TEM), high-speed video microscopy (HSVM), immunofluorescence and genetic testing. The patient from which PCD-NTHi 5 was obtained was diagnosed as "highly likely" to have PCD. This diagnosis was reached in the past before the current set of diagnostic tests, such as immunofluorescent staining of ALI cultures, were available. The patient is managed as a confirmed PCD case and the discrepancies between diagnostic algorithms<sup>278</sup> meant that this isolate was considered a PCD-NTHi isolate for the purpose of this work.

Table 2.1: Diagnostic and clinical details of patients from whom Non-typeable *Haemophilus*influenzae isolates were obtained. Pathogenic of likely pathogenic genetic mutations of PCD genes are bi-allelic unless otherwise stated. NTHi history is quoted as reported by clinicians. NTHi – Non-Typeable *Haemophilus influenzae*, PCD – Primary Ciliary Dyskinesia, TEM – Transmission Electron Microscopy.

Strain	Age at diagnosis	Ciliary motion (HSV)	Nasal nitric oxide (ppb)	Ciliary ultrastructural defect (TEM)	Genetics	NTHi history	Antibiotic history
PCD- NTHi 1	2у	Static	70	Outer Dynein Arms	DNAI1	frequent	nil current
PCD- NTHi 2	<1y	Static	32	Outer Dynein Arms	DNAI2	No previous samples	nil current
PCD- NTHi 3	8y	Static & Twitching	41	Outer Dynein Arms	CCDC151	mostly growing HI	No prophylaxis but several courses of co-amoxiclay
PCD- NTHi 4	<3mo	Static	25	Outer Dynein Arms	Heterozygous DNAI1	intermittent	no prophylaxis
PCD- NTHi 5	7у	Static & Twitching	25	Normal	Heterozygous DNAH11	frequent	no prophylaxis
PCD- NTHi 6	>18y	Rotating	47	Normal	HYDIN	no previous samples	Infrequent from GP

A Green Fluorescent Protein (GFP) expressing NTHi strain (NTHi-GFP-375<sup>SR</sup> with a stable chromosomal insertion of GFP gene and a streptomycin resistance gene) was kindly provided by Dr Derek Hood. This strain was originally derived from a clinical otitis media isolate from a Finnish pneumococcal vaccine study on children undergoing tympanocentesis in 1994-1995<sup>279,280</sup>

#### 2.1.2 Media and Plate Preparation

NTHi cultures were grown in brain heart infusion (BHI, Oxoid, UK) supplemented (sBHI) with hemin (10  $\mu$ l/mL) and nicotinamide adenine dinucleotide (NAD) (2  $\mu$ l/mL). Both supplements were filter sterilised prior to addition, Haemin was stored at room temperature and NAD stored as frozen aliquots. Supplemented BHI was made up fresh for every assay.

Chocolate blood agar (CBA) plates were prepared using Blood Agar Base No.2 (Oxoid, UK), according to manufacturer's instructions, with 5% defibrinated horse blood. The blood was lysed in a water bath at approximately 60°C for 2 h with manual shaking every 30 min. Plates were poured and allowed to set at room temperature and stored at 4°C until use.

# 2.1.3 Planktonic Growth Conditions and Glycerol Stocks of Bacterial Isolates

Clinical NTHi isolates were received on CBA plates from PHE. Colonies from these plates were subcultured in sBHI and grown to approximately exponential phase as determined by optical density (OD). The culture was vortexed briefly and incubated under static conditions at 37°C and 5% CO<sub>2</sub>.

Long term stocks were prepared by mixing the planktonic NTHi cultures with 40% glycerol (in  $dH_2O$ ) at a 1:1 ratio, for a final concentration of 20% glycerol. 1 mL aliquots were then stored in cryovials at -80°C.

For all subsequent assays, fresh CBA streak plates were prepared in a laminar flow hood. While streaking the plate, the glycerol stock was kept on dry ice to avoid complete thawing, scraping off a sample from the top of the stock with a sterile loop. The CBA plates were incubated overnight (static, 37°C, 5% CO<sub>2</sub>). Colonies were selected based on ease of removal while avoiding neighbouring colonies. Planktonic cultures were then inoculated as above, single colonies in sBHI, vortexed briefly and incubated to either exponential phase (5-8 h) or overnight (15-18 h) depending on the assay.

#### 2.1.4 Planktonic Growth Characterisation

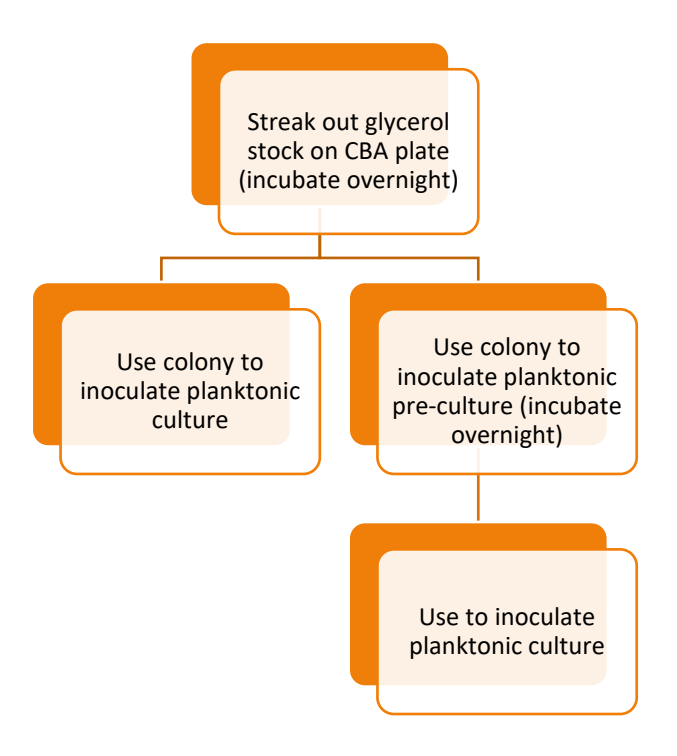


Figure 2.1 Schematic of the inoculation protocols investigated.

Two methods of inoculation were used during the characterisation of planktonic growth: a single colony from a CBA (as described above, 2.1.3) or using 200  $\mu$ l from a planktonic overnight culture (Figure 2.1). The optical density (OD) of the planktonic cultures was measured 2 h post-inoculation and every subsequent hour for the duration of the assay. 1 mL of culture was added to a cuvette and the OD was measured using a spectrophotometer (Jenway 6300, Keison Products, Chelmsford, UK) at a wavelength of 600 nm (OD<sub>600</sub>). sBHI was used as a blank measurement prior to taking readings.

In order to enumerate the number of viable bacterial cells in the planktonic cultures following overnight incubation (approx. 16 -18 h), the Miles and Misra method<sup>281</sup> was used to measure the number of colony forming units (CFUs) per mL. 10-fold dilutions of the culture were prepared in Hanks' Balanced Salt Solution (HBSS) to a  $10^7$  dilution. A  $10~\mu$ L sample of each dilution was spot plated on CBA plates in triplicate and incubated overnight (static,  $37^{\circ}$ C, 5% CO<sub>2</sub>). CFUs were enumerated and used to calculate the viable cell density in CFUs/mL which was then correlated to incubation time and OD (Section 3.2.1). This was replicated a minimum of 5 times for each strain, with 2 technical repeats each.

# 2.1.5 Inoculating NTHi Biofilms on Polystyrene

Planktonic cultures were grown overnight (approx. 16-18 h) to stationary phase as described in 2.1.4. The OD<sub>600</sub> was measured, and the corresponding CFUs/mL calculated using the previously established correlation (2.1.4). The culture was diluted so that each well was inoculated with 2 x  $10^8$  NTHi and supplemented with fresh sBHI according to assay (volumes detailed in appropriate method sections). Biofilms were incubated at  $37^{\circ}$ C and 5% CO<sub>2</sub> under static conditions and fed every 24 h by gently removing half the media and replacing it with an equal volume of fresh sBHI. Rapid application or removal of media led to the peeling off of biofilm layers and care was therefore taken when changing the media.

Once the 72 h biofilm growth period was selected for further work, biofilms were not fed daily due to logistical constrains of incubating over the weekend. The viability of biofilms after 72 h without fresh media was confirmed to be comparable.

# 2.1.6 Assessing Biomass using Crystal Violet

Crystal violet (CV) was used to estimate the total biomass of biofilms formed by each NTHi strain over 72 h. Biofilms were grown in 12-well tissue culture plates in a total volume of 2 mL sBHI media. 1 mL of used media was removed and replaced with an equal amount of fresh sBHI every 24 h.

For GFP-NTHi, PCD-NTHi 1 and PCD-NTHi 2, biofilms were analysed at 24, 48 and 72 h. All other strains were analysed at 72 h only. When processing, all media was removed, and the biofilms washed twice with 2 mL HBSS to remove non-adherent bacteria. The wells were stained with 2 mL of 0.1% CV solution for 20 min then washed twice with 2 mL HBSS. The plates were then air-dried overnight and the CV re-solubilised in 2 mL 30% acetic acid on a rotating platform for 15 min. 1 mL of re-solubilised CV was added to a cuvette and OD<sub>600</sub> was measured with a spectrophotometer (Jenway 6300, Keison Products, Chelmsford, UK), using 30% acetic acid as a blank.

# 2.1.7 Assessing Viability using CFUs

Biofilm viability over a 72 h period was measured using CFU counts. 6-well polystyrene tissue culture plates were inoculated as previously described (2.1.5) with a final volume of 4 mL sBHI. 2 mL of media was removed and replaced with an equal volume of fresh sBHI every 24 h.

For GFP-NTHi, PCD-NTHi 1 and PCD-NTHi 2, biofilms were analysed at 24, 48 and 72 h. All other strains (PCD-NTHi 3 to 6) were analysed at 72 h only. When processing, the media was removed, and the biofilms gently washed twice with 4 mL HBSS to remove non-adherent bacteria. The biofilms were re-suspended in 1 mL of HBSS using a cell scraper and transferred to a microcentrifuge tube. Following a brief vortex, a CFU count performed using the Miles and Misra method as described in (2.1.4).

Assessment of biofilm viability following antibiotic and macrophage exposure was performed in the same way at the assay endpoint.

# 2.1.8 Confocal Microscopy

For confocal microscopy, biofilms were grown in tissue culture (TC) treated cell-view dishes (Greiner Bio One, 8.7 cm²) in a total volume of 4 mL sBHI. 2 mL of media was removed every 24 h and replaced with an equal amount of fresh sBHI. At 72 h, the media was removed and replaced with 1 mL live/dead BacLight stain (containing Syto9 & propidium iodide, used according to manufacturer's instructions (Life Technologies)). The mixture was then incubated wrapped in foil for 15 min at room temperature in dark conditions to prevent photobleaching. The stain was removed, and the biofilm gently washed twice with 4 mL HBSS to remove unattached cells and excess stain. 1 mL of 60 % glycerol in dH<sub>2</sub>O was carefully added on top of the biofilm and images recorded using an inverted Leica SP8 confocal microscope.

Three random fields of view were imaged per plate using a 63x oil immersion objective. Z-stacks of the biofilms were recorded in  $0.3 \mu m$  steps, the total height varied by strain (Figure 3.10).

## 2.1.9 Confocal Image analysis

Confocal biofilm images were analysed using IMARIS (Bitplane, Oxford Instrument Company, Concord, MA, USA). Biofilms were reconstructed as surface objects for both channels (Live/Dead) and analysed using the Biofilm Analysis XTension (M. Gastinger, 2016). The values for "BioVolume", "Max thickness" and "Mean thickness" were taken for both live and dead populations for every field of view. The maximum and mean thickness were measured from the culture well surface while the biovolume measurement only included the IMARIS surface. Analysis data was extracted using a custom code and values averaged across all fields of view of each biofilm. Values for all biofilms of the same strain were then averaged and the standard deviation calculated using python (v2.7). The

ratio between the mean and the maximum thickness was calculated to give an indication of biofilm surface uniformity.

## 2.1.10 Antibiotic Susceptibility

The antibiotic susceptibility of planktonic NTHi was measured using Azithromycin and Ceftazidime etest strips (Biomérieux, France). Overnight planktonic cultures (2.1.4) were grown and 100  $\mu$ L spread evenly on a CBA plate. E-test strips were added gently to the centre of the plate, ensuring no large air bubbles were trapped underneath the strip. Plates were incubated overnight (static, 37°C, 5% CO<sub>2</sub>) and minimum inhibitory concentration (MIC) recorded.

The antibiotic susceptibility of NTHi biofilms was investigated by growing biofilms on plastic as described above (2.1.5) for 72 h. Antibiotics (Azithromycin and Ceftazidime) were diluted in sBHI and added to the biofilms at multiples of the previously determined MIC (1, 10, 100 MIC, Table 3.1). Media (sBHI) alone was used as a control treatment. Biofilms were incubated for 24 h (static, 37°C, 5% CO<sub>2</sub>) before being processed for CV and CFUs as described above (2.1.6 & 2.1.7 respectively).

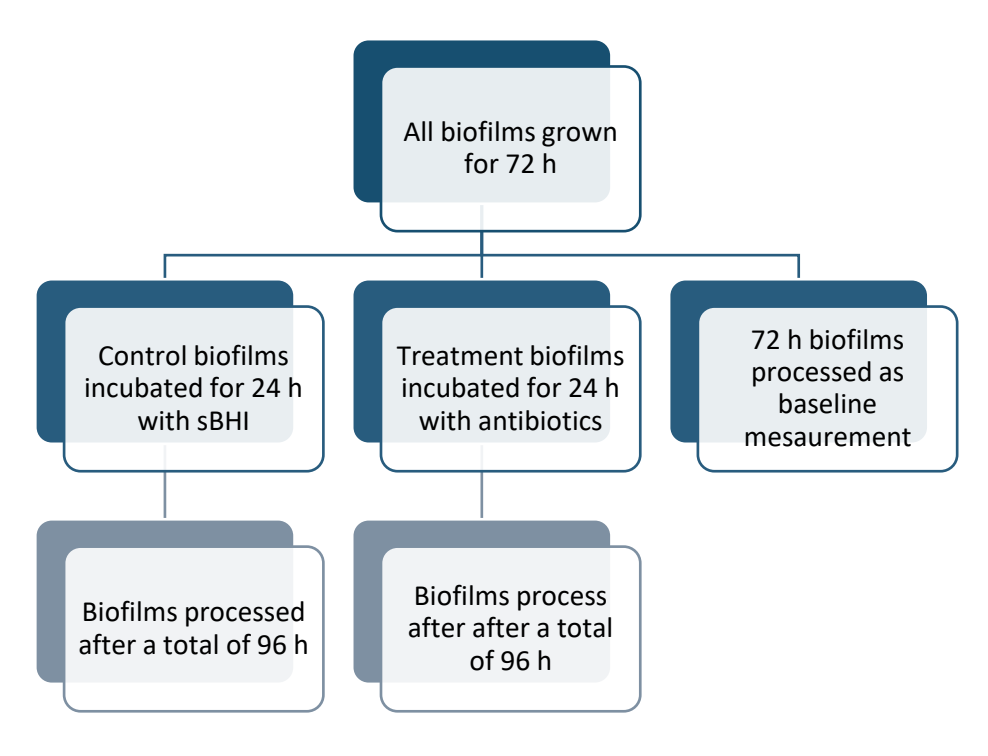


Figure 2.2 Overview of antibiotic tolerance assay

# 2.2 Cell Culture Methods

# 2.2.1 Participants

Nasal brushings were taken from healthy volunteers that were recruited from the National PCD centre at the University Hospital Southampton, UK, with ethical approvals by Southampton and South West Hampshire Research Ethics Committee (A) (REC numbers: 06/Q1702/109 and 08/H0502/126, UOS ERGO II 53155). All volunteers gave written informed consent, collected by trained PCD team personnel.

# 2.2.2 Culturing and Biobanking Nasal Brushing Samples

In preparation for cell culture, all plasticware was collagen-coated with 0.3 mg/mL PureCol (AdvancedBioMatrix, US) diluted in ultra-high-quality water. After a 1 h incubation, the collagen solution was aspirated off, followed by letting the plasticware air dry for a minimum 1 h in a biological safety cabinet.

Nasal brushing biopsies were taken using 2 mm diameter cytology brushes (Olympus Keymed Ltd, UK) and stored in in Pneumacult Ex-Plus Basal Medium (made according to manufacturer's

instructions with 1% streptomycin/penicillin and 0.2% nystatin) (StemCell Technologies, Canada), henceforth referred to as basal media. Cells were removed from the brushes through vigorous pipetting and centrifuged (400x g, 7 min, 10 °C). The cell pellet was resuspended in 1 mL basal media and seeded on to 2-3 wells of a collagen-coated 12-well plate depending on yield as judged by visual inspection of the cell pellet. Basal media was added to each well for a total of 2 mL and cells were incubated (37°C, 5% CO<sub>2</sub>) with 1 mL of basal media being replaced every 2-3 days.

Once 50% - 70% confluent, cells were passaged by aspirating media and replacing it with 500  $\mu$ L trypsin/EDTA (Sigma), incubating for 2 min (37°C, 5% CO<sub>2</sub>) and transferring trypsinised cells to 7 mL HBSS to dilute trypsin. Cells were centrifuged (400x g, 7 min) and resuspended in 1 mL HBSS followed by further centrifugation (400x g, 7 min, to wash off remaining trypsin) and resuspension in 5 mL basal media. Each well was processed in this way and seeded into collagen-coated T25 cm<sup>2</sup> culture flasks (Corning life sciences, UK). Flasks were incubated and 4 mL basal media replaced every 2-3 days.

At a confluency of 50% - 70%, flasks contained approximately  $2x10^6$  cells. Spend media was aspirated off and 1 mL of trypsin/EDTA added (2 min,  $37^{\circ}$ C, 5% CO<sub>2</sub>) to remove cells from the flask surface. The cell suspension was centrifuged (400x g, 7 min) and resuspended in 1 mL HBSS, centrifuged again (400x g, 7 min) and resuspended in 3 mL of 1:1 basal media/CryoStor® CS10 (StemCell Technologies, Canada). The suspension was split across three cryovials in 1 mL aliquots and control-frozen to -80°C.

Nasal brushings were taken by the PCD clinical team and the biobanking of samples was performed by the PCD research group<sup>230</sup>.

# 2.2.3 Culturing nasal epithelial cells for infection

Cell cultures were performed as described by Coles et al<sup>230</sup>. Cells stored at -80°C were defrosted at room temperature and the required number of cryovials combined, centrifuged (400x g, 7 min, 10 °C) and resuspended basal media (supplemented with 0.1% hydrocortisone, 1% streptomycin/penicillin and 0.2% nystatin). A cell count was performed using a 1:1 solution of cell suspension and 0.4% trypan blue with a haemocytometer chamber (Weber Scientific International, US).

Previously collagen-coated 24-well transwell inserts (6.5 mm diameter, 0.4  $\mu$ m pore size) (Corning Life Sciences, UK) were seeded apically with approximately 70,000 cells suspended in 250  $\mu$ L basal media each. 350  $\mu$ L basal media was added to the basolateral side of the Transwell membrane. Cells

were incubated at 37°C and 5% CO $_2$ , replacing media (200  $\mu$ L apical, 350  $\mu$ L basolateral) every 2-3 days.

Once cells had reached confluence, the apical media was removed to bring the cells to the air liquid interface (ALI) and the basolateral media replaced with 350  $\mu$ L Pneumacult Ex-Plus ALI Medium (supplemented with 0.5% hydrocortisone, 0.2% heparin, 1% streptomycin/penicillin and 0.2% nystatin) (StemCell Technologies, Canada), henceforth referred to as ALI medium. Cells were incubated (37°C, 5% CO<sub>2</sub>) for 4 weeks to allow differentiation to a ciliated, pseudostratified phenotype<sup>282</sup> (Horton – unpublished), replacing media (350  $\mu$ L basolateral) and performing an ALI media wash (100 $\mu$ l) every 2-3 days.

# 2.2.4 Co-culture preparation and Trans-epithelial Electrical Resistance

Once cells had been differentiated at ALI for a minimum of 4 weeks, the wells were prepared for coculturing with bacteria by changing the basolateral media to 350  $\mu$ L antibiotic free ALI media 24 hours prior to infection. The cells were then returned to the incubator (37°C, 5% CO<sub>2</sub>).

Transepithelial electrical resistance (TEER) was used as a surrogate indicator of cell membrane integrity and tight junction formation. The apical and basolateral media were replaced with HBSS (200  $\mu$ L and 500  $\mu$ L respectively) and incubated for 30 min (37°C, 5% CO<sub>2</sub>) to allow an equilibration of ions. TEER measurements were taken using a EVOM 2 epithelial voltohmmeter (World Precession Instruments, US). Three measurements were taken using chopstick probes per well, allowing time for the reading to stabilise each time.

One transwell was sacrificed for each assay and a cell count performed in order to calculate the number of bacterial cells required for desired multiplicities of infection (MOIs). To do this, the transwell was moved to a separate plate and 25% trypsin/EDTA (Gibco, Thermo Fisher Scientific) added to the apical and basolateral side (200  $\mu$ L and 500  $\mu$ L respectively). Following a 5 min incubation (37°C, 5% CO<sub>2</sub>), the plate was shaken gently, and the apical solution pipetted into 7 mL HBSS following gentle agitation of the cell layer with the pipette tip. A further 200  $\mu$ L trypsin/EDTA was added to the apical side, incubated again for 5 min and pipetted into the same 7mL HBSS. The cell suspension was centrifuged (400x g, 7 min) and pelleted cells resuspended in 1 mL HBSS. A cell count was performed on a 1:1 solution of cell suspension and 0.4% trypan blue (Gibco, Thermo Fisher Scientific, final concentration 0.2% trypan blue) with a haemocytometer chamber (Weber Scientific International, US).

# 2.2.5 Co-culture with non-typeable *Haemophilus influenzae* at the Air Liquid Interface

An overnight planktonic culture of NTHi was set up the day prior to infection as described in 2.1.4. PNECs were cultured at ALI for 4 weeks to form a ciliated pseudostratified phenotype as described in 2.2.3, a cell count and a baseline TEER reading were taken. Cultures with TEER readings below 100  $\Omega$ .cm² were excluded due to implied lack of epithelial cell layer integrity. Based on the cell count, a corresponding volume of briefly vortexed overnight culture was taken to achieve the desired multiplicity of infection (MOI). The bacteria were centrifuged (13,000rpm, 5min), resuspended in 50  $\mu$ L HBSS and added to the apical side of the epithelial cells. 350  $\mu$ L antibiotic free ALI media was added to the basolateral side of the transwells. Non-adherent bacteria were removed after 24 h and the co-culture was incubated for a further 48 h, 72 h in total (37°C, 5% CO<sub>2</sub>). As the project progressed and different NTHi strains used it was noted that leaving the NTHi suspension on the culture for 24 h may contribute to a decline in epithelial layer integrity. In response, a 1 h NTHi incubation period was introduced followed by the removal of any non-attached NTHi and the remaining suspension, reducing bacterial load and returning the culture to an ALI status. Comparisons between these two protocols – with and without the removal of non-adherent bacteria after 1 h - were performed and protocols adjusted accordingly (section 4.3.2).

After 72 h, TEER measurements were taken by replacing media with 200  $\mu$ L and 500  $\mu$ L HBSS on the apical and basolateral side respectively. Following a 30 min incubation period (37°C, 5% CO<sub>2</sub>) to allow ions to equilibrate, the TEER was measured at three points per well, allowing the reading to stabilise each time. The probe was sterilised between wells using 70% ethanol, allowed to air dry and washed in HBSS to avoid transferring ethanol to the co-culture.

To remove any non-adhered bacterial cells the apical surface of the wells was washed by removing the HBSS from the TEER process, replacing it with 200  $\mu$ L HBSS and gently rocking the plate by hand. The HBSS was removed and the process repeated, washing the co-culture surface three times.

The membrane of each well was excised using a sterile scalpel and transferred to 1 mL HBSS in a fresh 12-well plate. Bacterial cells were removed from the membrane through vigorous scraping using a cell scraper and the suspension vortexed for 10 s to ensure bacterial cells were as evenly suspended as possible.

Serial dilutions of each suspension were performed as described in 2.1.4 and 10  $\mu$ L spots plated out in triplicate on CBA plates. CFUs were enumerated for each biofilm and the CFUs per area calculated.

Investigation of the effect of macrophages on established biofilms were set up the same way, but instead of processing the co-cultures after 72 h, macrophages were added and the culture processed following a further 24 h incubation period.

# 2.2.6 Confocal imaging of NTHi-epithelial cell co-cultures

Primary human respiratory epithelial cells were infected with NTHi for 72 h as described in 2.2.5. To fix the sample, apical and basolateral media were replaced with 4% paraformaldehyde in 0.1M phosphate buffer (pH 7.2) for 15 min. This was followed by three washes using PBS, each for 5 min. The transwell membranes were cut out using a scalpel. When required, membranes were cut in half to provide more samples for staining. Membrane sections were added to 96 well plate wells along with PBS-triton x-100 (PBS-t). The PBS-t was removed, and 5% milk blocking solution added to the membranes for 1 h. Following three 5 min washes with PBS-t, primary antibodies were added (in the relevant dilutions, see Table 2.2) for 2 h. One well of each sample was kept as a control, so did not have primary antibodies added.

Table 2.2: Summary of antibodies used for immunofluorescent staining including dilutions.

Antibody type	Antibody	Fluorophore	Target	Ratio
Primary	Rabbit	-	RSPH4a	1:200
Primary	Mouse	-	Alpha-tubulin	1:50
Secondary	-	Alexa Fluor 594	Rabbit	1:2500
Secondary	-	Alexa Fluor 647	Mouse	1:2500

Following incubation with primary antibodies and three 5 min washes with PBS-t, secondary antibodies were added to all samples for 30 min. A further three 5 min washes with PBS-t were followed by 10 min DAPI staining (300nM). Membranes were washed three times for 5 min with PBS-t, followed by one PBS wash. Membranes were then mounted on glass slides using Mowiol mounting medium and kept at 4 °C until imaging. Slides were imaged using an SP8 confocal microscope (Leica, UK) using a 63x oil immersion objective lens.

# 2.2.7 Scanning electron microscopy of NTHi-epithelial cell co-cultures

Primary human respiratory epithelial cells were infected with NTHi as described in 2.2.5. For NTHi biofilms and macrophages on an abiotic surface, biofilms were grown and co-cultured as described in (REFERENCE). To fix the sample, media (apical and basolateral in the case of Transwells), were replaced with 4% paraformaldehyde in 0.1M phosphate buffer (pH 7.2) for 15 min. This was followed by three washes using PBS, each for 5 min. In preparation for SEM the sample was treated with fixative (3% glutaraldehyde, 4% formaldehyde in 0.1 M PIPES buffer (pH 7.2)) for 1 h, followed by two 10 min buffer rinses (0.1 M PIPES buffer (pH 7.2)). The sample was left in post-fixative (1% osmium tetroxide in 0.1 M PIPES buffer at pH 7.2) for 1 h, buffer rinsed twice for 10 min as before. The sample was dehydrated using an ethanol gradient (30%, 50%, 70% and 95% ethanol for 10 min each), followed by two 20 min treatments with absolute ethanol. Finally, the sample was critical point dried, mounted and sputter-coated with platinum using a Q150T ES sputter coater (Quorum, UK). The samples were then examined using a FEI Quanta 200 scanning electron microscope (FEI company, The Netherlands).

# 2.3 Macrophage Culture Methods

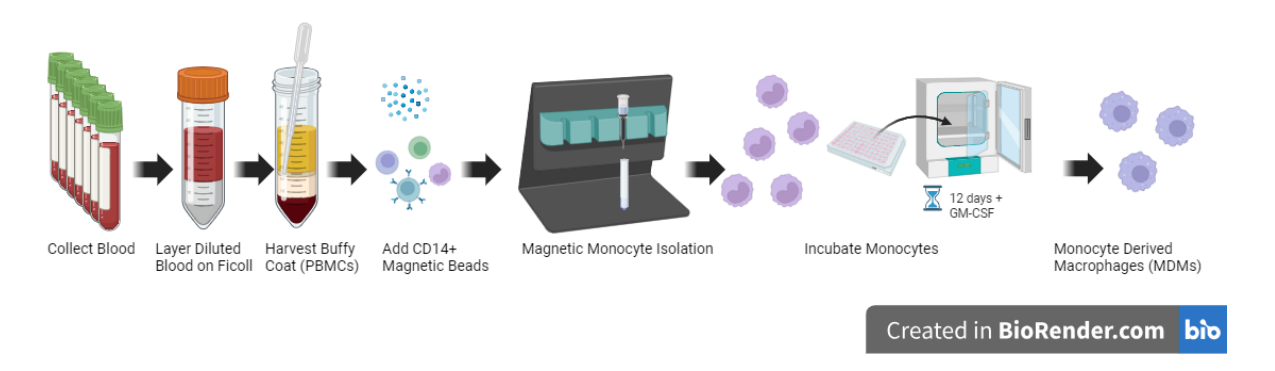


Figure 2.3 Schematic of Peripheral Blood Mononuclear Cell (PBMC) isolation and differentiation to Monocyte Derived Macrophages (MDMs)

# 2.3.1 Monocyte Derived Macrophage culture

Blood was obtained from healthy volunteers at the University Hospital Southampton, UK. The study was approved by the Hampshire A Research Ethics Committee (13/SC/0416, Leukocytes: Inflammation Model Systems (LIMS)). The inclusion criteria for healthy donors were as follows:

between the ages of 18 - 65

- able to give informed consent
- free from respiratory infections in the previous month
- not using anti-inflammatory, antibacterial or antiviral medication within the previous month

Up to 120 mL of blood was obtained from healthy volunteers into BD vacutainer lithium heparin blood collection tubes (BD Biosciences, Oxford, UK), in some cases less blood was collected to avoid excess discomfort once the blood flow slowed. Blood was mixed with an approximately equal volume of Dulbecco's Phosphate-Buffered Saline (PBS) (Sigma-Aldrich, Gillingham, UK) and slowly layered onto Ficoll Plaque-Plus (GE Healthcare, Little Chalfont, UK). The blood was centrifuged at (800 g, 30 min, 20°C) with minimal acceleration and braking. The Peripheral blood mononuclear cells (PBMC) were collected from the buffy coat at the interface between plasma and erythrocytes. The cells were washed in 50 mL PBS, centrifuged (400g, 10 min, 20°C), counted using a haemocytometer and washed again in PBS (50 mL, 400g, 5 min, 20°C). Cells were resuspended in 80 μl cold Monocyte Isolation Buffer (MIB (2mM EDTA, 0.5% (v/v) Bovine Serum Albumin (BSA) in PBS)) and 10 µL CD14+ magnetic microbeads (Miltenyi Biotec, UK) per 10<sup>7</sup> PBMCs. Cells were incubated in the fridge for 20 min and then washed with 10 mL of MIB (400g, 5 min, 4°C). Meanwhile a LS MACS column (Miltenyi Biotec) was prepared with 3 x 1 mL MIB washes. PBMCs were resuspended in 500 μl MIB per 108 of cells and added to the column. The column was washed with 3 x 3mL of MIB, removed from the magnet and isolated monocytes (CD14+ cells) eluted in 5 mL of MIB using a plunger. The eluted monocytes were made up to 10mL using PBS and counted using a haemocytometer. The cells were centrifuged (400g, 5 min, 4°C) and resuspended in 1 mL GM-CSF media (RPMI media with 2 mg/mL Lglutamine, 0.05 μ/mL penicillin, 50 μg/mL streptomycin, 0.5 μg/mL amphotericin B (all Sigma-Aldrich), 10% heat-inactivated foetal bovine serum (FBS) and 2 ng/mL GM-CSF (R&D Systems, Abingdon, UK)) per 10<sup>6</sup> cells. Cells were seeded at 5 x 10<sup>5</sup> cells per well in a 48-well plate, avoiding the outermost wells to avoid excess media evaporation. Plates were incubated at 37°C, 5% CO<sub>2</sub> for 12 days, topping the GM-CSF media up to 1 mL after 24 h and then carefully replacing the GM-CSF media every 48 h (72 h across weekends). The protocol is shown in Figure 2.3.

# 2.3.2 Macrophage-NTHi co-culture

Following differentiation of PBMC derived MDMs as described in section 2.3.1, differentiated cells were washed twice in PBS to remove media. Cells were washed for 30s with warmed EDTA-trypsin with the wash being collected. Fresh EDTA-trypsin was added, and cells incubated for 20 min at 37°C Supernatant was pipetted up and down, to help detach cells, and collected in 10% FBS media without antibiotics. MDMs were centrifuged (400g, 5 min, 20°C) and resuspended in 0.1% FBS media

without antibiotics. A 20  $\mu$ L sample of re-suspended cells was taken with 20  $\mu$ L of trypan blue and 10  $\mu$ L used to perform a viability check and cell count with a haemocytometer. MDMs remained over 97% viable post trypsinisation. The suspended cells were made up to the required concentration and added to biofilms and ALI cultures that had been cultured for 72 h as described in 2.1.5 and 2.2.5. They were then incubated for a further 24 h.

Two ratios of MDMs to NTHi cells were used on biofilms grown on an abiotic surface: 1 macrophage per 100 bacterial cells within the established biofilm (an effective MOI of 100), and 10 macrophages per 100 bacterial cells (an effective MOI of 10). As it is the macrophages being added to an established biofilm rather than bacterial cells being added to "infect" macrophages, these two ratios will be referred to as Macrophage Bacteria Ratio (MBR) for ease of reference. An MBR of 0.1 is equivalent to an MOI of 10 and an MBR of 0.01 is equivalent to an MOI of 100. MBR control will refer to the same number of macrophages that would be added to a biofilm to achieve the stated MBR, but without the biofilm, acting as a control for the macrophage response to the assay process rather than the bacteria.

The biofilms grown on plastic had a previously established bacterial count of  $3x10^6$  so to achieve an MBR of 0.1 and 0.01,  $3x10^5$  and  $3x10^4$  macrophages were added respectively (Summarised in Table 2.3). For ALI cultures, an MOI of 100 (MBR 0.01) was used which was equivalent to  $1x10^4$  MDMs.

Table 2.3 Summary of MBR and corresponding MOIs and actual number of macrophages that were added to plastic biofilms.

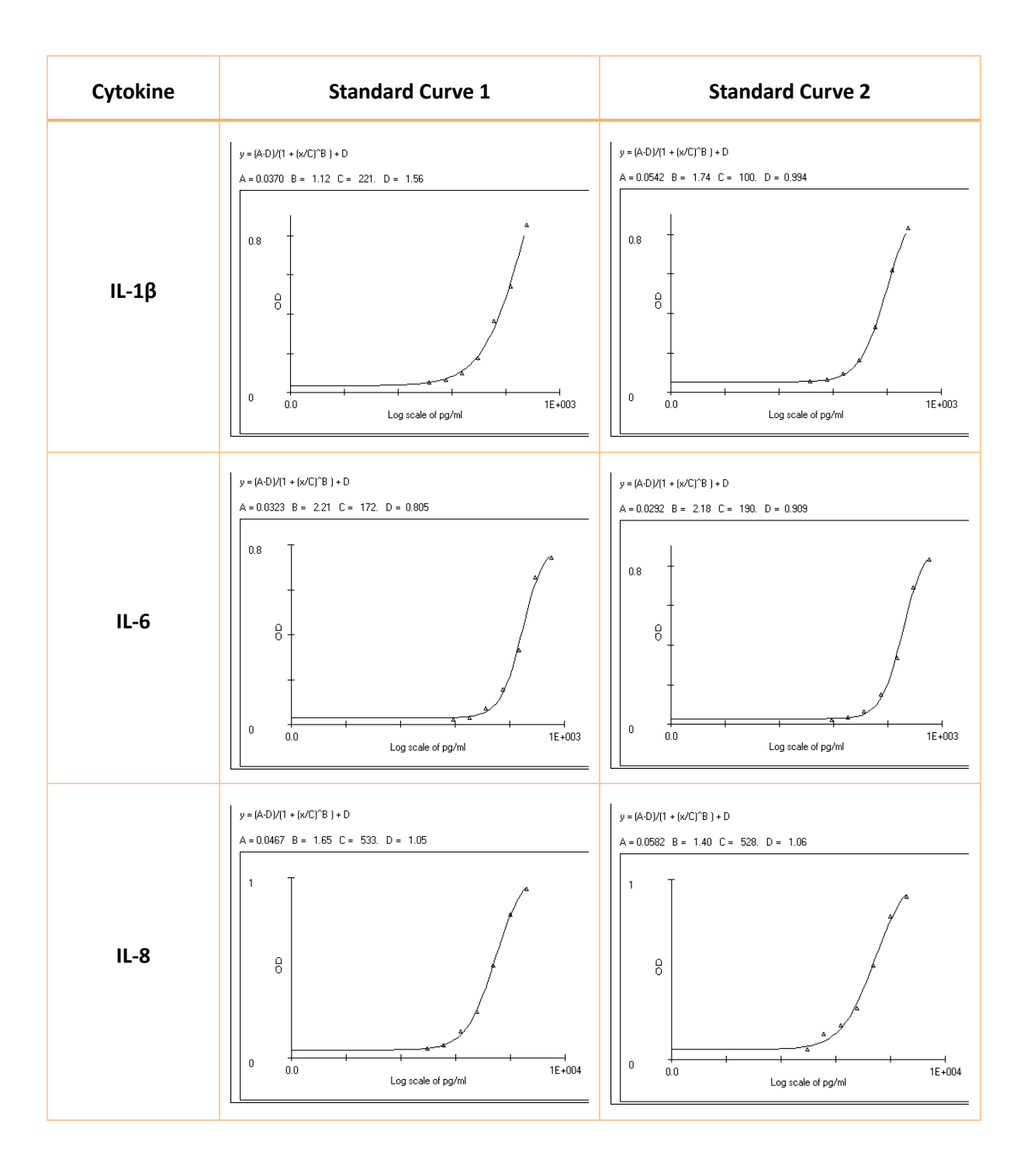
Macrophage Bacteria Ratio (MBR)	Equivalent MOI	Macrophages used on plastic	
0.1	10	300k	
0.01	100	30k	

# 2.4 Supernatant Analysis

## 2.4.1 Enzyme-Linked Immunosorbent Assay (ELISA)

To measure cytokine release from different co-cultures and their respective controls, supernatants collected from plastic biofilm cultures as described in 2.1.5 and ALI cultures (apical and basolateral) as described in 2.2.5 (Macrophage addition for both described in 2.3.2) were stored at -80°C and analysed at the same time using Enzyme-Linked Immunosorbent Assays (ELISAs).

IL-1 $\beta$ , IL-10, IL-6, IL-8 and TNF- $\alpha$  release was quantified using DuoSet ELISA kits (R&D Systems, Abingdon, Oxford) according to the manufacturer's instructions. Briefly, 96-well plates were coated with 50 $\mu$ l of capture antibody (re-constituted in PBS) overnight at room temperature. The plates were washed three times with 0.05% Tween 20 wash buffer and blocked using 1% BSA PBS reagent diluent for at least 1h at room temperature. The wash step was repeated and 50  $\mu$ L of standards and supernatant samples were added in duplicate, some diluted in reagent diluent or distilled water, as required and according to manufacturer's instructions. Samples were incubated for a minimum of 2 h at room temperature before being washed three times as before. 50 $\mu$ l of detection antibody was added for a minimum of 2 h at room temperature. The plates washed three times and 50 $\mu$ l streptavidin-horseradish peroxidase (streptavidin-HRP) was added for 20 min at room temperature, shielded from direct light. The was step was repeated and substrate solution was added for 20 min at room temperature, out of direct light. 25 $\mu$ l of stop solution (1M H<sub>2</sub>SO<sub>4</sub>) was added to each well and optical density was determined using a microplate reader at wavelength 450nm with a 550nm correction. Standard curves were calculated using a 4-parameter logistic curve fit. The resulting curves are shown in Figure 2.4.



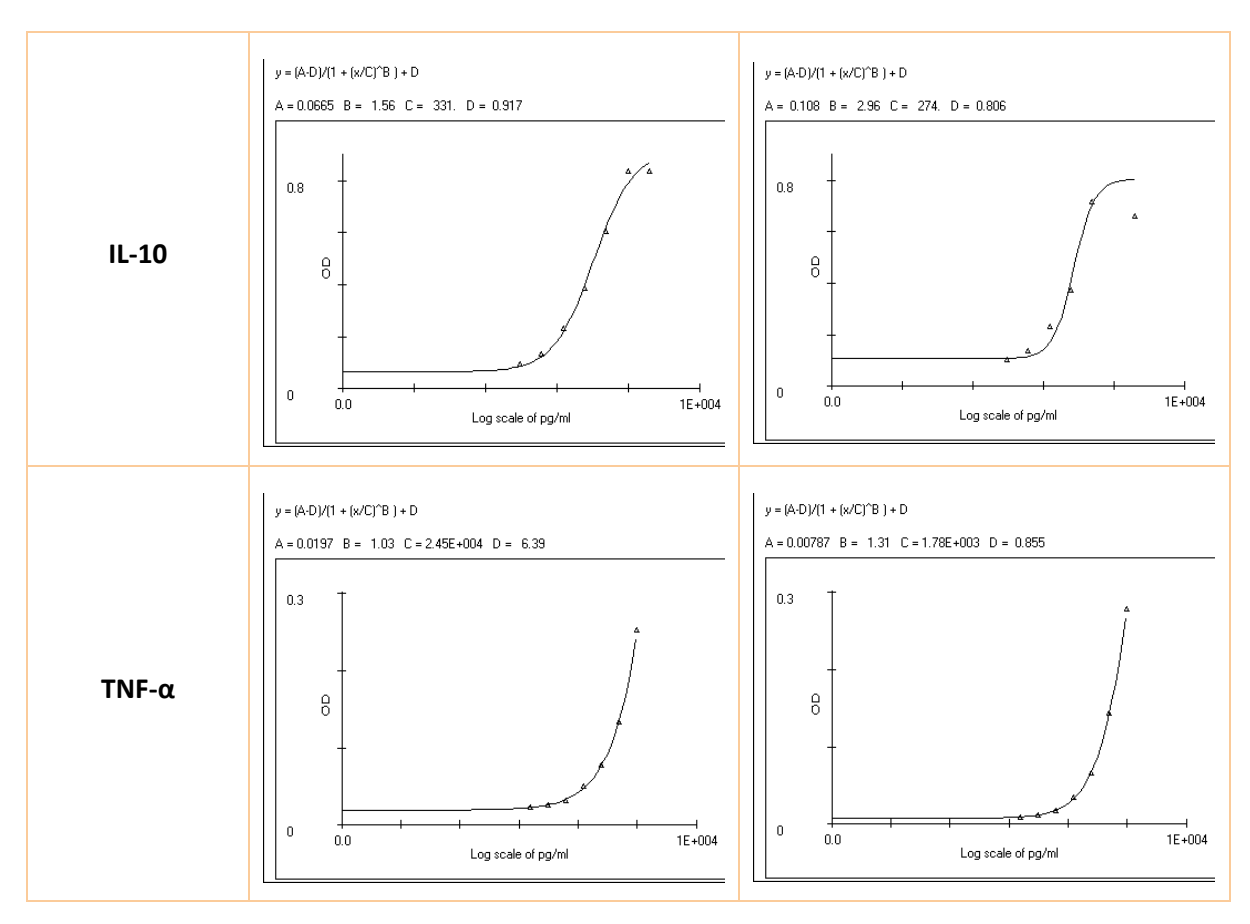


Figure 2.4 ELISA standard curves

As demonstrated in Figure 2.4, some, curves did not saturate fully meaning some OD readings were not able to be converted into the corresponding concentration. Missing data were extrapolated using the last three points of incomplete standard curves. These were used to calculate a straight-line equation, which was used to calculate a concentration based on the measured OD (as a log(concentration)) the inverse of which was taken to get the concentration. All cytokine graphs have a line denoting the maximum reading within the standard curve. All points above these were extrapolated. The detection limits are shown in Table 2.4, with dilution factors taken into account when displaying detection limits on graphs.

Table 2.4 Summary of ELISA detection limits, taking into account the dilution of samples.

Cytokine	Lower Detection Limit (pg/mL)	Upper Detection Limit (pg/mL)	Dilution factor	Effective Detection Limit (pg/mL)
IL- 8	31.3	2,000	20	626 - 40,000
IL-6	9.38	600	5	46.9 - 3,000
IL-16	3.91	250	1	3.91 - 250
TNF-α	15.6	1,000	2	31.2 - 2,000
IL-10	31.3	2,000	1	31.3 - 2,000

# 2.4.2 Lactate Dehydrogenase (LDH) assay

As a measure of cell lysis within co-cultures, the collected supernatants were analysed using a Lactate Dehydrogenase (LDH) assay kit - CytoTox 96 Non-Radioactive (Promega, USA). 50  $\mu$ L of samples were combined with 50 $\mu$ L of Cytotox 96 reagent in a 96-well plate. The plates were incubated at room temperature in darkness for 30 min followed by the addition of stop solution. Plates were tapped gently to mix the reagents fully and larger air bubbles were removed with a syringe needle. Optical density was measured using a plate reader at 490 nm wavelength. Due to limited sample availability, maximum lysis samples could not be taken so all results are displayed as OD rather than % maximum cytotoxicity.

# 2.5 Statistical Analysis

All biofilm assays had a minimum of two biological replicates, with a minimum of two technical replicates per biological repeat. 3 or more biological replicates were performed whenever possible. Each biological repeat had at least one untreated control. Biological replicates refer to assays carried out on different days, using different donors or combination of MDM and PNEC donors. Technical

replicates are described as taking place within biological repeats, this means separate wells exposed to the same treatment. Technical replicates were averaged and a mean for each biological replicate reported.

A sigmoid nonlinear least squares model was fitted to planktonic growth curves using RStudio (Version 1.3.1056) in order to identify the mid exponential time point and the maximum growth rate. Planktonic growth curves were compared by performing pairwise comparisons of timepoints using the "Compare Groups of Growth Curves (CGGC) permutation test" described in Elso et al (2004) and Baldwin et al (2007)<sup>283,284</sup>.

Data was processed using R Studio (version 2023.03.1, R version 4.3.0) and statistical analysis was performed using GraphPad Prism (Version 10, San Diego, USA) and R Studio. Both programmes were used for graphing results. Technical replicates were averaged within each biological repeat. For the purpose of graphing zero values on semi-log scale graphs (e.g. for colony forming units), 0.01 was used instead which was over 1000 fold smaller than any non-zero value in the data set. These adjusted values were labelled as 0 on the graphs.

Non-parametric tests were used throughout the analysis due to low numbers of biological replicates and Shapiro-wilk tests showing normality varying between groups. Paired data was analysed using Wilcoxon tests for two groups and Friedman tests with Dunn's post hoc analysis for multiple comparisons. Non-paired data was analysed using Kruskal-Wallis with Dunn's post hoc test for comparing multiple groups and Mann—Whitney U tests for comparing 2 groups. Levels of corelation were tested using Pearson tests. A p value of ≤0.05 was considered significant.

# Chapter 3 Characterisation of Planktonic Growth and Biofilm Formation of Non-typeable *Haemophilus* influenzae Strains

# 3.1 Introduction

Non-Typeable *Haemophilus influenzae* (NTHi) is an opportunistic bacterial pathogen that acts as a commensal of the upper airway in much of the healthy population. Due to underlying conditions, NTHi can become pathogenic and invade the lower respiratory tract. The formation of aggregates of bacterial cells encased in an extracellular matrix, termed biofilms, makes NTHi infections very persistent and difficult to treat. Biofilms form through the attachment of planktonic cells to a surface, followed by replication and matrix production. The increased difficulty to reach the bacterial cells due to the extracellular matrix make bacteria within biofilms more resistant to antibiotic treatment and targeting by the host immune response. Changes in cell metabolism linked to biofilm formation additionally reduced antibiotic efficacy as these drugs often target the cellular replication process.

Understanding the host pathogen interaction is a key factor in developing treatments, with different *in vitro* models being used to answer specific questions. There is a general push towards making *in vitro* models more representative of *in vivo* conditions. This often means increasing the complexity of the model to include more cell types such endothelial cells<sup>285</sup> and immune cells<sup>50,286</sup>. The aim of this project was to co-culture NTHi biofilms on primary epithelial cells and expose these to primary macrophages. As a preliminary step, six clinical strains of NTHi from PCD patients and a GFP-tagged NTHi strain were characterised in order to select a suitable strain to take forward for co-culturing. A laboratory GFP-strain (gifted by Dr Derek Hood) was utilised for its imaging potential as it would not need additional staining for confocal microscopy. As NTHi is very heterogenous, a range of clinical isolates were investigated in order to select one with good biofilm forming capabilities. Initially, planktonic growth was characterised to optimise biofilm inoculation protocols. Biofilms grown on an abiotic surface were characterised to show biofilm viability, biomass production and biofilm structure. The use of an abiotic surface, i.e. on culture plates, allowed for preliminary work to be done with fewer variable factors such as the epithelial cell response, at a faster rate as no cell

cultures had to be grown prior to biofilm inoculation, and at a lower cost, both in terms of samples and consumables.

The antibiotic tolerance of GFP-NTHi and clinical isolate 4 (PCD-NTHi 4) biofilms was also tested. The two antibiotics used in this work were Azithromycin and Ceftazidime. Both are commonly prescribed to patients to combat bacterial infections, both acutely<sup>287</sup> and prophylactically<sup>288</sup>. Ceftazidime is a beta-lactam, which acts through inhibiting cell wall synthesis, leading to bacterial lysis. Azithromycin is a macrolide that inhibits protein synthesis, thereby having a bacteriostatic effect.

# 3.2 Aims

## 3.2.1 Planktonic characterisation

Aim: To quantify the planktonic growth of a laboratory GFP-NTHi strain and six clinical isolates in order to inform protocol design for downstream assays.

# Objectives:

- Measure the planktonic growth of NTHi using optical density and colony forming unit
   (CFU) count over 24 h.
- Quantify the time taken for planktonic NTHi to reach the mid-exponential growth phase and determine if growth rate can be increased using different methods of inoculation.
- Correlate optical density measurements of planktonic NTHi cultures with the corresponding number of viable bacterial cells to inform future inoculation volumes.

## 3.2.2 Biofilm characterisation

Aim: To characterise biofilm development of a laboratory GFP-NTHi strain and six clinical isolates to identify the best biofilm forming strain.

# Objectives:

- Investigate NTHi biofilm formation over 72 h on polystyrene plates (an abiotic surface)
  as measured with crystal violet (CV) staining and viable bacterial cell counts. Use the
  findings to determine a suitable timepoint for future biofilm assays.
- Demonstrate GFP production of 72 hr GFP-NTHi biofilms using confocal microscopy.

- Visualise biofilm structure and viability of clinical isolates using confocal microscopy and live/dead (Syto9/PI) staining.
- Identify the most robust biofilm forming isolate of NTHi based on the structure, the biomass produced and the viability of the bacterial cells. This will inform which strain is taken forward to co-culture development.
- Determine the minimum inhibitory concentration (MIC) of clinically relevant antibiotics
   Azithromycin and Ceftazidime against planktonic GFP-NTHi and PCD-NTHi 4 then
   compare the impact of concentrations up to 100x higher on 72 hr NTHi biofilms in order
   to demonstrate increased antibiotic tolerance.

# 3.3 Results

#### 3.3.1 Planktonic Growth

Biofilm assays are typically inoculated using planktonic cultures with a standardised number of planktonic bacterial cells. It was therefore necessary to characterise the planktonic growth kinetics of NTHi strains to enable a consistent inoculation number for downstream assays.

The impact of two different inoculation techniques on planktonic growth was compared in order to maximise the planktonic growth rate, thus reaching the desired number of viable bacterial cells quickly and therefore optimising the experimental logistics of subsequent assays. Previous work by W. Walker<sup>274</sup> used planktonic cultures at the mid-exponential growth phase to inoculate biofilm assays. Building on this, the time taken by planktonic NTHi to reach the mid-exponential growth phase was quantified.

Two inoculation methods were investigated: a single colony from a chocolate blood agar (CBA) streak plate and 200  $\mu$ L from a planktonic overnight pre-culture (approx. 18 h, as described in methods 2.1.4). The optical density (OD) was measured two hours after inoculation and every subsequent hour for 12 h. A final time point was measured 24 h post inoculation. Separate planktonic cultures were inoculated in the evening, grown overnight, and measured every hour 14 to 18 h after inoculation.

For GFP-NTHi, planktonic growth curves were compared by performing pairwise comparisons of timepoints using the "Compare Groups of Growth Curves (CGGC) permutation test" described in Elso et al (2004) and Baldwin et al (2007)<sup>283,284</sup>. The inoculation method did not have a significant impact on the growth curve of planktonic GFP-NTHi (Figure 3.1). Using an overnight pre-culture led to a higher OD at every time point compared to inoculating with a single colony from a CBA plate. Inoculation with an overnight pre-culture led to a maximum OD of 0.64 while inoculating with a single colony led to a maximum OD of 0.56. A sigmoid curve was fitted to the growth curve to identify the time take to reach the mid exponential growth phase. Cultures inoculated from a plate took 6.8 h while those inoculated using an overnight culture took 6.2 h, a decrease of 36 min.

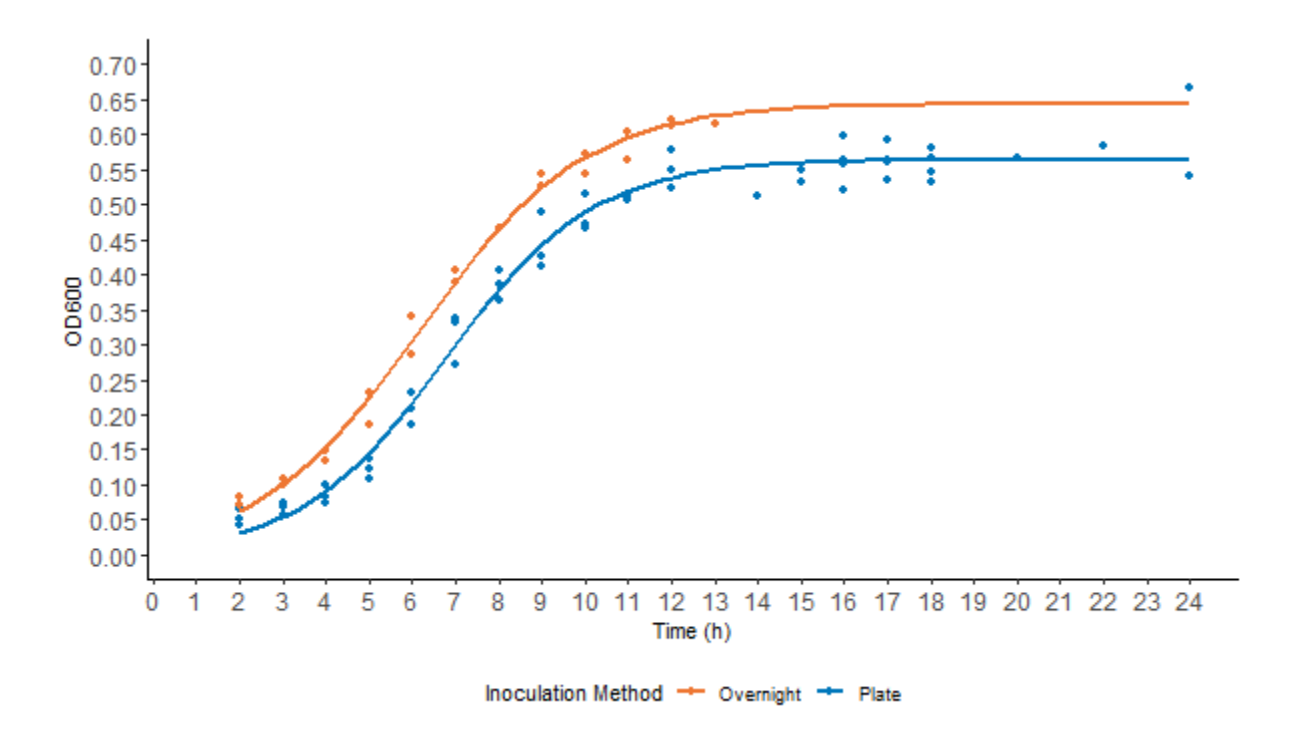


Figure 3.1: GFP-NTHi planktonic growth curves comparing inoculation method. Planktonic growth was measured using optical density (OD600) readings over a 24 h period. Cultures were inoculated either with 200  $\mu$ L of a planktonic pre-culture grown overnight (Orange) or a single colony selected from a chocolate agar plate prepared the day before (Blue). Overnight: n = 2 for 2-12 h, n = 1 for 13 & 24 h. Plate: n  $\geq$  2 for 2-12 h, n  $\geq$  4 for 16-18 h, n  $\geq$  1 for 14-15 and 20-24 h. Datapoints represent separate biological replicates and are shown as means of a minimum of duplicate cultures, lines represent a fitted non-linear model. The difference between the inoculation methods was not statistically significant (Compare Groups of Growth Curves permutation test)

Planktonic growth of the two clinical isolates acquired first, PCD-NTHi 1 and PCD-NTHi 2, was investigated in a similar manner, comparing the growth rate between different inoculation methods. The clinical isolates took between 8 and 12 h to reach mid exponential growth (Figure 3.2). Using an overnight culture to inoculate the planktonic culture decreased the time to reach mid exponential growth by 1.4 h and 2.5 h for PCD-NTHi 1 and 2 respectively. Both PCD-NTHi 1 and PCD-NTHi 2 reached a similar maximum OD (0.64 and 0.61 respectively). Cultures inoculated using an overnight culture were not assessed past 13 h since no increase in growth rate was identified in the exponential phase. As the aim of this section of work was to identify a logistically viable biofilm inoculation protocol, further investigation of an overnight inoculated planktonic culture was deemed superfluous.

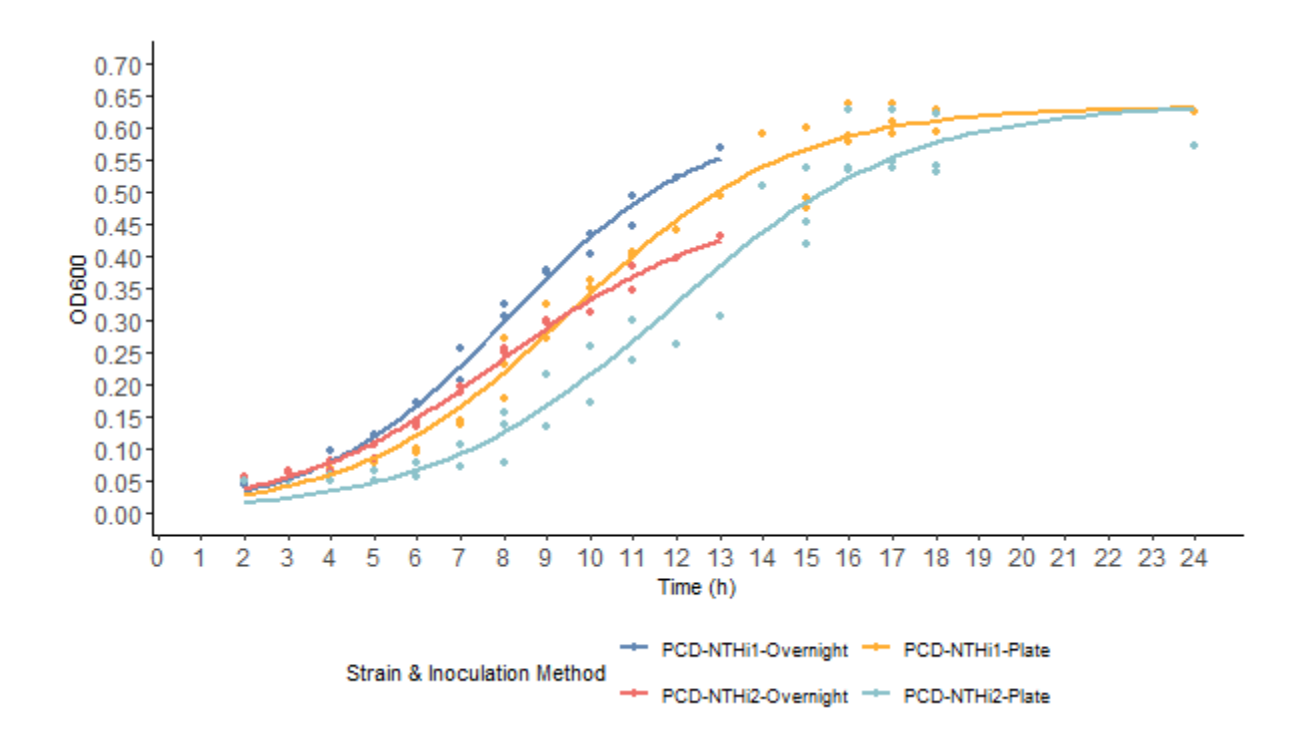


Figure 3.2 Growth curves of clinical NTHi isolates from PCD patients comparing inoculation method. Planktonic growth was measured using optical density (OD600) readings over a 24-hour period. Two clinical strains were used, PCD-NTHi 1 (Dark Blue & Yellow) and PCD- NTHi 2 (Orange & Teal), for both cultures were inoculated either with 200 μL of a planktonic pre-culture grown overnight (Dark Blue – PCD-NTHi 1, Orange – PCD-NTHi 2) or a single colony selected from a chocolate agar plate prepared the day before (Yellow – PCD-NTHi 1, Teal – PCD-NTHi 2). Overnight: n = 2 for 2-11 h, n = 1 for 12-13 h. Plate n = 2 for 2-11 h, n = 3 for 15-18 h, n = 1 for 12-14 h and 24 h. Datapoints represent separate biological replicates and are shown as means of duplicate cultures. The difference between the inoculation methods was not statistically significant for either strain (Compare Groups of Growth Curves permutation test).

Due to the time taken by planktonic NTHi to reach the mid exponential growth phase being over 6 h, regardless of inoculation method, it was deemed logistically unfeasible to use mid exponential cultures to inoculate biofilm assays. Instead, planktonic cultures grown overnight to a stationary growth phase were investigated as an alternative to growing planktonic cultures for 6 h on the day of setting up downstream assays.

The OD of planktonic GFP-NTHi cultures grown overnight (14-18 h) to the stationary growth phase was measured and the corresponding CFUs enumerated to determine the number of viable cells in

CFUs/mL as described in methods 2.1.4 (Figure 3.3). Time was not found to have a significant impact on OD or number of bacterial cells (Spearman). Furthermore, no significant correlation between OD and CFUs was identified (Spearman). The average OD and number of bacteria across all planktonic GFP-NTHi cultures grown overnight (14- 18 h) was  $0.548 \pm 0.032$  and  $7.40 \pm 1.93 \times 10^8$  CFUs/mL respectively.

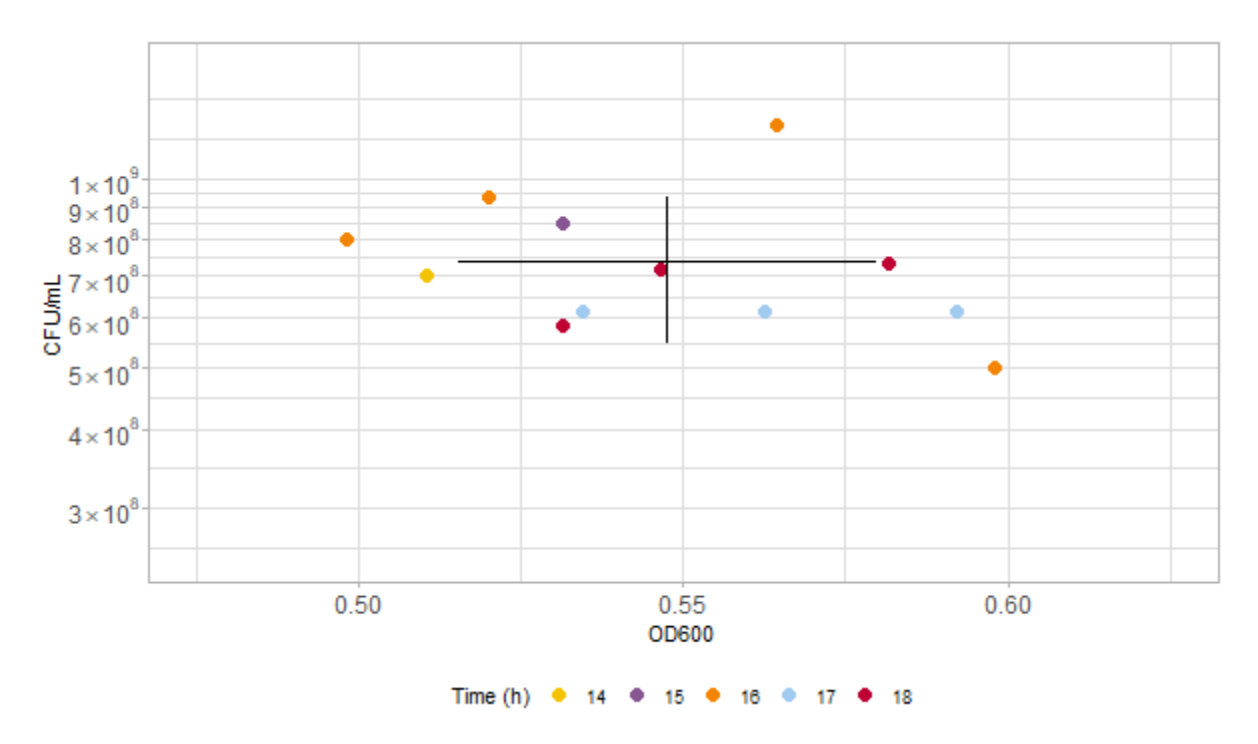
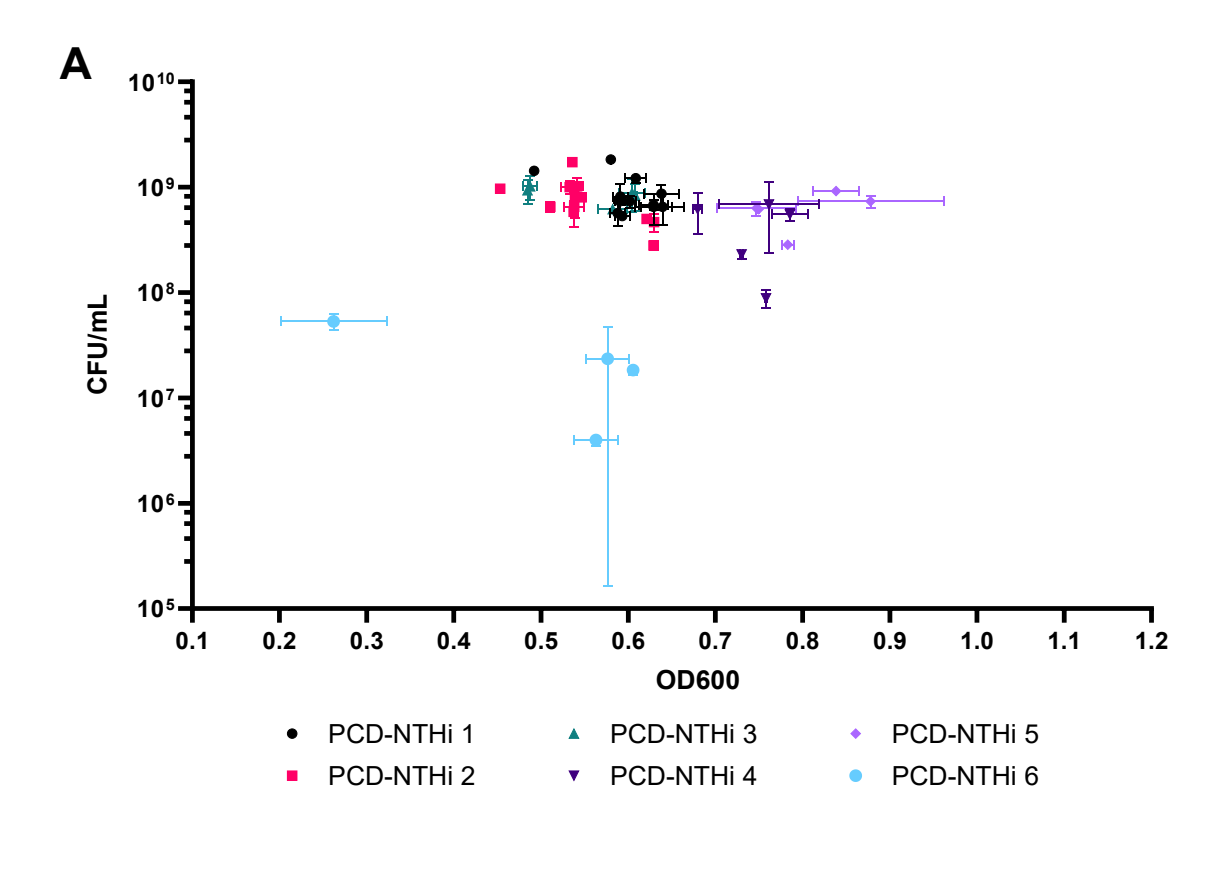


Figure 3.3: Stationary phase regression of GFP-NTHi planktonic cultures grown overnight. Planktonic cultures were inoculated using a colony form a plate and optical density and CFU counts were measured at a range of time points (14-18 h) during incubation. Time points are differentiated by colour, see figure legend for details. n ≥ 3 for 16-18 h, n = 1 for 14-15 h. Datapoints represent separate biological replicates and are shown as the means of duplicate cultures. The mean and standard deviation of all time points is represented by the black lines.

As the planktonic growth of the two clinical isolates of NTHi was equally unsuitable for using cultures in the exponential growth phase as GFP-NTHi, the relationship between OD and the number of viable bacteria (CFUs/mL) during the stationary growth phase was characterised in the same way as for the GFP-NTHi strain. Having previously identified that time had no significant impact on either variable, cultures were measured in the same 14-18 h time frame as GFP-NTHi. As more clinical strains were obtained at this point in time, this was done for six clinical isolates in total (PCD-NTHi 1-6).



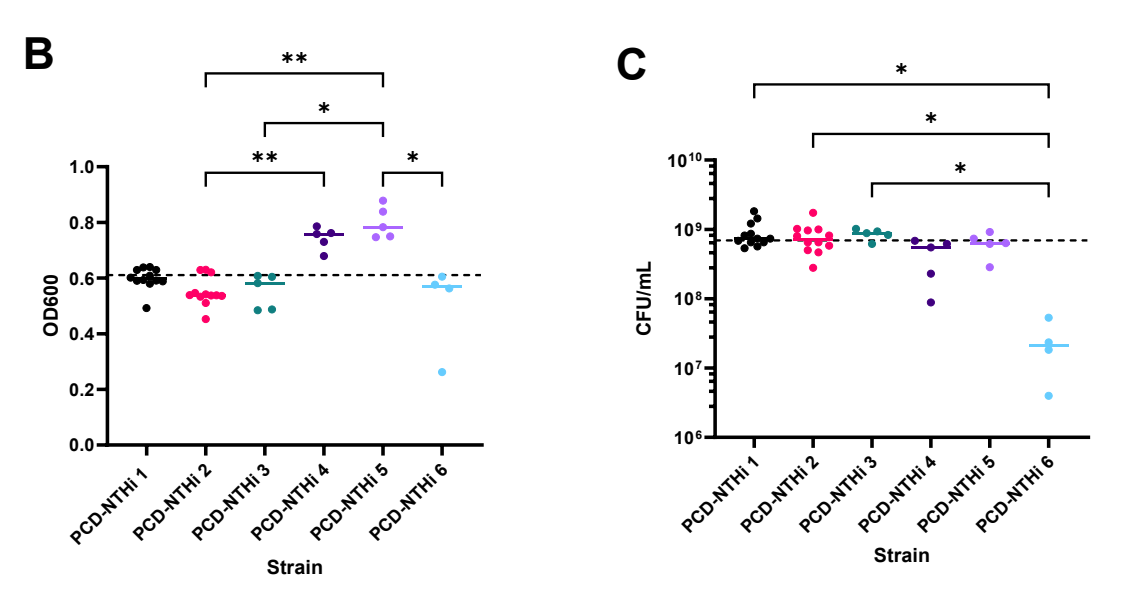


Figure 3.4 Stationary phase planktonic cultures of six clinical NTHi isolates characterised by optical density and CFU counts. Media was inoculated using a colony from an agar plate and incubated for up to 18 h with readings being taken between 14 – 18h. PCD-NTHi strains are shown in different colours, see figure legend for details. n = 12 for PCD-NTHi 1 & 2, n = 5 for PCD-NTHi 3-5, n = 4 for PCD-NTHi 6. Data points represent separate biological

replicates and are shown as means of duplicate cultures with the exception of two points for PCD-NTHi 1 & 2 (single cultures). (A) shows the mean OD versus the CFU density for each biological replicate with error bars showing SD. Only PCD-NTHi 2 had a correlation between OD and CFU (Spearman, p < 0.05) (B) shows OD by strain, with solid lines depicting the median for each strain. The dashed line represents the global mean OD (0.611). (B) shows the mean CFU density by strain, solid lines depict the median and the dashed line shows the average across all strains (6.96x108 CFU/mL). The impact of strain on OD and CFU was analysed using Kruskal-Wallis with Dunn's post hoc test (only significant comparisons shown - \*p<0.05, \*\*p<0.01)

The number of viable bacteria and the corresponding optical density of the planktonic culture is shown in Figure 3.4A, breakdowns by strain of both metrics (optical density and bacterial cell density) are shown in Figure 3.4B and Figure 3.4C. PCD-NTHi 2 showed a significant correlation between OD and CFUs/mL (Spearman test, p < 0.05). All other strains tested did not demonstrate a significant correlation. The heterogeneity of strains had a significant effect on the number of CFUs/mL in each planktonic culture during the stationary growth phase (Kruskal-Wallis, p < 0.005) as well as on OD (Kruskal-Wallis, p < 0.0001). Four strains grew to an optical density of approximately 0.5 (PCD 1, 2, 3 & 6). The other two strains growing to an optical density above 0.7 (PCD 4 & 5) as shown in Figure 3.4B. PCD-NTHi 6 showed a greater variation on OD across biological replicates (range of 0.34 compared to 0.11 – 0.18 across the other strains) as well as a lower number of bacterial cells. All isolates, except PCD-NTHi 6, were found to grow to a viable cell population of comparable magnitude, ranging from 4 - 9 x108 CFUs/mL in an overnight planktonic culture (Figure 3.4C).

#### 3.3.2 Biofilm Formation

Having established a biofilm inoculation protocol, the biofilm formation of GFP-NTHi, PCD-NTHi 1 and PCD -NTHi 2 was investigated. This work was done on an abiotic surface to initially demonstrate GFP-NTHi was capable of forming biofilms before moving on to co-culture assays. Previous work<sup>274,275</sup> had used a 72 h timeframe for biofilm assays, therefore 24 h increments up to 72 h were selected to characterise the biofilm formation. The aim was to determine a suitable timepoint for future biofilm assays based on the development of a robust biofilm. Viability, biomass, antibiotic tolerance and visualisation through microscopy were used to assess this aim.

Crystal violet (CV) staining was used for initial confirmation of biofilm growth and as a quantification of the total biomass produced by GFP-NTHi, PCD-NTHi 1 & 2 as described in methods 2.1.6. CV is a cationic dye that binds to the bacterial cell surface, regardless of viability, and components of the extracellular matrix to provide a measurement of total biomass. Following staining, the presence of biofilms was visible to the naked eye, confirming the capacity for biofilm formation over 72 h.

The length of incubation was shown to have a significant effect on the biomass formation of GFP-NTHI (Friedman, p<0.005), but not on PCD-NTHi 1 & 2 (Figure 3.5). The median OD increased by 131% for GFP-NTHi and 80% and 18% for PCD-NTHi 1 & 2 respectively.

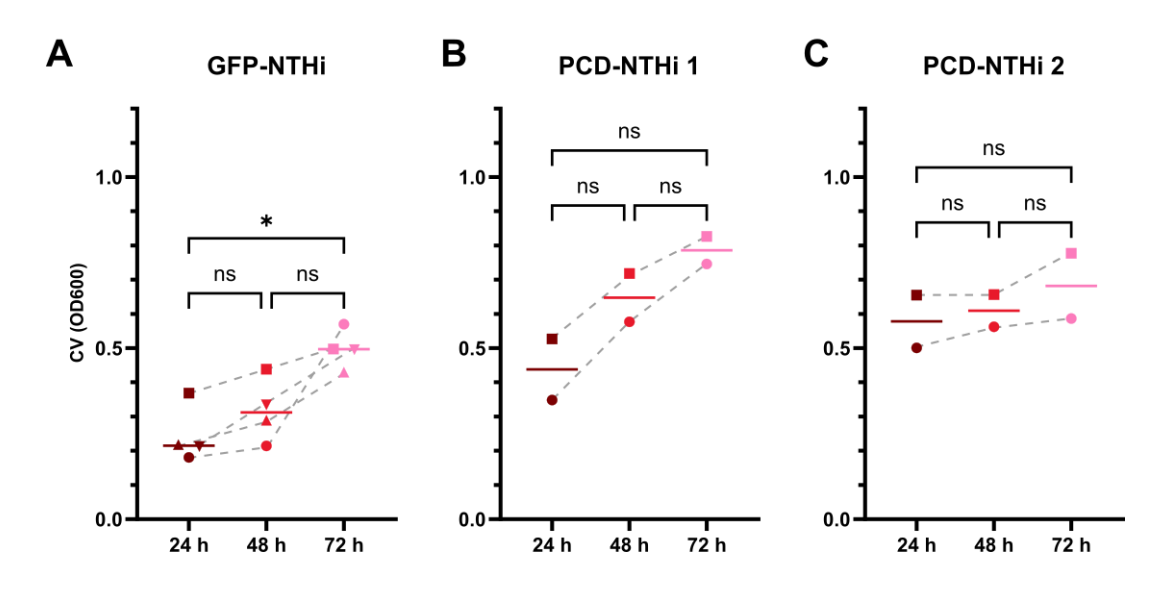


Figure 3.5: Biomass of produced by NTHi strains after 72 h as measured using CV staining. Stationary phase planktonic cultures were used to seed culture plates and incubated statically up to a stated time point. Biofilms were then washed and stained followed by stain quantification through OD measurements. Strains used were (A) GFP-NTHi (n = 4), (B) PCD-NTHi 1 (n = 2) and (C) PCD-NTHi 2 (n = 2). Datapoints are shown as means of at a minimum of duplicates (GFP-NTHi in triplicates) with separate biological replicates shown as different shapes joined by dashed grey line, solid lines depict the median. Data was analysed using Friedman tests with Dunn's post hoc analysis (\*p<0.05).

In conjunction with measuring the biomass produced by NTHi biofilms over a 72 h period, the bacterial viability was quantified using culturable cell counts by scraping surface associated cells that remained after washing the biofilm and performing a serial dilution to obtain a CFU count as described in methods section 2.1.7.

There was no significant difference in the number of viable cells recovered from GFP-NTH and PCD-NTHi 1 & 2 biofilms at each timepoint (Figure 3.6). Viable cell counts were in the magnitude range of  $10^7 - 10^8$  CFUs/cm<sup>2</sup> across all time points.

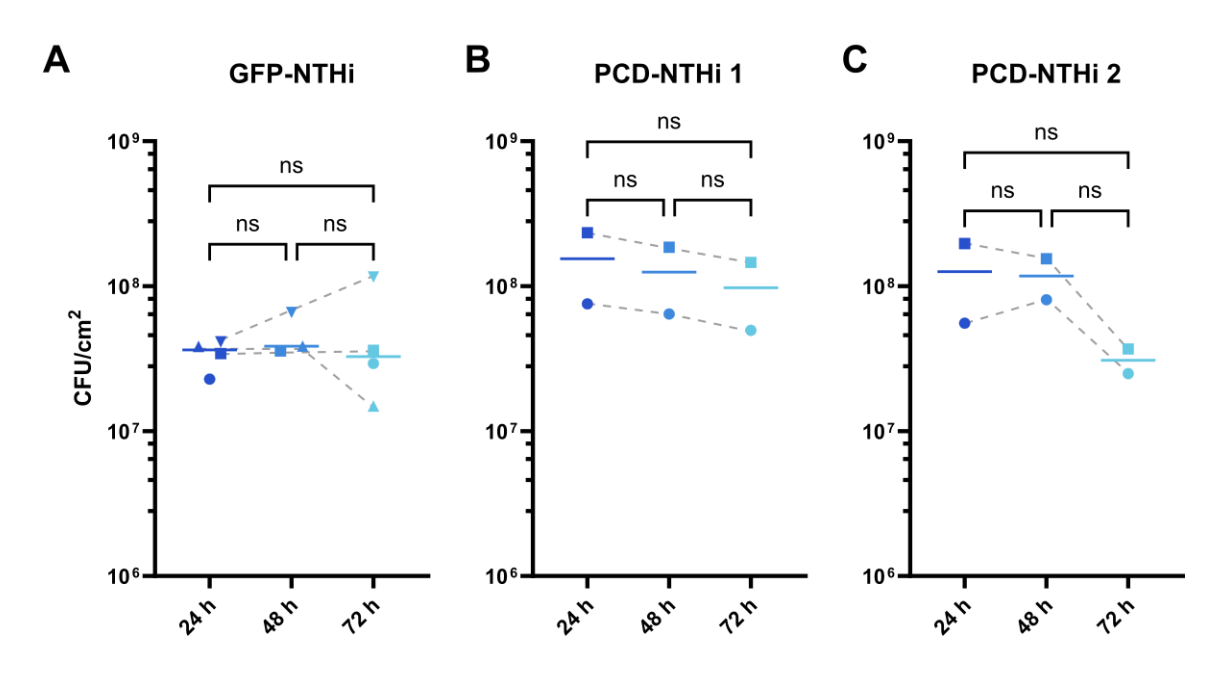


Figure 3.6: Viable cells in NTHi biofilms grown over 72 h on an abiotic surface. Biofilms of three strains were inoculated using 200 μL of overnight planktonic culture in sBHI. At each timepoint, biofilms were washed, cells were resuspended and colony forming units enumerated. Data points represent separate biological replicates (joined by grey dashed lines) and show means of technical duplicate (GFP-NTHi in triplicate) wells with solid lines showing medians. (A) GFP-NTHi (n = 4, 3 for 48 h time point). (B) PCD-NTHi 1 (n = 2) (C) PCD-NTHi 2 (n=2) No statistically significant differences were observed between timepoints (Friedman with Dunn's Post hoc analysis (Kruskal-Wallis for GFP-NTHi))

## 3.3.3 Green Fluorescent Protein Production

Having determined 72 h to be a suitable time point at which to assess GFP-NTHi biofilm formation, confocal microscopy was used to visualise the ultrastructure and to confirm the GFP fluorescence of the NTHi strain as described in methods 2.1.8. Additionally, computational analysis of captured images was used to complement and validate the CV and CFU findings. Confocal microscopy made it possible to obtain three dimensional images without disrupting the biofilm layer, enabling the ultrastructure to be characterised.

Biofilms were grown for 72 h, followed by a wash to remove any non-adhered, planktonic bacteria. The biofilm was then stained with Syto9 and propidium iodide, a combination of stains commonly used to indicate bacterial viability. Syto9 enters viable cells with intact membranes, binds to nucleic acids and emit green fluorescence when excited at a 488 nm wavelength causing them to fluoresce green. Propidium iodide is only able to pass through a membrane with increased permeability, commonly indicating a loss of viability, displacing the Syto9 and causing far red fluorescence emission when excited at a wavelength of 493 nm.

As it was not established whether GFP-NTHi fluorescence would be sufficient to successfully visualise the biofilm using confocal microscopy both unstained and stained GFP-NTHi biofilms were imaged. Though dead bacteria would no longer be producing GFP, residual signals may still be detected from GFP produced before loss of viability. Both stained and un-stained biofilms showed aggregates of bacteria on a thin lawn (Figure 3.7).

The green staining of the non-stained biofilm appeared sparser than the stained biofilm, suggesting that not all cells which would stain with Syto9 were producing detectable levels of GFP. Computational analysis of the detected biovolume using IMARIS image analysis software was used to quantify the biovolume for three fields of view for stained and unstained GFP-NTHi biofilms. Mean GFP staining at  $1.16 \pm 0.54 \times 10^4 \, \mu m^3$  per field of view was seen in unstained biofilms compared with  $2.88 \pm 1.00 \times 10^4 \, \mu m^3$  for Syto9 staining, a reduction of approximately 60%. Mean and maximum thickness of detected biovolume showed a similar reduction, going from  $5.81 \pm 1.62 \, \mu m$  to  $1.95 \pm 0.57 \, \mu m$  and  $1.84 \, \mu m$  to  $1.85 \, \mu m$  for mean and maximum height respectively.

Propidium iodide staining was seen on images of stained biofilms (Figure 3.7B). The average total biovolume staining (Syto9 and propidium iodide staining) was  $5.9 \pm 1.2 \times 10^4 \, \mu m^3$  with 49% consisting of "live" Syto9 staining.

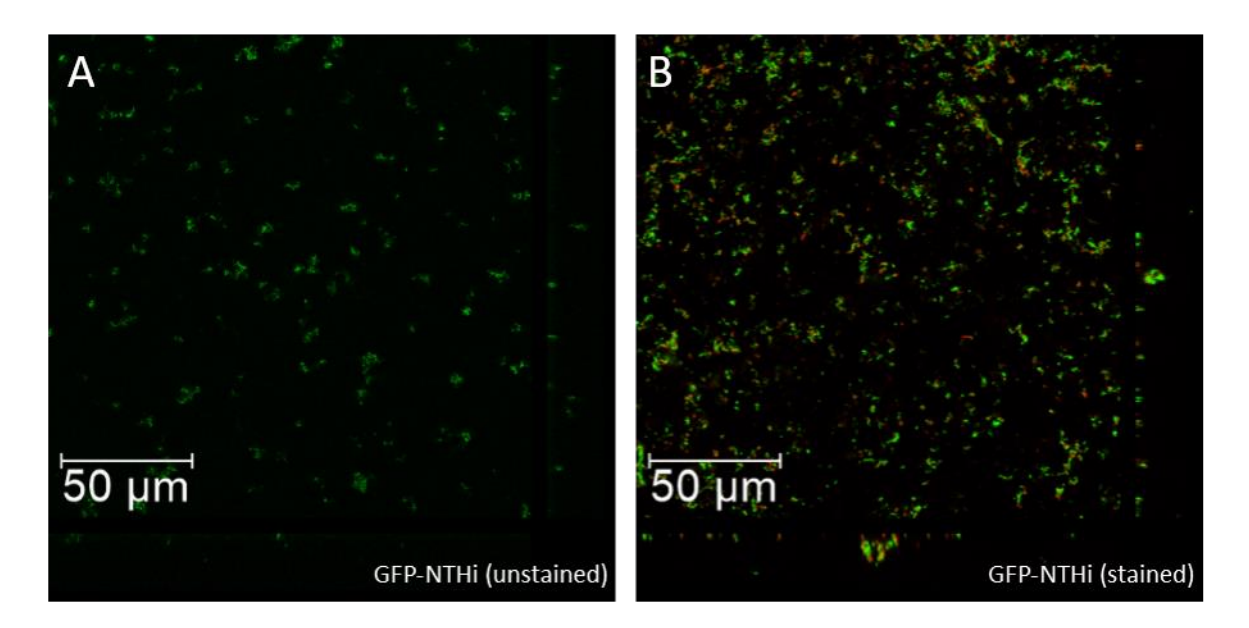


Figure 3.7: Representative orthogonal sections of confocal images GFP-NTHi biofilms grown for 72 h on an abiotic surface. Biofilms were inoculated with 200 μL of overnight planktonic culture and grown in sBHI for 72 h before being washed, stained with live/dead stain, and fixed with 60 % glycerol. (A) Unstained bacteria were imaged for GFP expression (B) bacteria were stained with Syto9 and propidium iodide. Images were taken on a Leica SP8 laser scanning confocal microscope (63x (Oil) objective). Stained images were recorded three separate occasions (biological replicates, n=3) with three random FOVs recorded each time. Non-stained images were recorded on one occasion with four random FOVs.

# 3.3.4 Comparing Clinical Isolates

With biofilm formation by the clinical isolates PCD-NTHi 1 & 2 confirmed after 72 h, four additional strains of NTHi were obtained from PCD patients and biofilm formation was compared in order to find the optimal candidate strain to take forwards on to an epithelial cell co-culture.

First, all strains were assessed for biomass formation at a 72 h (Figure 3.8A). Strain was found to significantly affect the total biomass formed after 72 h, though post hoc analysis did not identify any one significant comparison. PCD-NTHi 4, 5 and 6 were found to produce the most biomass out of the strains investigated. Viability of 72 h biofilms of all six clinical strains was compared. Biofilms of all strains contained a similar number of culturable cells after the 72 h period, with medians ranging from  $1.8 \times 10^7$  to  $9.8 \times 107$  CFUs / cm² (Figure 3.8B). No statistical difference in the number of culturable cells was found between the strains.

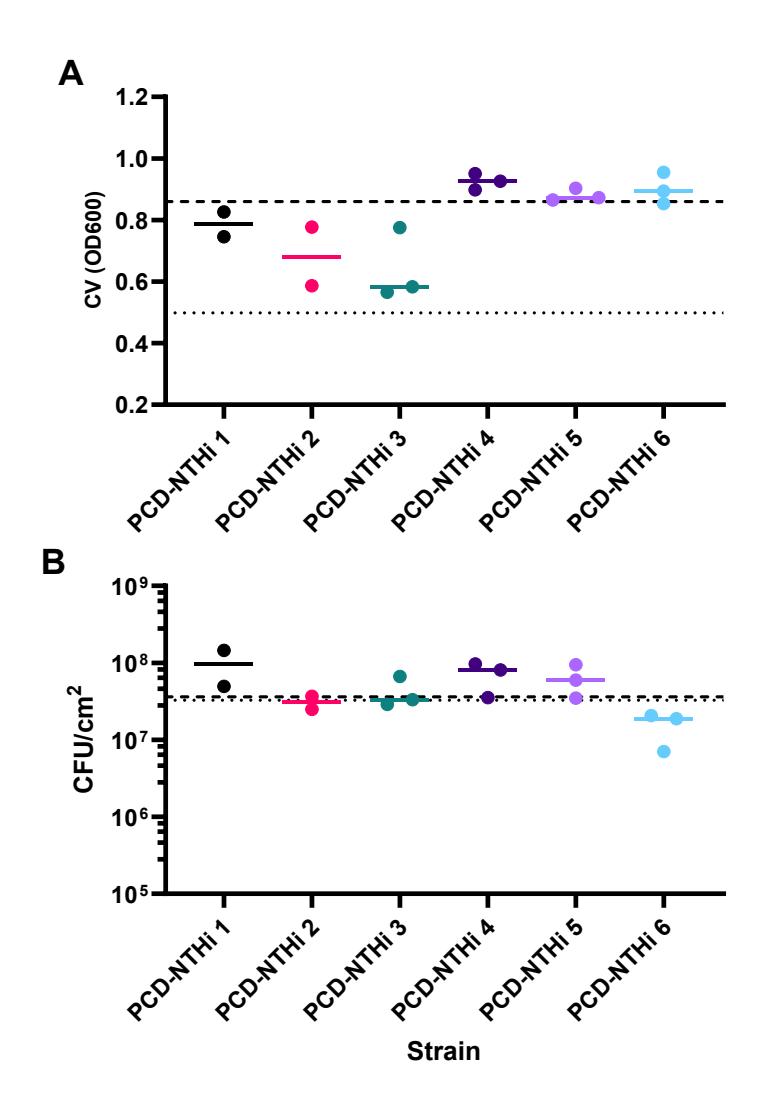


Figure 3.8 Characterisation of NTHi biofilms after 72 h of incubation on an abiotic surface. Planktonic overnight cultures of six clinical NTHi isolates from PCD patients were cultured in sBHI. After 72 h, biofilms were washed, and either (A) biomass was quantified using CV staining or (B) bacteria were resuspended and CFUs enumerated. Data points represent separate biological replicates (PCD-NTHi 1 & 2: n = 2, PCD-NTHi 3-6: n = 3), and are shown as means of duplicate wells solid line depict median. Dashed line represents global median of across all strains (0.86 for biomass, 3.61 x 10<sup>7</sup> for CFUs). The dotted lines represent the median biomass of GFP-NTHi for reference (0.50 biomass, 3.26 x 10<sup>7</sup> CFUs). The Strain had a significant effect on biomass formed (Kruskal Wallis p < 0.05) but post hoc analysis (Dunn's) did not identify a significant pair comparison. No significant difference was found in CFUs recovered (Kruskal Wallis)

After the confirmation of all six clinical NTHi isolates forming biofilms after 72 h through biomass and culturable cell readouts, confocal microscopy was used to visualise these validate CV and CFU readouts. Computational image analysis was used to quantify biofilm parameters for each recorded field of view. Images were collected and analysed as described in methods 2.1.8.

A high level of heterogeneity in structure was observed between the biofilms formed by the clinical NTHi isolates. Cross sections of biofilms formed by PCD-NTHi 1, 2 & 3 showed a lower density of cells compared with PCD-NTHi 4, 5 & 6 (Figure 3.9). Visual inspection suggested a greater number of viable cells, in biofilms formed by PCD-NTHi 1 & 5 and to a lesser extent PCD-NTHi 2 & 3. These biofilms show an equal distribution of cells staining "live" and "dead". In contrast, PCD-NTHi 4 biofilms formed a dense layers of cells three distinct layers could be seen. Yellow staining near the substratum, suggesting of mixed viability (red and green staining overlapping), followed by a less viable layer with more red staining and finally a layer of green staining viable cells on surface. The PCD-NTHi 6 biofilm appeared to consist predominantly of non-viable red staining cells, with individual viable green staining cells distributed throughout the comparatively thick, dense biofilm. Visual differences in density could also be observed, with the biofilm of PCD-NTHi 3 containing more gaps than biofilms formed by PCD-NTHi 4, 5 and 6.

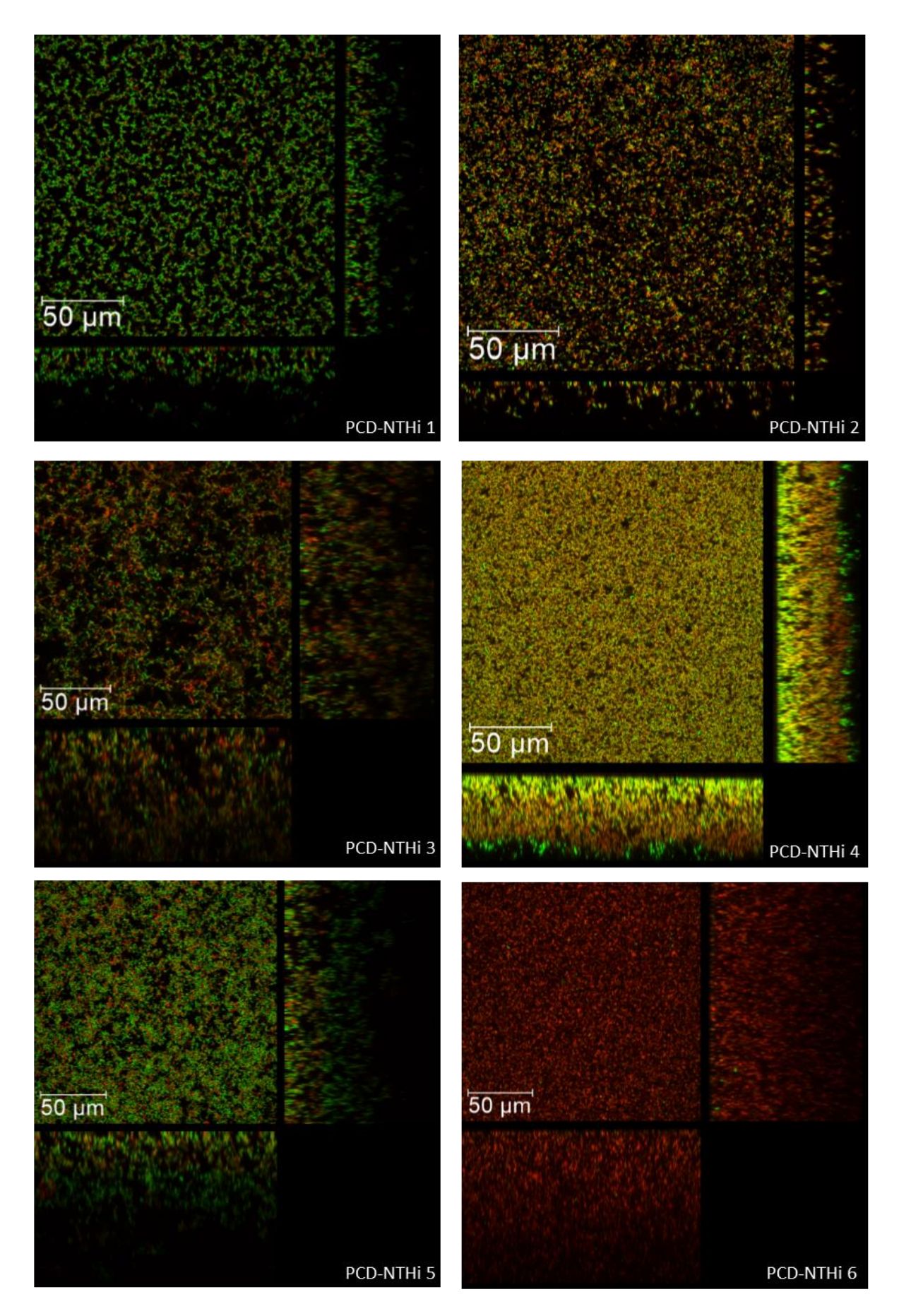


Figure 3.9 Representative orthogonal sections of CLSM images of NTHi biofilms after 72 h of incubation. 6 clinical isolates obtained from PCD patients were used. Following incubation, biofilms were washed and stained with the live/dead stains (Syto9 and propidium iodide, Green: live, Red: dead). The main panel shows orthogonal views from one x-y plane towards the base of the biofilm and the side panels below and right show the x-z and y-z planes respectively (the size of the panel reflects biofilm thickness).

Images were taken using a Leica SP8 confocal laser scanning microscope using a x63 (oil immersion) objective. Images are representative of n = 4 biological replicates, each with 3 FOVs.

IMARIS image analysis software was used to analyse the confocal images. Biovolume was calculated based on the total stained volume within each image (Figure 3.10A). PCD-NTHi 4 produced the largest amount of biovolume (median  $1.93 \times 10^6 \, \mu m^3$ ) while PCD-NTHi 2 produced the lowest (median  $2.84 \times 10^5 \, \mu m^3$ ). Strain was found to have a significant impact on biovolume.

The volumes of cells staining green ("live") and red ("dead") were analysed separately, giving an indication of overall viability of the biofilm. PCD-NTHi 5 had the highest viability (65%) and PCD-NTHi 6 the lowest (34%), though the difference between "live" and "dead" staining was not found to be statistically significant for any strain (Wilcoxon). All other strains had a comparable viability ranging from 48 – 55% (Figure 3.10B).

Besides viability, image analysis was also used to characterise the morphology of the PCD-NTHi biofilms. The maximum and average thickness was quantified for each field of view and averaged across each biological repeat (Figure 3.10C & D). PCD-NTHi 3 was found to form the thickest biofilm with a median maximum height of 107  $\mu$ m and a median mean height of 63.6  $\mu$ m. The thinnest biofilm formed by a clinical isolate was PCD-NTHi 2 with a median maximum thickness of 30.2  $\mu$ m and a median mean thickness of 12.0  $\mu$ m. Strain had a significant impact on biofilm thickness both on the maximum and the mean thickness.

In order to numerically compare the surface of the biofilms, the ratio between the average and the maximum thickness was calculated for each field of view (Figure 3.10E). A higher ratio would imply a higher similarity between the mean and the maximum height and therefore a smoother biofilm surface. PCD-NTHi 4 was found to have the highest ratio (median 0.68) while PCD-NTHi 2 had the lowest amongst clinical isolates (median 0.39). GFP-NTHi biofilms had a median ratio of 0.31.

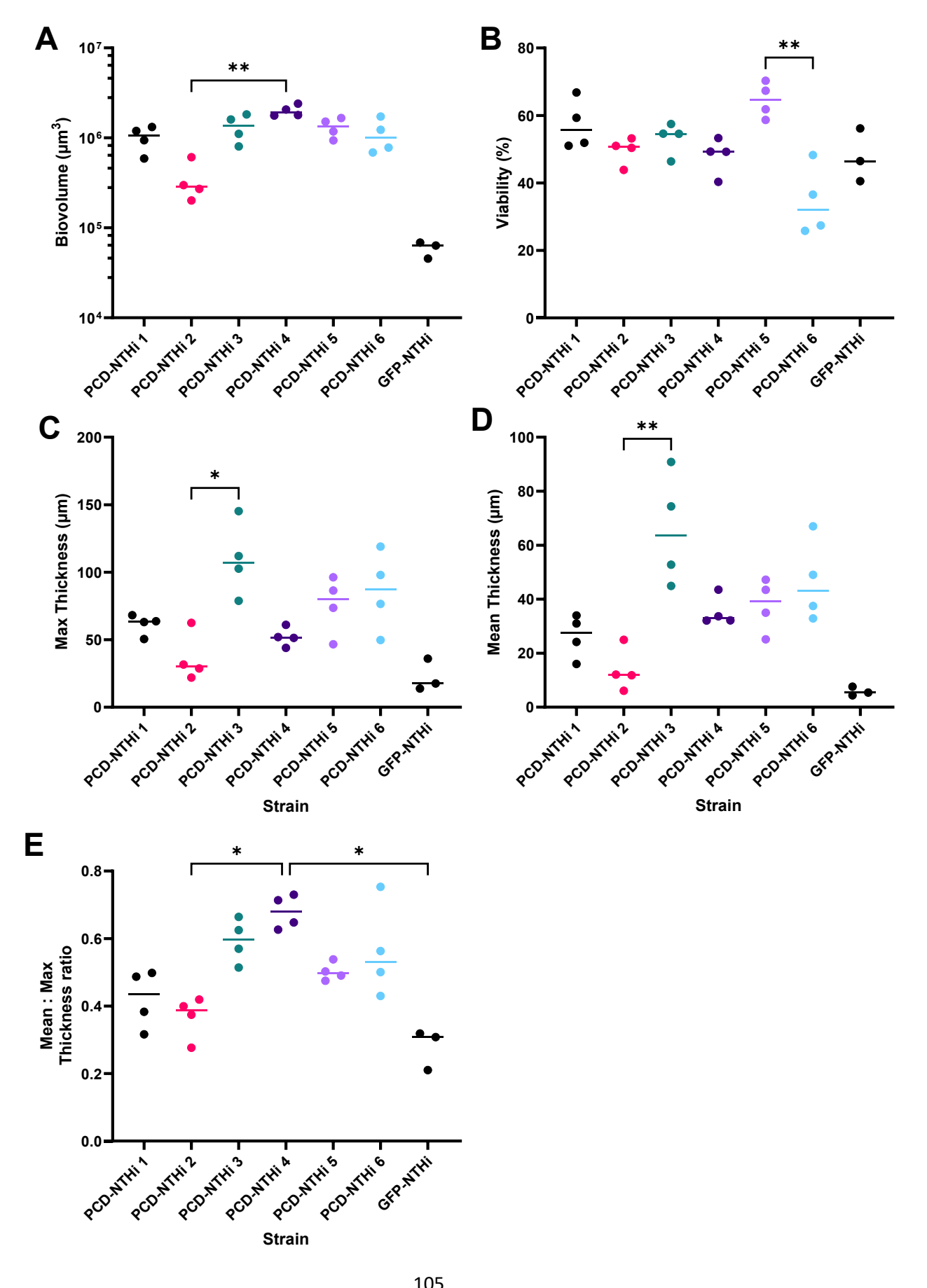


Figure 3.10 Biovolume of biofilms formed by clinical NTHi isolates from PCD patients. Biofilms were grown for 72 h, stained using live/dead stain (Syto9 and propidium iodide) and imaged using SP8 laser scanning confocal microscopy. Images were analysed using IMARIS image analysis software and stained biovolume was quantified. Data points are shown as means of three random FOVs from n = 4 separate biological replicates (n = 3 for PCD-NTHi 6), solid lines show median. (A) Total biovolume (B) Viability as calculated from live and dead staining biovolumes. (C) Maximum height from substratum (D) Mean height from Substratum (E) Ratio of mean to maximum thickness as an indicator of biofilm surface smoothness. Data were analysed using Kruskal Wallis with Dunn's post hoc analysis, strain had a significant effect on biovolume formed, viability, thickness, and surface (graphs show significant comparisons only).

## 3.3.5 Antibiotic Tolerance

Having demonstrated biofilm formation by GFP-NTHi and PCD-NTHi 4 after 72 h, the antibiotic tolerance of these biofilms was investigated as described in methods 2.1.10. Antibiotic tolerance is a key hallmark of biofilms, contributing to the difficulty of treating persistent biofilm infections. Planktonic cultures and biofilms were exposed to the commonly used antibiotics azithromycin and ceftazidime; a macrolide and a third-generation cephalosporin respectively. The Minimum Inhibitory Concentration (MIC) of both antibiotics for planktonic GFP-NTHi and PCD-NTHi 4 cultures were determined first using e-test strips, results are shown in Table 3.1.

Table 3.1 MICs of azithromycin and ceftazidime for two strains of planctonic NTHi, GFP-NTHi and cliical isolate PCD-NTHi 4 in  $\mu g/mL$  (n = 3)

	Azithromycin	Ceftazidime
GFP-NTHi	2	0.064
PCD-NTHi 4	4	0.47

NTHi biofilms were grown for 72 h before being incubated with antibiotics concentrations 1, 10 and 100 times the identified planktonic MIC for 24 h and assessed using CV and CFU counts to identify any effect on biomass and cell culturability (as in indicator of viability) respectively. A control biofilm was incubated with no antibiotics alongside the treated biofilms.

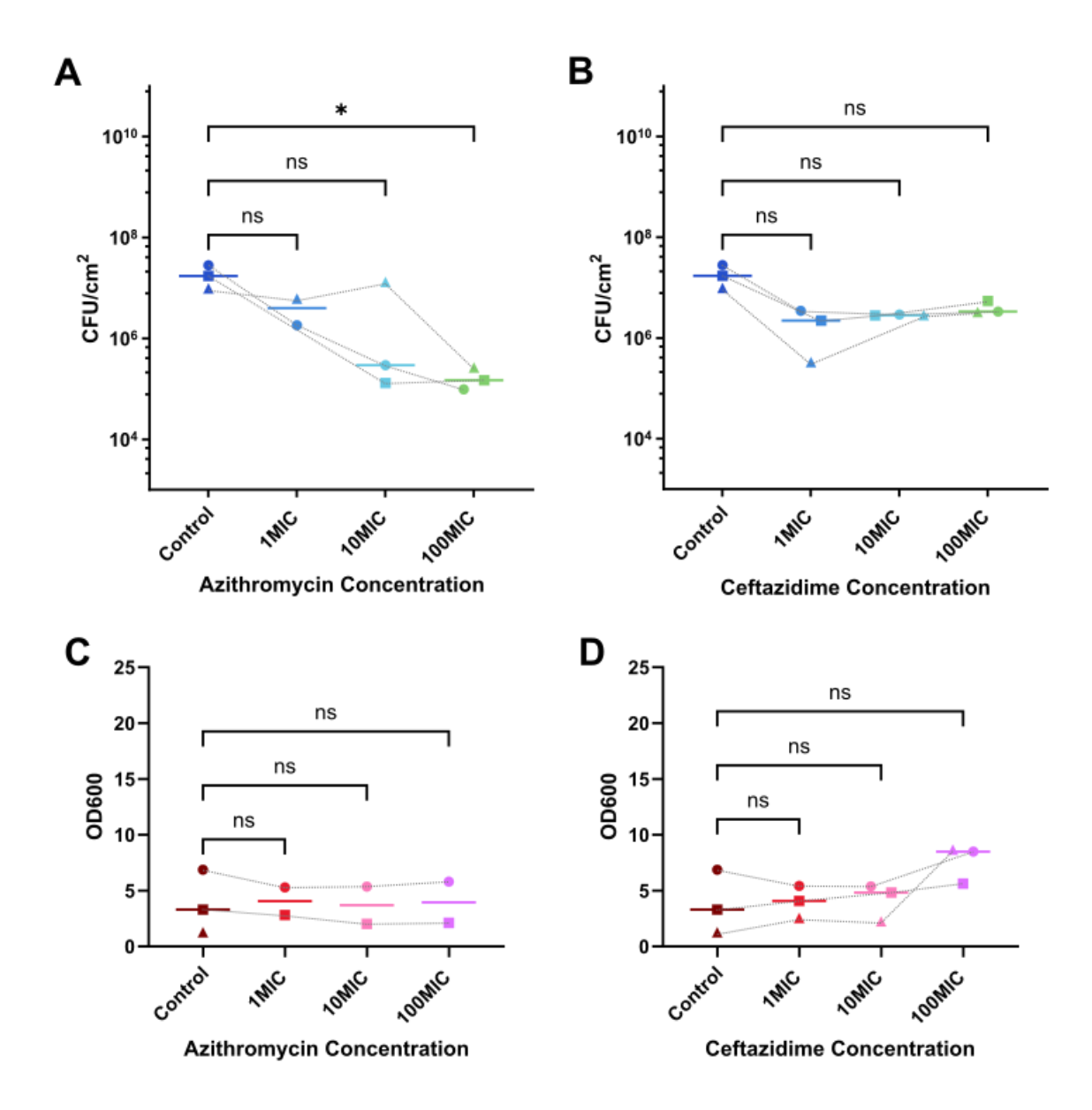


Figure 3.11: GFP-NTHi biofilm response to antibiotics. Azithromycin and ceftazidime were added to 72 h biofilms at 1, 10 and 100 times the planktonic MIC and incubated for 24 h. No antibiotics were added to the controls. Biofilms were then washed and either scraped and CFUs enumerated or stained with CV to assess biomass. Data points are shown as means of duplicate wells with separate biological replicates denote by shapes and

datapoints from the same biological replicate being joined by grey lines; coloured lines depict medians. (A) CFU counts following azithromycin treatment, n=3 except 1 MIC n=2 (B) CFU counts following ceftazidime treatment, n=3 (C) Biomass following azithromycin treatment, n=2 (D) biomass following ceftazidime treatment, n=3. Data were analysed using Kruskal-Wallis with Dunn's post hoc for Azithromycin and Friedman test with Dunn's post hoc for Ceftazidime (\* p < 0.05)

Antibiotic treatment had no significant impact on bacterial culturability of GFP-NTHi biofilms with the exception of azithromycin at 100MIC (200  $\mu$ g/mL), leading to a 100-fold reduction in the number of viable bacterial cells (Figure 3.11A), ceftazidime did not affect bacterial culturability (Figure 3.11B). All treatments failed to reduce the number of viable bacterial cells to below 10<sup>5</sup>. There was no significant change in biomass in response to any of the antibiotic treatments compared with the control biofilm (Figure 3.11C & D).

For PCD-NTHi 4 biofilms, azithromycin reduced the viable cell count to zero in all treatments excepts one 1 MIC case (Figure 3.12A) though the difference was not found to be statistically significant. Cells remained viable when biofilms were exposed to ceftazidime, with only 100 MIC showing a significant reduction in viable cell count compared to the untreated control (Figure 3.12B). Like with GFP-NTHi, the viable cell count was not reduced below 10<sup>5</sup> CFU/cm<sup>2</sup> by ceftazidime. Biomass was significantly reduced by azithromycin at 100 time the planktonic MIC (Figure 3.12C), at lower concentrations the amount of biomass remaining was not significantly affected. Ceftazidime caused an increase in biomass compared to the untreated control biofilm at 10 MIC (Figure 3.12D), but no significant change in biomass as seen at 1 MIC and 100 MIC.

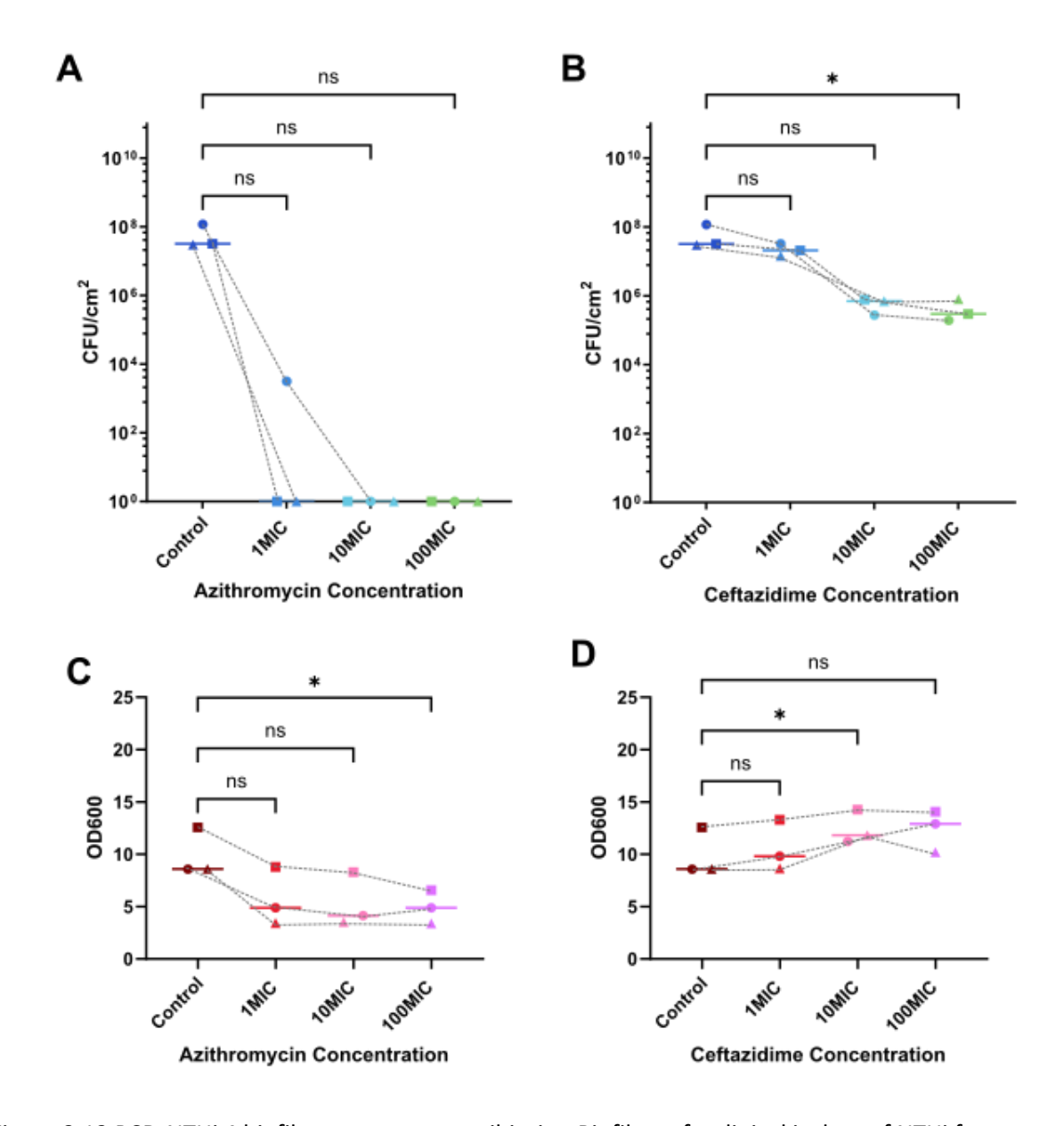


Figure 3.12 PCD-NTHi 4 biofilm response to antibiotics. Biofilms of a clinical isolate of NTHi from a PCD patient were grown for 72 and azithromycin and ceftazidime were added at 1, 10 and 100 times the planktonic MIC and incubated for 24 h. No antibiotics were added to the controls. Biofilms were then washed and either scraped and CFUs enumerated or stained with CV to assess biomass. Data points are shown as means of duplicate wells; coloured lines depict medians. Separate biological replicates are shown as different shapes joined by grey lines. n = 3 for all treatments (A) CFU counts following azithromycin treatment (B) CFU counts following ceftazidime treatment (C) Biomass

following azithromycin treatment (D) biomass following ceftazidime treatment. Data were analysed with Friedman tests with Dunn's post hoc (\* p <0.05)

## 3.4 Discussion

NTHi biofilm formation was demonstrated for six clinical isolates from PCD patients and a GFP expressing laboratory strain. NTHi is a highly heterogeneous species so both planktonic and biofilm growth needed characterisation before moving on to the co-cultures presented in subsequent chapters. Slow planktonic growth led to the biofilm inoculation protocols being adapted from previous work<sup>274,275</sup> to use stationary instead of exponential phase cultures to inoculate biofilms. Biofilm growth after 72 h was confirmed and characterised for all seven strains (GFP-NTHi and PCD-NTHi 1-6). Based on this characterisation, PCD-NTHi 4 was selected for further work alongside GFP-NTHi. Antibiotic tolerance, a hallmark of biofilms, was demonstrated for both strains. The work presented in this chapter was the first step to developing a clinically relevant and logistically viable model of bacterial infections of the airway.

Planktonic cultures of NTHi were to be used to inoculate biofilms and infect co-cultures, so as a first step, these cultures had to be characterised. Previous work<sup>274,275</sup> done by this research group had established an inoculation protocol taking approximately 2 days: first NTHi was streaked on a CBA plate from a frozen stock and incubated overnight. On the second day a single colony was used to inoculate a planktonic culture which was grown to the exponential growth phase and then then used to inoculate biofilm assays, this took 2 - 6 h depending on strain. As this work was using newly acquired NTHi strains and the heterogeneity of NTHi is well established<sup>178,236,274</sup>, the growth kinetics were investigated in order to confirm the feasibility of the previously used protocol. For this, the first two clinical strains acquired (PCD-NTHi 1&2) and GFP-NTHi were used. The decision to include GFP-NTHi was made based on the potential benefits to imaging biofilms and co-cultures down the line.

The heterogeneity of NTHi may extend to metabolic enzymes<sup>289</sup>, leading to a heterogeneity in growth rates. As initial growth curves showed slower growth than previously observed (over 6 h for GFP-NTHi and 8-12 h for PCD-NTHi 1 & 2), the method of inoculating the planktonic culture was adapted from using a bacterial colony from a CBA plate to using an overnight culture. This decision was made in an attempt to adhere to previous protocols and therefore allow comparisons between findings. However, the change in inoculation method did not significantly decrease the time taken to reach the mid-exponential phase by any of the strains. As the aim of this work was the development of a logistically feasible model, the six-hour delay before setting up any downstream assay was not amenable to the desired outcome. Instead, using a planktonic overnight culture grown to the stationary growth phase was characterised. This added a day to the whole process compared

to the previously used protocol, as a streak plate was incubated overnight in order to inoculate the overnight planktonic culture that was then used to inoculate the biofilm assay on day three. However, the planktonic overnight culture could be ready earlier in the day, improving the logistics of the downstream assays. Additionally, stationary phase bacteria are more representative of bacteria exposed to *in vivo* conditions of limited nutrient availability and other stressors, which triggers biofilm formation<sup>290,291</sup>.

Stationary phase planktonic cultures were measured at 14-18 h. A range of time points was investigated to determine if there was flexibility in this new protocol that would ease logistic pressure on experimental days. In this growth phase, the bacterial population remains steady as growth slows and bacteria die off at a similar rate as the growth rate. OD and the number of viable bacteria was quantified hourly in the stated time range. Neither OD nor CFU correlated with time in these cultures, making the planktonic culture suitable for inoculating downstream assays at any point within this timeframe.

With the exception of PCD-NTHi 2, OD did not directly correlate to CFUs when the culture is in the stationary growth phase. It was therefore decided to use the average CFUs/mL of a stationary planktonic culture as reference for determining the volume of planktonic culture used to inoculate downstream assays. Across all timepoints, the planktonic culture grew to a viable bacteria population with the magnitude of 10<sup>8</sup> CFU/mL, with the exception of PCD-NTHi 6 where the viable bacterial count was over 10-fold lower. For PCD-NTHi 2 cultures, CFUs were found to negatively correlate with OD, implying a higher OD corresponded to a lover viable bacteria count. PCD-NTHi 5 cultures had the highest OD readings but no corresponding increase in CFU. Both PCD-NTHi 2 and 6 had lower OD readings than other strains, however, only PCD-NTHi 6 had a correspondingly lower CFU count compared to other strains. The variation between the characterised clinical strains demonstrates the heterogeneity of NTHi and underlines the need for using a range of strains once the model is established before drawing conclusions.

Previous work had established a 72 h timepoint for biofilm growth<sup>274</sup> after finding that strain depend variation of CFU counts could not be detected after 24 h and that some strains produced a significant increase in biomass between 24 h and 72 h. To confirm this timepoint, the first three strains that were obtained (GFP-NTHi, PCD-NTHi 1 & 2) were characterised every 24 h for 72 h. Biofilm formation was confirmed across all three time points for all three strains, both through CV staining and through viable CFU recovery. There was no significant change in either metric across the time points investigated with the exception of a significant biomass increase by GFP-NTHi biofilms

between 24 h and 72 h. This increase without a corresponding increase in viable bacteria suggests increased EPS production, a strategy used by bacteria to create a physical and chemical barrier against both antibiotics and host immune responses<sup>292</sup>. Similar trends have been observed in other NTHi strains<sup>274,293</sup>. The stability of the viable cell population and the aim of keeping the protocol logistically viable meant that 72 h was deemed a sufficiently long biofilm incubation timespan. This work consisted of a low number of biological repeats, so no significant statistical analysis was possible. As on each occasion, duplicate (PCD-NTHi) and triplicate (GFP-NTHi) wells were used, and the purpose was to confirm biofilm formation at the previously used 72 h time point this was deemed sufficient in order to move the project forward. For more robust statistical analysis and direct strain comparisons, more biological replicates would be needed.

Once the biofilm inoculation protocol was established, further clinical NTHi strains (PCD-NTHi 3 -6) were characterised at the confirmed 72 h endpoint and all strains were compared in order to identify the strain with the most robust biofilm forming capabilities. To achieve this, CFU counts and CV staining was used as before with the addition of confocal imaging, the computational analysis of which was used to verify the findings of the former. NTHi isolates from individuals with PCD and CF, both genetic conditions that pre-dispose patients to recurrent bacterial airway infection, have been shown to be highly heterogeneous previously<sup>224,233</sup>, with strains from chronic infections forming thicker biofilms than those from more recent infections<sup>224</sup>. This wasn't seen in the strains in this work as no significant difference in CV staining and CFU counts was found between clinical isolates despite varying infection histories (section 2.1.1). However, confocal imaging demonstrated a strain dependent heterogeneity in biofilm structure. All strains formed lawns of bacteria, however, the density of the cells varied from strain to strain. For example, PCD-NTHi 3 contained large gaps in the staining while PCD-NTHi 4 was densely packed with cells. The absence of staining indicated an absence of cells, but not of all biofilm material, so it is possible that EPS was present in these gaps. PCD-NTHi 3 was found to have the thickest biofilms, as measured by biovolume height, but no significant increase in CV staining, which supports the interpretation that the biofilms are less dense, containing less total material but in a larger overall volume than other strains.

EPS presence may also be indicated by differences in CV staining and live/dead biovolume staining as SYTO9/PI staining does not stain matrix protein while CV stains biofilm material more broardly<sup>294</sup>. For example, comparing the trends across strains for total biovolume and CV staining showed general concurrence between the readouts, however PCD-NTHi 2 and 6 had a lower biovolume than expected given the CV readouts. A fluorescent stain like SYPRO RUBY could be used in the future to

visualise the EPS component of the biofilm<sup>295</sup> on confocal images. SEM imaging of NTHi biofilms on abiotic surfaces has previously shown variation in EPS production<sup>274</sup>, so additional SEM imaging of the strains used for this work would help clarify the observed discrepancies between CV staining and confocal biovolume staining.

CFU counts and "live" staining was found to generally have a similar trend across strains with the exception of PCD-NTHi 1 where CFUs were comparatively high compared to "live" biovolume staining and PCD-NTHi 3 where CFUs were comparatively low. Confocal images of PCD-NTHi 1 biofilms showed individual bacteria above the main lawn, potentially due to cells being embedded in EPS. It is possible that this layer of sparce bacteria was taller than initially identified, therefore sufficiently tall z stacks were not recorded. Viable biovolume may therefore not have been included in the image analysis while the whole biofilm was included for CFU counts. The discrepancy between CFUs and SYTO9 staining seen in PCD-NTHi 3 biofilms may have been due to VBNCs as these would show up on confocal imaging following staining with SYTO9<sup>296</sup> but not on culture plates for CFU counts. The VBNC state is a bacterial survival strategy that has been demonstrated by NTHi in the past<sup>297</sup>, so the suggestion that this PCD-NTHi 3 may be more prone towards this state made it less suitable for this work which would rely on CFU counts as an indicator for bacterial viability. Future work with an expanded range of NTHi strains would need to take care to characterise bacterial viability in multiple ways such as microscopy and PCR. Unfortunately, this was not possible as part of this project.

Using computational image analysis tools, the confocal images were quantified. Comparing "live" and "dead" staining biovolumes revealed that there was an approximately 50/50 split in viable and non-viable cells within each biofilm. There was a significant difference in viability between PCD-NTHi 5 and 6 biofilms, with PCD-NTHi 5 biofilms containing more "live" staining cells and PCD-NTHi 6 biofilms containing more "dead" staining cells. This was reflected in the appearance of the confocal images.

PCD-NTHi 6 produced a comparable biofilm in terms biomass, total biovolume, thickness and CFU counts as the other PCD isolates. However, live/dead staining gave a median viability of 32.0% and the confocal images showed predominantly red (propidium iodide) staining. The viable cell counts suggest that this staining may not be representative, instead the cells may be viable but with a more porous membrane. This allows the stain to enter the cells and leads to cells being detected as "dead" when using the live/dead staining method. PCD-NTHi 6 also produced a less consistent planktonic cell culture, which would lead to more inconsistent inoculation numbers. Combining the

unreliability of the inoculum and the staining, PCD-NTHi 6 was discounted as a potential candidate for future work.

GFP-NTHi biofilms formed less biomass than the clinical PCD isolates which correlates with findings that clinical isolates from chronically infected patients often form more robust biofilms<sup>298</sup> than labstrains. The number of viable cells withing GFP-NTHi biofilms was comparable to the clinical strains. GFP-NTHi biofilms were observed to consist of a thin lawn of bacteria with occasional aggregates of bacterial cells. The structure was unlike the thicker lawns observed in other NTHi strains<sup>274,293</sup> and those observed in the clinical strains here. The quantification of the confocal biofilm images showed GFP-NTHi formed thinner biofilms containing less biomass compared to biofilms formed by clinical isolates. The viability was similar with a median of 46.5%.

The aim of using confocal microscopy to verify GFP fluorescence was achieved. Unstained biofilms were clearly visible, however unstained biofilms showed a 60% reduction in green fluorescence compared to biofilms stained with SYTO9I. This may be due to a combination of GFP-NTHi not producing the same level of fluorescence as SYTO9 and the fact that SYTO9 stains nucleic acids and may therefore be staining any extracellular DNA as well as intracellular DNA. GFP-NTHi biofilms stained with SYTO9/PI showed a red staining "dead" population that may not have been detected within an unstained biofilm. However, GFP has been found to have a half-life of 2.8 h in fibroblasts<sup>299</sup>, so a cell that was staining red due to loss of viability may still have contained enough GFP to be been detected in an unstained sample.

GFP production on its own may not be enough to fully characterise a biofilm as these contain EPS, dead cells and cells with reduced metabolic activity. It is however a useful tool for initial imaging that reduces the complexity and requirement for optimisation that other methodologies such as FISH may require.

Combining the biofilm characterisation readouts from across the clinical isolates underlines the heterogeneity of clinical NTHi. PCD-NTHi 4 biofilms were among the most viable and highest in biomass as measured by CV staining. They also produced the highest amount of biovolume as measured by the staining of bacterial cells alone. Despite this, the average height of PCD-NTHi 4 biofilms did not stand out compared to other isolates, and the ratio between mean and maximum height was the highest of any strain suggesting a dense, uniform biofilm. This is supported by the confocal images. Biofilm uniformity has been used as an indicator of maturity is *S. aureus* biofilms<sup>300</sup>

besides suggesting a more robust structure. Based on these observations, PCD-NTHi 4 was chosen for further work, having demonstrated robust biofilm forming capabilities.

Conversely, PCD-NTHi 2 was among the lowest biomass producing strain, the lowest amount of biovolume as measured by stained cells and the thinnest biofilms. Additionally, the ratio between the mean and the maximum thickness of PCD-NTHi 2 biofilms suggests that the biofilm surface is uneven, and therefore may be more prone to attack by immune cells and antibiotic factors as well as possibly being more vulnerable to sheer forces. PCD-NTHi 3 produced the least biomass but was found to be the thickest biofilms through confocal microscopy, suggesting a less dense biofilm compared with the other strains investigated. This could be seen on the orthogonal confocal slices, which showed a greater number of un-stained "channels" between bacterial cells.

Once the decision to use GFP-NTHi and PCD-NTHi 4 in further work had been made, the antibiotic tolerance of the two strains was investigated to further verify biofilm formation as antibiotic tolerance is a key hallmark of biofilm formation<sup>301</sup>. Planktonic MICs were identified using e-test strips and biofilms exposed to concentrations 1, 10 and 100-fold higher. The MIC of azithromycin against planktonic GFP-NTHi and PCD-NTHi 4 was identified as 2  $\mu$ g/mL and 4  $\mu$ g/mL respectively. Azithromycin MICs have been found to range from 0.25 to 8  $\mu$ g/mL<sup>238,272,302</sup> across various NTHi strains. Ceftazidime MICs against planktonic GFP-NTHi and PCD-NTHi 4 were found to be 0.064  $\mu$ g/mL and 0.47  $\mu$ g/mL respectively. There is generally more susceptibility to ceftazidime than azithromycin in clinical NTHi strains<sup>174</sup>.

Previous work had found that biofilms of some clinical NTHi strains showed an 10 fold increase in MIC compared to planktonic cultures, while others showed no difference<sup>274</sup>. Based on this, the concentration ranges of 1-100 fold planktonic MICs were selected for this work.

Antibiotic tolerance of GFP-NTHi biofilms to azithromycin and ceftazidime was demonstrated, with only 100 MIC azithromycin causing a significant reduction in culturable cells after 24 h of treatment. All biofilms retained a viable cell population above 10<sup>5</sup> CFUs/cm<sup>2</sup>, meaning that viable biofilm remained following treatment. Biomass was not significantly affected by 24 h antibiotic treatment. This suggests that the antibiotics are not disrupting the biofilm structure enough to dislodge biomass from the attached biofilm.

Clinical isolate PCD-NTHi 4 biofilms remained susceptible to azithromycin, with a near complete loss of culturable cells following exposure to the planktonic MIC. Biomass remained unaffected except for a significant reduction in biomass following treatment with 100 MIC azithromycin, perhaps

indicating a biofilm matrix with enough structural integrity as to not be removed during the washing process, despite no longer containing viable bacteria. The effect of azithromycin on NTHi biofilm biomass in the literature varies: previous work using a clinical isolate of NTHi found an increase in CV staining following two hour azithromycin exposure of a 72 h biofilm *in vitro*<sup>275</sup>, while exposing a previously formed NTHi biofilm to sub-inhibitory concentrations of azithromycin in a flow cell has been shown to decrease biomass<sup>302</sup>, possibly due the sufficient weakening of the structural integrity so that the shear forces of the flow-cell were sufficient to disrupt the established biofilm. Sub-inhibitory concentrations of azithromycin have been found to decrease static biofilm formation<sup>302</sup>, however this was using mid-exponential planktonic NTHi to inoculate the biofilm, not stationary phase bacteria. It is therefore possible that the bacteria were more susceptible to azithromycin while being more metabolically active and without the protection of a biofilm matrix.

The loss of CFU counts following azithromycin exposure may also indicate a shift towards a VBNC phenotype and thus a loss of viability detection using culture plate methods. PCR has been found to detect chronic *P. aeruginosa* and *S. aureus* infections in cystic fibrosis patients that had negative culture tests, the majority of which were on long term azithromycin treatment. To my knowledge, no work has been done investigating if azithromycin can induce a VBNC phenotypes in NTHi to date, though increased resistance as an effect of antibiotic treatment has been found<sup>303</sup> and the cause of transitioning to a VBNC state being quoted as "starvation"<sup>304</sup>. As discussed previously, imaging techniques could be used to confirm loss of viability in future, though this fell outside the scope of this project.

PCD-NTHi 4 biofilms remained viable following ceftazidime exposure, with only the highest tested concentration, 100 MIC, causing a significant (but not total) reduction in viable cells compared to the untreated control. A significant increase in biomass was observed following incubation with 10 MIC ceftazidime, but not at higher or lower concentrations.

Overall, the GFP-NTHi biofilms were either unaffected by the addition of antibiotics up to 100 times the concentration that would have killed planktonic cultures, or only partially decreased in viability. Equally, clinical isolate PCD-NTHi 4 remained viable following exposure to ceftazidime, though not azithromycin. As biofilms have been observed to tolerate antimicrobial concentrations 10-1000 times higher than those tolerated by equivalent planktonic bacteria<sup>305</sup>, the findings supported the hypothesis that both GFP-NTHi and PCD-NTHi 4 are forming biofilms on abiotic surfaces leading to reduced antibiotic susceptibility.

In general, there were only a maximum of three biological replicates of all antibiotic tolerance assays, so the statistics will lack robustness even though each contained two technical replicates. As the purpose of these assays was to demonstrate a tolerance to antibiotics (or lack thereof) rather than a fundamental insight, a lower number of biological replicates was deemed acceptable to meet logistical constraints. Further biological replicates would be needed if comparisons of antibiotic susceptibility were to be made between the strains.

## 3.5 Summary and Conclusion

This chapter described the characterisation of GFP-NTHi and six clinical strains of NTHi from PCD patients (PCD-NTHi 1-6). First, the planktonic growth in order to optimise the inoculation protocol for downstream assays and the biofilm growth in order to verify the 72 h timepoint was determined. Stationary phase planktonic bacteria were determined to be most practical and representative choice to model the planktonic bacteria that would form biofilms *in vivo*. All strains were found to form biofilms on an abiotic surface as demonstrated through biomass staining, viable bacteria recovery, confocal imaging though a high level of heterogeneity was observed between strains.

PCD-NTHi 4 and 2 were identified as best and worse biofilm formers respectively based on viability, biomass formation, and confocal image analysis. Antibiotic tolerance, a key hallmark of biofilm formation, was demonstrated by both GFP-NTHi and PCD-NTHi 4. PCD-NTHi 4 was therefore taken forward for co-culture biotic airway epithelial cell cultures from healthy volunteers.

# Chapter 4 Non-typeable *Haemophilus influenzae* on Epithelial Cell Cultures at the Air-Liquid Interface

## 4.1 Introduction

Biofilms have been found to develop differently on biotic vs non-biotic surfaces<sup>224</sup>, possibly due to varying nutrient availability and the host response mediated by the epithelial cells. This chapter will be focusing on optimising the co-culture protocol in order to produce viable biofilms on the apical surface of the epithelium while maintaining the integrity of the epithelial cell layer. This work will form the basis of the development of a model using bacteria, epithelial cells and, eventually, macrophages.

Having determined a suitable inoculation protocol based on planktonic growth characterisation in the last chapter along with demonstrating biofilm formation on an abiotic surface, two strains of NTHi (GFP-NTHi and PCD-NTHi 4) were taken forward to be used in ALI co-cultures with PNECs.

## 4.2 Aims

Aim: Co-culture GFP- NTHi and the clinical strain PCD-NTHi 4 biofilms on the apical surface of PNEC ALI cultures

## Objectives:

- Optimise MOI (1-100) and attachment period (1 h and 24 h) for NTHi/ALI co-cultures to maximise epithelial layer integrity and biofilm formation.
  - Measure bacterial recovery after 72 h through CFU count.
  - Validate epithelial cell layer integrity through TEER.
- Visualise the location of GFP-NTHi in relation to PNECs after 72 h of co-culture using confocal microscopy and scanning electron microscopy (SEM) in order to confirm apical biofilm formation.
- Visualise PCD-NTHi 4 clinic strain on PNECs using SEM and characterise morphology and integrity of co-culture.

## 4.3 Results

### 4.3.1 Co-Culturing GFP-NTHi with Primary Nasal Epithelial Cells

Having established the capability of GFP-NTHi for forming biofilms on an abiotic surface, the next stage of developing this model of airway infections with increased clinical relevance was to grow GFP-NTHi biofilms on epithelial cells. PNECs from healthy volunteers were grown at ALI for at least 4 weeks in order to differentiate into a pseudostratified, ciliated phenotype (section 2.2.3). Planktonic GFP-NTHi was grown to the stationary growth phase as previously characterised (Section 3.3.1), then used to infect the apical surface of the PNEC ALI culture. A range of MOIs were investigated: 10:1, 50:1 and 100:1.

TEER measurements of differentiated PNEC ALI cultures were taken before infection with NTHi and 72 h afterwards.

No significant drop in TEER was detected over a 72 h co-culture period, neither in the uninfected control nor at any MOI (Figure 4.1). Comparing matched TEER readings within each PNEC donor sample showed that individual TEER trends were not consistent i.e., all increasing or all decreasing.

A larger spread of TEER readings was observed at 72 h post co-culture at MOI 50 and MOI 100 (ranges of 464 and 385  $\Omega$ .cm<sup>2</sup> respectively). Lower ranges were observed for the uninfected control and MOI 10 cultures (170 and 188  $\Omega$ .cm<sup>2</sup> respectively). TEER readings of one biological replicate dropped below 100  $\Omega$ .cm<sup>2</sup> in for all treatments except MOI 50, including the uninfected control.

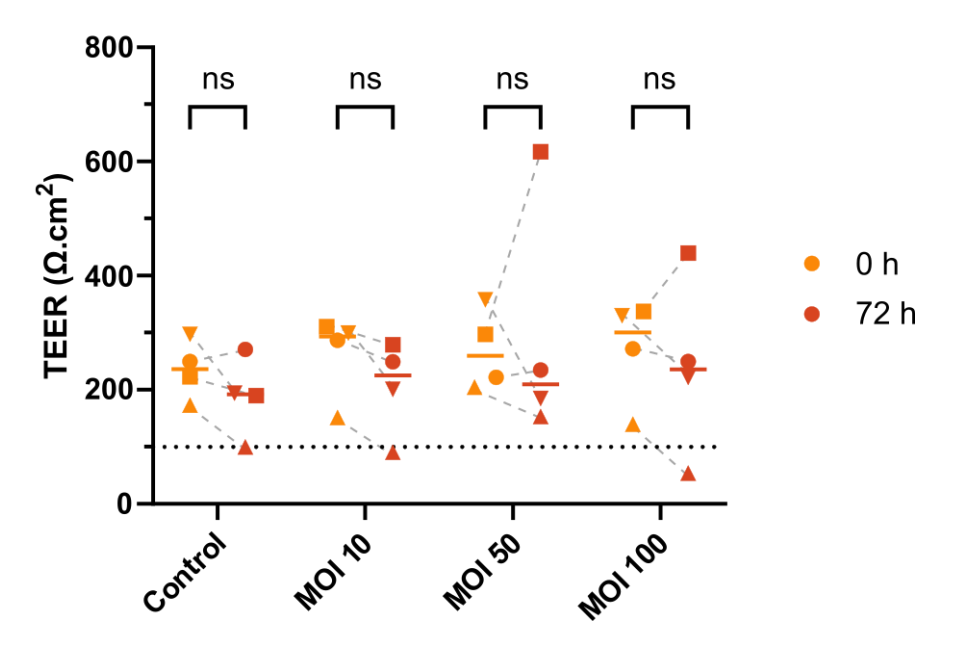


Figure 4.1: TEER of PNEC ALI culture measured before and after 72 h co-culture with GPF-NTHi to represent cell layer integrity. n=4 PNEC donors (separate biological replicates depicted by shapes joined by grey dashed lines), each datapoint is shown as the mean of duplicate wells (except the uninfected control which had only had a single well). Solid lines show the median, the dotted line marks a  $100~\Omega.cm^2$ . No statistically significant differences between pre-infection and post 72 hr co-culture were observed (Wilcoxon signed-rank test).

Viable bacteria were recovered from co-cultures after 72 h of infection (Figure 4.2). There was no statistically significant difference in the number of bacteria recovered between MOIs. Cultures at all MOIs maintained a viable bacterial cell population of the magnitude of 10<sup>7</sup> CFUs/cm<sup>2</sup> or above.

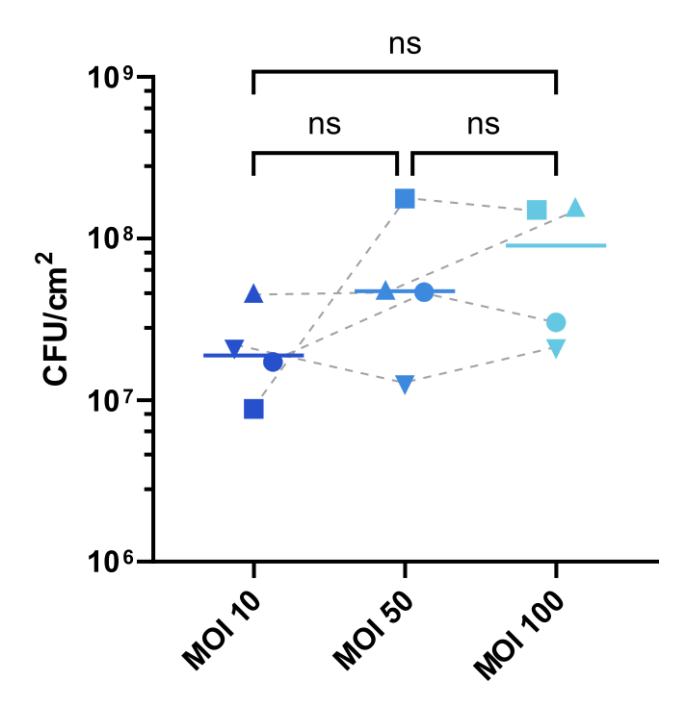


Figure 4.2 Viable GFP-NTHi cells per area recovered after 72 h co-culture on healthy volunteer PNECs at ALI. n=4 separate biological replicates (different shapes joined by dashed grey lines), data points show the mean of duplicate wells with solid lines indicating the median.

Datapoint shapes distinguish biological replicates i.e. PNEC donors. No statistically significant difference was identified between MOIs (Friedman test with Dunn's post hoc analysis). No bacterial cells were recovered from uninfected controls.

As the presence of viable bacteria and the maintenance of the epithelial layer integrity was demonstrated, microscopy was used to further understand the interaction between GFP-NTHi and PNECs in a 72 h co-culture. Confocal microscopy was used to visualise the three-dimensional organisation of the co-cultures to assess biofilm formation and possible internalisation of bacteria into the epithelial cells (section 2.2.6).

Confocal imaging of the co-culture revealed that GFP-NTHi had invaded the epithelial layer (Figure 4.3A). No GFP-NTHi could be identified on the surface of the epithelial layer. Bacteria were only observed in areas without ciliation (Figure 4.3B). Ciliated areas did not have bacteria within the epithelial layer (Figure 4.3C).

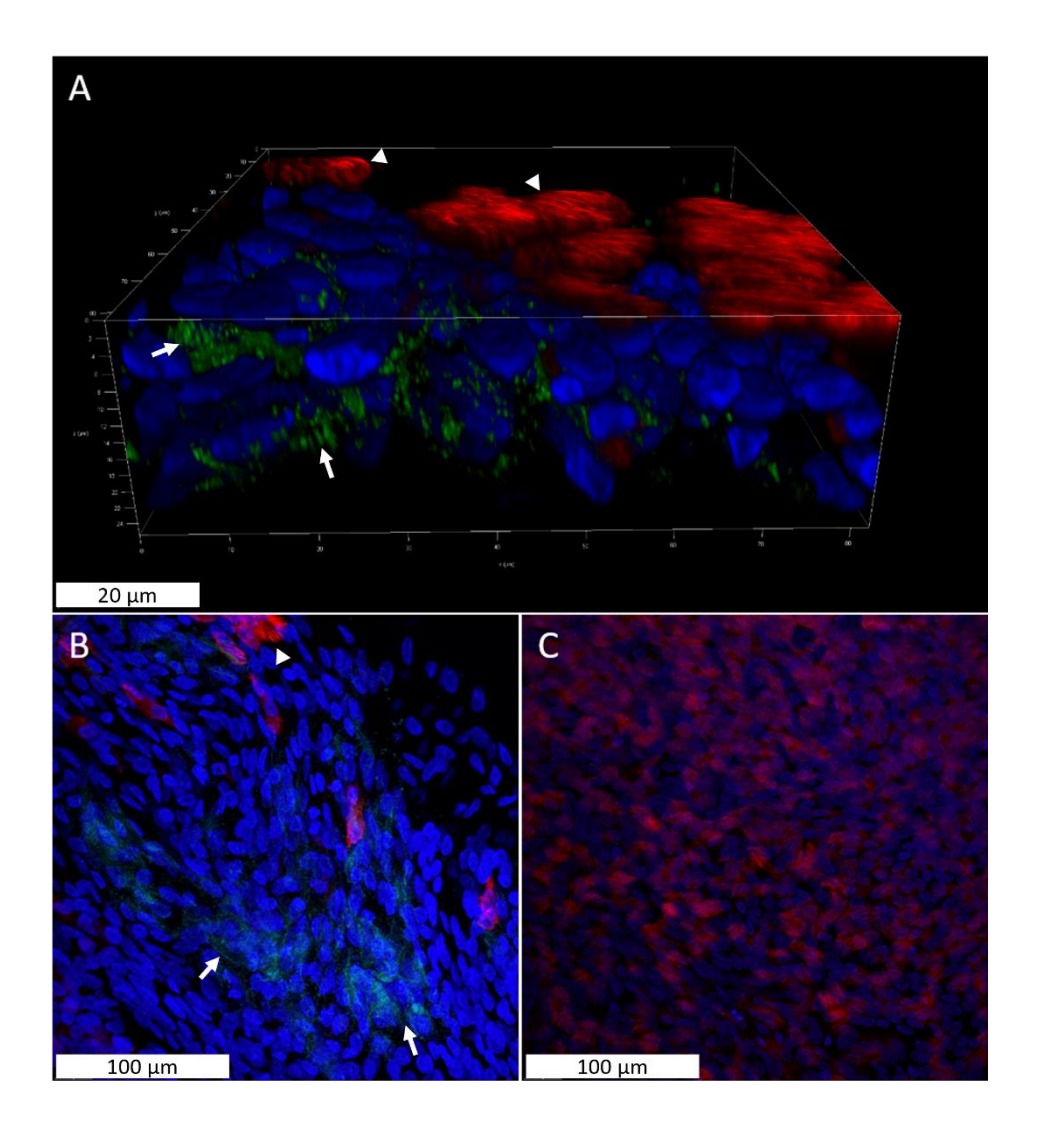


Figure 4.3 Confocal microscopy images of GFP-NTHi co-cultured for 72 h on healthy volunteer PNECs at ALI. Bacteria were added to the epithelial cell layer at an MOI of 50 and incubated for 72 h before being washed and stained. Cilia were labelled using a RSPH4a antibody with Alexa Fluor 594 as secondary antibody (red), DAPI was used to stain nuclei (blue), while the GFP-strain is green. Examples of GFP-NTHi within the epithelial cell layer are marked by white arrows, examples of cilia by white arrowheads. A) 3D view showing NTHi within the cell layer B) representative max projection of infected non-ciliated area C) representative max projection of a ciliated area without bacteria. Bacteria were observed withing the epithelial layer, not on its surface. Bacteria only appeared in non-ciliated areas (B). Images were taken on a Leica SP8 confocal microscope. One biological repeat was performed as a preliminary investigation. Scale bars represent 20 µm.

SEM was used to validate the confocal imaging and provide a better resolution of the epithelial cell surface in order to identify if any bacterial aggregates were present (section 2.2.7). Images showed extensive ciliation of the cell surface (Figure 4.4A). The SEM images confirmed no significant biofilm formation on the epithelial cell surface. Some isolated clusters were observed in the few areas of lower ciliation (Figure 4.4B-C), however it was difficult to determine if these were bacterial clusters or other debris. These data indicate that the GFP strain could not form a biofilm on ALI cultures and therefore the laboratory strain was not taken forwards for this project.

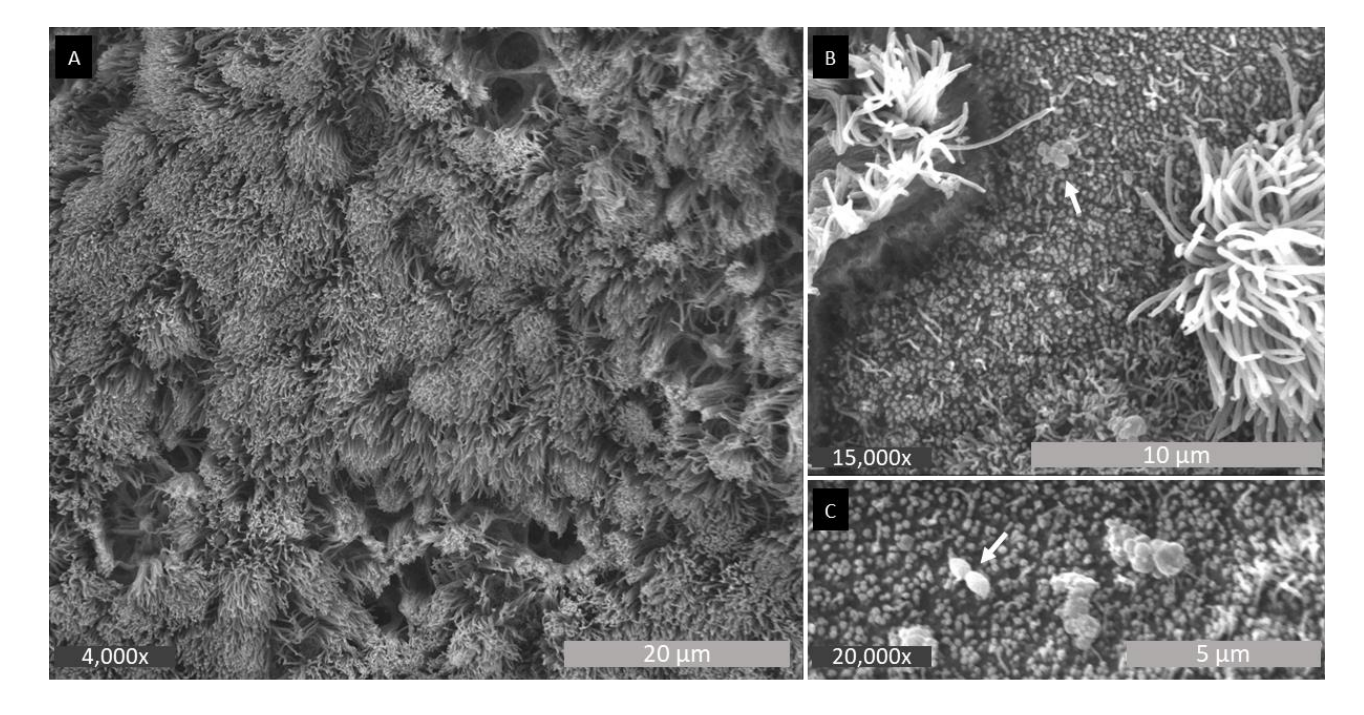


Figure 4.4 SEM images of GFP-NTHi/PNEC co-cultures at ALI. Bacteria were added apically to the epithelial cell layer at MOI 50. Co-cultures were incubated for 72 h before being washed, fixed and stained. The majority of the culture was well ciliated (A) with few areas lacking cilia (B). There were no obvious biofilm aggregates identified. Small aggregates such those shown in (B-C, white arrows) were observed, however they could not be reliably distinguished from debris. Uninfected controls showed the same level of ciliation as infected epithelial cell layers. (A) was taken at 4000x magnification, (B) at 15000x magnification (C) at 20,000x magnification. Respective scale bars shown on images. Images taken with a FEI Quanta 200 SEM

## 4.3.2 Clinical NTHi isolate Co-Cultured on Primary Epithelial Cells

Initially, the clinical strain PCD-NTHi 4 was taken forward for co-culture assays alongside GFP-NTHi with the aim of providing additional clinical relevance that the laboratory strain GFP-NTHi would be lacking. However, as it became apparent that GFP-NTHi did not form biofilms on the apical surface of PNEC ALI cultures, PCD-NTHi 4 was selected for the sole strain for further investigations.

SEM was used to confirm apical biofilm growth on the ALI cultures using this clinical NTHi strain. Isolated aggregates of bacterial cells could be seen (Figure 4.5).

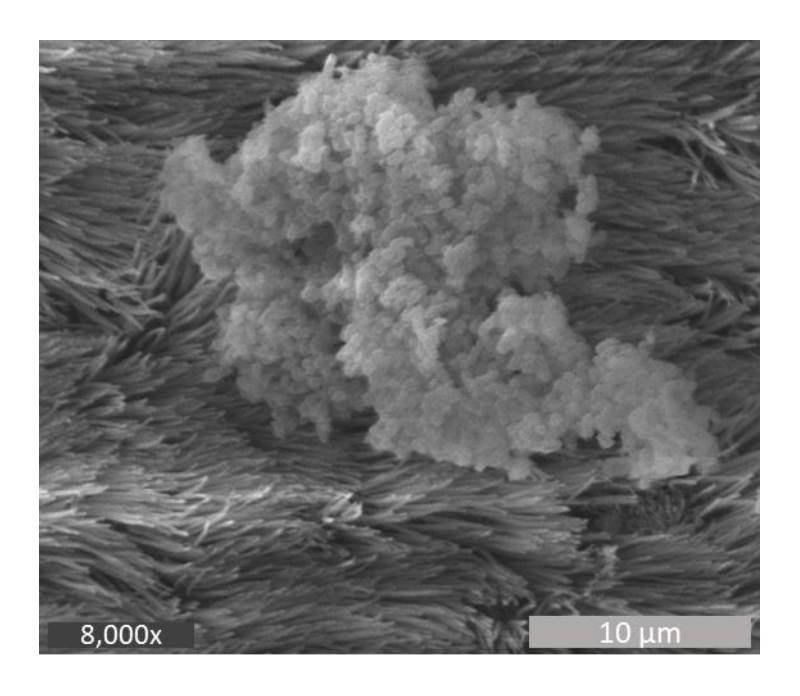


Figure 4.5 SEM image of PCD-NTHi 4 NTHi co-cultured on healthy PNECs at ALI for 72 h. Planktonic bacteria were added to the epithelial cell layer at MOI 50 for 24 h before the suspension was removed. Co-cultures were incubated for a total of 72 h before being fixed and processed for SEM.

However, as with GFP-NTHi-PNEC co-cultures (Figure 4.1), 24 h infection with the clinical strain PCD-NTHi 4 caused a drop in TEER that suggested a loss of epithelial cell layer integrity (Figure 4.6A). Due to this the attachment time of PCD-NTHi 4 was reduced to 1 h and the TEER and CFUs compared to the previously used 24 h attachment period. Reducing the NTHi attachment time led to TEER remaining above  $100 \Omega \cdot \text{cm}^2$  at all MOIs (Figure 4.6B). No statistical difference was observed between pre and post 72 h co-culture for any MOIs at either attachment time (Figure 4.6).

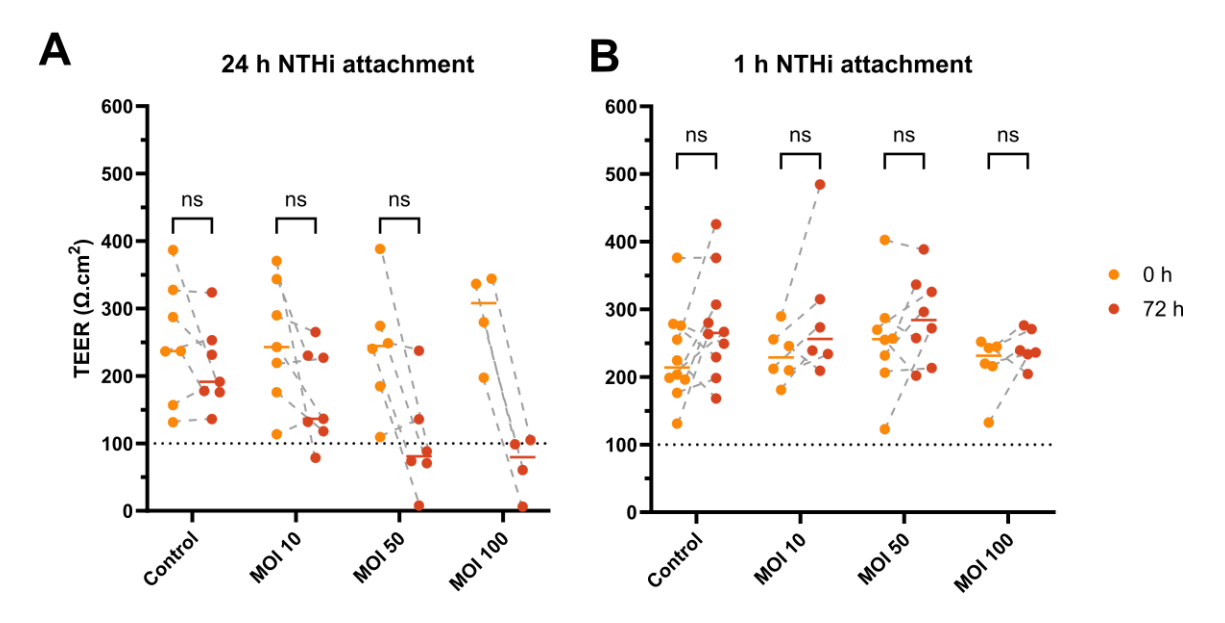


Figure 4.6 Integrity of PNEC layer before and after (yellow and orange respectively) 72 h of coculture with PCD-NTHi 4 at ALI represented by TEER. Ciliated cell cultures were infected with stationary phase planktonic NTHi at a range of MOIs. Bacterial suspensions were removed after (A) 24 h or (B) 1 h. TEER was measured in three positions on each Transwells, averaged per well and corrected for background readings. n > 6 separate biological replicates (each linked by grey dashed lines) except for MOI 100 at 24 h attachment (n = 4). Datapoints show means of a minimum of two duplicate wells except non-infected control treatments which only had single replicates. Solid lines depict medians, the dotted black line marks  $100 \Omega \cdot \text{cm}^2$ . TEER at 0 h and 72 h was compared for each treatment using multiple Wilcoxon tests (except 24 h MOI 100), no significant difference was observed.

While no significant decrease in TEER was seen when comparing readings within each co-culture, comparing the change in TEER between MOIs showed that MOI 100 led to a significantly larger decrease compared to the uninfected control when using a 24 h NTHi attachment time (Figure 4.7A). MOI did not have a significant effect on TEER change at any MOI when an attachment time of 1 h was used (Figure 4.7B). The attachment time was found to significantly affect the TEER change across all cultures (Figure 4.7C).

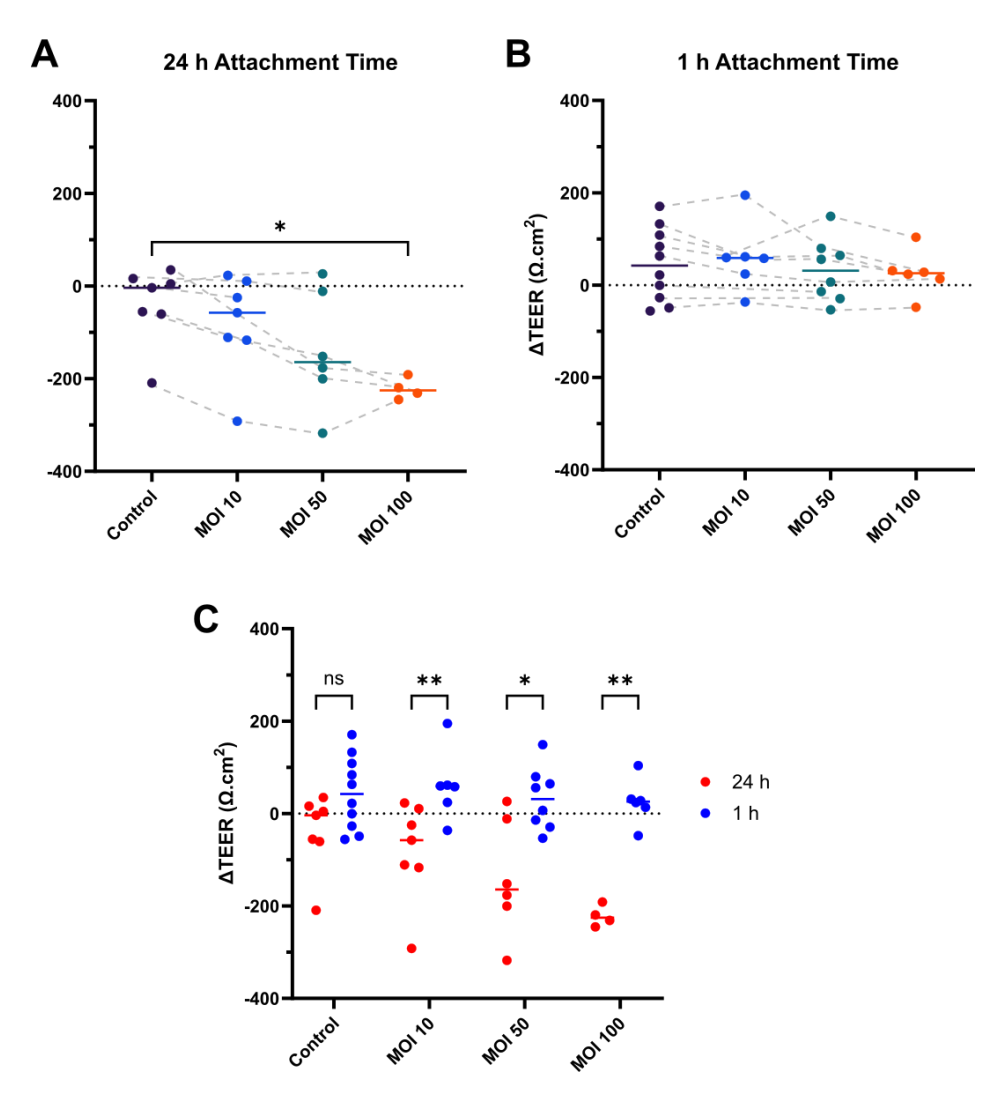


Figure 4.7 TEER change within co-cultures before and after 72 h NTHi-PNEC ALI co-culture.

Planktonic PCD-NTHi 4 cell suspension was added for 1 or 24 h before being removed (Attachment time). TEER of PNEC ALI cultures was measured before infection and following 72 h of co-culture. n > 6 separate biological replicates except for MOI 100 at 24 h attachment (n = 4). Datapoints show the calculated difference ( $\Delta\Omega$ .cm²) as a mean of duplicate wells (uninfected controls had single replicate). Solid lines represent the median. Datapoints from the same biological replicates are joined by dashed grey lines. (A) TEER change following an NTHi attachment time of 24 h. (B) TEER change following an NTHi attachment time of 24 h. (B) TEER change between the two attachment times. TEER change by MOI for each attachment time (A&B) was analysed using Kruskal-Wallis tests with Dunn's post hoc analysis comparing each MOI to the uninfected control – only significant differences are shown. TEER change by

attachment time (C) was compared using multiple Mann-Whitney tests (\*p<0.05, \*\*p<0.01)

Comparing the number of viable bacterial cells recovered from 72 h co-cultures showed that there was a significant increase in recovered CFUs between MOI 10 and MOI 100 when using a 24 h attachment time (Figure 4.8A) but not between MOI 10 and MOI 50 nor between MOI 50 and MOI 100. There was no statistically significant difference in recovered CFUs between MOIs when a 1 h infection period was used (Figure 4.8B). The bacterial attachment time had a significant impact on PCD-NTHi 4 CFUs recovered after 24 h of co-culture. CFU recovery was significantly lower when non-attached bacteria were removed after 1 h compared to a 24 h attachment period (Figure 4.8C). However, recovery remained above a magnitude of  $10^6$  CFU/mL for the 1 h attachment period, a range that was feasible to use for this work going forward.

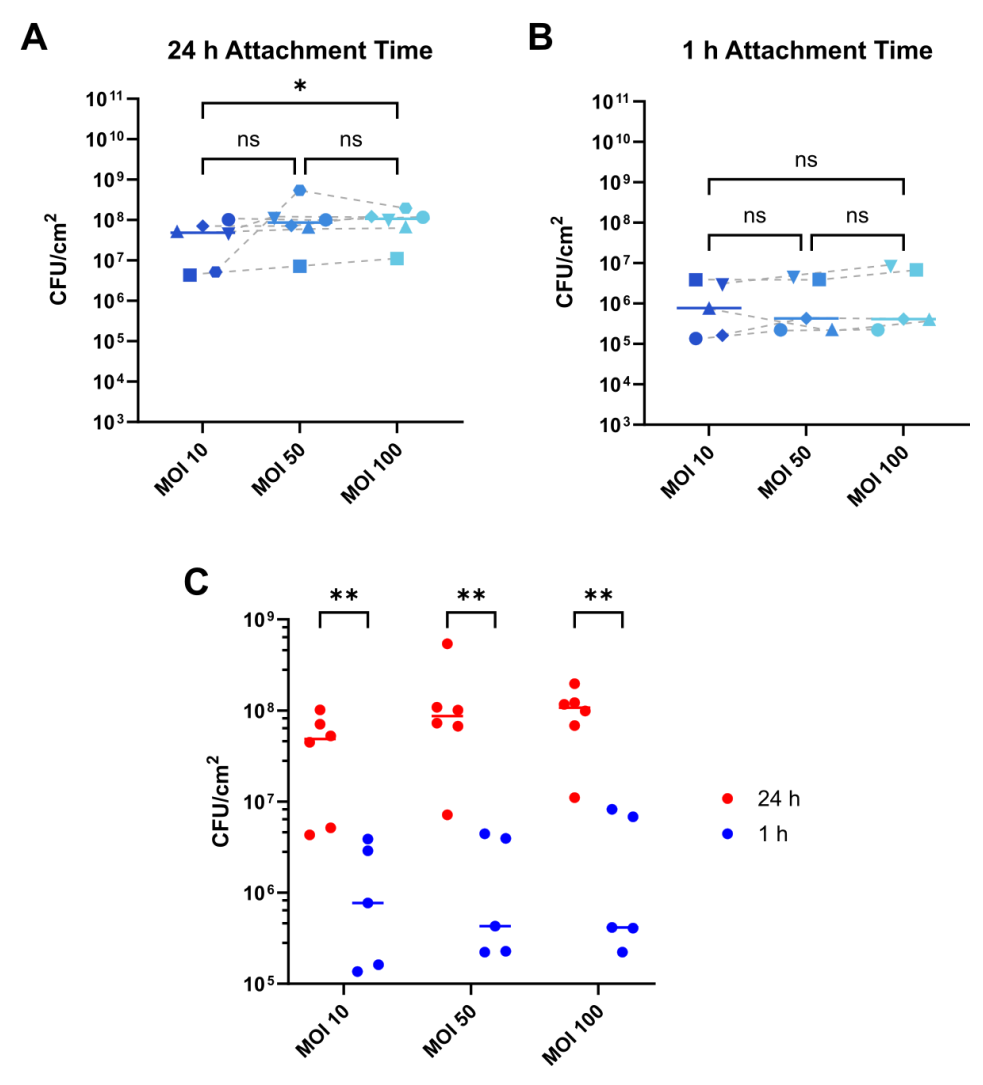


Figure 4.8 Viable PCD-NTHi 4 cells per area recovered after 72 h co-culture on healthy volunteer PNECs at ALI. Ciliated epithelial cell cultures were infected with a clinical strain of NTHi at a range of MOIs and co-cultured for 72 h before being scraped, re-suspended and CFU counts performed. Attachment time (before removing the apical media containing NTHi) was either 24 h or 1 h (A and B respectively). Data shown as paired averages of duplicate wells, n = 6 separate biological replicates for 24 hr attachment, n = 5 for 1 hr attachment, biological replicates shown as different shapes joined by dashed grey lines, solid lines depicting the median. Note that shapes are not equivalent between graph (A) and (B). (C) Comparison of bacterial attachment periods for each MOI. Data was analysed using Friedman tests with Dunn's post hoc analysis (A & B) and multiple Mann-Whitney tests, comparing the difference within each MOI (C) (\*p<0.05, \*\*p<0.01).

## 4.4 Discussion

The aim of this chapter was to co-culture NTHi apically on ALI cultures and recover CFU while TEER remained viable. Apical biofilms were desired as the overall hypothesis of this project was that the addition of macrophages onto established biofilms on ALI cultures would cause a reduction in biofilm viability. The initial objective was to optimise the GFP strain for use in this work for ease of imaging, but it was unable to form apical biofilms. Subsequent work with the clinical strain went on to optimise the MOIs used in order to maximise the CFU recovery, and thus biofilm formation, from a 72 h co-culture. However, it became apparent that the associated drop in TEER, the chosen indicator of epithelial cell layer integrity, meant that the ALI cultures did not consistently remain viable using the current protocol. In response, the time that planktonic NTHi suspensions were incubated on the ALI cultures before aspiration, termed "Attachment Time", was reduced from 24 h to 1 h reducing bacterial recovery (while remaining at acceptable levels) whilst maintaining epithelial integrity. This potentially even acted as an advantage as lower numbers of macrophages were now needed to achieve the desired macrophage/NTHi ratios.

#### 4.4.1 Strain comparison

TEER readings did not change significantly before and after 72 h co-culture under any conditions used in this work (Figure 4.1.& Figure 4.6). The range of TEERs following infection was found to increase with higher MOIs of GFP-NTHi, but not with PCD-NTHi 4. The maintenance of TEER across 72 h of co-culture has been observed previously  $^{224}$ . However, the majority of the observed TEER measurements, even prior to infection, fell below the threshold of approximately  $400~\Omega$ .cm<sup>2</sup> that is generally quoted for primary airway ALI cultures in the literature.  $^{224,230,306,307}$  Visual inspection showed good ciliation, ciliary movement and no visible holes in the cell layer. Culture protocols were interrogated for potential problems, but an underlying cause could not be identified. Since no clear indication of unsuitability could be identified, the samples were used and change in TEER used as an indication of excess cellular damage due to bacterial infection. If more time was available, it would have been worth investigating these comparatively low TEERs and confirm the ALI culture health for cultures with low TEER using methods such as tight junction staining, paracellular permeability measurements, viability stains and cytotoxicity assays as well as assessing ciliary health through CBF and percentage ciliation with the use of HSVM.

MOI did not appear have a significant effect on GFP-NTHi CFU recovery (Figure 4.2). While a significantly higher number of PCD-NTHi 4 CFUs were recovered at MOI 100 at an attachment time of 24 h (Figure 4.8). Similar median CFUs were recovered from GFP-NTHi and PCD-NTHi 4 co-cultures, suggesting that neither strain is more susceptible to the epithelial host defences than the other.

Confocal microscopy provided a 3D, cross-section of the co-culture that clearly visualised bacterial cell localisation. The choice to include GFP-NTHi in the co-culture work despite forming comparatively poor biofilms on an abiotic surface (Section 3.3.2) was made due to the imaging potential of a GFP tagged strain and to serve as a comparison between a lab strain and a clinical isolate for this project. However, the strain was found to be unsuitable when GFP-NTHi cells were observed within a ciliated co-culture through immunofluorescent confocal microscopy but not on the apical surface (Figure 4.3A). A different laboratory strain of NTHi has been observed to invade PNEC ALI cultures within 24 h while simultaneously maintaining an apical biofilm<sup>308</sup>. Labelling the cilia showed a clear distinction between non-ciliated areas where bacterial cells had entered the epithelium and ciliated areas where GFP-NTHi could not be seen (Figure 4.3 B & C respectively). Similar preferences for non-ciliated cells as targets of NTHi invasions have been observed previously<sup>308,309</sup>. Previous observations have shown that CBF and percentage ciliation of PNECs is not affected by 24 - 72 h co-culture with clinical PCD isolates of NTHi<sup>224</sup> though these observations may be strain dependent as other work has found CBF of primary PNECs to be reduced by NTHi laboratory strain 49247<sup>308</sup> and of primary bovine BECs to be reduced by NTHi supernatant within 1 min, though the CBF did increase again but not to pre-exposure levels within the 48 h observed<sup>310</sup>. As NTHi is a human restricted pathogen, the latter work may be less representative. LOS and Protein D have been suggested as causes for reductions in CBF<sup>131,311</sup>. So, while functioning cilia may have initially prevented GFP-NTHi from reaching the epithelial cell surface, virulence factors may have contributed to the loss ciliary function that opened up areas for colonisation. Further work with HSVM for ciliary function and western blots for virulence factors would help elucidate this further.

The lack of apical GFP-NTHi cells was confirmed using SEM (Figure 4.4). A few isolated aggregates were found on areas without cilia, though these were difficult to find. Furthermore, it was difficult to definitively identify these as bacteria or other debris. Different strains of NTHi have been observed to form biofilms on PNECs in the past<sup>84</sup>, though NTHi invasion of the epithelium has also been seen, with preferential invasion of PNECs compared to PBECS<sup>312</sup>. These findings cemented the decision to not take GFP-NTHi forwards for the macrophage work. Both imaging techniques were performed

only once due to logistical constraints and to provide an initial insight into the distribution of bacteria. GFP-NTHi was used as a proof of concept to demonstrate the capability to image the bacteria in co-culture without the need for staining. The aim of this project is to develop a model examining apical biofilm formation on airway epithelium, so while additional biological replicates would be beneficial to reliably demonstrate that internalisation of GFP-NTHi is consistently observed, this work fell outside of the direction of this project. Instead, the characterisation of clinical NTHi isolates from PCD patients was prioritised (Section 4.3.2), and any further co-culture characterisation was performed using clinical isolates.

## 4.4.2 Attachment time comparison

Though no significant drop in TEER was observed, the objective reading for some cultures dropped below a 100 Ω.cm<sup>2</sup> threshold where viability was in doubt when a NTHi attachment time of 24 h was used, both for GFP-NTHi and PCD-NTHi 4. Previous work had shown no negative effect for 24 h NTHi infections of HBEC cultures<sup>9</sup> and PNEC ALI cultures<sup>308</sup>, though this work did not incubate to cocultures for a further 48 h following removal of unattached bacteria. Other work using PBECs and a clinical NTHi strain infected for 24 h and incubated for up to 8 days<sup>232</sup>. Responding to the drop seen in this work, a 1 h attachment period for PCD-NTHi 4 was tested. One potential explanation was that the longer incubation period before the removal of the apical fluid was causing a loss of cellular differentiation in the pseudostratified ALI culture. This was found to be unlikely as comparing the change in TEER between cultures using 1 h and 24 h attachment times only showed a significant difference in infected cultures (MOI 10 - 100) and not in the uninfected control (Figure 4.7C). Alternatively, the length of the attachment period was allowing too much bacterial attachment, which was overloading and reducing the viability of the epithelial cell layer, though attachment of NTHi to ciliated ALI cultures has been observed within 5 min<sup>308</sup>. NTHi may be able to cause cell detachment through LOS or protein D<sup>310</sup>, so loss of host cell-cell adhesion may have been seen in the reduction in TEER. Longer exposure to soluble bacterial virulence factor may also have contributed. NTHi endotoxin mediated upregulation of the adhesion molecule ICAM-19 might also contribute to an increase in NTHi adhesion sites, so longer exposure leads to more adhesion opportunities. Preferential binding to structurally damaged cells by NTHi<sup>313</sup> may also led to a vicious cycle where damage causes increased attachment which in turn causes more damage, so bacterial attachment may be non-linear and there might a be a "tipping point" where the epithelium gets overwhelmed and loses integrity.

MOI did not have a significant effect on TEER change at 1 h attachment time of PCD-NTHi 4 (Figure 4.7B), but there was a significant drop in TEER comparing the uninfected control with MOI 100 when an attachment time of 24 was used (Figure 4.7A), potentially due to the prolonged exposure to a comparably high dose.

It is possible that the fact that there was an MOI based difference in CFU recovery for PCD-NTHi 4 at 24 h attachment, and not when using a 1 h attachment, could be due to these culture conditions allowing a majority of planktonic bacteria to attach to the PNEC surface before the suspension is removed. Shorter attachment periods may limit the total number of bacterial cells that is able to adhere to the surface, making the total cells in the suspension irrelevant. This is supported by the observation that attachment time had a significant effect on CFU recovery at every MOI of PCD-NTHi 4, decreasing the median CFU recovery from a magnitude of 10<sup>7</sup> to 10<sup>5</sup> (Figure 4.8C). It would be worth investigating this further by enumerating the CFUs that are removed following the attachment time, however this work fell outside the scope of this project.

Apical PCD-NTHi 4 was seen on SEM (Figure 4.5), however, SEMs images were only available for cultures using a 24 h attachment as time was limited to repeat this once it was decided to move forward with a 1 h attachment period. Later work on the triple co-culture model showed that PCD-NTHi 4 was forming biofilms following 96 h of co-culture in the NTHi-ALI controls (Figure 6.2A-B). Had more time been available, a more thorough microscopic investigation of PCD-NTHi localisation with methodology such as fluorescence *in situ* hybridization (FISH) would have been ideal as NTHi has been previously observed in both<sup>178,186</sup>. This could be done by staining membrane protein such as ZO-1 or E-Cadherin and visualising the localisation of bacteria in relation to these proteins. Additionally, dissociating the epithelial cells from the membrane and each other and sorting infected and non-infected individual cells using flow cytometry could be used to investigate the proportion of PNECs associated with bacteria.

# 4.5 Summary and Conclusion

This chapter set out to optimise the parameters for co-culturing NTHi on ciliated PNEC ALI cultures.

TEER was used as an indicator of epithelial cell layer integrity and CFU recovery as representative of biofilm formation and survival.

As a result of the data discussed above, GFP-NTHi was excluded from further work due to bacterial infection taking place within the epithelial cell layer and PCD-NTHi 4 was used to infect ALI cultures

for 1 h as this reduced the decrease of TEER during the co-culturing process. As MOI did not affect TEER or CFU recovery, an MOI of 50 was selected as a starting point for developing triple co-cultures that include macrophages.

# Chapter 5 Primary Macrophages and Non-typeable Haemophilus influenzae Biofilms on an Abiotic Surface

## 5.1 Introduction

Following the characterisation and optimisation of PCD-NTHi 4 biofilms on both an abiotic surface and on primary epithelial cells at ALI, the impact of MDMs on these biofilms was investigated.

Biofilms are often formed by opportunistic pathogens such as NTHi in individuals whose immune defences have become compromised, for example in cystic fibrosis<sup>314</sup>, COPD<sup>292</sup> or PCD<sup>315</sup>. Though there are a range of mechanisms that contribute to opportunistic infections in each of these conditions, macrophages are likely to play a role in perpetuating chronic inflammatory conditions. The macrophage response is often dysregulated and ineffective in chronic conditions, however, it is unclear if this is inherently due to macrophages being altered in these conditions or whether a combination of factors such as reduced mucociliary clearance contributes to a general lack of biofilm clearance. It was therefore hypothesised that macrophages from healthy volunteer PBMCs could reduce the viability and biomass of NTHi biofilm grown on an abiotic surface. To address this hypothesis, biofilms were grown on plastic as described previously (Sections 2.1.5 & 3.3.4) for 72 h before macrophages were added and the co-culture incubated for a further 24 h. Treatments are summarised in Figure 5.1: "No media change" indicates that the biofilms remain in the same media in which they were incubated for the initial 72 h, for all other treatments, old media was removed and replaced with either NTHi media (sBHI), MDM media (low serum RPMI) or MDMs suspended in MDM media for the additional 24 h incubation. Initially MBRs of 0.1 and 0.01 were used (MOI 10 and 100 respectively). However, further assays were performed using only MBR 0.01 due to variability in PBMC yield from volunteers. MDM controls meant MDMs were added to empty wells, not containing NTHi biofilms. The impact of MDMs on the biofilms was assessed by investigating biofilm viability and the macrophage response was characterised by measuring cytokine release and cytotoxicity. This chapter will discuss these results, demonstrating a co-culture model that remains viable for 24 h, the effect of MDMs on NTHi biofilms and limitations of the protocol used.

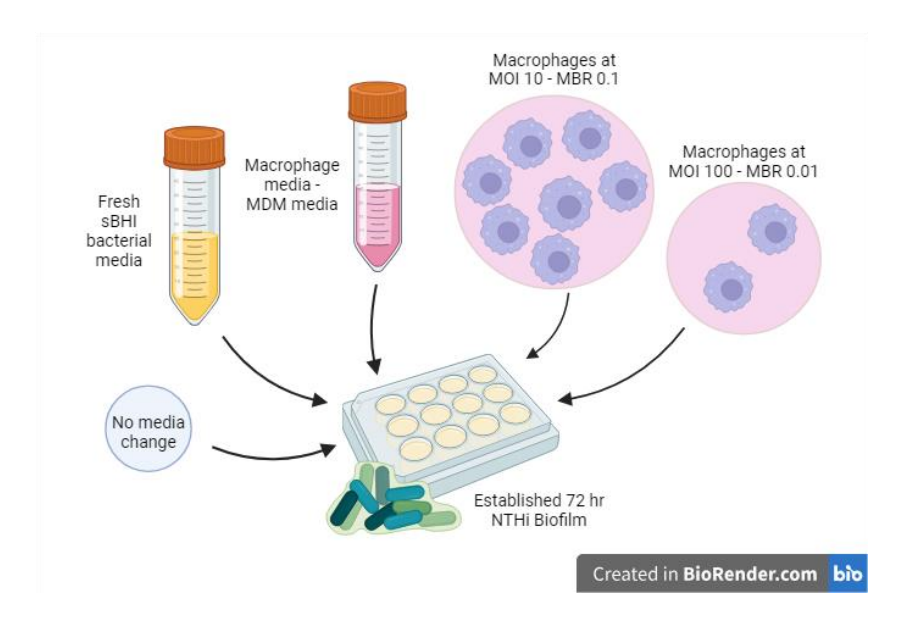


Figure 5.1 Summary of NTHi biofilm treatments following 72 h of incubation. Co-cultures were incubated for 24 h before being processed.

## 5.2 Aims

Aim: To assess the ability of MDMs to reduce established NTHi biofilms on plastic controlling for the impact of MDM media.

## Objectives:

- Visualise the MDM-biofilm interaction through SEM
- Measure changes in biofilm viability through CFU counts and in biomass through CV staining
- Characterise MDM cytokine response through ELISA
- Confirm MDM viability through LDH assay

## 5.3 Results

## 5.3.1 Visualising MDM-NTHi co-cultures

To confirm the presence of MDMs and NTHi biofilms on an abiotic surface after 24 h of co-culture, scanning electron microscopy was used. Intact macrophages could be observed adhering to the glass surface at both macrophage concentrations, MBR 0.1 and MBR 0.01 (Figure 5.2) Macrophages were equally spread over the area (Figure 5.2A & C). MDM cells were generally round with a rough surface and surrounded by areas of filamentous protrusions or cellular debris (Figure 5.2B & D).

Comparing same-sized fields of view, the number of macrophages observed between the MDM control and the MDM-NTHi co-culture suggests that about a third of macrophages remain intact when exposed to the biofilm compared to those added to an empty well.

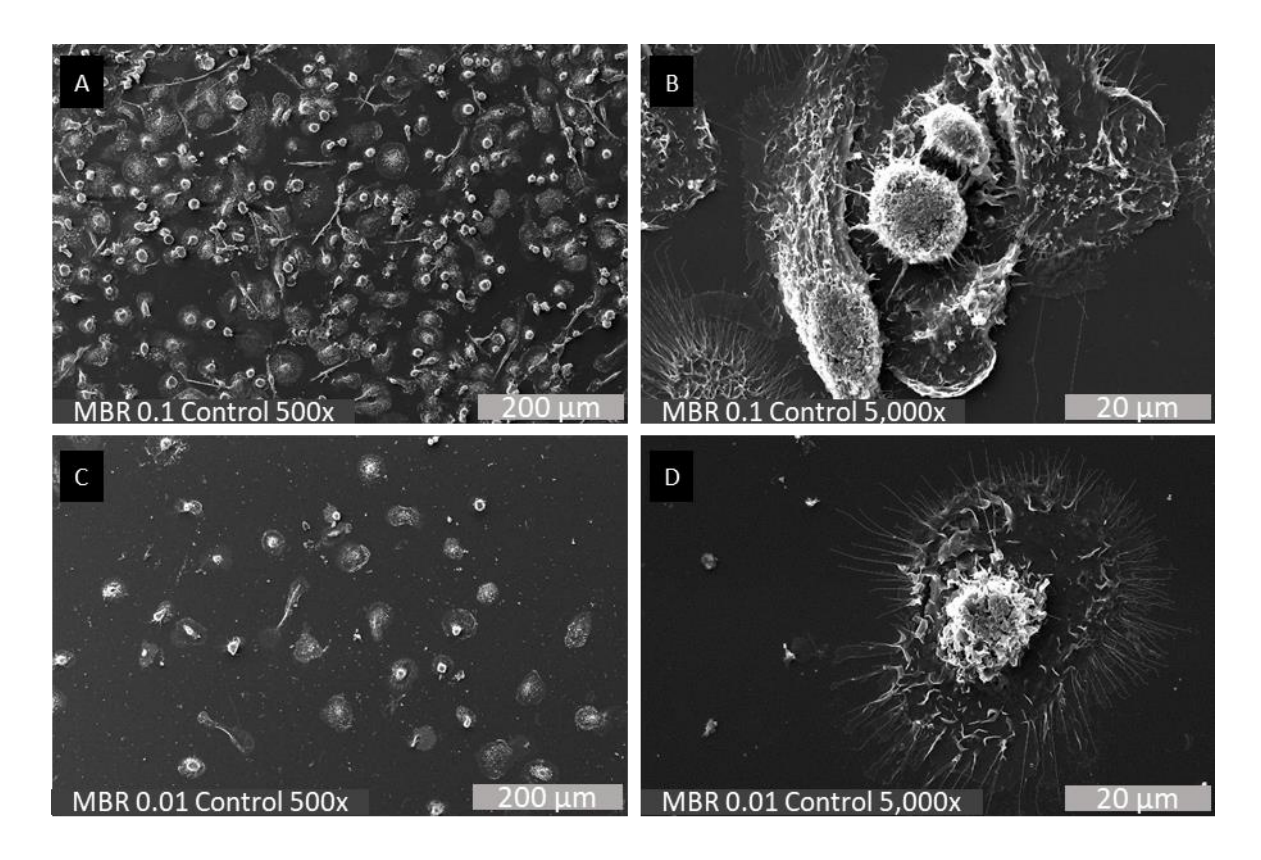


Figure 5.2 SEM images of MDMs on sterile glass coverslips. Macrophages differentiated from monocytes in GM-CSF for 12 days before being dissociated and cultured in low serum antibiotic free medium for 24 h. Macrophage Bacteria Ratio (MBR) refers to the corresponding ratio if the same number of macrophages had been added to an established NTHi biofilm. Intact cells were predominately round with some extending

pseudopodia. Light grey bars for scale with representative lengths. (A & B) MBR 0.1 control (300k MDMs) at 500x and 5,000x magnification respectively. (C & D) MBR 0.01 control (30k MDMs) at 500x and 5,000x magnification respectively.

SEM images of the abiotic MDM-NTHi co-culture show intact macrophages surrounded by bacterial biofilm (Figure 5.3). MDMs were often surrounded by an area cleared of bacteria, but with bacterial cells on the surface of the macrophage cell (Figure 5.3B&C). An extracellular matrix surrounding the bacterial cells could not be clearly identified.

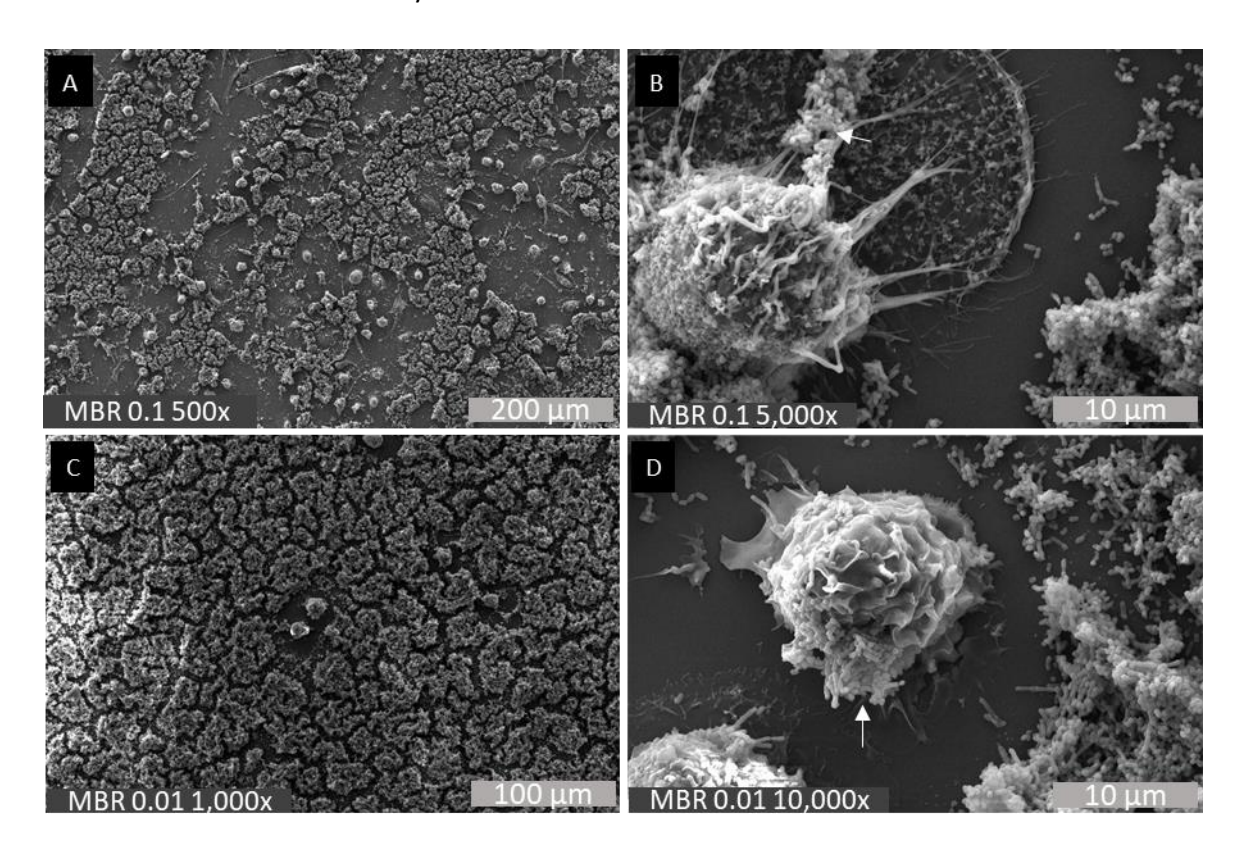


Figure 5.3 SEM images of MDMs and PCD-NTHi 4 biofilms after 24 h co-culture. Primary monocytes were cultured with GM-CSF for 12 days before being added to established NTHi biofilms grown in sBHI for 72 h on sterile glass coverslips. Areas surrounding MDMs are cleared of bacteria and bacteria can be seen on the MDM surface at both MBRs (White Arrows) Light grey bars for scale with representative lengths. (A & B) MBR 0.1 at magnification of 500x and 5,000 respectively. Representative images of MDMs evenly spaced out

across the co-culture. (C & D) MBR 0.01 at magnifications of 1,000x and 10,000x respectively.

### 5.3.2 Biofilm Viability

Following the confirmation of biofilm presence after 24 h of co-culture with MDMs, biofilm viability was quantified using CV staining and CFU counts. CV staining was used as an indicator of total biomass remaining as it binds protein and DNA and could therefore be used to quantify both bacterial cells and any extracellular matrix.

To rule out the possibility of any observed effects on biofilm viability being due to changing the media from bacterial sBHI to MDM RPMI, experiments were conducted using culture media alone without any MDM present. There was no significant effect to bacterial cell culturability between the addition of fresh NTHi media and fresh MDM media when added for 24 h following 72 h of biofilm growth (Figure 5.4A), however biomass was significantly higher when NTHi media was added compared to MDM media (Figure 5.4B).

Not replacing the NTHi media on 72 h biofilms and incubating for a further 24 h (96 h total incubation) lead to a loss of viable CFUs in all but on biological replicate, with the addition of both fresh NTHi media and fresh MDM leading to a significant increase in CFUs (Figure 5.4A). Biomass remained detectable after 96 h without media change, with media replacement after 72 h not leading to a significant change in biomass (Figure 5.4B).

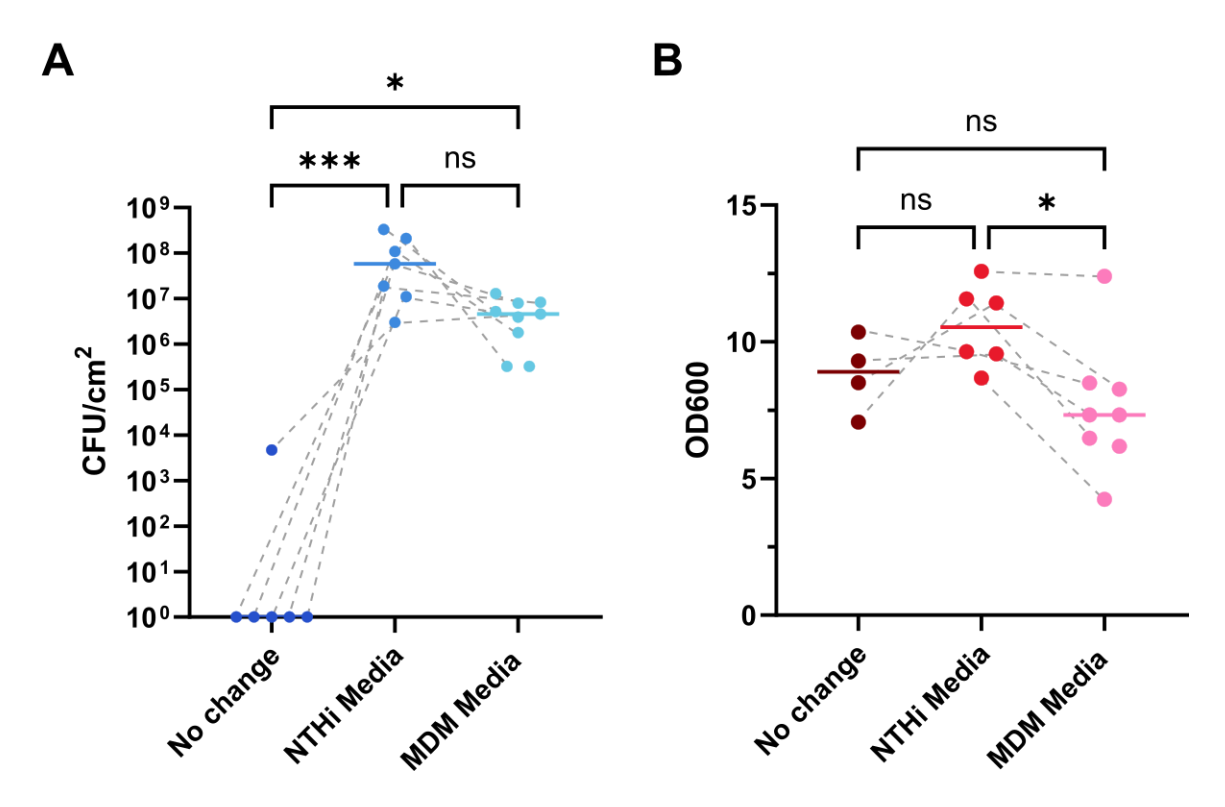


Figure 5.4 Impact of media change on NTHi biofilms grown on an abiotic surface. PCD-NTHi 4 biofilms were grown for 72 h in sBHI before the media was either changed to MDM media (RPMI), fresh NTHi media (sBHI) or not changed and subsequently incubated for a further 24 h. Biofilms were then washed and either resuspended for CFU enumeration or stained using CV (A) Biofilm viability as indicated by culturable CFU counts. (B) Biomass shown as CV OD readings. CFU: n ≥ 6, Biomass: n ≥ 4 of separate biological replicates (linked by dashed grey lines) with data points shown as means of technical duplicates where available, otherwise from single wells per biological replicate. Solid lines indicate the median. Data were analysed using Kruskal-Wallis with Dunn's post hoc analysis test (\*p<0.05, \*\*\*p<0.001).

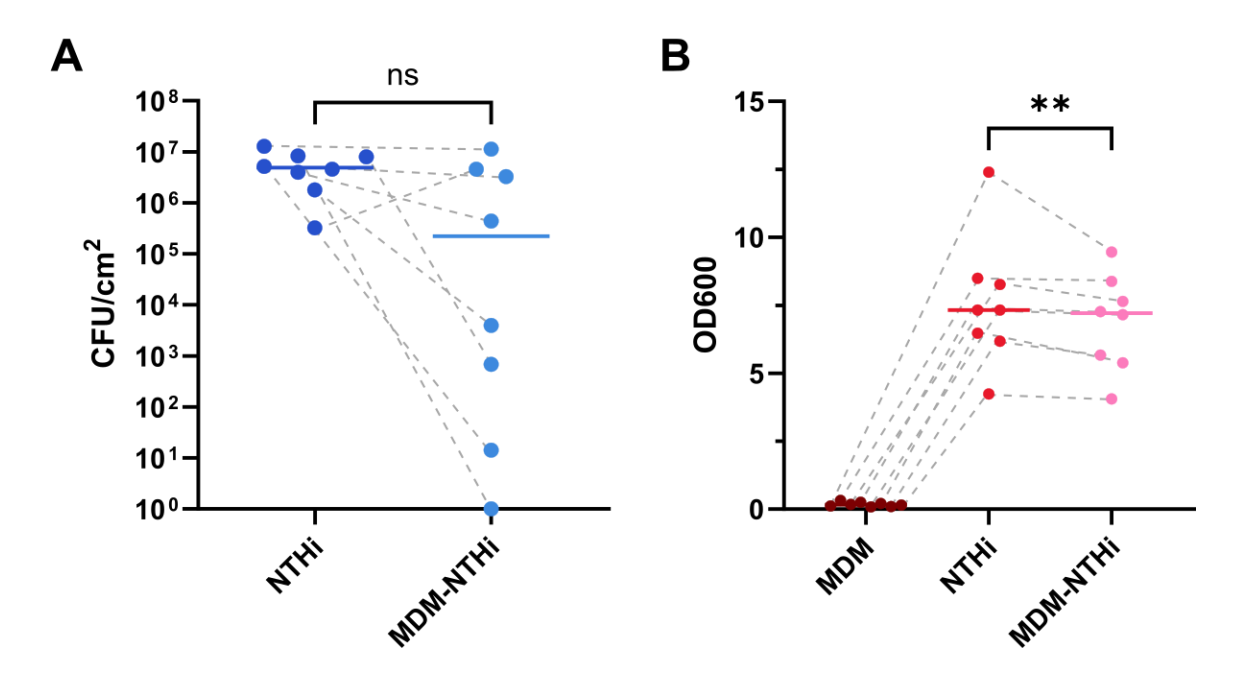


Figure 5.5 Biofilm characterisation following 24 h MDM-NTHi co-culture. PCD-NTHi 4 biofilms were grown for 72 h followed by the addition of MDMs at a 0.01 MDM:NTHi ratio and a further 24 h incubation before being washed and processed for CFU enumeration of CV staining (A) Viable CFU counts (B) Biomass shown as CV OD readings. n = 8 biological replicates (linked by dashed grey lines), paired datapoints are shown as averages of technical duplicates where available, some as single wells per biological replicate. Solid lines depict the median. NTHi and MDM-NTHi co-cultures were compared using Wilcoxon test (\*\*p<0.01)

The addition of macrophages did not have a significant effect on biofilm viability, as measured by culturable CFU counts, after 24 h of co-culture and a ratio of 0.01 macrophages to NTHi (Figure 5.5A, p = 0.078). The CFUs had a large range following the addition of MDMs compared the CFUs on the media control,  $0 - 1.13 \times 10^7$  and  $3.25 \times 10^5 - 1.28 \times 10^7$  for the MDM-NTHi co-culture and NTHi respectively, a difference in range of  $1.2 \times 10^6$ .

There was a statistically significant decrease in biomass following the addition of MDMs to established NTHi biofilms (Figure 5.5B), though the change in median was only 0.115.

## **5.3.3** Macrophage Response

The macrophage response to co-culturing macrophages and established NTHi biofilms for 24 h on an abiotic surface was investigated through the analysis of cytokine release into the culture

supernatants using ELISAs. A significant increase in pro-inflammatory cytokine release was detected when MDMs were exposed to NTHi biofilms for 24 h compared to MDM control cultures (Figure 5.6A-D). There was no statistically significant release of the anti-inflammatory cytokine, IL-10, in the same co-cultures (Figure 5.6E). The cytokine response of MDMs to MDM-NTHi co-cultures showed a large range compared to the baseline MDM cytokine release with a 5 - 40 fold increase in range for pro-inflammatory cytokines.

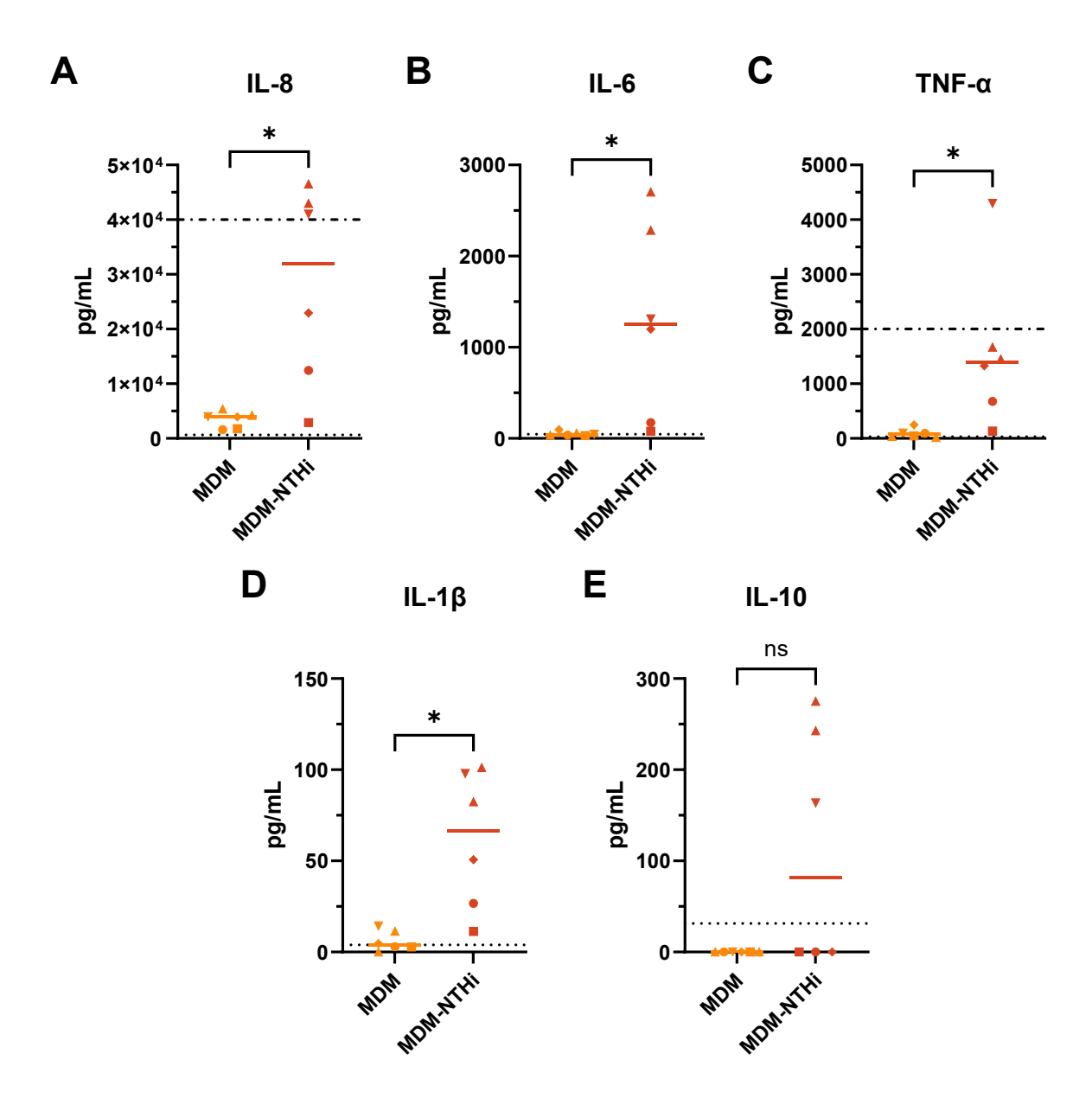


Figure 5.6 Cytokine release by MDM-NTHi co-cultures compared with MDM culture controls. Primary MDMs were co-cultured with established 72 h PCD-NTHi 4 biofilms for 24 h, supernatants were collected and analysed using ELISAs. Pro-inflammatory cytokines IL-8

(A), IL-6 (B), TNF- $\alpha$  (C) and IL-1 $\beta$  (D) and anti-inflammatory cytokine IL-10 (E) were quantified. n = 6 separate biological replicates (shapes depicting readings from the same biological replicates), paired datapoints show means of duplicate ELISA wells from same supernatant sample. Medians depicted by solid lines. Dot-dash line shows upper detection limit, dotted line shows lower detection limit. Data were analysed using Wilcoxon tests (\*p<0.05).

As an indicator of cell lysis, LDH release into the supernatant was quantified to assess the cytotoxicity of MDM exposure to biofilms. All readings were corrected for the media background reading of 0.06 OD. A significant difference was observed between the MDM-NTHi co-cultures and both MDM and NTHi controls. The NTHi and MDM control cultures, were not compared with each other. The ranges were 0.064, 0.153 and 0.236 for the NTHi control, the MDM control and the MDM-NTHi co-culture respectively. The fold change of LDH release between matched MDM and MDM-NTHi co-cultures ranged between 1.6 and 6 with one MDM-NTHi leading to a 129-fold increase in LDH release compared to the paired MDM culture.

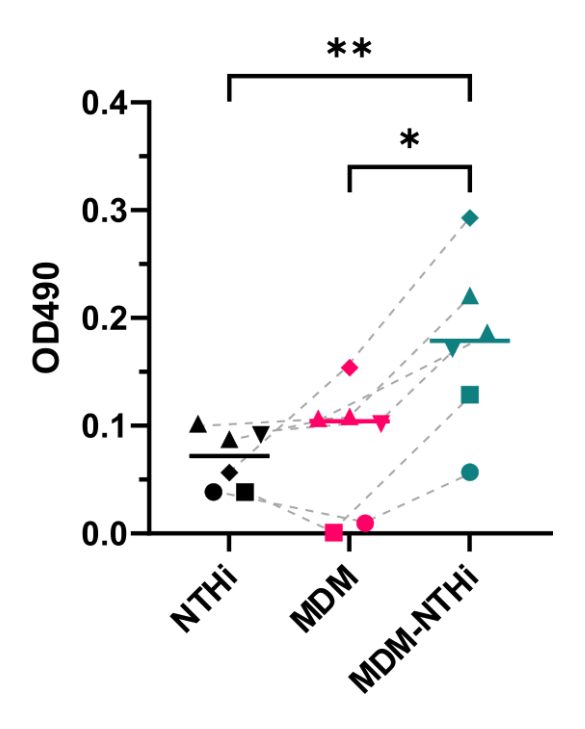


Figure 5.7 Supernatant LDH released by MDM-NTHi co-culture. Primary MDMs were co-cultured with established 72 h PCD-NTHi 4 biofilms for 24 h, supernatants were collected and LDH levels quantified. n = 6 separate biological replicates (shapes linked by dashed grey lines), paired datapoints show means of duplicate assay wells from same supernatant

sample. Medians depicted by solid lines. Friedman test with Dunn's post-hoc analysis only comparing MDM-NTHi to each control (NTHi only and MDM only cultures), all comparisons shown (\*p<0.05, \*\*p<0.01)

## 5.4 Discussion

The work presented in this chapter demonstrated that primary MDMs fail to significantly reduce PCD- NTHi 4 biofilm viability after 24 h of co-culture on a plastic surface. MDMs remain viable during this co-culture incubation and produce a pro-inflammatory cytokine response, though a high degree of variability was observed between donors/biological replicates.

To the best of our knowledge, this work had been the first to attempt adding macrophages to established NTHi biofilms on an abiotic surface. Similar work has been done with *Staphylococcus aureus* by Thurlow et al at MOI 10 (MBR 0.1), co-culturing macrophages with the biofilms for 1 h and 24 h<sup>300</sup>. Intercellular survival of NTHi has previously been observed<sup>276</sup>, though that work was done with planktonic bacteria rather than biofilms and on an abiotic surface, it showed that NTHi was able to infect MDMs within 2 h and both NTHi and MDMs remained viable for 24 h.

Macrophage viability prior to co-culture was confirmed using trypan blue (97% viability, Section 2.3.2). Ideally, the effect of the low serum media and the trypsinisation process would have been thoroughly characterised. Though used in other work<sup>316</sup>, trypsinisation has been shown to decrease cell surface markers in an incubation time dependent manner, affecting cell function<sup>317</sup>, so the effect of the dissociation process was not negligible. Unfortunately, the monocyte yield and time constraints limited the amount of characterisation possible. Intact MDMs could be observed via SEM following 24 h culture either alone or with NTHi biofilms, indicating that MDMs remained viable throughout the co-culture process. Measurable cytokine release further supported this. Further viability assays such as MTT assays, live/dead staining microscopy and flow cytometry would help quantify the cytotoxic effect of the co-culturing process on MDMs.

The SEM images of MDM-NTHi co-cultures showed lawns of bacteria, interrupted by areas of clearance surrounding macrophages. This was reflected in a statistically significant decrease in CV staining in MDM-NTHi co-cultures compared to NTHi only controls. As bacteria could be seen on the surface of macrophages it is unclear if the bacteria had moved onto the macrophages from the surface or if the area was cleared by the macrophage and surviving bacteria had multiplied on the macrophage. This work only used a single endpoint, so more frequent time points or timelapse

microscopy with staining methods like Cell-Tracker would lead to a better understanding of the NTHi-MDM interaction. No clear extracellular matrix could be identified surrounding the bacterial cells. SEM biofilm images of other NTHi strains have shown an extracellular matrix in the past, but it was also noted that there is a strain-based heterogeneity of matrix protein<sup>318</sup>. The absence of an extracellular matrix in these SEM images is therefore likely to be a strain specific feature, that may not be observed in other strains. SEM images of other clinical isolates such as those used in Chapter 3 may have demonstrated this heterogeneity if more time was available.

As the MDM medium is not designed for biofilm growth, the effect of media changes on the NTHi biofilms was investigated. Following 72 h undisturbed incubation in sBHI, the media was replaced with either fresh sBHI, MDM media or not replaced.

Not replacing media, effectively keeping the NTHi biofilm undisturbed for 96 h, led to a loss of culturable bacteria in all but one case, suggesting that media has been depleted to the point of bacterial death at this time point. PCD-NTHi 4 biofilm viability after 72 h of incubation was previously confirmed (3.3.4). Another explanation for the decline in CFU counts following 96 h of incubation is the entry into a VBNC state, previously observed in NTHi<sup>319</sup>, which can be induced by a range of factors including changes in pH nutrient starvation<sup>320</sup>. As VBNC bacteria remain intact and metabolically active<sup>321</sup>, live/dead staining and PCR would be useful methods to determine the viability after a 96 h incubation period.

There was no significant difference in biomass between keeping the biofilms in spent media and replacing it with either NTHi media or MDM media, suggesting that the media change does not reduce the biomass in isolation. Replacing the media with fresh sBHI led to a significant increase in biomass compared to replacing it with MDM media. This may reflect an increased growth and production of biofilm matrix due to the availability of the biofilm optimal, nutrient rich media which was not possible with the suboptimal MDM media. However, as fresh sBHI does not increase viability compared to MDM media, it is possible that there's a difference between cells being "reactivated" by any fresh media and having enough nutrients to produce more biomass. This increase in biomass could potentially come from an increased cell size. Alternatively, it may reflect a more structurally stable biofilm that is less susceptible to damage through washing. Washing the biofilm before processing it removes any non-adherent cells, it is therefore a method for measuring the biofilm alone. However, though care is taken, the detachment of small sections of the biofilm as a result of washing cannot be ruled out. SEM microscopy and confocal microscopy staining for EPS material could be used to further understand the structural changes caused by the different media

treatments. A more in-depth investigation of gene expression through RNA-Seq could elucidate the bacterial response further, but this lay considerably outside the remit of this project. The lack of significant difference in viable CFU between the MDM and the bacterial media suggests that biofilms recover to a similar viability following the media change, so addition of MDM after 72 h is a viable model for studying the effects of macrophages on the biofilm.

NTHi biofilms remained intact and viable over the 24 h MDM-NTHi co-culture as seen on SEM images, CFU recovery and CV staining. The addition of MDMs did not significantly affect the median number of viable CFUs in the co-culture, though in some cases, no CFUs were recovered from the biofilm following MDM-NTHi co-culture. In these cases, the paired NTHi-only cultures remained viable, ruling out experimental failures such as contamination or technical issues such as incubator failure. Planktonic NTHi has been observed to survive better in the presence of MDMs compared to being cultured alone, this effect increasing with length of co-culture<sup>236</sup>. The range of viable CFU recovery following 24 h MDM-NTHi co-culture suggests that MDM may have an effect on NTHi biofilm viability, but that this may be donor dependent and therefore not demonstrated here to a statistically significant level due to relatively low numbers of biological replicates. Additionally, experimental variation cannot be ruled out. Ideally, MDMs from the same donors would be used on multiple occasions to clarify the cause of the observed variation.

MDMs responded to MDM-NTHi co-culture with significant increases in pro-inflammatory cytokine release. Increased levels of IL-8, IL-1 $\beta$  and TNF- $\alpha$  were detected in the supernatant compared to the MDM cultures without NTHi biofilms, while no increase in the anti-inflammatory cytokine IL-10 was observed. The GM-CSF differentiation method Similar levels of IL-6 and IL-1 $\beta$  release has been observed in primary MDMs in response to 24 h planktonic NTHi infection<sup>236</sup>. As with CFU recovery, a large range in cytokine responses was observed. Anecdotally, one donor provided MDMs on two separate occasions and cytokine release was similar in both instances which is an indication towards donor-based variability, though clearly more samples from the same donor and multiple samples from other donors would be needed to fully substantiate this conclusion.

LDH release, typically used as an indicator of cell lysis, increased significantly in the MDM-NTHi cocultures compared to both MDM and NTHi mono-cultures. Limitations in MDM yield meant that it was not possible to collect fully lysed control samples of co-cultures against which the LDH release could be compared. Since cytokine release was detected in all of these co-cultures and *in vivo* degradation of cytokines ranges between 18 min and 15 h<sup>322</sup> it may be more likely that the increased LDH levels observed are due to increased metabolic activity as the macrophages responded to the NTHi biofilm since LDH plays a role in glycolysis<sup>323</sup>, catalysing the production of lactate. Live/dead or TOTO3<sup>300</sup> staining and confocal microscopy could have been used to visualise the co-culture and verify viability. Additionally, LDH release was seen in the NTHi control culture here and in previous planktonic NTHi work<sup>236</sup>, so NTHi lysis may also contribute to LDH levels in the MDM-NTHi co-cultures.

Generally, the same biological replicates consistently had the highest levels across all proinflammatory cytokines measured. The LDH release in these co-cultures was around the overall
median with similar trends observed in the MDM monoculture. The two co-cultures with the lower
cytokine release also had the lower LDH release and higher CFU counts, suggesting lower MDM
activity and therefore less effect on biofilm viability. On the other hand, lower cytokine release may
correspond to higher MDM lysis and thus LDH release which was observed in one co-culture which
also showed no reduction in CFUs. LDH inhibition has been observed to reduce the release of
inflammatory cytokines by macrophages in response to LPS<sup>323</sup> and addition of LDH has been seen to
lead to an increase in inflammatory cytokine release<sup>324</sup>. It is therefore possible that LDH, either as
by-product of the macrophage metabolism or as a result of MDM lysis, is further enhancing the
inflammatory response and possibly leading to a feedback mechanism. The co-cultures in this work
were only incubated for 24 h, however there is evidence that prolonged exposure to lactate
eventually induces a more anti-inflammatory phenotype in macrophages in order to repair damage
caused by the inflammation process<sup>325</sup>.

As mentioned previously, this work did not have enough biological replicates to draw firm conclusions on this, rather it should be viewed as preliminary data for future work. The suggested connection between cytokine release, LDH and biofilm CFU counts highlights the importance of acquiring matched readouts for co-cultures. Doing so may help explain observations beyond simply the impact of MDM-NTHi co-culture and increase our understanding of donor variation which could aid experimental design in the future. Additionally, methods such as flow-cytometry, microscopy, PCR and MTS assays would help to confidently differentiate between differences in metabolic activity and viability of MDMs.

While this work used a variety of primary MDM donors, only one clinical isolate of NTHi was used. NTHi is very heterogeneous, for example, planktonic NTHi persistence in primary MDMs has been shown to be strain dependent<sup>181,183,236</sup>. Therefore, not only does MDM donor variation need to be accounted for in future work but NTHi strain heterogeneity should also be considered.

### 5.5 Summary and Conclusion

This chapter showed that primary MDMs could be co-cultured with established PCD-NTHi 4 biofilms for 24 h. Small areas of biofilm appear to be cleared surrounding the macrophages and there is a decrease in biomass, however the bacterial viability does not appear to be affected by MDM presence. The biofilms are not affected by the change in media. Macrophages produce a measurable pro-inflammatory response when exposed to NTHi biofilms as well as an increased release in LDH. The protocol established here provides the necessary tools to move on to developing a NTHi-MDM-PNEC triple co-culture in the following chapter.

# Chapter 6 Non-typeable *Haemophilus influenzae*, Macrophage and Epithelial Cell Triple Co-Culture

#### 6.1 Introduction

Protocol Summary:

# PNECs NTHI Differentiated for 4+ weeks attachment for 72 hrs addition addition attachment for 24 hrs

#### **Treatment Summary:**



Figure 6.1 Summary of ALI culture protocol and treatment definitions for triple co-cultures and controls. Following ALI differentiation, 50  $\mu$ L of NTHi suspensions (or HBSS) was added for 1 h and after 72 h 10  $\mu$ L of MDM suspension (or MDM media) was added for 24 h. Control – ALI culture only, NTHi-ALI – Biofilm on ALI culture, MDM-ALI – Macrophages on ALI, Triple – Macrophages on Biofilms on ALI culture. Created with Biorender.com.

In the previous chapter, a protocol for dissociating viable MDMs from their culture well was established and it was demonstrated that MDMs could be added to an established biofilm on an abiotic surface and co-cultured for 24 h. To investigate if this interaction is affected by the presence of primary airway epithelium, PNECs were cultured at ALI to resemble a ciliated, pseudostratified epithelium. NTHi cells were grown on this ALI culture for 72 h before MDMs were added at the same MBR as the with the biofilms grown on plastic in the previous section (Chapter 5), an MBR of 0.01. This corresponds to an effective MOI of 100. This ratio was selected to serve as a comparison

between the MDM response to NTHi biofilms on plastic. The four co-culture treatments of ALI cultures that will be compared in this chapter are summarised in Figure 6.1.

#### 6.2 Aims

Aim: Characterise the impact of MDM addition to established NTHi biofilms on airway epithelium ALI cultures, including controls for ALI, ALI-MDM and ALI-NTHi in each experiment.

#### Objectives:

- Visualise MDM impact, localisation, and cell viability through SEM.
- Confirm epithelial cell integrity through TEER.
- Measure co-culture cytotoxicity through LDH.
- Characterise the combined cytokine response of PNECs and MDMs through ELISA.
- Measure changes in biofilm viability through CFU counts.

#### 6.3 Results

#### 6.3.1 Visualising Co-Cultures

SEM was used to visualise co-cultures and confirm the presence of viable MDMs and bacterial cells following 72 h NTHi infection and subsequent 24 h MDM addition (see section 6.1 & 2.3.2 for details). Viable macrophages were observed on the MDM-ALI cultures (Figure 6.2C & D), often in clusters around the outside of the ALI culture, rarely towards the centre. Bacterial aggregates could be seen in areas of reduced ciliation on NTHi-ALI co-cultures (Figure 6.2A & B).

Viable MDMs on triple co-cultures were observed in proximity to bacterial aggregates, predominantly in direct contact with bacteria (Figure 6.3C & D). These were seen both on ciliated and non-ciliated areas. Additionally, bacterial aggregates on triple cultures could be seen on non-ciliated areas with no MDMs nearby (Figure 6.3A). Bacteria were also observed on ciliated areas where they were associated with larger, smooth, rounded globules which could potentially be mucus (Figure 6.3B).

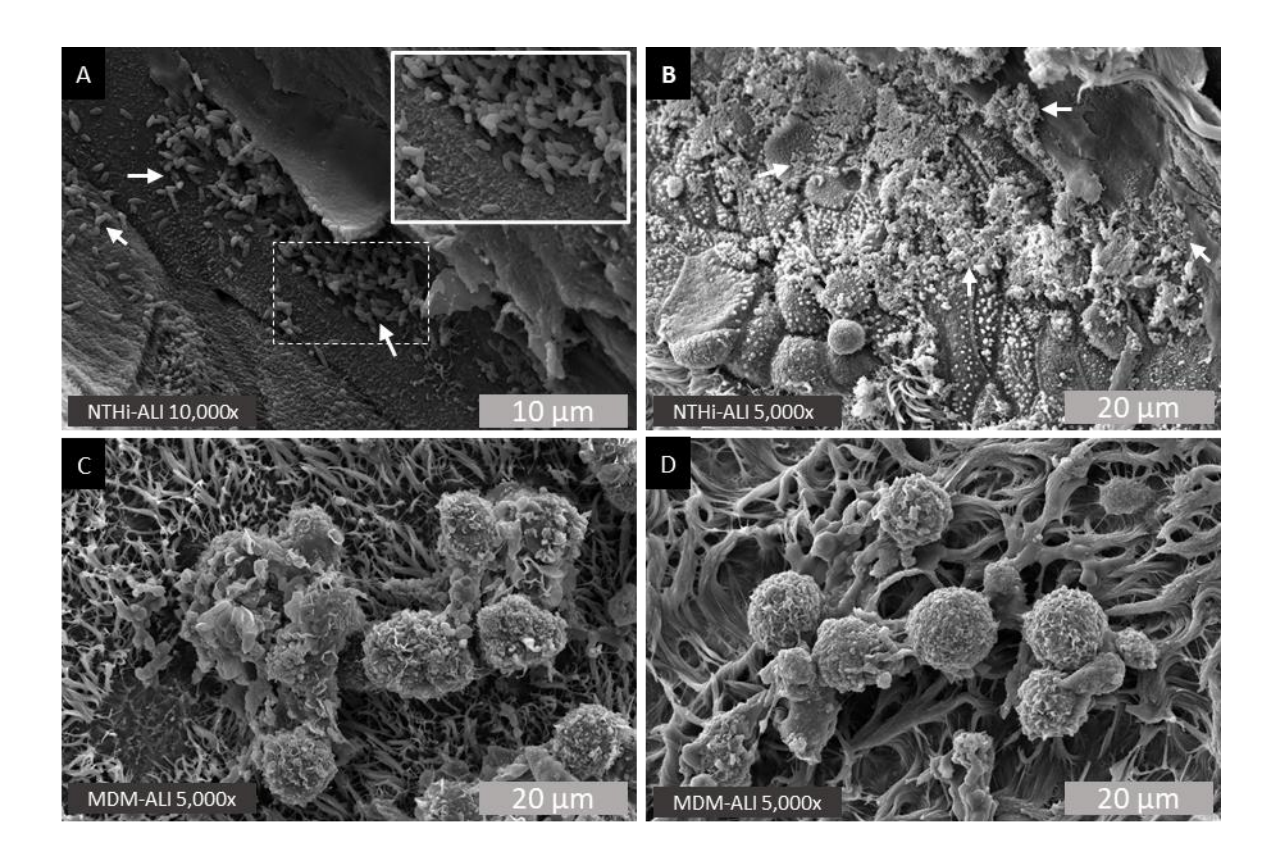


Figure 6.2 SEM images of MDMs and NTHi on ciliated airway epithelial cells. These cultures acted as controls for the triple co-cultures. (A-B) Bacterial aggregates are shown by white arrows (A) in-lay shows zoomed in dashed window. NTHi-ALI cultures were infected with PCD-NTHi 4 and co-cultured for 72 h to allow the formation of biofilms before washing the apical side, replacing the basal media and culturing for a further 24 h. (C-D) MDMs in clusters on ciliated epithelium. MDM-ALI cultures were not infected with NTHi and had MDMs added in antibiotic free media and the co-culture incubated for 24 h. Images are representative of n = 3 biological replicates.

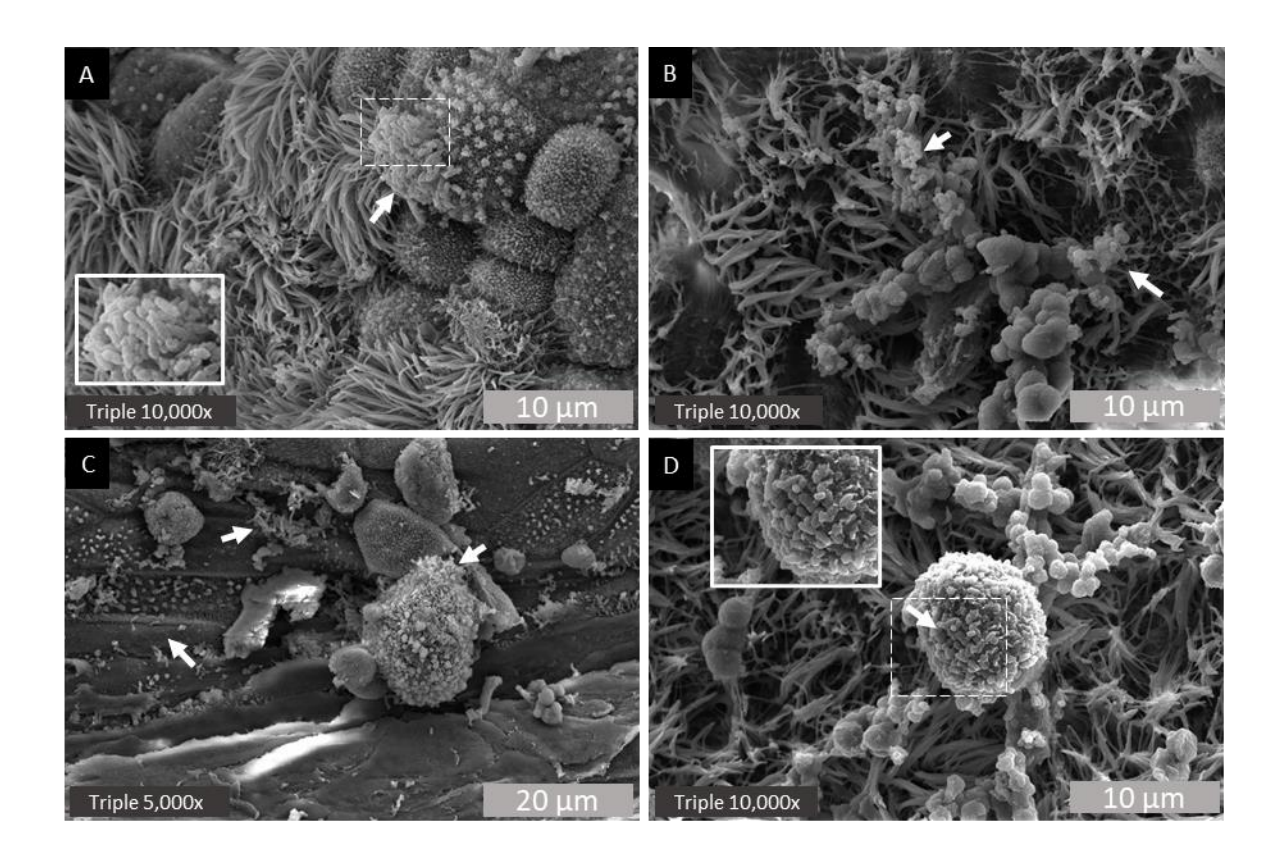


Figure 6.3 SEM images of triple co-cultures on ALI airway epithelial cells. Ciliated ALI cultures were infected with PCD-NTHi 4 for 72 h before MDMs were added and the triple cultures incubated for a further 24 h. White arrows show examples of NTHi cells. In-lays show zoomed in dashed windows A) shows a biofilm on a non-ciliated epithelial cells near a ciliated area. (B) Bacteria on a ciliated area (C) Bacteria on the surface of a macrophage with further bacterial aggregates on the epithelial cell surface. (D) Macrophage on a ciliated area surrounded by mucus with bacteria on its surface. Images are reprasentative of n = 3 biological replicates.

#### 6.3.2 ALI culture integrity and viability

TEER was used as an indicator of epithelial cell layer integrity and thus a representation of co-culture health. These readings were taken both to investigate the impact of co-culturing on TEER and to ensure that infections and treatments did not compromise the cells in a significant manner so that subsequent readouts of cytokines and CFUs corresponded to a viable culture. No statistically significant changes in TEER between the timepoints for any of the co-culture treatments was observed (Figure 6.4) as well as all readings being above  $250 \,\Omega.\text{cm}^2$ . The spread of the TEER readings decreased at each stage of the co-culture, with triple co-culture TEER readings going from a range of  $555 \,\Omega.\text{cm}^2$  before infection to a range of  $383 \,\Omega.\text{cm}^2$  after 72 h NTHi infection followed by  $205 \,\Omega.\text{cm}^2$  following 24 h triple co-culture. Similar trends were observed in the uninfected controls, NTHi-ALI and MDM-ALI co-cultures over the experimental time course.

Previous experiments using primary cells, both PNECs and MDMs, have shown that donor variability or inherent and unavoidable experimental variability, like room temperature, may have a larger impact than experimental conditions such as co-culture treatments. Therefore, the TEER data was analysed from a donor perspective rather than a treatment perspective. Assessing the TEER readings by ALI donor/biological replicate and grouping all treatments together revealed a consistent trend in TEER changes over time within each biological replicate (Figure 6.5). In most cases, no significant changes in TEER were observed between time points within each donor, however different cultures could be seen either decreasing or increasing in TEER in the same time frame (Figure 6.5B & C). Additionally, one ALI donor was used in two separate biological repeats (with different MDM donors). The TEER trend was different between the two biological repeats (Figure 6.5E & F), suggesting experimental variation rather than a donor specific difference.

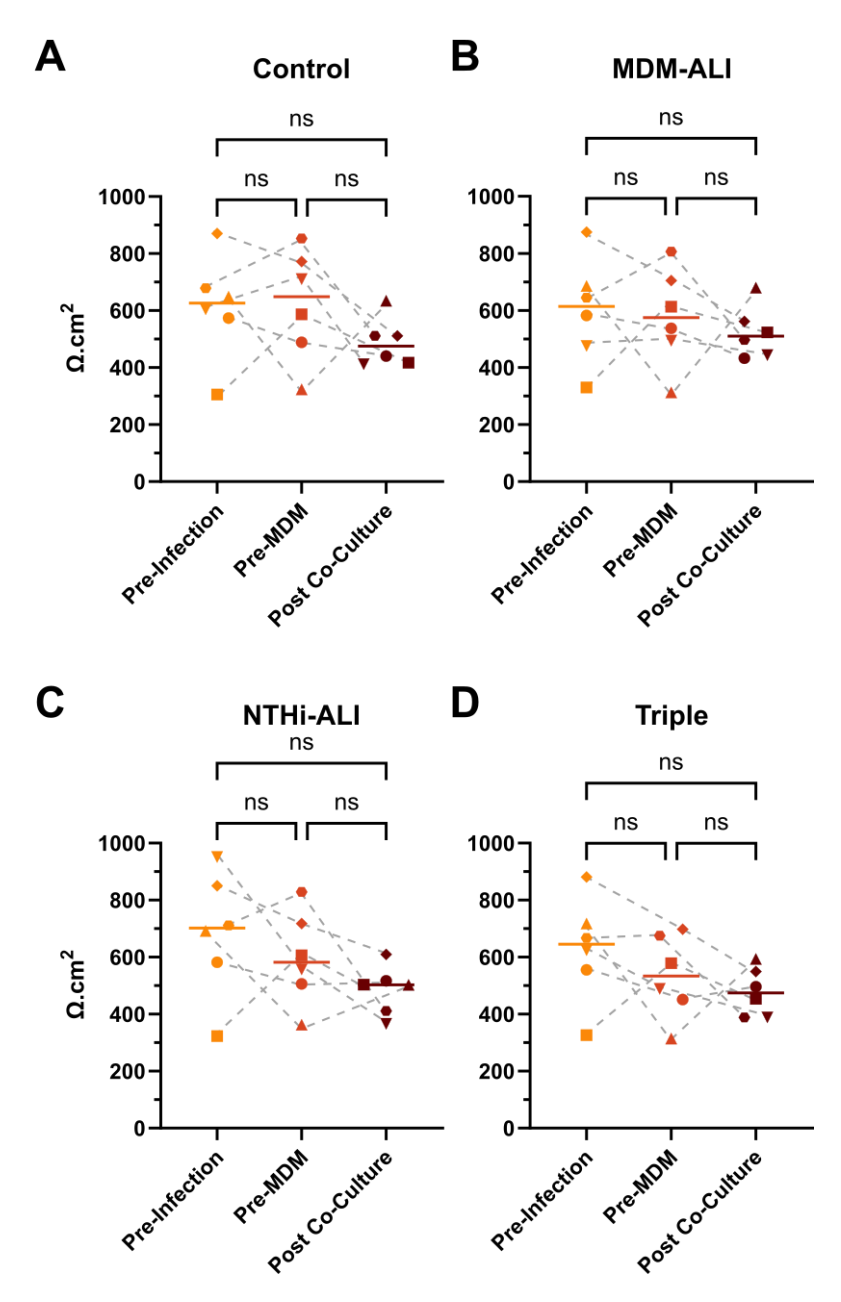


Figure 6.4 Epithelial cell layer integrity during triple co-cultures of MDMs on NTHi infected, differentiated PNEC ALI cultures and associated control co-cultures. Ciliated PNEC ALI cultures were infected with PCD-NTHi 4 for 1 h before 72 h co-culture followed by 24 h MDM addition. X axis labelling refers to these time points, A-C will not have NTHi and MDMs added at the corresponding time points (A) Control culture had no bacteria or MDMs added. (B) MDM-ALI was not infected with NTHi but did have MDMs added. (C) NTHi-ALI was infected with NTHi but had no MDMs added. (D) Triple co-culture had both NTHi and MDMs added. TEER was measured in three positions per culture, the

mean calculated and corrected for background TEER. n = 6 biological replicates (shapes joined by dashed grey lines), datapoints show the mean of duplicate wells (single technical replicate for Control cultures (A)), solid lines represent the median. Time points were compared using Friedmann Tests with Dunn's post hoc analysis, no significant differences were observed.

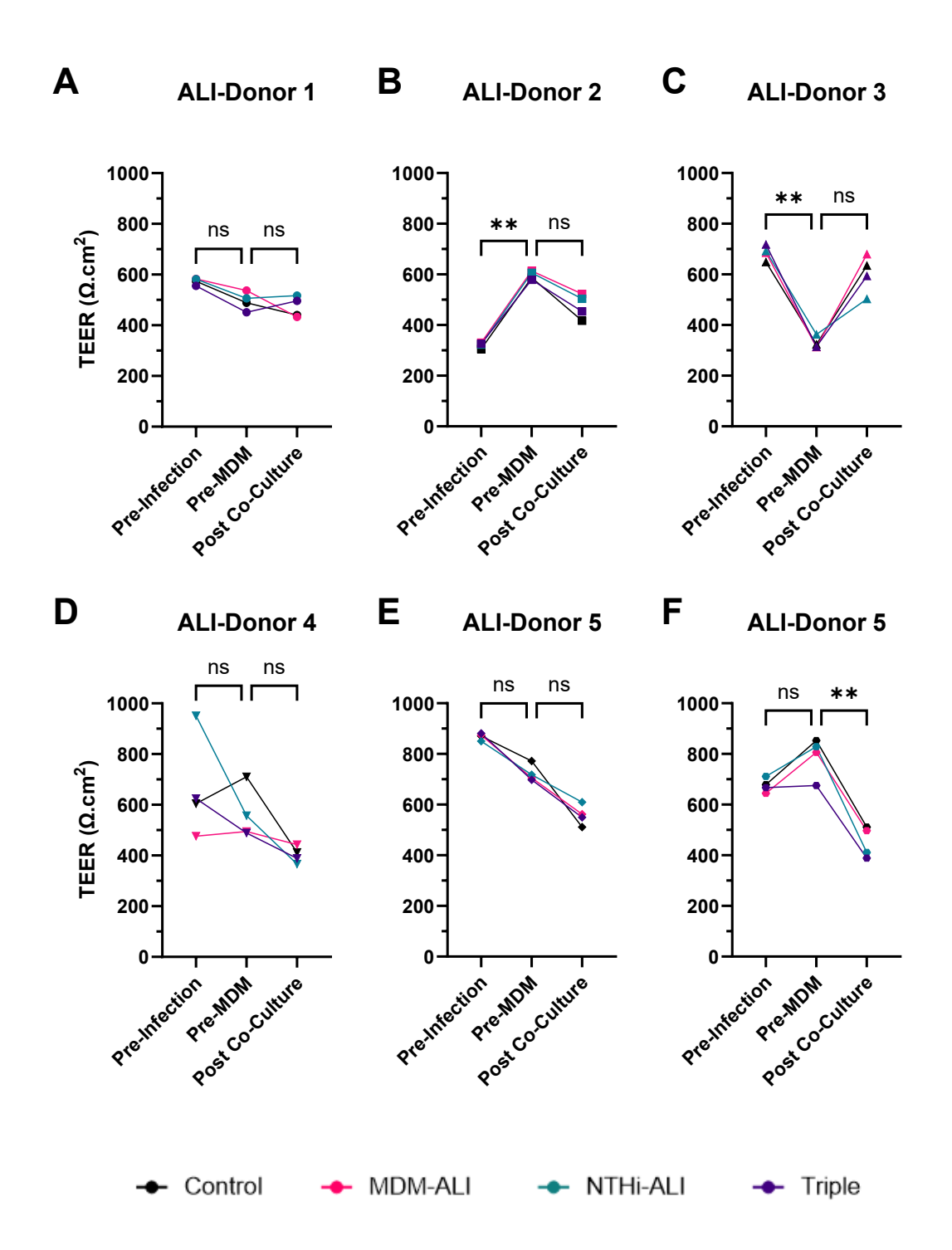


Figure 6.5 Epithelial cell layer integrity (measured through TEER) of PNEC ALI cultures from different donors during co-culture with PCD-NTHi 4 and MDMs. For Triple co-cultures, ciliated ALI cultures were infected with bacteria for 1 h, co-cultured for 72 h followed by the addition of MDMs for a further 24 h. Control cultures (black) were only ALI cultures, MDM-ALI (magenta) were not infected with bacteria and NTHi-ALI (teal) did not have MDMs added. n=4 treatments per 6 biological repeats, data is shown as means of

duplicate wells (Control treatment only had single technical replicates). ALI donor 5 (E-F) was used twice, with different MDM donors. Data was analysed using Friedman tests with Dunns post hoc analysis for adjacent time points (\*\*p < 0.01).

As an additional measure of culture viability, a LDH assay was used as an indicator of cytotoxicity by quantifying the levels of LDH released into the supernatant, both apical and basolateral. A significant increase in LDH release was observed in the apical supernatant compared to the basolateral side in the MDM-ALI and triple cultures (Figure 6.6), the two that included MDMs in the apical compartment. No significant differences were seen in cultures that did not involve MDMs (Control and NTHi-ALI). Apical supernatants from co-cultures with MDMs had a larger range in LDH readings than basolateral supernatants or apical supernatants from non-MDM co-cultures, with ranges of 0.72 and 0.67 for MDM-ALI and Triple co-cultures respectively, and ranges below 0.18 for all other supernatants.

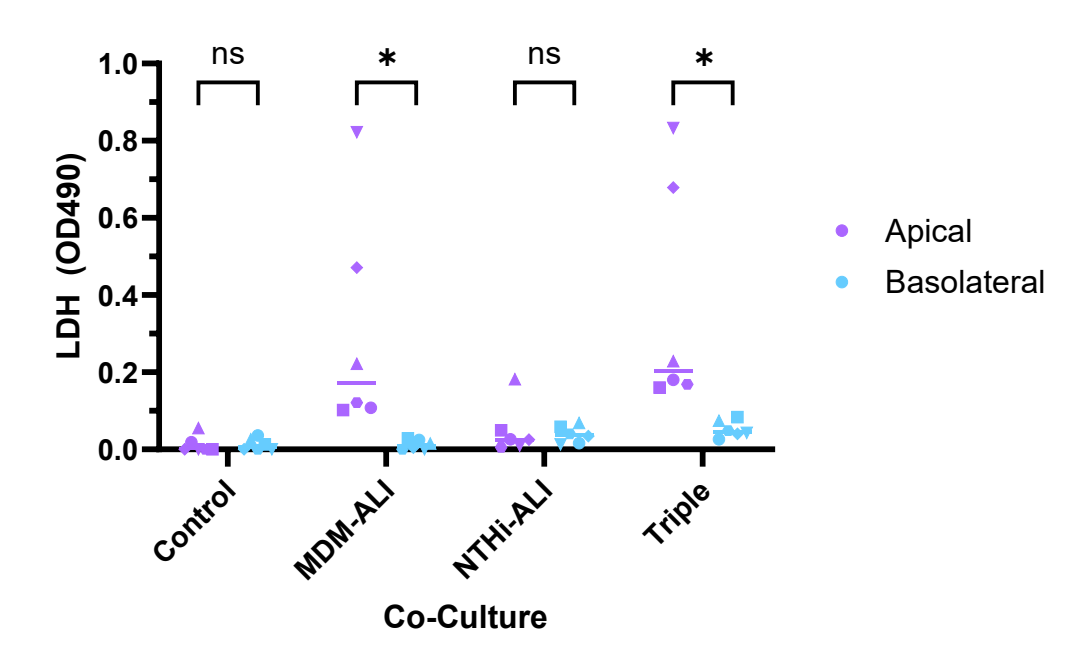


Figure 6.6 Co-culture viability indicated by LDH release. PNEC ALI cultures were infected with NTHi for 1 h, co-cultured for 72 h and then co-cultured with MDMs for 24 h. Apical washes and basolateral supernatants were collected and analysed in duplicate, subtracting media background. n = 6 separate biological replicates (shapes), paired data shows mean OD readings of duplicates. Medians are depicted by solid lines. Differences

between Transwell sides were compared by Wilcoxon tests for all treatments (\*p < 0.05).

Comparing LDH release in apical supernatant shows a significant increase caused by the presence on MDMs compared to treatments without MDMs (Figure 6.7). The presence of NTHi did not cause a statistically significant increase in LDH release, both when comparing Control cultures to NTHi-ALI co-cultures and when comparing MDM-ALI cultures to Triple co-cultures. All cultures maintained their TEER readings (Figure 6.4), regardless of LDH levels.

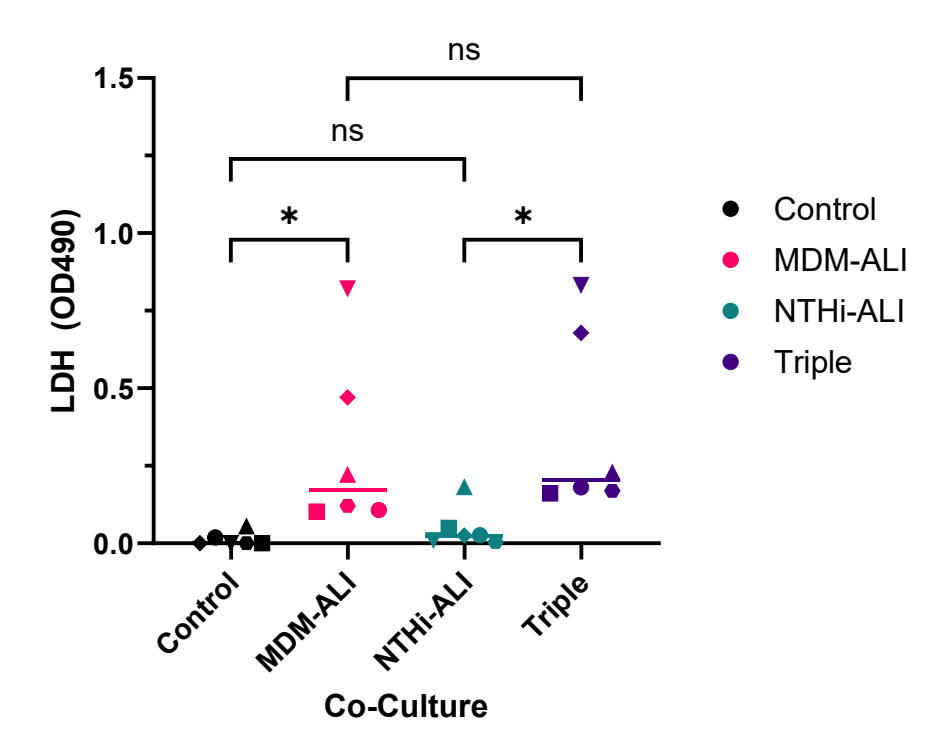


Figure 6.7 LDH released into apical supernatant by PNEC ALI cultures following co-culutres with PCD-NTHi 4, MDMs or both. Ciliated ALI culutres were infected with NTHi for 1 h, co-cultutred for 72 h followed by MDM addition for 24 h. Apical washes were collected and analysed in duplicate and adjusted for media background. n = 6 separate biological replicates (shapes), paired data shows mean OD readings of duplicates. Medians are depicted by solid lines. Data was analysed using Friedmans test with Dunn's post hoc analysis for relevant comparisons, all shown (\*p < 0.05).

#### 6.3.3 Cytokine response

To characterise the immune response of both epithelial cells and MDMs within the co-cultures, the levels of cytokine release in basolateral supernatant and apical washes were analysed. The cytokines investigated were IL-8, IL-1 $\beta$ , IL-6, TNF- $\alpha$  and IL-10. Significant differences between the apical and the basolateral supernatant were only observed in three cases: IL-6 in Triple co-culture and IL-1 $\beta$  in MDM-ALI and Triple co-cultures (Wilcoxon test p<0.05). No significant differences between apical and basolateral supernatant were observed for other co-cultures and cytokines.

There was a significant increase in IL-1 $\beta$ , IL-8 and IL-6 between NTHi-ALI and triple co-cultures (Figure 6.8). No statistical difference was observed between MDM-ALI and triple co-cultures or between the control and MDM-ALI/NTHi-ALI.

IL-10 and TNF- $\alpha$  was not detected beyond the lower limit of detection in the majority of biological replicates and no statistically relevant difference was seen in apical levels across the treatments (Figure 6.9).

Only IL-8 and IL-6 were detected in the basolateral supernatant beyond background (Figure 6.10A & B), There was a significant increase in IL-8 between MDM-ALI and triple co-cultures. No significant difference in IL-6 between co-cultures was observed. IL-1 $\beta$  was detected above the lower limit of detection in two triple co-cultures only (Figure 6.10C). IL-10 and TNF- $\alpha$  were not detected in the basal supernatant above the minimum detection threshold in any culture.

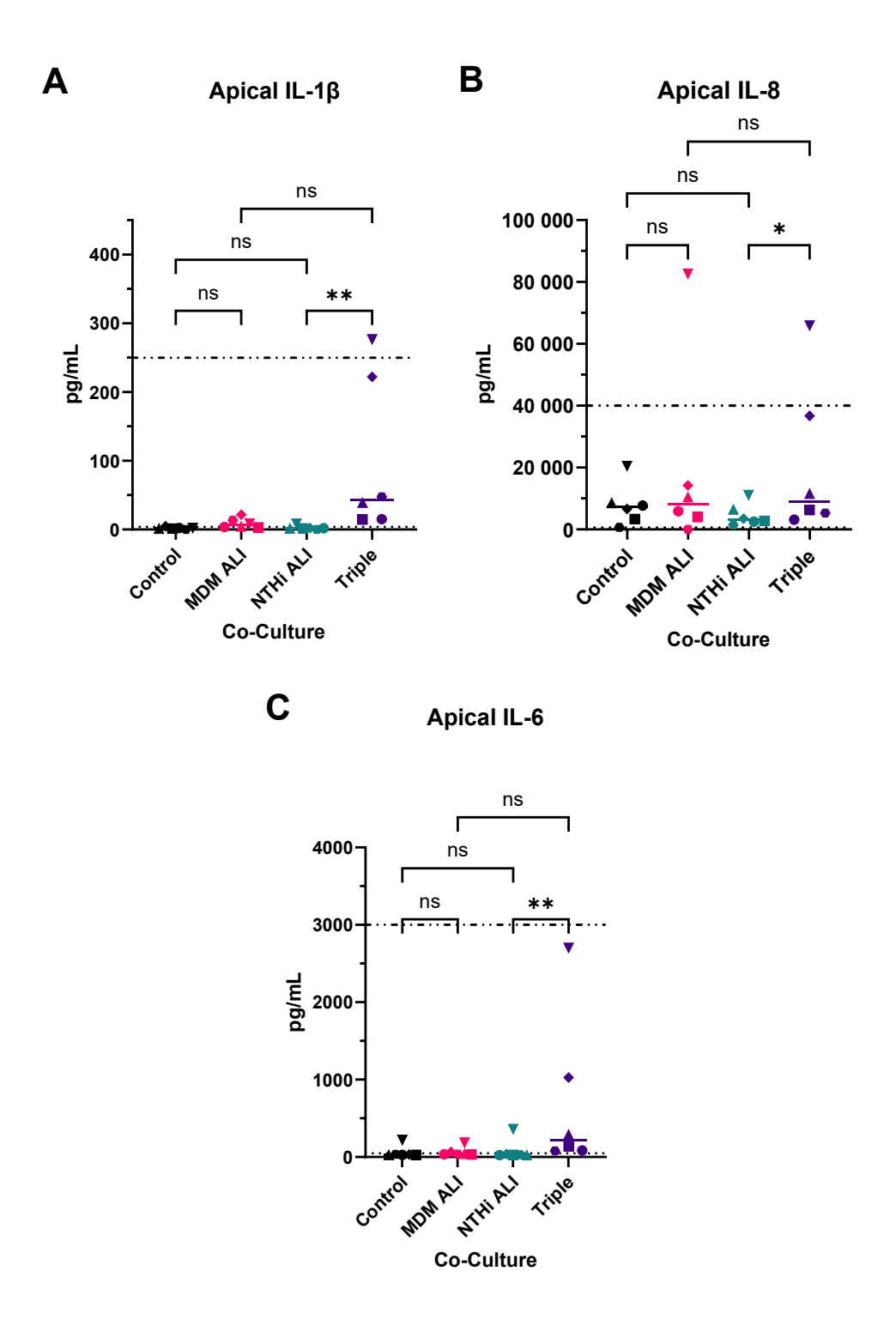


Figure 6.8 Pro-inflammatory cytokines in apical supernatants of PNEC ALI co-cultures. Ciliated PNEC cultures were infected with PCD-NTHi 4 for 1 h, co-cultured for 72 h followed by MDM addition for 24 h. Control co-cultures containing only MDM or NTHi are labelled. Co-cultures were washed apically, and the supernatants assessed for cytokines in duplicate. (A) IL-1 $\beta$  (B) IL-8 (C) IL-6. n = 6 separate biological replicates (shapes), data points are

shown as means of technical duplicates, medians are depicted by solid lines. Upper limits of detection are shown by dot/dash lines, lower limits by dotted lines. Data was analysed using Friedman tests with Dunn's post hoc analysis for relevant comparisons, all shown (\*p<0.05, \*\*p<0.01)

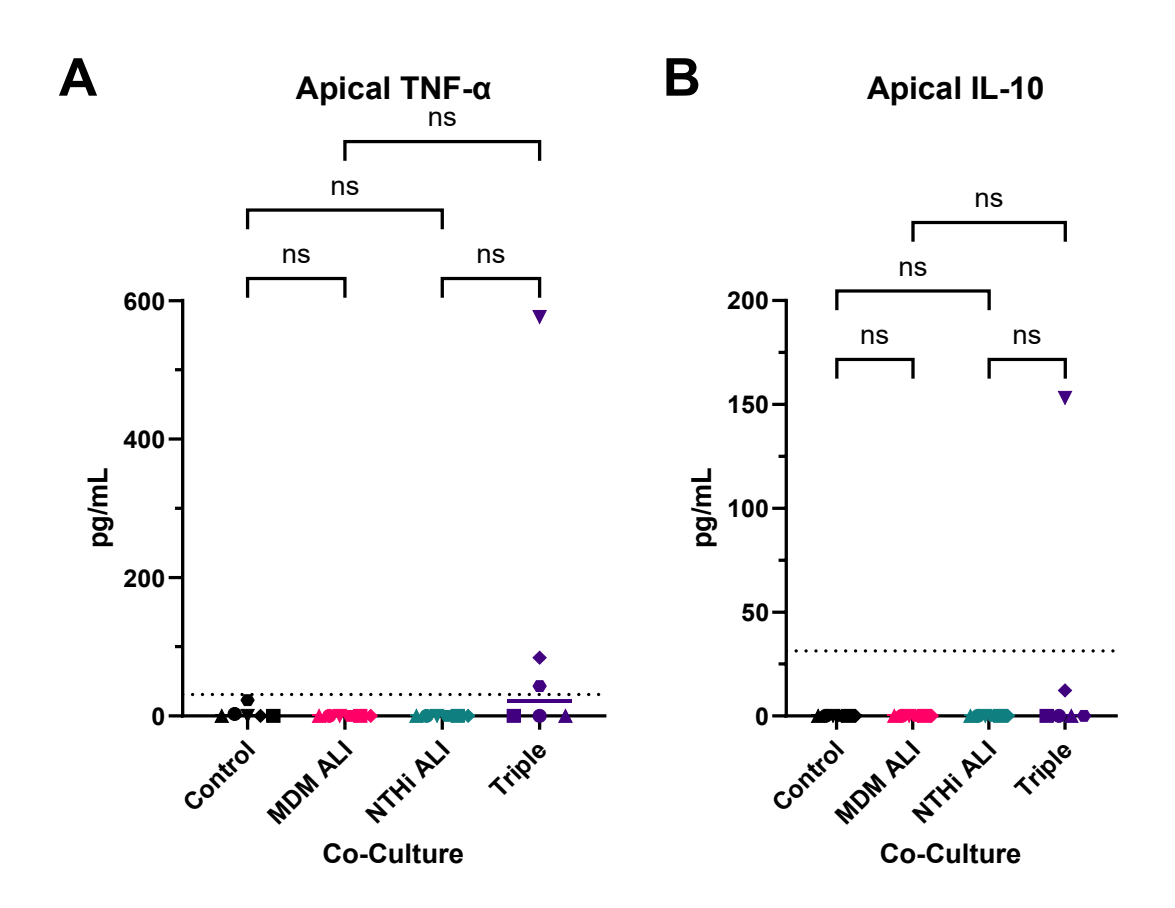


Figure 6.9 Cytokines with low detection in apical supernatants of PNEC ALI co-cultures. Ciliated PNEC cultures were infected with PCD-NTHi 4 for 1 h, co-cultured for 72 h followed by MDM addition for 24 h. Control co-cultures containing only MDM or NTHi are labelled. Co-cultures were washed apically, and the supernatants assessed for cytokines in duplicate.

(A) TNF-α (B) IL-10. n = 6 separate biological replicates (shapes), data points are shown as means of technical duplicates, medians are depicted by solid lines. Lower limits shown by dotted lines. No statistical difference was found (Friedman tests with Dunn's post hoc analysis for relevant comparisons, all shown)

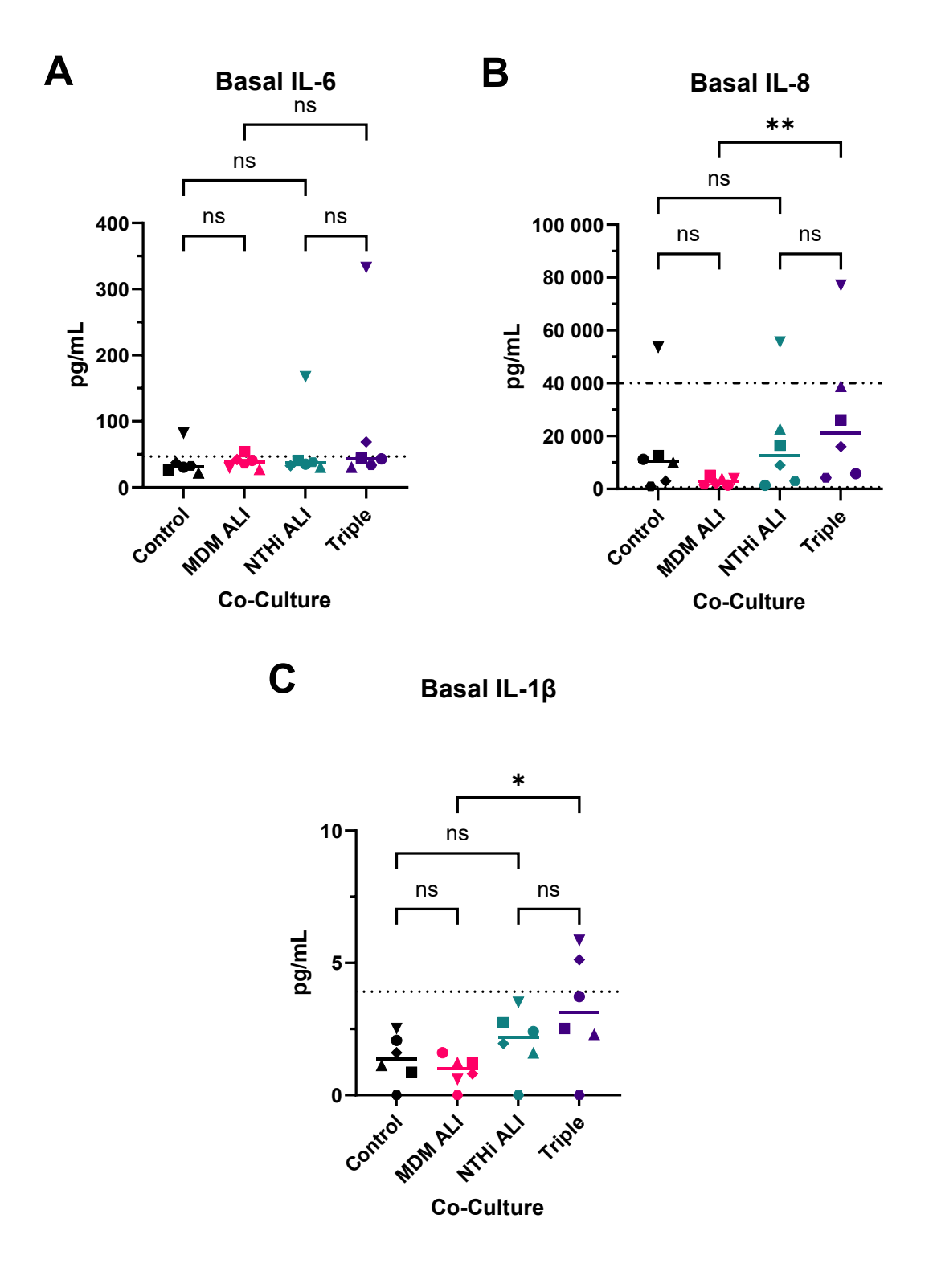


Figure 6.10 Cytokines detected in basal supernatent of PNEC ALI cultures. Ciliated PNEC cultures were infected with PCD-NTHi 4 for 1 h, co-cultured for 72 h followed by MDM addition for 24 h. Control co-cultures containing only MDM or NTHi are labelled. Basolateral supernatants were collected and assessed for cytokines in duplicate. (A) IL-6 (B) IL-8 (C)

IL-1 $\beta$ . n = 6 separate biological replicates (shapes), data points are shown as means of technical duplicates, medians are depicted by solid lines. Upper limits of detection are shown by dot/dash lines, lower limits by dotted lines. Data was analysed using Friedman tests with Dunn's post hoc analysis for relevant comparisons, all shown (\*p<0.05, \*\*p<0.01)

#### 6.3.4 Biofilm Viability

As the triple co-culture was shown to remain viable and significant increases in inflammatory mediators could be detected in response to NTHi, the final step was to investigate the impact that macrophage addition had on the NTHi viability within the Ali culture system.

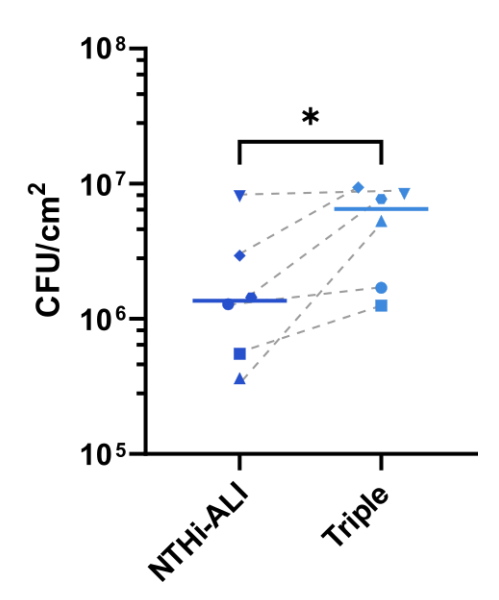


Figure 6.11 NTHi CFU recovered from PNEC ALI co-culture after 72 h of co-culture followed by 24 h MDM exposure (triple) or non-MDM control (NTHi-ALI). Following co-culture,

Transwells were excised, scrapped, cells resuspended and CFUs enumerated. n= 6
(shapes joined by dashed grey lines), data are shown as means of duplicate wells, solid lines depict median. All non-infected controls were free of bacteria. Data were analysed using Wilcoxon test (\*p<0.05)

A significant increase in the median bacterial recover was observed in Triple co-cultures, from  $1.4 \times 10^6$  to  $6.5 \times 10^6$  CFU/cm<sup>2</sup> (Figure 6.11). The addition of MDMs to a NTHi-ALI co-culture increased the CFU count in all biological replicates, by a median average of  $2.8 \times 10^6$  CFU/cm<sup>2</sup>, compared to NTHi-ALI co-cultures where MDMs were not added.

#### 6.4 Discussion

Viable Triple co-cultures showed that monocyte-derived macrophage addition to established PCD-NTHi 4 biofilms on ciliated epithelium failed to reduce bacterial viability, instead increasing CFU counts while producing a pro-inflammatory response. Triple co-cultures were characterised using SEM, TEER readings, LDH and cytokine release and bacterial CFU counts. The work presented in this chapter moved from MDM-NTHi co-cultures on an abiotic surface (Chapter 5) to a more complex model on primary ciliated epithelium which allowed the host-pathogen interaction to be investigated under more clinically representative conditions.

Previous macrophage to epithelial cell co-cultures have used ratios between 1:1 and 1:5 with MDM adhesion periods of 2-24 h<sup>326</sup>. As the 24 h addition of apical media was suggested not to affect epithelial TEER, MDMs were added for 24 h. Aiming for MOI 100 (MBR 0.01) between NTHi and MDMs meant that the MDM to epithelial ratio was about 1:100.

The viability of co-cultures was assessed using multiple methods. Visually, SEMs showed intact MDMs and bacteria on ciliated epithelium. The integrity of the PNEC layer was confirmed using TEER readings throughout the co-culturing process, no significant effect of culture time or treatment on TEER was seen.

Ciliary beating was observed through light microscopy but not quantified as part of this work. Using HSVM to quantify the ciliary beat frequency and percentage ciliation could be used in future work to gain more insight into the epithelial cell health of this co-culture, especially since NTHi has been seen to affect CBF<sup>310</sup>. High levels of cytokine release by in MDM-ALI and Triple co-cultures suggest MDM viability while cultures with lower cytokine levels did not have comparatively high LDH levels that would suggest high levels of cell lysis. ALI survival of macrophages has been demonstrated by Wu et al using the A549 cell line, which induced a more representative alveolar macrophage phenotype<sup>327</sup>.

SEM images provided insight into the spatial aspects of the co-cultures. MDMs were observed around the outside of the MDM-ALI cultures which likely reflects an inability to reach the surface of the epithelial cell layer due to ciliary beating. This corresponds to observations made using light microscopy where macrophages could be seen moving across the culture. It is possible that the trypsinisation of MDMs following differentiation from monocytes lead to a loss of adhesion molecules, reducing the ability of MDMs to adhere to the epithelial cell surface. As MDMs were

often observed in clusters on MDM-ALI cultures, it is possible that MDM-MDM adhesion was easier to achieve than MDM-PNEC adhesion.

Bacterial aggregates could be seen in areas of reduced ciliation, it is not clear from this work if bacterial colonisation led to loss of ciliation or if the lack of cilia in certain areas was a predisposing factor for bacterial attachment in these cultures, though previous work has demonstrated that NTHi supernatant exposure lead to a shedding of ciliated BBECs in submerged cultures<sup>310</sup> and the exfoliation of ciliated epithelial cells in response to NTHi infection<sup>328</sup>.

The functioning cilia and associated mucociliary clearance reflects *in vivo* conditions where pathogens are moved away from the airway surface. However, this protocol did not remove apical fluids during the co-culture process, so non-adherent bacteria remained in the culture well while *in vivo* they would be moved up and out of the airway. Therefore, the release of bacterial toxins, such as LOS<sup>329</sup> and Protein D<sup>131</sup>, may still cause damage to the epithelial cells and thus enable subsequent colonisation as NTHi has been shown to have an increased affinity to structurally damaged epithelial cells<sup>313</sup>.

The addition of MDMs to NTHi-ALI co-cultures led to an increase in CFUs in all biological replicates and a statistically significant increase overall. The fact that macrophages could be observed on the ciliated epithelial cell layer with bacteria on their surface suggested that MDMs may be acting as niches for NTHi survival that were not available when cilia prevented easy attachment and colonisation. It therefore appears that the macrophages, while being ineffective at clearing the infection, are actually providing the bacteria with more opportunity for infection and persistence than if they were not present. The presence of MDMs has been shown to enhance planktonic NTHi CFU recovery compared to planktonic NTHi alone<sup>236</sup>. Nutrient sequestration is a host defence mechanism against pathogens<sup>330</sup> and bacteria will be exposed to minimal culture media in ALI cultures, so metabolically active MDMs may be a source of nutrients for bacteria. Alternatively, MDMs may provide a non-ciliated surface for attachment as NTHi biofilms were generally observed in non-ciliated areas or on MDM surfaces.

Although SEM gave some insight of the localisation of bacteria and MDMs on the ALI cultures, there was no way to measure internalisation. Future work using flow cytometry and gentamycin protection assays would help demonstrate the level of intra and para-cellular NTHi, both associated with macrophages and with epithelial cells as demonstrated for NTHi-ALI cultures by Brown et al<sup>312</sup>. Additionally, time-lapse microscopy would help with understanding the temporal elements of the

MDM-NTHi interaction. The use of TEM may also elucidate the integrity of the epithelial cell layer as demonstrated by Ren et al, where the apical surface appeared intact but the basal cell layer showed increased disorganisation and intercellular spacing following 5 day NTHi infection<sup>232</sup>.

Comparing apical supernatant LDH release showed that the presence of NTHi does not increase LDH release by PNECs or MDMs. No significant increase in LDH was seen between the ALI control and NTHi-ALI co-culture nor between MDM-ALI and Triple co-cultures.

Adding MDMs significantly increased apical LDH release both comparing ALI control to MDM-ALI and comparing NTHi-ALI to Triple co-cultures. This suggests that NTHi infection does not cause a significant amount of cell lysis in either epithelial cells or MDMs. Instead, the process of adding MDMs to an ALI culture leads to an increase in LDH release, either from the macrophages themselves or through a feedback system between epithelial cells and macrophages. The increase in total cells could also be playing a role, but the number of MDMs added made up about 1% of the total number of host cells in the co-cultures, so it is unlikely that the increase in LDH is due to an increase in cell numbers alone.

Previous work by Ackland has shown that planktonic NTHi added to MDMs at an MOI of 100 (same MOI as used here) did not significantly increase LDH release compared to an uninfected control over 24 h<sup>236</sup>, supporting the finding that NTHi addition does not inherently increase MDM LDH release. Furthermore, Bossche et al found that some, but not all, of the lower respiratory tract bacterial pathogens investigated reduced LDH activity<sup>331</sup>. These observations were found to be dose, time and strain dependent for different species and although NTHi was not one of the species tested, it raises a valid point for further investigation for the infection model presented here.

As discussed in Chapter 5, though LDH is often used as a measurement of cytotoxicity, it also plays a role in cellular metabolism and may therefor indicate actively metabolising cells rather than lysed cells. This project was limited by samples and therefore supernatant to analyse, but future work would benefit from using metabolic assays such as MTS and viability staining such as trypan blue or propidium iodide to confirm whether high levels of LDH correlate with increased metabolic activity or cytolysis.

The cytokine response of the co-cultures was primarily seen in the apical supernatant, the location of the MDMs. Van riet et al found primary epithelium alone did not have a significant il-6 and IL-8 response to LPS without the presence of primary macrophages<sup>332</sup>. They hypothesised that the presence of macrophages stimulates an epithelial cell response which contributes to the levels of

cytokines observed in co-cultures. Similar observations were made in this work, with NTHi-ALI cultures not producing a significant inflammatory response but Triple co-cultures showing a significant increase in apical IL-6, IL-8 and IL-1β. Furthermore, basolateral release of IL-8 and IL-1β increased significantly between MDM-NTHi and Triple co-cultures though IL-1β readings were below the lower limits of detection and should be treated with caution. As there was no significant difference between Control and NTHi-ALI co-cultures, the presence of NTHi does not stimulate this response. Previous work on NTHi-ALI cultures showed similar concentrations of IL-6 and IL-8 in the basolateral media that also did not increase significantly over a 72 h co-culture period<sup>224</sup>. NTHi-ALI and Triples co-cultures did not show a significant basolateral difference either. These observations could be due to the PNEC response to NTHi infection (NTHi-ALI) being slightly elevated but not enough to achieve statistical significance with the current number of replicates, and as the Triple coculture response is elevated again in the same way, only the comparison between MDM-ALI and Triple co-culture achieves significance. As multiple groups were statistically compared for this work, the nature of multiple statistical tests means that the threshold for significance becomes higher. As this model is investigated further in the future, more focused hypotheses, and targeted comparisons along with higher numbers of biological replicates may delineate the role played by each cell type in the inflammatory response better.

IL-8 release has been found to be NTHi strain dependent in PNECs after 96 h of submerged coculture with a more invasive strain inducing a stronger response<sup>312</sup>. The same work found that this was not the case when using the CALU-3 cell line. NTHi heterogeneity has therefore been demonstrated to play a significant factor in the host-pathogen interaction, especially when using primary host cells, and supports the need for testing a variety of strains within any model that is developed.

The pro-inflammatory cytokine response taken together with the increasing CFU counts correspond to a chronic inflammation scenario, where inflammatory signals are produced, but bacteria are not cleared. *In vivo* these signals would lead to the recruitment of further immune cells, which was not simulated in this model.

Comparing the results of MDM-NTHi co-culture on an abiotic surface (Chapter 5) with what was seen in this chapter demonstrates the importance of developing more complex *in vitro* models to study host-pathogen interactions. The presence of and contact with epithelial cells had been shown to alter macrophage behaviour in the past<sup>50,333</sup>, so this work was looking to compare the results between the two scenarios.

SEM images of MDM-NTHi co-cultures show macrophages spread equally across the culture surface. MDM-ALI co-cultures, by comparison, showed macrophages cluster together around the edges of the culture. Only when NTHi was present in triple co-cultures, could macrophages be seen separated from other macrophages, instead interacting with bacteria. In MDM-NTHi co-cultures and MDM-only controls, even MDMs distribution was likely due to the fact that well mixed MDM suspensions being added to homogenous surfaces such as an equal lawn of NTHi biofilm or an empty well detected no signal gradient along which macrophages may have gathered. On ALI co-cultures, the ciliary beating prevented macrophages from settling on the surface due to gravity as they would have done on plastic. Instead, detection of NTHi may have guided MDMs to bacterial aggregates which were often in areas of reduced ciliation, thus allowing macrophage attachment and resulting in a less even spread.

On plastic, LDH and pro-inflammatory cytokine release increased when MDMs were exposed to NTHi biofilms whereas on ALI cultures, the difference in LDH release between MDM-ALI and triple co-cultures was not significant. This could be due to the interaction of MDMs and PNECs producing a more varied response than MDMs alone on plastic, and therefore higher numbers of biological replicates are needed to detect a significant difference. While NTHi survival was not impacted by MDMs in plastic co-cultures, there was an increase in survival when MDMs were present in ALI co-cultures.

When working with primary cells, potential donor variation means that the need for sufficient biological replicates is greater than when immortalised cell lines are used. In spite of this, the appeal of primary cells and their increased biological relevance often makes this an avenue worth pursuing. Donor variation of TEER has been observed by Bovard et al in both primary bronchial and primary small airway cell ALI cultures<sup>334</sup> as well as donor Variation in response to viral infections being observed with possible explanations including receptor distributions and cytokine responses<sup>335</sup>. As discussed in Chapter 4 and Chapter 5, there are indications of donor variation in this work, though the relatively low number of replicates prevent the formation of any substantial conclusions. During the Triple co-culture work presented in this chapter, additional observations were made to add to this consideration. The TEER trends of ALI cultures were shown to correlate more with biological replicate than co-culture type (NTHi/MDM presence). Additionally, one ALI donor was used twice, displaying different TEER trends. Though different MDM donors were used in each replicate, the fact that TEER change was consistent across all co-cultures regardless of MDM inclusion suggests that experimental variation had a greater impact than either ALI or MDM donor. Two MDM donors

provided two samples each, and similar LDH release was observed for both donors regardless of differing ALI donors.

One of the main shortcomings of this work were the limited availability of MDMs reducing the number of samples and thus readouts that could be acquired. For example, no lysis controls were available for the LDH assays and not all readouts could be acquired for every biological replicate. Having this level of matched data would strengthen any interpretations regarding the effects and responses of macrophages to NTHi biofilms in this advanced co-culture system. Increased MDM availability would also allow increased MBRs and additional time points to be investigated. Furthermore, the MDMs and PNECs were not able to be donor matched due to logistical barriers. Doing so in future may provide a clearer delineation in host responses to infection.

#### 6.5 Summary and Conclusion

In conclusion, MDMs are able to be co-cultured with NTHi infected PNEC epithelium at ALI for 24 h. The macrophages are not able to reduce bacterial viability in this time, rather they appear to enhance NTHi survival. The epithelial cell layer integrity was maintained throughout the co-culture process and was not affected significantly by the presence of MDMs or NTHi. LDH and cytokine levels rose in response to Triple co-cultures and were predominantly detected in the apical supernatant. This work provides a basis for further development of a more clinically relevant and complex model to study the host-pathogen interaction and may be applied to a variety of conditions and pathogens.

# **Chapter 7** Summary and Future Work

#### 7.1 Summary of Results

Understanding the host-pathogen interaction will often hold the key to identifying new targets for treatments. The complexity of the immune response with its many cell types and signals means that any work done outside of whole organisms will be a simplified version of this system. While great strides have been made modelling the interactions of a single cell type, be it epithelial cells or immune cells, and a range of pathogens, the next step bridging *in vitro* and *in vivo* models is combining multiple host cells within co-cultures.

The human airway encounters a myriad of challenges through the air we breathe. In order to prevent catastrophic damage to our lungs a system of defences, both physical and chemical, work to remove pathogens and irritants. Epithelial cells line the airway, denying access to the deeper layers of the mucosa, detecting pathogens and signalling to the immune system. Both local and recruited immune cells such as macrophages respond to pathogens, removing them through phagocytosis and orchestrating a long-term immune response. Additionally, the airway is lined with cilia which move mucus and any threats trapped within out of the airway through mucociliary clearance.

Bacteria such as NTHi cause biofilm infections in the human airway. This species is often found as a commensal in the upper airway, but acts as an opportunistic pathogen when the host defences are compromised by underlying conditions such as cystic fibrosis, asthma or primary ciliary dyskinesia. The latter is a heterogenous condition that manifests as a loss of ciliary function leading to an increase in airway infections by the likes of NTHi.

This work set out to build on previous work investigating NTHi biofilms on PNEC ALI cultures<sup>274,275</sup> and NTHi MDM interactions<sup>236</sup> by combining the two host cell types with NTHi into a triple co-culture model.

NTHi is Highley heterogeneous so as new strains of NTHi were to be used for this work, the first step was to characterise the planktonic and biofilm growth in bacterial monocultures. Six isolates from PCD patients were collected along with a GFP producing strain that was kindly provided by Dr Derek Hood. The strains were found to grow slower in planktonic cultures than the strains that were previously used, so the biofilm inoculation protocol was adapted to use stationary phase planktonic cultures rather than the exponential growth phase cultures used in previous work.

Biofilm formation on plastic was demonstrated after 72 h by all strains, with significant heterogeneity in size, viability and structure observed. PCD-NTHi 4 was selected as a suitable clinical strain to take forward alongside GFP-NTHi onto the PNEC ALI culture model.

The work on comparing these strains was important in demonstrating the heterogeneity in NTHi, both in planktonic and in biofilm behaviour, even within isolates from the same underlying condition. This must always be kept in mind when working with this bacterial species as any findings may be strain dependent. Future work will therefore always benefit from using several strains of NTHi.

Optimising the MOI of GFP-NTHi and PCD-NTHi 4 on PNEC ALI cultures to maximise the epithelial cell layer integrity and the bacterial viability after 72 h of co-culture led to the realisation that GFP-NTHi does not form biofilms on the apical side culture, instead penetrating the PNEC layer. Differences in cellular invasion capabilities are another aspect of NTHi heterogeneity that must therefore be considered in future models. GFP-NTHi was deemed unsuitable for this work aiming to look at apical biofilms and was therefore excluded from further work within this project.

The length of incubation before removing unattached NTHi from the apical side of the co-culture appeared to play a role in epithelial cell layer integrity, with 24 h attachment periods leading to a drop in TEER that suggested a breakdown of epithelial cell junctions following 72 h co-culture. In response, the NTHi attachment time was reduced to 1 h, leading to the maintenance of TEER and a drop in CFU recovery. The latter remained within a suitable level for this work. This insight is a valuable reminder that in order to investigate biofilms and their interactions with the host, the whole life cycle must be considered. Biofilms can not be added pre-formed to a culture, instead the planktonic and attachment phases will have an impact on the overall model and every step warrants detailed investigation to fully understand the host-pathogen interaction.

The novel 24 h co-culture of primary MDMs with established PCD-NTHi 4 biofilms on plastic showed that both bacteria and macrophages were surviving the process. Macrophages were failing to reduce the number of viable bacteria, though did reduce the biomass within the cultures. A pro-inflammatory cytokine response was detected suggesting active, viable macrophages and SEM showed intact macrophages surrounded by bacteria. The failure of immune cells and antibiotics to reduce bacterial viability is a major factor in the challenge posed by biofilm infections. This was reflected in these observations and has been seen with other bacterial species<sup>300</sup>.

The modulation of immune responses by host cell interactions is an expanding area of understanding and the fundamental motivation for this project<sup>50,336,337</sup>. The addition of MDMs to NTHi biofilms grown on PNEC ALI cultures was therefore the final stage of this work. All three cell types could be observed on SEM images and a macrophage cytokine response detected. The maintenance of TEER across co-cultures supported the sustained viability of all components of this model. The number of NTHi cells recovered from the co-cultures increased in response to the addition of macrophages.

#### 7.2 Shortcomings and Future Work

The methodology of combining cell types in this work was selected based on previously established protocols. This meant that ALI cultures were infected apically with NTHi for 72 h before separately cultured MDMs were added apically. The method of NTHi addition is representative of the *in vivo* scenario as NTHi is acquired through the airway where it settles on the apical surface of the epithelium. The subsequent modelling is simplified however in the fact that no immune cells are present for the 72 h over which NTHi colonisation takes place. This means that no significant immune response is present as seen by the lack of significant cytokine response between uninfected control ALI cultures and NTHi-ALI co-cultures. Future work would benefit from adding NTHi to established MDM-ALI co-cultures to investigate the potential impact of an increased immune response in NTHi colonisation of airway epithelium. Macrophage-ALI co-cultures have been developed previously to study the effect of inhaled factors such as cigarette smoke<sup>316</sup> and ozone<sup>326</sup>, so the concept of using these models for infection studies is not farfetched.

In addition to the sequential nature of the bacteria and MDM addition, the method of MDM addition requires refining for a more accurate model in the future. *In vivo* macrophages may be recruited from the interstitial space or from the blood stream<sup>338</sup>, this means that they are arriving at the site of infection from the basolateral side of the epithelium. In this project, the established and well characterised MDM differentiation protocol meant that Transwells containing ALI cultures could not be added on top of the wells in which MDMs were cultured. Instead MDMs required dissociation to be added to the Transwell system. There are several examples of immune cells being co-cultured in the literature, for example by allowing differentiated macrophages to adhere to inverted Transwell inserts<sup>337</sup> or adding them to the basolateral side<sup>336</sup>. Utilising these methods was not possible as part of this project due to the time that fully characterising them would have taken, but combing the insight gained from these alternative methods with the primary cell approach used in

this project is a promising future avenue for understanding the host-pathogen interaction of opportunistic pathogens such as NTHi and beyond.

Working with primary cells will always pose more of a challenge in terms of sample availability that using cell lines, however the increased biological relevance justifies this decision, especially when investigating complex host-pathogen interactions.

The main limiting factor of this work was the yield of primary MDMs following the differentiation process. Loss of macrophages during the trypsin dissociation process prior to the addition to biofilms and co-cultures meant that there was a limit to the NTHi:MDM ratios that were achievable as well as the number of assays that could be performed within each co-culture. The latter would have provided more matched readouts (eg cytokines, CFUs, LDH and SEMs) so that co-culture behaviour could be better understood. Alternative, less aggressive, MDM dissociation methods that maintain surface protein integrity may also have affected the ability for MDMs to adhere to the epithelial cell layer. However, due to time and donor limitations it was not possible to optimise the MDM dissociation protocol fully.

Increasing the number of co-cultures that can be tested per donor would increase the supernatant available to be analysed. This would allow the suspected impact of planktonic NTHi on ALI culture health when using a 24 h attachment period to be explored further as a greater number of virulence factors could be tested for including LOS and protein D. Additional host defence signals and molecules could also be measured including GM-CSF and LL-37 as previously done<sup>274</sup>.

Increasing the number of time points investigated would also shed more light on the host-pathogen interaction. As many assays such as CFU counts and imaging require the co-culture to be broken up or fixed, more samples would allow matched time points.

As internalisation of NTHi was seen in this work and the wider literature<sup>312,339</sup>, a more thorough characterisation of this aspect of the host-pathogen interaction within this model would be very valuable. Methodologies such as gentamycin washes<sup>236</sup> through to flow cytometry<sup>340</sup> have been used for this in the past and could be applied here. Creating a GFP producing clinical NTHi strain would also represent the best of the two strains used here: increased imaging ease and clinical relevance.

Once this model is fully optimised and characterised, its function can be applied in many different directions. Testing antibiotics would be a relatively straightforward application, but using primary cells from individuals with PCD or asthma may help understand the host dysregulation that

contributes to the increased infection rates emblematic of these conditions. Furthermore, other bacterial species and virus infections could be investigated as well as multi-species infections and commensal behaviour.

## Appendix A Bibliography

- 1. Wanner, A., Salathé, M. & O'Riordan, T. G. Mucociliary clearance in the airways. *Am. J. Respir. Crit. Care Med.* **154**, 1868–902 (1996).
- 2. Rayner, R. E., Makena, P., Prasad, G. L. & Cormet-Boyaka, E. Optimization of Normal Human Bronchial Epithelial (NHBE) Cell 3D Cultures for in vitro Lung Model Studies. *Sci. Rep.* **9**, (2019).
- 3. Aijaz, S., Balda, M. S. & Matter, K. Tight Junctions: Molecular Architecture and Function. in *International review of cytology* **248**, 261–298 (Int Rev Cytol, 2006).
- 4. Soyka, M. B. *et al.* Defective epithelial barrier in chronic rhinosinusitis: The regulation of tight junctions by IFN-γ and IL-4. *J. Allergy Clin. Immunol.* **130**, 1087-1096.e10 (2012).
- 5. Guttman, J. A. & Finlay, B. B. Tight junctions as targets of infectious agents. *Biochim. Biophys. Acta Biomembr.* **1788**, 832–841 (2009).
- 6. Nava, P., Kamekura, R. & Nusrat, A. Cleavage of transmembrane junction proteins and their role in regulating epithelial homeostasis. *Tissue Barriers* **1**, (2013).
- 7. Chen, S., Einspanier, R. & Schoen, J. Transepithelial electrical resistance (TEER): a functional parameter to monitor the quality of oviduct epithelial cells cultured on filter supports.

  Histochem. Cell Biol. 144, 509 (2015).
- 8. Asgrimsson, V., Gudjonsson, T., Gudmundsson, G. H. & Baldursson, O. Novel Effects of Azithromycin on Tight Junction Proteins in Human Airway Epithelia. *Antimicrob. Agents Chemother.* **50**, 1805 (2006).
- 9. Khair, O. *et al.* Effect of Haemophilus influenzae endotoxin on the synthesis of IL-6, IL-8, TNF-alpha and expression of ICAM-1 in cultured human bronchial epithelial cells. *Eur. Respir. J.* **7**, 2109–2116 (1994).
- Sleigh, M. A., Blake, J. R. & Liron, N. The Propulsion of Mucus by Cilia. *Am. Rev. Respir. Dis.* 137, 726–741 (1988).
- 11. Ibanez-Tallon, I., Heintz, N. & Omran, H. To beat or not to beat: roles of cilia in development and disease. *Hum. Mol. Genet.* **12**, 27R 35 (2003).

- 12. Boisvieux-Ulrich, E., Laine, M. C. & Sandoz, D. The orientation of ciliary basal bodies in quail oviduct is related to the ciliary beating cycle commencement. *Biol. Cell* **55**, 147–150 (1985).
- 13. Hariri, B. M. & Cohen, N. A. New insights into upper airway innate immunity. in *American Journal of Rhinology and Allergy* **30**, 319–323 (OceanSide Publications Inc., 2016).
- 14. Kaliner, M., Marom, Z., Patow, C. & Shelhamer, J. Human respiratory mucus. *J. Allergy Clin. Immunol.* **73**, 318–323 (1984).
- 15. Button, B. *et al.* A periciliary brush promotes the lung health by separating the mucus layer from airway epithelia. *Science (80-. ).* **337**, 937–941 (2012).
- 16. Martin, T. R. & Frevert, C. W. Innate immunity in the lungs. in *Proceedings of the American Thoracic Society* **2**, 403–411 (American Thoracic Society, 2005).
- 17. Nicod, L. P. Lung defences: An overview. European Respiratory Review 14, 45–50 (2005).
- 18. Tong, H. H. *et al.* Expression of cytokine and chemokine genes by human middle ear epithelial cells induced by formalin-killed Haemophilus influenzae or its lipooligosaccharide htrB and rfaD mutants. *Infect. Immun.* **69**, 3678–3684 (2001).
- 19. Deshmane, S. L., Kremlev, S., Amini, S. & Sawaya, B. E. Monocyte chemoattractant protein-1 (MCP-1): An overview. *Journal of Interferon and Cytokine Research* **29**, 313–325 (2009).
- 20. Ellison, R. T. & Giehl, T. J. Killing of gram-negative bacteria by lactoferrin and lysozyme. *J. Clin. Invest.* **88**, 1080–1091 (1991).
- 21. Dryden, M. Reactive oxygen species: a novel antimicrobial. *Int. J. Antimicrob. Agents* **51**, 299–303 (2018).
- 22. Bals, R., Weiner, D. J., Moscioni, A. D., Meegalla, R. L. & Wilson, J. M. Augmentation of Innate Host Defense by Expression of a Cathelicidin Antimicrobial Peptide. INFECTION AND IMMUNITY 67, (1999).
- 23. Byfield, F. J. *et al.* Cathelicidin LL-37 Increases Lung Epithelial Cell Stiffness, Decreases

  Transepithelial Permeability, and Prevents Epithelial Invasion by Pseudomonas aeruginosa . *J. Immunol.* **187**, 6402–6409 (2011).
- 24. Singh, P. K. et al. Production of-defensins by human airway epithelia. Medical Sciences 95,

(1998).

- 25. Schutte, B. C. & McCray, P. B. B-Defensins in Lung Host Defense. *Annu. Rev. Physiol.* **64**, 709–748 (2002).
- 26. Iwasaki, H. & Akashi, K. Myeloid Lineage Commitment from the Hematopoietic Stem Cell. *Immunity* **26**, 726–740 (2007).
- 27. Tarling, J. D., Lin, H. & Hsu, S. Self-Renewal of Pulmonary Alveolar Macrophages: Evidence From Radiation Chimera Studies. *J. Leukoc. Biol.* **42**, 443–446 (1987).
- 28. Guilliams, M. *et al.* Alveolar macrophages develop from fetal monocytes that differentiate into long-lived cells in the first week of life via GM-CSF. *J. Exp. Med.* **210**, 1977–1992 (2013).
- 29. Yona, S. & Jung, S. Monocytes: Subsets, origins, fates and functions. *Curr. Opin. Hematol.* **17**, 53–59 (2010).
- 30. Norris, D. A., Morris, R. M., Sanderson, R. J. & Kohler, P. F. Isolation of functional subsets of human peripheral blood monocytes. *J. Immunol.* **123**, 166–172 (1979).
- 31. Narasimhan, P. B., Marcovecchio, P., Hamers, A. A. J. & Hedrick, C. C. Nonclassical Monocytes in Health and Disease. *Annu. Rev. Immunol.* **37**, 439–456 (2019).
- 32. Ziegler-Heitbrock, L. The CD14+ CD16+ blood monocytes: their role in infection and inflammation. *J. Leukoc. Biol.* **81**, 584–592 (2007).
- 33. Martinez, F. O. & Gordon, S. The M1 and M2 paradigm of macrophage activation: Time for reassessment. *F1000Prime Rep.* **6**, (2014).
- 34. Stein, M., Keshav, S., Harris, N. & Gordon, S. Interleukin 4 potently enhances murine macrophage mannose receptor activity: A marker of alternative immunologic macrophage activation. *J. Exp. Med.* **176**, 287–292 (1992).
- 35. Abramson, S. L. & Gallin, J. I. IL-4 inhibits superoxide production by human mononuclear phagocytes. *J. Immunol.* **144**, 625–30 (1990).
- 36. da Silva, M. D. *et al.* IL-10 Cytokine Released from M2 Macrophages Is Crucial for Analgesic and Anti-inflammatory Effects of Acupuncture in a Model of Inflammatory Muscle Pain. *Mol. Neurobiol.* **51**, 19–31 (2014).

- 37. Murray, P. J. *et al.* Macrophage Activation and Polarization: Nomenclature and Experimental Guidelines. *Immunity* **41**, 14–20 (2014).
- 38. Xue, J. *et al.* Transcriptome-Based Network Analysis Reveals a Spectrum Model of Human Macrophage Activation. *Immunity* **40**, 274–288 (2014).
- 39. Aderem, A. & Underhill, D. M. MECHANISMS OF PHAGOCYTOSIS IN MACROPHAGES. *Annu. Rev. Immunol.* **17**, 593–623 (1999).
- 40. Akira, S., Uematsu, S. & Takeuchi, O. Pathogen recognition and innate immunity. *Cell* **124**, 783–801 (2006).
- 41. Kawasaki, T. & Kawai, T. Toll-like receptor signaling pathways. *Frontiers in Immunology* **5**, 461 (2014).
- 42. Dale, D. C., Boxer, L. & Conrad Liles, W. The phagocytes: Neutrophils and monocytes. *Blood* **112**, 935–945 (2008).
- 43. Farhat, K. *et al.* Heterodimerization of TLR2 with TLR1 or TLR6 expands the ligand spectrum but does not lead to differential signaling. *J. Leukoc. Biol.* **83**, 692–701 (2008).
- 44. Long, E. M., Millen, B., Kubes, P. & Robbins, S. M. Lipoteichoic Acid Induces Unique Inflammatory Responses when Compared to Other Toll-Like Receptor 2 Ligands. *PLoS One* **4**, e5601 (2009).
- 45. Dalpke, A., Frank, J., Peter, M. & Heeg, K. Activation of toll-like receptor 9 by DNA from different bacterial species. *Infect. Immun.* **74**, 940–946 (2006).
- 46. MacMicking, J., Xie, Q. & Nathan, C. NITRIC OXIDE AND MACROPHAGE FUNCTION. *Annu. Rev. Immunol.* **15**, 323–350 (1997).
- 47. Ragland, S. A. & Criss, A. K. From bacterial killing to immune modulation: Recent insights into the functions of lysozyme. *PLoS Pathogens* **13**, e1006512 (2017).
- 48. Aggarwal, N. R., King, L. S. & D'Alessio, F. R. Diverse macrophage populations mediate acute lung inflammation and resolution. *American Journal of Physiology Lung Cellular and Molecular Physiology* **306**, L709 (2014).
- 49. Stříž, I., Slavčev, A., Kalanin, J., Jarešová, M. & Rennard, S. I. Cell-Cell Contacts with Epithelial

- Cells Modulate the Phenotype of Human Macrophages. Inflammation 25, 241–246 (2001).
- 50. Bauer, R. N. *et al.* Interaction with Epithelial Cells Modifies Airway Macrophage Response to Ozone. *Am J Respir Cell Mol Biol* **52**, 285–294 (2015).
- 51. Ishii, H. *et al.* Alveolar macrophage-epithelial cell interaction following exposure to atmospheric particles induces the release of mediators involved in monocyte mobilization and recruitment. *Respir. Res.* **6**, 87 (2005).
- 52. Fujii, T. et al. Interaction of Alveolar Macrophages and Airway Epithelial Cells Following

  Exposure to Particulate Matter Produces Mediators that Stimulate the Bone Marrow. Am. J.

  Respir. Cell Mol. Biol 27, (2002).
- 53. Hung, L. Y. *et al.* Macrophages promote epithelial proliferation following infectious and non-infectious lung injury through a Trefoil factor 2-dependent mechanism. *Mucosal Immunol.* **12**, 64–76 (2019).
- 54. Kuebler, W. M., Parthasarathi, K., Wang, P. M. & Bhattacharya, J. A novel signaling mechanism between gas and blood compartments of the lung. *J. Clin. Invest.* **105**, 905–913 (2000).
- 55. Bourdonnay, E. *et al.* Transcellular delivery of vesicular SOCS proteins from macrophages to epithelial cells blunts inflammatory signaling. *J. Exp. Med.* **212**, 729–742 (2015).
- 56. Cerri, C. *et al.* Monocyte/Macrophage-Derived Microparticles Up-Regulate Inflammatory Mediator Synthesis by Human Airway Epithelial Cells. *J. Immunol.* **177**, 1975–1980 (2006).
- 57. Thorley, A. J. *et al.* Innate immune responses to bacterial ligands in the peripheral human Lung Role of alveolar epithelial TLR expression and signalling. *PLoS One* **6**, (2011).
- 58. Martin, F. J. & Prince, A. S. TLR2 Regulates Gap Junction Intercellular Communication in Airway Cells. *J. Immunol.* **180**, 4986–4993 (2008).
- 59. Bhattacharya, J. & Westphalen, K. *Macrophage-epithelial interactions in pulmonary alveoli*. *Seminars in Immunopathology* **38**, 461–469 (Springer Verlag, 2016).
- 60. Westphalen, K. *et al.* Sessile alveolar macrophages communicate with alveolar epithelium to modulate immunity. *Nature* **506**, 503–506 (2014).

- 61. Pfeiffer, R. I. Preliminary communication on the exciting causes of influenza. *Br. Med. J.* **1**, 128 (1892).
- 62. Smith, W., Andrewes, C. H. & Laidlaw, P. P. A VIRUS OBTAINED FROM INFLUENZA PATIENTS. *Lancet* **222**, 66–68 (1933).
- 63. Winslow, C. E. *et al.* The Families and Genera of the Bacteria: Final Report of the Committee of the Society of American Bacteriologists on Characterization and Classification of Bacterial Types. *J. Bacteriol.* **5**, 191–229 (1920).
- 64. Murphy, T. F. & Apicella, M. A. Nontypable Haemophilus influenzae: a review of clinical aspects, surface antigens, and the human immune response to infection. *Reviews of infectious diseases* **9**, 1–15 (1987).
- 65. Meats, E. *et al.* Characterization of Encapsulated and Noncapsulated Haemophilus influenzae and Determination of Phylogenetic Relationships by Multilocus Sequence Typing. *J. Clin. Microbiol.* **41**, 1623–1636 (2003).
- 66. Martí-Lliteras, P. *et al.* Nontypable Haemophilus influenzae Displays a Prevalent Surface Structure Molecular Pattern in Clinical Isolates. *PLoS One* **6**, e21133 (2011).
- 67. Poje, G. & Redfield, R. J. General methods for culturing Haemophilus influenzae. *Methods Mol. Med.* **71**, 51–56 (2003).
- 68. Morey, P. *et al.* Evidence for a non-replicative intracellular stage of nontypable Haemophilus influenzae in epithelial cells. *Microbiology* **157**, 234–250 (2011).
- 69. Foxwell, A. R., Kyd, J. M. & Cripps, A. W. Nontypeable Haemophilus influenzae: pathogenesis and prevention. *Microbiol. Mol. Biol. Rev.* **62**, 294–308 (1998).
- 70. Rao, V. K., Krasan, G. P., Hendrixson, D. R., Dawid, S. & St. Geme, J. W. Molecular determinants of the pathogenesis of disease due to non-typable *Haemophilus influenzae*. *FEMS Microbiol. Rev.* **23**, 99–129 (1999).
- 71. Howard, A. J., Dunkin, K. T. & Millar, G. W. Nasopharyngeal carriage and antibiotic resistance of Haemophilus influenzae in healthy children. *Epidemiol. Infect.* **100**, 193–203 (1988).
- 72. Sethi, S., Evans, N., Grant, B. J. B. & Murphy, T. F. New Strains of Bacteria and Exacerbations of Chronic Obstructive Pulmonary Disease. *N. Engl. J. Med.* **347**, 465–471 (2002).

- 73. Hiltke, T. J., Schiffmacher, A. T., Dagonese, A. J., Sethi, S. & Murphy, T. F. Horizontal transfer of the gene encoding outer membrane protein P2 of nontypeable Haemophilus influenzae, in a patient with chronic obstructive pulmonary disease. *J. Infect. Dis.* **188**, 114–117 (2003).
- 74. Murphy, T. F., Sethi, S., Klingman, K. L., Brueggemann, A. B. & Doern, G. V. Simultaneous Respiratory Tract Colonization by Multiple Strains of Nontypeable *Haemophilus influenzae* in Chronic Obstructive Pulmonary Disease: Implications for Antibiotic Therapy. *J. Infect. Dis.* **180**, 404–409 (1999).
- 75. Hargreaves, R. M., Slack, M. P. E., Howard, A. J., Anderson, E. & Ramsay, M. E. Changing patterns of invasive Haemophilus influenzae disease in England and Wales after introduction of the Hib vaccination programme. *Br. Med. J.* **312**, 160–161 (1996).
- 76. King, P. Haemophilus influenzae and the lung ( Haemophilus and the lung). *Clin. Transl. Med.*1, (2012).
- 77. Kress-Bennett, J. M. *et al.* Identification and characterization of msf, a novel virulence factor in Haemophilus influenzae. *PLoS One* **11**, (2016).
- 78. Shen, K. *et al.* Identification, distribution, and expression of novel genes in 10 clinical isolates of nontypeable Haemophilus influenzae. *Infect. Immun.* **73**, 3479–3491 (2005).
- 79. Dongari-Bagtzoglou, A. Pathogenesis of mucosal biofilm infections: Challenges and progress. *Expert Rev. Anti. Infect. Ther.* **6**, 201–208 (2008).
- 80. Donlan, R. M. Biofilm Formation: A Clinically Relevant Microbiological Process. *Clin. Infect. Dis.* **33**, 1387–1392 (2001).
- 81. Molin, S. & Tolker-Nielsen, T. Gene transfer occurs with enhanced efficiency in biofilms and induces enhanced stabilisation of the biofilm structure. *Curr. Opin. Biotechnol.* **14**, 255–261 (2003).
- 82. Jurcisek, J. A. & Bakaletz, L. O. Biofilms Formed by Nontypeable Haemophilus influenzae In Vivo Contain both Double-Stranded DNA and Type IV Pilin Protein. *J. Bacteriol.* **189**, 3868–3875 (2007).
- 83. Mokrzan, E. M., Ward, M. O. & Bakaletz, L. O. Type IV pilus expression is upregulated in nontypeable Haemophilus influenzae biofilms formed at the temperature of the human

- nasopharynx. J. Bacteriol. 198, 2619–2630 (2016).
- 84. Collins, S. A. *et al.* Cephalosporin-3'-Diazeniumdiolate NO Donor Prodrug PYRRO-C3D Enhances Azithromycin Susceptibility of Nontypeable Haemophilus influenzae Biofilms. *Antimicrob. Agents Chemother.* **61**, e02086-16 (2017).
- 85. Murphy, T. F. & Kirkham, C. Biofilm formation by nontypeable Haemophilus influenzae: Strain variability, outer membrane antigen expression and role of pili. *BMC Microbiol.* **2**, 1–8 (2002).
- 86. Thulborn, S. J. *et al.* Detection of Cell-Dissociated Non-Typeable <em>Haemophilus influenzae</em> in the Airways of Patients with Chronic Obstructive Pulmonary Disease
  Int. J. Chron. Obstruct. Pulmon. Dis. Volume 15, 1357–1365 (2020).
- 87. Linke, D., Riess, T., Autenrieth, I. B., Lupas, A. & Kempf, V. A. J. Trimeric autotransporter adhesins: variable structure, common function. *Trends Microbiol.* **14**, 264–270 (2006).
- 88. St Geme, J. W., Kumar, V. V., Cutter, D. & Barenkamp, S. J. Prevalence and distribution of the hmw and hia genes and the HMW and Hia adhesins among genetically diverse strains of nontypeable Haemophilus influenzae. *Infect. Immun.* **66**, 364–368 (1998).
- 89. Osman, K. L., Jefferies, J. M., Woelk, C. H., Cleary, D. W. & Clarke, S. C. The adhesins of non-typeable Haemophilus influenzae. *Expert Rev. Anti. Infect. Ther.* **16**, 187–196 (2018).
- 90. Ecevit, I. Z. *et al.* Prevalence of the hifBC, hmw1A, hmw2A, hmwC, and hia genes in Haemophilus influenzae isolates. *J. Clin. Microbiol.* **42**, 3065–3072 (2004).
- 91. De Chiara, M. *et al.* Genome sequencing of disease and carriage isolates of nontypeable Haemophilus influenzae identifies discrete population structure. *Proc. Natl. Acad. Sci. U. S. A.* **111**, 5439–5444 (2014).
- 92. Atack, J. M. *et al.* The HMW2 adhesin of non-typeable Haemophilus influenzae is a human-adapted lectin that mediates high-affinity binding to 2–6 linked N-acetylneuraminic acid glycans. *Biochem. Biophys. Res. Commun.* **503**, 1103–1107 (2018).
- 93. Noel, G. J., Barenkamp, S. J., St. Geme, J. W., Haining, W. N. & Mosser, D. M. High-molecular-weight surface-exposed proteins of haemophilus influenzae mediate binding to macrophages. *J. Infect. Dis.* **169**, 425–429 (1994).
- 94. St. Geme, J. W., Falkow, S. & Barenkamp, S. J. High-molecular-weight proteins of nontypable

- Haemophilus influenzae mediate attachment to human epithelial cells. *Proc. Natl. Acad. Sci. U. S. A.* **90**, 2875–2879 (1993).
- 95. Vuong, J. *et al.* Absence of high molecular weight proteins 1 and/or 2 is associated with decreased adherence among non-typeable Haemophilus influenzae clinical isolates. *J. Med. Microbiol.* **62**, 1649–1656 (2013).
- 96. Fink, D. L., Buscher, A. Z., Green, B., Fernsten, P. & St. Geme, J. W. The Haemophilus influenzae Hap autotransporter mediates microcolony formation and adherence to epithelial cells and extracellular matrix via binding regions in the C-terminal end of the passenger domain. *Cell. Microbiol.* **5**, 175–186 (2003).
- 97. Spahich, N. A. *et al.* Structural determinants of the interaction between the Haemophilus influenzae Hap autotransporter and fibronectin. *Microbiol. (United Kingdom)* **160**, 1182–1190 (2014).
- 98. Fink, D. L., Green, B. A. & St. Geme, J. W. The Haemophilus influenzae Hap autotransporter binds to fibronectin, laminin, and collagen IV. *Infect. Immun.* **70**, 4902–4907 (2002).
- 99. Hendrixson, D. R. & St. Geme, J. W. The Haemophilus influenzae Hap serine protease promotes adherence and microcolony formation, potentiated by a soluble host protein. *Mol. Cell* **2**, 841–850 (1998).
- 100. Meng, G., Spahich, N., Kenjale, R., Waksman, G. & St Geme, J. W. Crystal structure of the Haemophilus influenzae Hap adhesin reveals an intercellular oligomerization mechanism for bacterial aggregation. *EMBO J.* **30**, 3864–3874 (2011).
- 101. Euba, B. et al. Relative contribution of P5 and Hap surface proteins to nontypable Haemophilus influenzae interplay with the host upper and lower airways. PLoS One 10, e0123154 (2015).
- 102. Chul Hee Lee *et al.* Distribution of secretory leukoprotease inhibitor in the human nasal airway. *Am. Rev. Respir. Dis.* **147**, 710–716 (1993).
- 103. Atack, J. M. *et al.* The nontypeable haemophilus influenzae major adhesin hia is a dual-function lectin that binds to human-specific respiratory tract sialic acid glycan receptors. *MBio* 11, 1–15 (2020).

- 104. St Geme Iii, J. W. & Cutter, D. The Haemophilus influenzae Hia Adhesin Is an Autotransporter Protein That Remains Uncleaved at the C Terminus and Fully Cell Associated. JOURNAL OF BACTERIOLOGY **182**, (2000).
- 105. Atack, J. M. *et al.* Selection and Counterselection of Hia Expression Reveals a Key Role for Phase-Variable Expression of Hia in Infection Caused by Nontypeable Haemophilus influenzae. *J. Infect. Dis.* **212**, 645–653 (2015).
- 106. Webster, P. *et al.* Distribution of bacterial proteins in biofilms formed by non-typeable Haemophilus influenzae. *J. Histochem. Cytochem.* **54**, 829–842 (2006).
- 107. Cardines, R. *et al.* Haemophilus influenzae in children with cystic fibrosis: Antimicrobial susceptibility, molecular epidemiology, distribution of adhesins and biofilm formation. *Int. J. Med. Microbiol.* **302**, 45–52 (2012).
- 108. Tchoupa, A. K., Lichtenegger, S., Reidl, J. & Hauck, C. R. Outer membrane protein P1 is the CEACAM-binding adhesin of Haemophilus influenzae. *Mol. Microbiol.* **98**, 440–455 (2015).
- 109. Avadhanula, V., Rodriguez, C. A., Ulett, G. C., Bakaletz, L. O. & Adderson, E. E. Nontypeable Haemophilus influenzae adheres to intercellular adhesion molecule 1 (ICAM-1) on respiratory epithelial cells and upregulates ICAM-1 expression. *Infect. Immun.* **74**, 830–838 (2006).
- 110. Frick, A. G. *et al.* Haemophilus influenzae Stimulates ICAM-1 Expression on Respiratory Epithelial Cells . *J. Immunol.* **164**, 4185–4196 (2000).
- 111. Burns, J. L. & Smith, A. L. A major outer-membrane protein functions as a porin in Haemophilus influenzae. *J. Gen. Microbiol.* **133**, 1273–1277 (1987).
- 112. Regelink, A. G. *et al.* Variation in the composition and pore function of major outer membrane pore protein P2 of Haemophilus influenzae from cystic fibrosis patients. *Antimicrob. Agents Chemother.* **43**, 226–232 (1999).
- 113. Duim, B., Alphen, L., Eijk, P., Jansen, H. M. & Dankert, J. Antigenic drift of non-encapsulated Haemophilus influenzae major outer membrane protein P2 in patients with chronic bronchitis is caused by point mutations. *Mol. Microbiol.* 11, 1181–1189 (1994).
- 114. Sikkema, D. J. & Murphy, T. F. Molecular analysis of the P2 porin protein of nontypeable Haemophilus influenzae. *Infect. Immun.* **60**, 5204–5211 (1992).

- 115. Reddy, M. S., Bernstein, J. M., Murphy, T. F. & Faden, H. S. *Binding between Outer Membrane Proteins of Nontypeable Haemophilus influenzae and Human Nasopharyngeal Mucin.*INFECTION AND IMMUNITY **64**, (1996).
- 116. Su, Y.-C. *et al.* Haemophilus influenzae P4 Interacts With Extracellular Matrix Proteins Promoting Adhesion and Serum Resistance Europe PMC Funders Group. *J Infect Dis* **213**, 314–323 (2016).
- 117. Michel, L. V. *et al.* Dual orientation of the outer membrane lipoprotein P6 of nontypeable Haemophilus influenzae. *J. Bacteriol.* **195**, 3252–3259 (2013).
- 118. Murphy, T. F., Kirkham, C. & Lesse, A. J. Construction of a mutant and characterization of the role of the vaccine antigen P6 in outer membrane integrity of nontypeable Haemophilus influenzae. *Infect. Immun.* **74**, 5169–5176 (2006).
- 119. Berenson, C. S., Murphy, T. F., Wrona, C. T. & Sethi, S. Outer Membrane Protein P6 of Nontypeable Haemophilus influenzae Is a Potent and Selective Inducer of Human Macrophage Proinflammatory Cytokines. *Infect. Immun.* 73, 2728–2735 (2005).
- 120. Chang, A., Kaur, R., Michel, L. V., Casey, J. R. & Pichichero, M. Haemophilus influenzae vaccine candidate outer membrane protein P6 is not conserved in all strains. *Hum. Vaccin.* **7**, 102–105 (2011).
- 121. Sikkema, D. J., Nelson, M. B., Apicella, M. A. & Murphy, T. F. Outer membrane protein P6 of Haemophilus influenzae binds to its own gene. *Mol. Microbiol.* **6**, 547–554 (1992).
- 122. Preciado, D. *et al.* A proteomic characterization of NTHi lysates. *Int. J. Pediatr. Otorhinolaryngol.* **80**, 8–16 (2016).
- 123. Wu, S. *et al.* Biofilm-specific extracellular matrix proteins of nontypeable Haemophilus influenzae. *Pathog. Dis.* **72**, 143–160 (2014).
- 124. Das, S. *et al.* Improving patient care via development of a protein-based diagnostic test for microbe-specific detection of chronic rhinosinusitis. *Laryngoscope* **124**, 608–615 (2014).
- 125. Singh, B., Al-Jubair, T., Mörgelin, M., Thunnissen, M. M. & Riesbeck, K. The unique structure of haemophilus influenzae protein E reveals multiple binding sites for host factors. *Infect. Immun.* 81, 801–814 (2013).

- 126. GODIER, A. & HUNT, B. J. Plasminogen receptors and their role in the pathogenesis of inflammatory, autoimmune and malignant disease. *J. Thromb. Haemost.* **11**, 26–34 (2013).
- 127. Su, Y.-C. *et al. Haemophilus influenzae* acquires vitronectin via the ubiquitous Protein F to subvert host innate immunity. *Mol. Microbiol.* **87**, 1245–1266 (2013).
- 128. Jalalvand, F. *et al.* Haemophilus influenzae protein F mediates binding to laminin and human pulmonary epithelial cells. *J. Infect. Dis.* **207**, 803–813 (2013).
- Su, Y. C. et al. The Laminin Interactome: A Multifactorial Laminin-Binding Strategy by Nontypeable Haemophilus influenzae for Effective Adherence and Colonization. J. Infect. Dis. 220, 1049–1060 (2019).
- 130. Ahrén, I. L., Janson, H., Forsgren, A. & Riesbeck, K. Protein D expression promotes the adherence and internalization of non-typeable Haemophilus influenzae into human monocytic cells. *Microb. Pathog.* **31**, 151–158 (2001).
- 131. Janson, H. *et al.* Effects on the Ciliated Epithelium of Protein D–Producing and –Nonproducing Nontypeable *Haemophilus influenzae* in Nasopharyngeal Tissue Cultures. *J. Infect. Dis.* **180**, 737–746 (1999).
- 132. Davoudi, A. *et al.* Immunization with Protein D from Non-Typeable Haemophilus influenzae (NTHi) Induced Cytokine Responses and Bioactive Antibody Production. *Jundishapur J Microbiol* **9**, 36617 (2016).
- 133. Jurcisek, J. A. *et al.* The PilA protein of non-typeable Haemophilus influenzae plays a role in biofilm formation, adherence to epithelial cells and colonization of the mammalian upper respiratory tract. *Mol. Microbiol.* **65**, 1288–1299 (2007).
- 134. Novotny, L. A. & Bakaletz, L. O. Intercellular adhesion molecule 1 serves as a primary cognate receptor for the Type IV pilus of nontypeable Haemophilus influenzae. *Cell. Microbiol.* **18**, 1043–1055 (2016).
- 135. Bakaletz, L. O. *et al.* Demonstration of type IV pilus expression and a twitching phenotype by Haemophilus influenzae. *Infect. Immun.* **73**, 1635–1643 (2005).
- 136. Carruthers, M. D. *et al.* Biological roles of nontypeable Haemophilus influenzae type IV pilus proteins encoded by the pil and com operons. *J. Bacteriol.* **194**, 1927–33 (2012).

- 137. Mokrzan, E. M., Johnson, T. J. & Bakaletz, L. O. Expression of the nontypeable haemophilus influenzae type IV pilus is stimulated by coculture with host respiratory tract epithelial cells. *Infect. Immun.* 87, (2019).
- 138. Baddal, B. Characterization of biofilm formation and induction of apoptotic DNA fragmentation by nontypeable Haemophilus influenzae on polarized human airway epithelial cells. *Microb. Pathog.* **141**, 103985 (2020).
- 139. Kubiet, M., Ramphal, R., Weber, A. & Smith, A. Pilus-mediated adherence of Haemophilus influenzae to human respiratory mucins. *Infect. Immun.* **68**, 3362–3367 (2000).
- 140. Weber, A., Harris, K., Lohrke, S., Forney, L. & Smith, A. L. Inability to express fimbriae results in impaired ability of Haemophilus influenzae b to colonize the nasopharynx. *Infection and Immunity* **59**, 4724–4728 (1991).
- 141. Swords, W. E., Jones, P. A. & Apicella, M. A. Review: The lipo-oligosaccharides of Haemophilus influenzae: an interesting array of characters. *J. Endotoxin Res.* **9**, 131–144 (2003).
- 142. Allen, S., Zaleski, A., Johnston, J. W., Gibson, B. W. & Apicella, M. A. Novel sialic acid transporter of Haemophilus influenzae. *Infect. Immun.* **73**, 5291–5300 (2005).
- 143. Swords, W. E. *et al.* Sialylation of Lipooligosaccharides Promotes Biofilm Formation by Nontypeable Haemophilus influenzae. *Infect. Immun.* **72**, 106–113 (2004).
- 144. Greiner, L. L. *et al.* Nontypeable Haemophilus influenzae strain 2019 produces a biofilm containing N-acetylneuraminic acid that may mimic sialylated O-linked glycans. *Infect. Immun.* **72**, 4249–4260 (2004).
- 145. Jurcisek, J. *et al.* Role of sialic acid and complex carbohydrate biosynthesis in biofilm formation by nontypeable Haemophilus influenzae in the chinchilla middle ear. *Infect. Immun.* **73**, 3210–3218 (2005).
- 146. Johnston, J. W. *et al.* Characterization of the N-acetyl-5-neuraminic acid-binding site of the extracytoplasmic solute receptor (SiaP) of nontypeable Haemophilus influenzae strain 2019. *J. Biol. Chem.* **283**, 855–865 (2008).
- 147. Swords, W. E. *et al.* Non-typeable Haemophilus influenzae adhere to and invade human bronchial epithelial cells via an interaction of lipooligosaccharide with the PAF receptor. *Mol.*

- Microbiol. 37, 13-27 (2000).
- 148. West-Barnette, S., Rockel, A. & Swords, W. E. Biofilm growth increases phosphorylcholine content and decreases potency of nontypeable Haemophilus influenzae endotoxins. *Infect. Immun.* **74**, 1828–1836 (2006).
- 149. Johnson, R. W., McGillivary, G., Denoël, P., Poolman, J. & Bakaletz, L. O. Abrogation of nontypeable Haemophilus influenzae Protein D function reduces phosphorylcholine decoration, adherence to airway epithelial cells, and fitness in a chinchilla model of otitis media. *Vaccine* **29**, 1211–1221 (2011).
- 150. Hong, W. *et al.* Phosplioiylclioline decreases early inflammation and promotes the establishment of stable biofilm communities of nontypeable Haemophilus influenzae strain 86-028NP in a chinchilla model of otitis media. *Infect. Immun.* **75**, 958–965 (2007).
- 151. Pang, B. *et al.* Lipooligosaccharides containing phosphorylcholine delay pulmonary clearance of nontypeable Haemophilus influenzae. *Infect. Immun.* **76**, 2037–2043 (2008).
- 152. Hong, W., Pang, B., West-Barnette, S. & Swords, W. E. Phosphorylcholine expression by nontypeable Haemophilus influenzae correlates with maturation of biofilm communities in vitro and in vivo. in *Journal of Bacteriology* **189**, 8300–8307 (American Society for Microbiology (ASM), 2007).
- 153. Lundström, S. L. *et al.* Application of capillary electrophoresis mass spectrometry and liquid chromatography multiple-step tandem electrospray mass spectrometry to profile glycoform expression during Haemophilus influenzae pathogenesis in the chinchilla model of experimental otitis media. *Infect. Immun.* **76**, 3255–3267 (2008).
- 154. Daines, D. A. *et al.* Haemophilus influenzae luxS mutants form a biofilm and have increased virulence. *Microb. Pathog.* **39**, 87–96 (2005).
- 155. Armbruster, C. E. *et al.* LuxS promotes biofilm maturation and persistence of nontypeable Haemophilus influenzae in vivo via modulation of lipooligosaccharides on the bacterial surface. *Infect. Immun.* **77**, 4081–4091 (2009).
- 156. Armbruster, C. E. *et al.* RbsB (NTHI-0632) mediates quorum signal uptake in nontypeable Haemophilus influenzae strain 86-028NP. *Mol. Microbiol.* **82**, 836–850 (2011).

- 157. Pang, B. et al. Autoinducer 2 (AI-2) Production by Nontypeable Haemophilus influenzae 86-028NP Promotes Expression of a Predicted Glycosyltransferase That Is a Determinant of Biofilm Maturation, Prevention of Dispersal, and Persistence In Vivo. (2018).
- 158. Ünal, C. M. *et al.* QseC controls biofilm formation of non-typeable Haemophilus influenzae in addition to an Al-2-dependent mechanism. *Int. J. Med. Microbiol.* **302**, 261–269 (2012).
- 159. Surette, M. G., Miller, M. B. & Bassler, B. L. Quorum sensing in Escherichia coli, Salmonella typhimurium, and Vibrio harveyi: A new family of genes responsible for autoinducer production. *Proc. Natl. Acad. Sci. U. S. A.* **96**, 1639–1644 (1999).
- 160. Flemming, H. C. & Wingender, J. The biofilm matrix. Nat. Rev. Microbiol. 8, 623–633 (2010).
- 161. Marti, S. *et al.* Bacterial Lysis through Interference with Peptidoglycan Synthesis Increases
  Biofilm Formation by Nontypeable Haemophilus influenzae. *mSphere* **2**, 329–345 (2017).
- 162. Jurcisek, J. A., Brockman, K. L., Novotny, L. A., Goodman, S. D. & Bakaletz, L. O. Nontypeable Haemophilus influenzae releases DNA and DNABII proteins via a T4SS-like complex and ComE of the type IV pilus machinery. (2017). doi:10.1073/pnas.1705508114
- 163. Goodman, S. D. *et al.* Biofilms can be dispersed by focusing the immune system on a common family of bacterial nucleoid-associated proteins. *Mucosal Immunol.* **4**, 625–637 (2011).
- 164. Devaraj, A., Buzzo, J., Rocco, C. J., Bakaletz, L. O. & Goodman, S. D. The DNABII family of proteins is comprised of the only nucleoid associated proteins required for nontypeable *Haemophilus influenzae* biofilm structure. *Microbiologyopen* **7**, e00563 (2018).
- 165. Brockson, M. E. *et al.* Evaluation of the kinetics and mechanism of action of anti-integration host factor-mediated disruption of bacterial biofilms. *Mol. Microbiol.* **93**, 1246–1258 (2014).
- 166. Kamashev, D. *et al.* Comparison of histone-like HU protein DNA-binding properties and HU/IHF protein sequence alignment. *PLoS One* **12**, 1–24 (2017).
- 167. Brandstetter, K. A., Jurcisek, J. A., Goodman, S. D., Bakaletz, L. O. & Das, S. Antibodies directed against integration host factor mediate biofilm clearance from nasopore. in *Laryngoscope* **123**, 2626–2632 (NIH Public Access, 2013).
- 168. Novotny, L. A., Jurcisek, J. A., Goodman, S. D. & Bakaletz, L. O. Monoclonal antibodies against DNA-binding tips of DNABII proteins disrupt biofilms in vitro and induce bacterial clearance in

- vivo. EBioMedicine 10, 33–44 (2016).
- 169. Novotny, L. A. *et al.* Antibodies against the majority subunit of type IV pili disperse nontypeable H aemophilus influenzae biofilms in a LuxS-dependent manner and confer therapeutic resolution of experimental otitis media. *Mol. Microbiol.* **96**, 276–292 (2015).
- 170. C Reygaert, W. An overview of the antimicrobial resistance mechanisms of bacteria. *AIMS Microbiol.* **4**, 482–501 (2018).
- 171. Kaji, C., Watanabe, K., Apicella, M. A. & Watanabe, H. Antimicrobial effect of fluoroquinolones for the eradication of nontypeable haemophilus influenzae isolates within biofilms. *Tohoku J. Exp. Med.* **214**, 121–128 (2008).
- 172. Reimche, J. L., Kirse, D. J., Whigham, A. S. & Swords, W. E. Resistance of non-typeable Haemophilus influenzae biofilms is independent of biofilm size. *Pathog. Dis.* **75**, 112 (2017).
- 173. Dabernat, H. & Delmas, C. Epidemiology and evolution of antibiotic resistance of Haemophilus influenzae in children 5 years of age or less in France, 2001-2008: A retrospective database analysis. *Eur. J. Clin. Microbiol. Infect. Dis.* **31**, 2745–2753 (2012).
- 174. Li, X. X. *et al.* Molecular Epidemiology and Antimicrobial Resistance of Haemophilus influenzae in Adult Patients in Shanghai, China. *Front. Public Heal.* **8**, 95 (2020).
- 175. St.Geme, J. W. & Falkow, S. Haemophilus influenzae adheres to and enters cultured human epithelial cells. *Infect. Immun.* **58**, 4036–4044 (1990).
- 176. Forsgren, J. *et al.* Haemophilus influenzae resides and multiplies intracellularly in human adenoid tissue as demonstrated by in situ hybridization and bacterial viability assay. *Infect. Immun.* **62**, 673–679 (1994).
- 177. Van Schilfgaarde, M. *et al.* Haemophilus influenzae localized in epithelial cell layers is shielded from antibiotics and antibody-mediated bactericidal activity. *Microb. Pathog.* **26**, 249–262 (1999).
- 178. Clementi, C. F. & Murphy, T. F. Non-Typeable Haemophilus influenzae Invasion and Persistence in the Human Respiratory Tract. *Front. Cell. Infect. Microbiol.* **1**, 1–9 (2011).
- 179. Hardison, C. L. *et al.* Transient Nutrient Deprivation Promotes Macropinocytosis-Dependent Intracellular Bacterial Community Development. **3**, 286–304 (2018).

- 180. Craig, J. E., Nobbs, A. & High, N. J. The Extracytoplasmic Sigma Factor, E, Is Required for Intracellular Survival of Nontypeable Haemophilus influenzae in J774 Macrophages. *Infect. Immun.* **70**, 708–715 (2002).
- 181. Craig, J. E., Cliffe, A., Garnett, K. & High, N. J. Survival of nontypeable Haemophilus influenzae in macrophages. *FEMS Microbiol. Lett.* **203**, 55–61 (2001).
- 182. Forsgren, J. *et al.* Persistence of nontypeable Haemophilus influenzae in adenoid macrophages: A putative colonization mechanism. *Acta Otolaryngol.* **116**, 766–773 (1996).
- 183. KING, P. *et al.* Effect of interferon gamma and CD40 ligation on intracellular monocyte survival of nontypeable *Haemophilus influenzae* . *APMIS* **116**, 1043–1049 (2008).
- 184. Lazou Ahrén, I. et al. The Importance of a b-Glucan Receptor in the Nonopsonic Entry of Nontypeable Haemophilus influenzae into Human Monocytic and Epithelial Cells. The Journal of Infectious Diseases 184, (2001).
- 185. Goyal, M., Singh, M., Ray, P., Srinivasan, R. & Chakraborti, A. Cellular interaction of nontypeable Haemophilus influenzae triggers cytotoxicity of infected type II alveolar cells via apoptosis. *Pathog. Dis.* **73**, 1–12 (2014).
- 186. Van Schilfgaarde, M., Van Alphen, L., Eijk, P., Everts, V. & Dankert, J. Paracytosis of Haemophilus influenzae through cell layers of NCI-H292 lung epithelial cells. *Infect. Immun.*63, 4729–4737 (1995).
- 187. VanWagoner, T. M. *et al.* The modA10 phasevarion of nontypeable Haemophilus influenzae R2866 regulates multiple virulence-associated traits. *Microb. Pathog.* **92**, 60–67 (2016).
- 188. Phillips, Z. N. *et al.* Analysis of invasive nontypeable Haemophilus influenzae isolates reveals selection for the expression state of particular phase-variable lipooligosaccharide biosynthetic genes. *Infect. Immun.* **87**, (2019).
- 189. Cholon, D. M. *et al.* Serial isolates of persistent Haemophilus influenzae in patients with chronic obstructive pulmonary disease express diminishing quantities of the HMW1 and HMW2 adhesins. *Infect. Immun.* **76**, 4463–4468 (2008).
- 190. Davis, G. S. *et al.* Phase variation and host immunity against high molecular weight (HMW) adhesins shape population dynamics of nontypeable Haemophilus influenzae within human

- hosts. J. Theor. Biol. 355, 208-218 (2014).
- 191. Barenkamp, S. J. Human Antibodies (Abs) Specific for the High Molecular Weight (HMW) Adhesion Proteins of Nontypable Haemophilus influenzae (NTHI) are Opsonophagocytic. *Pediatr. Res.* **45**, 156A-156A (1999).
- 192. Nakamura, S. *et al.* Molecular basis of increased serum resistance among pulmonary isolates of non-typeable Haemophilus influenzae. *PLoS Pathog.* **7**, (2011).
- 193. Weiser, J. N., Love, J. M. & Moxon, E. R. The molecular mechanism of phase variation of H. influenzae lipopolysaccharide. *Cell* **59**, 657–665 (1989).
- 194. Lysenko, E. S., Gould, J., Bals, R., Wilson, J. M. & Weiser, J. N. Bacterial phosphorylcholine decreases susceptibility to the antimicrobial peptide LL-37/hCAP18 expressed in the upper respiratory tract. *Infect. Immun.* **68**, 1664–1671 (2000).
- 195. Weiser, J. N. *et al.* Phosphorylcholine on the lipopolysaccharide of Haemophilus influenzae contributes to persistence in the respiratory tract and sensitivity to serum killing mediated by C-reactive protein. *J. Exp. Med.* **187**, 631–640 (1998).
- 196. Langereis, J. D. *et al.* Nontypeable haemophilus influenzae invasive blood isolates are mainly phosphorylcholine negative and show decreased complement-mediated killing that is associated with lower binding of IgM and CRP in comparison to colonizing isolates from the oropharynx. *Infect. Immun.* **87**, (2019).
- 197. Richter, K. *et al.* Phosphocholine-modified lipooligosaccharides of Haemophilus influenzae inhibit ATP-induced IL-1β release by pulmonary epithelial cells. *Molecules* **23**, (2018).
- 198. Apicella, M. A. Nontypeable Haemophilus influenzae: the role of N-acetyl-5-neuraminic acid in biology. *Frontiers in cellular and infection microbiology* **2**, 19 (2012).
- 199. Fox, K. L. *et al.* Identification of a bifunctional lipopolysaccharide sialyltransferase in Haemophilus influenzae: Incorporation of disialic acid. *J. Biol. Chem.* **281**, 40024–40032 (2006).
- 200. Atack, J. M. *et al.* A biphasic epigenetic switch controls immunoevasion, virulence and niche adaptation in non-typeable Haemophilus influenzae. *Nat. Commun.* **6**, 1–12 (2015).
- 201. Atack, J. M., Murphy, T. F., Pettigrew, M. M., Seib, K. L. & Jennings, M. P. Non-typeable

- Haemophilus influenzae isolates from patients with chronic obstructive pulmonary disease contain new phase-variable modA methyltransferase alleles controlling phasevarions. *Sci. Rep.* **9**, (2019).
- 202. Brockman, K. L. *et al.* The ModA2 Phasevarion of nontypeable Haemophilus influenzae Regulates Resistance to Oxidative Stress and Killing by Human Neutrophils. *Sci. Rep.* **7**, 1–11 (2017).
- 203. Brockman, K. L. *et al.* Epigenetic regulation alters biofilm architecture and composition in multiple clinical isolates of nontypeable haemophilus influenzae. *MBio* **9**, (2018).
- 204. Brockman, K. L. *et al.* ModA2 phasevarion switching in nontypeable haemophilus influenzae increases the severity of experimental otitis media. *J. Infect. Dis.* **214**, 817–824 (2016).
- 205. Plaut, A. G., Qiu, J. & St. Geme, J. W. Human lactoferrin proteolytic activity: Analysis of the cleaved region in the IgA protease of Haemophilus influenzae. *Vaccine* **19**, 148–152 (2000).
- Fernaays, M. M., Lesse, A. J., Cai, X. & Murphy, T. F. Characterization of igaB, a second immunoglobulin A1 protease gene in nontypeable Haemophilus influenzae. *Infect. Immun.* 74, 5860–5870 (2006).
- 207. Roos, A. *et al.* Human IgA Activates the Complement System Via the Mannan-Binding Lectin Pathway. *J. Immunol.* **167**, 2861–2868 (2001).
- Sharpe, S. W., Kuehn, M. J. & Mason, K. M. Elicitation of epithelial cell-derived immune effectors by outer membrane vesicles of nontypeable haemophilus influenzae. *Infect. Immun.* 79, 4361–4369 (2011).
- 209. Winter, L. E. & Barenkamp, S. J. Immunogenicity of Nontypeable Haemophilus influenzae Outer Membrane Vesicles and Protective Ability in the Chinchilla Model of Otitis Media. *Clin. Vaccine Immunol.* **24**, 1–12 (2017).
- 210. Shoemark, A. Haemophilus influenzae biofilms in primary ciliary dyskinesia: A moving story. *Eur. Respir. J.* **50**, (2017).
- 211. Wijers, C. D., Chmiel, J. F. & Gaston, B. M. Bacterial infections in patients with primary ciliary dyskinesia: Comparison with cystic fibrosis. *Chronic Respiratory Disease* **14**, 392–406 (2017).
- 212. O'Callaghan, C., Chetcuti, P. & Moya, E. High prevalence of primary ciliary dyskinesia in a

- British Asian population. Arch. Dis. Child. 95, 51–52 (2010).
- 213. Behan, L. *et al.* Diagnosing primary ciliary dyskinesia: an international patient perspective. *Eur Respir J* **48**, 1096–1107 (1096).
- 214. Kuehni, C. E. *et al.* Factors influencing age at diagnosis of primary ciliary dyskinesia in European children. *Eur. Respir. J.* **36**, 1248–58 (2010).
- 215. Shapiro, A. J. et al. Diagnosis, monitoring, and treatment of primary ciliary dyskinesia: PCD foundation consensus recommendations based on state of the art review. *Pediatr. Pulmonol.* 51, 115–32 (2016).
- 216. Horani, A., Ferkol, T. W., Dutcher, S. K. & Brody, S. L. Genetics and biology of primary ciliary dyskinesia. *Paediatr. Respir. Rev.* **18**, 18–24 (2016).
- 217. Ostrowski, L. E. *et al.* A Proteomic Analysis of Human Cilia. *Mol. Cell. Proteomics* **1**, 451–465 (2003).
- 218. Horani, A. *et al.* Establishment of the early cilia preassembly protein complex during motile ciliogenesis. *Proc. Natl. Acad. Sci.* **115**, E1221–E1228 (2018).
- 219. Gahleitner, F. *et al.* Lower airway clinical outcome measures for use in primary ciliary dyskinesia research: A scoping review. *ERJ Open Res.* **7**, (2021).
- 220. Pifferi, M. *et al.* Evaluation of pulmonary disease using static lung volumes in primary ciliary dyskinesia. *Thorax* **67**, 993–999 (2012).
- 221. Alanin, M. C. *et al.* A longitudinal study of lung bacterial pathogens in patients with primary ciliary dyskinesia. *Clin. Microbiol. Infect.* **21**, 1093.e1-1093.e7 (2015).
- 222. Noone, P. G. *et al.* Primary Ciliary Dyskinesia Diagnostic and Phenotypic Features. *Am. J. Respir. Crit. Care Med.* **169**, 459–467 (2004).
- 223. Walker, W., Jackson, C., Harris, A., Packham, S. & Lucas, J. Longitudinal microbiology of children with primary ciliary dyskinesia. *Eur. Respir. J.* **40**, P2959 (2012).
- 224. Walker, W. T. *et al.* Primary ciliary dyskinesia ciliated airway cells show increased susceptibility to Haemophilus influenzae biofilm formation. *Eur. Respir. J.* **50**, (2017).
- 225. Marrazzo, P. et al. 3D reconstruction of the human airway mucosa in vitro as an experimental

- model to study NTHi infections. PLoS One 11, (2016).
- 226. Carter, M. & Shieh, J. Chapter 14 Cell Culture Techniques. Guide to Research Techniques in Neuroscience (Elsevier Inc., 2015). doi:10.1016/B978-0-12-800511-8.00014-9
- 227. Huang, S., Wiszniewski, L. & Constant, S. The Use of In Vitro 3D Cell Models in Drug Development for Respiratory Diseases. in *Drug Discovery and Development Present and Future* (InTech, 2011). doi:10.5772/28132
- 228. Whitcutt, M. J., Adler, K. B. & Wu, R. A biphasic chamber system for maintaining polarity of differentiation of culture respiratory tract epithelial cells. *Vitr. Cell. Dev. Biol.* **24**, 420–428 (1988).
- 229. Grainger, C. I., Greenwell, L. L., Lockley, D. J., Martin, G. P. & Forbes, B. Culture of Calu-3 cells at the air interface provides a representative model of the airway epithelial barrier. *Pharm. Res.* **23**, 1482–1490 (2006).
- 230. Coles, J. L. *et al.* A Revised Protocol for Culture of Airway Epithelial Cells as a Diagnostic Tool for Primary Ciliary Dyskinesia. *J. Clin. Med.* **9**, 3753 (2020).
- 231. Hinks, T. S. C. *et al.* Steroid-induced Deficiency of Mucosal-associated Invariant T Cells in the Chronic Obstructive Pulmonary Disease Lung Implications for Nontypeable Haemophilus influenzae Infection. *Am. J. Respir. Crit. Care Med.* **194**, 1208–1218 (2016).
- 232. Ren, D. *et al.* Characterization of extended co-culture of non-typeable Haemophilus influenzae with primary human respiratory tissues. *Exp. Biol. Med.* **237**, 540–547 (2012).
- 233. Starner, T. D. *et al.* Haemophilus influenzae forms biofilms on airway epithelia: implications in cystic fibrosis. *Am. J. Respir. Crit. Care Med.* **174**, 213–20 (2006).
- 234. Hartwig, S. M., Ketterer, M., Apicella, M. A. & Varga, S. M. Non-typeable Haemophilus influenzae protects human airway epithelial cells from a subsequent respiratory syncytial virus challenge. *Virology* **498**, 128–135 (2016).
- 235. Hiraoka, M. *et al.* Tosufloxacin for eradicating Biofilm-Forming nontypeable haemophilus influenzae isolated from intractable acute otitis media. *Jundishapur J. Microbiol.* **12**, (2019).
- 236. Ackland, J. Investigating macrophage-pathogen interactions in asthma. (2021).

- 237. Hayden, P. J. et al. Mechanisms Of Goblet Cell Hyperplasia Induced By Simulated Viral Exposure Or TH2 Cytokines In The EpiAirway-FT<sup>TM</sup> In Vitro Human Airway Model. in American Thoracic Society International Conference Meetings Abstracts American Thoracic Society International Conference Meetings Abstracts A2051–A2051 (American Thoracic Society, 2011). doi:10.1164/airccm-conference.2011.183.1 meetingabstracts.a2051
- 238. Sekiya, Y. *et al.* Comparative efficacies of different antibiotic treatments to eradicate nontypeable Haemophilus influenzae infection. *BMC Infect. Dis.* **8**, 1–9 (2008).
- 239. Hong, W. *et al.* Nontypeable Haemophilus influenzae inhibits autolysis and fratricide of Streptococcus pneumoniae in vitro. *Microbes Infect.* **16**, 203–213 (2014).
- 240. Cope, E. K. *et al.* Regulation of Virulence Gene Expression Resulting from Streptococcus pneumoniae and Nontypeable Haemophilus influenzae Interactions in Chronic Disease. *PLoS One* **6**, e28523 (2011).
- 241. Fakih, M. G., Murphy, T. F., Pattoli, M. A. & Berenson, C. S. Specific binding of Haemophilus influenzae to minor gangliosides of human respiratory epithelial cells. *Infect. Immun.* **65**, 1695 (1997).
- 242. Gulraiz, F., Bellinghausen, C., Bruggeman, C. A. & Stassen, F. R. Haemophilus influenzae increases the susceptibility and inflammatory response of airway epithelial cells to viral infections. *FASEB J.* **29**, 849–858 (2015).
- 243. Lugade, A. A., Bogner, P. N., Murphy, T. F. & Thanavala, Y. The Role of TLR2 and Bacterial Lipoprotein in Enhancing Airway Inflammation and Immunity. *Front. Immunol.* **2**, (2011).
- 244. Clemans, D. L. *et al.* Induction of proinflammatory cytokines from human respiratory epithelial cells after stimulation by nontypeable Haemophilus influenzae. *Infect. Immun.* **68**, 4430–4440 (2000).
- 245. Ackland, J. *et al.* Macrophage inflammatory responses to Non-typeable Haemophilus influenzae (NTHi) are strain-dependent. in *European Respiratory Journal* **54**, PA5440 (European Respiratory Society (ERS), 2019).
- 246. Berenson, C. S. *et al.* Nontypeable Haemophilus influenzae-binding gangliosides of human respiratory (HEp-2) cells have a requisite lacto/neolacto core structure. *FEMS Immunol. Med. Microbiol.* **45**, 171–182 (2005).

- 247. Arrevillaga, G., Gaona, J., Sánchez, C., Rosales, V. & Gómez, B. Respiratory Syncytial Virus

  Persistence in Macrophages Downregulates Intercellular Adhesion Molecule-1 Expression and

  Reduces Adhesion of Non-Typeable <b&gt;&lt;i&gt;Haemophilus

  influenzae&lt;/i&gt;&lt;/b&gt; Intervirology 55, 442–450 (2012).
- 248. Gu, X. X., Tsai, C. M., Apicella, M. A. & Lim, D. J. Quantitation and biological properties of released and cell-bound lipooligosaccharides from nontypeable Haemophilus influenzae. *Infect. Immun.* **63**, 4115–4120 (1995).
- 249. Foxwell, A. R., Kyd, J. M. & Cripps, A. W. Kinetics of inflammatory cytokines in the clearance of non-typeable *Haemophilus influenzae* from the lung. *Immunol. Cell Biol.* **76**, 556–559 (1998).
- 250. Ahrén, I. L., Bjartell, A., Egesten, A. & Riesbeck, K. Lipopolysaccharide-Binding Protein Increases Toll-like Receptor 4—Dependent Activation by Nontypeable Haemophilus influenzae. *J. Infect. Dis.* **184**, 926–930 (2001).
- 251. Wieland, C. W. *et al.* The MyD88-Dependent, but Not the MyD88-Independent, Pathway of TLR4 Signaling Is Important in Clearing Nontypeable Haemophilus influenzae from the Mouse Lung . *J. Immunol.* **175**, 6042–6049 (2005).
- 252. Wieland, C. W., Florquin, S. & van der Poll, T. Toll-like receptor 9 is not important for host defense against Haemophilus influenzae. *Immunobiology* **215**, 910–914 (2010).
- 253. Punturieri, A., Copper, P., Polak, T., Christensen, P. J. & Curtis, J. L. Conserved Nontypeable Haemophilus influenzae -Derived TLR2-Binding Lipopeptides Synergize with IFN-β to Increase Cytokine Production by Resident Murine and Human Alveolar Macrophages. *J. Immunol.* 177, 673–680 (2006).
- 254. Provost, K. A., Smith, M., Arold, S. P., Hava, D. L. & Sethi, S. Calcium restores the macrophage response to nontypeable Haemophilus influenzae in chronic obstructive pulmonary disease. *Am. J. Respir. Cell Mol. Biol.* **52**, 728–737 (2015).
- 255. Leichtle, A. *et al.* CC Chemokine Ligand 3 Overcomes the Bacteriocidal and Phagocytic Defect of Macrophages and Hastens Recovery from Experimental Otitis Media in TNF –/– Mice. *J. Immunol.* **184**, 3087–3097 (2010).
- 256. Chen, A. C.-H. et al. Multiple inflammasomes may regulate the interleukin-1-driven

- inflammation in protracted bacterial bronchitis. ERJ Open Res. 4, 00130-02017 (2018).
- 257. Rotta detto Loria, J. *et al.* Nontypeable Haemophilus Influenzae Infection Upregulates the NLRP3 Inflammasome and Leads to Caspase-1-Dependent Secretion of Interleukin- $1\beta$  A Possible Pathway of Exacerbations in COPD. *PLoS One* **8**, (2013).
- 258. Kurabi, A. *et al.* The inflammasome adaptor ASC contributes to multiple innate immune processes in the resolution of otitis media. *Innate Immun.* **21**, 203–214 (2015).
- 259. Taylor, D. C., Cripps, A. W. & Clancy, R. L. *A possible role for lysozyme in determining acute exacerbation in chronic bronchitis. Clin Exp Immunol* **102**, (1995).
- 260. Prasad, J. et al. Nontypeable haemophilus influenzae (NTHi) and lung oxidative stress. Eur. Respir. J. 42, (2013).
- 261. King, P. T. *et al.* Nontypeable haemophilus influenzae induces sustained lung oxidative stress and protease expression. *PLoS One* **10**, (2015).
- 262. Ween, M. *et al.* A small volume technique to examine and compare alveolar macrophage phagocytosis of apoptotic cells and non typeable Haemophilus influenzae (NTHi). *J. Immunol. Methods* **429**, 7–14 (2016).
- 263. Lu, C. *et al.* Nontypeable Haemophilus influenzae DNA stimulates type I interferon expression via STING signaling pathway. *Biochim. Biophys. Acta Mol. Cell Res.* **1865**, 665–673 (2018).
- 264. Berenson, C. S. *et al.* Impaired Alveolar Macrophage Response to Haemophilus Antigens in Chronic Obstructive Lung Disease. *Am J Respir Crit Care Med* **174**, 31–40 (2006).
- 265. Berenson, C. S., Kruzel, R. L., Eberhardt, E. & Sethi, S. Phagocytic dysfunction of human alveolar macrophages and severity of chronic obstructive pulmonary disease. *J. Infect. Dis.* **208**, 2036–2045 (2013).
- 266. Provost, K. A., Smith, M., Miller-Larsson, A., Gudleski, G. D. & Sethi, S. Bacterial regulation of macrophage bacterial recognition receptors in COPD are differentially modified by budesonide and fluticasone propionate. *PLoS One* **14**, (2019).
- 267. Berenson, C. S. *et al.* Impaired innate immune alveolar macrophage response and the predilection for COPD exacerbations. *Thorax* (2014). doi:10.1136/thoraxjnl-2013-203669

- 268. Ween, M. P., Whittall, J. J., Hamon, R., Reynolds, P. N. & Hodge, S. J. Phagocytosis and Inflammation: Exploring the effects of the components of E-cigarette vapor on macrophages. *Physiol. Rep.* **5**, e13370 (2017).
- 269. Bhat, T. A. *et al.* Secondhand Smoke Induces Inflammation and Impairs Immunity to Respiratory Infections. *J. Immunol.* **200**, 2927–2940 (2018).
- 270. Hamon, R. *et al.* Bushfire smoke is pro-inflammatory and suppresses macrophage phagocytic function. *Sci. Rep.* **8**, (2018).
- 271. Hodge, S. *et al.* Nonantibiotic macrolides restore airway macrophage phagocytic function with potential anti-inflammatory effects in chronic lung diseases. *Am J Physiol Lung Cell Mol Physiol* **312**, 678–687 (2017).
- 272. Euba, B. *et al.* Relationship between azithromycin susceptibility and administration efficacy for nontypeable Haemophilus influenzae respiratory infection. *Antimicrob. Agents Chemother.* **59**, 2700–2712 (2015).
- 273. Khalaf, R. M., Lea, S. R., Metcalfe, H. J. & Singh, D. Mechanisms of corticosteroid insensitivity in COPD alveolar macrophages exposed to NTHi. *Respir. Res.* **18**, (2017).
- 274. Walker, W. Cilia, nitric oxide and non-typeable Haemophilus influenzae biofilm infection. (2014).
- 275. Collins, S. A. Epithelial-biofilm interaction in primary ciliary dyskinesia. 1, (2017).
- 276. Ackland, J. *et al.* Dual RNASeq Reveals NTHi-Macrophage Transcriptomic Changes During Intracellular Persistence. *Front. Cell. Infect. Microbiol.* **0**, 740 (2021).
- 277. Lucas, J. S. *et al.* European Respiratory Society guidelines for the diagnosis of primary ciliary dyskinesia. *European Respiratory Journal* **49**, (2017).
- 278. Nussbaumer, M. *et al.* Diagnosis of primary ciliary dyskinesia: discrepancy according to different algorithms. *ERJ Open Res.* **7**, 00353–02021 (2021).
- 279. Mulay, A. et al. An in vitro model of murine middle ear epithelium. 9, 1405–1417 (2016).
- 280. Hood, D. W. *et al.* Sialic acid in the lipopolysaccharide of Haemophilus influenzae: Strain distribution, influence on serum resistance and structural characterization. *Mol. Microbiol.*

- **33**, 679–692 (1999).
- 281. Miles, A. A., Misra, S. S. & Irwin, J. O. The estimation of the bactericidal power of the blood. *J. Hyg. (Lond).* **38**, 732–749 (1938).
- 282. Legebeke, J. *et al.* Temporal Whole-Transcriptomic Analysis of Characterized In Vitro and Ex Vivo Primary Nasal Epithelia. *Front. Cell Dev. Biol.* **10**, 1–12 (2022).
- 283. Elso, C. M. *et al.* Leishmaniasis host response loci (lmr1-3) modify disease severity through a Th1/Th2-independent pathway. *Genes Immun.* **5**, 93–100 (2004).
- 284. Baldwin, T. *et al.* Wound healing response is a major contributor to the severity of cutaneous leishmaniasis in the ear model of infection. *Parasite Immunol.* **29**, 501–513 (2007).
- 285. Wang, P. *et al.* A cross-talk between epithelium and endothelium mediates human alveolar–capillary injury during SARS-CoV-2 infection. *Cell Death Dis.* **11**, (2020).
- 286. Costa, A., de Souza Carvalho-Wodarz, C., Seabra, V., Sarmento, B. & Lehr, C. M. Triple coculture of human alveolar epithelium, endothelium and macrophages for studying the interaction of nanocarriers with the air-blood barrier. *Acta Biomater.* **91**, 235–247 (2019).
- 287. Chen, W., Shao, C., Song, Y. & Bai, C. Primary ciliary dyskinesia complicated with diffuse panbronchiolitis: A case report and literature review. *Clin. Respir. J.* **8**, 425–430 (2014).
- 288. Paff, T., Omran, H., Nielsen, K. G. & Haarman, E. G. Current and future treatments in primary ciliary dyskinesia. *International Journal of Molecular Sciences* **22**, (2021).
- 289. Hosmer, J. *et al.* Access to highly specialized growth substrates and production of epithelial immunomodulatory metabolites determine survival of Haemophilus influenzae in human airway epithelial cells. *PLoS Pathog.* **18**, (2022).
- 290. Navarro Llorens, J. M., Tormo, A. & Martínez-García, E. Stationary phase in gram-negative bacteria. *FEMS Microbiol. Rev.* **34**, 476–495 (2010).
- 291. Jaishankar, J. & Srivastava, P. Molecular basis of stationary phase survival and applications. *Front. Microbiol.* **8**, 2000 (2017).
- 292. Weeks, J. R., Staples, K. J., Spalluto, C. M., Watson, A. & Wilkinson, T. M. A. A. The Role of Non-Typeable Haemophilus influenzae Biofilms in Chronic Obstructive Pulmonary Disease.

- Front. Cell. Infect. Microbiol. 11, 1–17 (2021).
- 293. Pang, B. et al. Dps promotes survival of nontypeable Haemophilus influenzae in biofilm communities in vitro and resistance to clearance in vivo. (2012).
  doi:10.3389/fcimb.2012.00058
- 294. Puges, M. *et al.* A Narrative Review of Experimental Assessment to Study Vascular Biomaterials Infections and Infectability. *EJVES Vasc. Forum* **59**, 49–55 (2023).
- 295. Wilson, C. *et al.* Quantitative and Qualitative Assessment Methods for Biofilm Growth: A Mini-review. *Res. Rev. J. Eng. Technol.* **6**, (2017).
- 296. Wagley, S. *et al.* Bacterial dormancy: A subpopulation of viable but non-culturable cells demonstrates better fitness for revival. *PLoS Pathog.* **17**, (2021).
- 297. Rayner, M. G. *et al.* Evidence of Bacterial Metabolic Activity in Culture-Negative Otitis Media With Effusion. *JAMA* **279**, 296–299 (1998).
- 298. Sanchez, C. J. *et al.* Biofilm formation by clinical isolates and the implications in chronic infections. *BMC Infect. Dis. 2013 131* **13**, 1–12 (2013).
- 299. Halter, M., Tona, A., Bhadriraju, K., Plant, A. L. & Elliott, J. T. Automated live cell imaging of green fluorescent protein degradation in individual fibroblasts. *Cytom. Part A* **71**, 827–834 (2007).
- 300. Thurlow, L. R. *et al.* Staphylococcus aureus Biofilms Prevent Macrophage Phagocytosis and Attenuate Inflammation In Vivo. *J. Immunol.* **186**, 6585–6596 (2011).
- 301. Mah, T. Biofilm-specific antibiotic resistance. 1061–1072 (2012).
- 302. Starner, T. D., Shrout, J. D., Parsek, M. R., Appelbaum, P. C. & Kim, G. H. Subinhibitory

  Concentrations of Azithromycin Decrease Nontypeable Haemophilus influenzae Biofilm

  Formation and Diminish Established Biofilms. *Antimicrob. Agents Chemother.* **52**, 137 (2008).
- 303. Ehrlich, G. D. *et al.* Mucosal Biofilm Formation on Middle-Ear Mucosa in the Chinchilla Model of Otitis Media. *JAMA* **287**, 1710–1715 (2002).
- 304. Li, L., Mendis, N., Trigui, H., Oliver, J. D. & Faucher, S. P. The importance of the viable but non-culturable state in human bacterial pathogens. *Front. Microbiol.* **5**, 258 (2014).

- 305. Gilbert, P., Das, J. & Foley, I. Biofilm susceptibility to antimicrobials. *Adv. Dent. Res.* **11**, 160–167 (1997).
- 306. Martens, A. *et al.* An optimized, robust and reproducible protocol to generate well-differentiated primary nasal epithelial models from extremely premature infants. *Sci. Rep.* **9**, 1–10 (2019).
- 307. Papazian, D., Würtzen, P. A. & Hansen, S. W. K. Polarized Airway Epithelial Models for Immunological Co-Culture Studies. *Int. Arch. Allergy Immunol.* **170**, 1–21 (2016).
- 308. Petris, A.-M. NON-TYPEABLE HAEMOPHILUS INFLUENZAE AND RHINOVIRUS CO-INFECTION OF THE RESPIRATORY EPITHELIUM. (2019).
- 309. Petris, A. M. *et al.* Non-typeable Haemophilus influenzae infection of ciliated epithelium from healthy and chronic obstructive pulmonary disease donors. *Eur. Respir. J.* **52**, PA5300 (2018).
- 310. Bailey, K. L. et al. Non-typeable Haemophilus influenzae decreases cilia beating via protein kinase C epsilon. Respiratory Research 13, (2012).
- 311. Wilson, R., Roberts, D. & Cole, P. Effect of bacterial products on human ciliary function in vitro. *Thorax* **40**, 125–131 (1985).
- 312. Brown, M. A. *et al.* Epithelial immune activation and intracellular invasion by non-typeable Haemophilus influenzae. *Front. Cell. Infect. Microbiol.* **13**, (2023).
- 313. Chatziparasidis, G., Kantar, A. & Grimwood, K. Pathogenesis of nontypeable Haemophilus influenzae infections in chronic suppurative lung disease. *Pediatr. Pulmonol.* **58**, 1849–1860 (2023).
- 314. Saliu, F. *et al.* Chronic infection by nontypeable haemophilus influenzae fuels airway inflammation. *ERJ Open Res.* **7**, (2021).
- 315. Walker, W. T. *et al.* Ciliated cultures from patients with primary ciliary dyskinesia produce nitric oxide in response to Haemophilus influenzae infection and proinflammatory cytokines. *Chest* **145**, 668–669 (2014).
- 316. Lagowala, D. A. *et al.* Microphysiological Models of Lung Epithelium-Alveolar Macrophage Co-Cultures to Study Chronic Lung Disease. *Adv. Biol.* (2023). doi:10.1002/adbi.202300165

- 317. Chen, S., So, E. C., Strome, S. E. & Zhang, X. Impact of Detachment Methods on M2 Macrophage Phenotype and Function. *J. Immunol. Methods* **426**, 56–61 (2015).
- 318. Gallaher, T. K., Wu, S., Webster, P. & Aguilera, R. Identification of biofilm proteins in non-typeable Haemophilus Influenzae. *BMC Microbiol.* **6**, 65 (2006).
- 319. Tikhomirova, A., Trappetti, C., Paton, J. C. & Kidd, S. P. The outcome of H. influenzae and S. pneumoniae inter-species interactions depends on pH, nutrient availability and growth phase. *Int. J. Med. Microbiol.* **305**, 881–892 (2015).
- 320. Oliver, J. D. Recent findings on the viable but nonculturable state in pathogenic bacteria. *FEMS Microbiology Reviews* **34**, 415–425 (2010).
- 321. Del Mar Lleo, M., Pierobon, S., Tafi, M. C., Signoretto, C. & Canepari, P. mRNA detection by reverse transcription-PCR for monitoring viability over time in an Enterococcus faecalis viable but nonculturable population maintained in a laboratory microcosm. *Appl. Environ. Microbiol.* **66**, 4564–4567 (2000).
- 322. Liu, C. et al. Cytokines: From Clinical Significance to Quantification. Adv. Sci. 8, (2021).
- 323. Song, Y. J. *et al.* Inhibition of lactate dehydrogenase A suppresses inflammatory response in RAW 264.7 macrophages. *Mol. Med. Rep.* **19**, 629–637 (2019).
- 324. Daifuku, M., Nishi, K., Okamoto, T. & Sugahara, T. Activation of J774.1 murine macrophages by lactate dehydrogenase. *Cytotechnology* **66**, 937–943 (2014).
- 325. Manosalva, C. *et al.* Role of Lactate in Inflammatory Processes: Friend or Foe. *Front. Immunol.* **12**, 1–14 (2022).
- 326. He, R. W. *et al.* Optimization of an air-liquid interface in vitro cell co-culture model to estimate the hazard of aerosol exposures. *J. Aerosol Sci.* **153**, 105703 (2021).
- 327. Wu, J. *et al.* Characterization of air-liquid interface culture of A549 alveolar epithelial cells. *Brazilian J. Med. Biol. Res.* **51**, (2018).
- 328. Yamanaka, N., Ogra, P. L., Fujihara, K., Bernstein, J. M. & Hard, R. Morphologic and Motility Changes of Nasal Cilia in Primary Culture Caused by Haemophilus Influenzae. *Ann. Otol. Rhinol. Laryngol.* **105**, 452–457 (1996).

- 329. Choi, J., Cox, A. D., Li, J., McCready, W. & Ulanova, M. Activation of innate immune responses by Haemophilus influenzae lipooligosaccharide. *Clin. Vaccine Immunol.* **21**, 769–776 (2014).
- 330. Szelestey, B. R., Heimlich, D. R., Raffel, F. K., Justice, S. S. & Mason, K. M. Haemophilus Responses to Nutritional Immunity: Epigenetic and Morphological Contribution to Biofilm Architecture, Invasion, Persistence and Disease Severity. *PLOS Pathog.* **9**, e1003709 (2013).
- 331. Van den Bossche, S., Vandeplassche, E., Ostyn, L., Coenye, T. & Crabbé, A. Bacterial Interference With Lactate Dehydrogenase Assay Leads to an Underestimation of Cytotoxicity. *Front. Cell. Infect. Microbiol.* **10**, (2020).
- 332. Van Riet, S. *et al.* Modulation of Airway Epithelial Innate Immunity and Wound Repair by M(GM-CSF) and M(M-CSF) Macrophages. *J. Innate Immun.* **12**, 410–421 (2020).
- 333. Tao, F. & Kobzik, L. Lung Macrophage-Epithelial Cell Interactions Amplify Particle-Mediated Cytokine Release. Am. J. Respir. Cell Mol. Biol **26**, (2002).
- 334. Bovard, D. *et al.* Comparison of the basic morphology and function of 3D lung epithelial cultures derived from several donors. *Curr. Res. Toxicol.* **1**, 56–69 (2020).
- 335. Rijsbergen, L. C., van Dijk, L. L. A., Engel, M. F. M., de Vries, R. D. & de Swart, R. L. In Vitro Modelling of Respiratory Virus Infections in Human Airway Epithelial Cells A Systematic Review. *Front. Immunol.* **12**, 1–18 (2021).
- 336. Barreto-Duran, E. *et al.* The interplay between the airway epithelium and tissue macrophages during the SARS-CoV-2 infection. *Front. Immunol.* **13**, 1–14 (2022).
- 337. Noel, G. *et al.* A primary human macrophage-enteroid co-culture model to investigate mucosal gut physiology and host-pathogen interactions. *Sci. Rep.* **7**, 1–14 (2017).
- 338. Evren, E., Ringqvist, E. & Willinger, T. Origin and ontogeny of lung macrophages: from mice to humans. *Immunology* **160**, 126–138 (2020).
- Ackland, J. et al. Nontypeable Haemophilus influenzae infection of pulmonary macrophages drives neutrophilic inflammation in severe asthma. Allergy Eur. J. Allergy Clin. Immunol. 77, 2961–2973 (2022).
- 340. Horton, K. L. *et al.* Method development for flow-cytometric analysis of primary human airway epithelia infected with non-typeable Haemophilus influenzae. *Eur. Respir. J.* **60**, 3926

(2022).